Synthesis and evaluation of novel multidentate N-heterocyclic carbene ligand precursors built on calixarene, DOTA and DTPA scaffolds

Emma Karen Bullough

Submitted in accordance with the requirements for the degree of Doctor of Philosophy

The University of Leeds
School of Chemistry

February 2013

The candidate confirms that the work submitted is her own, except where work which has formed part of jointly-authored publications has been included. The contribution of the candidate and the other authors to this work has been explicitly indicated below. The candidate confirms that appropriate credit has been given within the thesis where reference has been made to the work of others.

Publications

- Emma K. Bullough, Colin A. Kilner, Marc A. Little and Charlotte E. Willans. **Tetrakis(methylimidazole) and tetrakis(methylimidazolium) calix[4]arenes: competitive anion binding and titration studies.** *Org. Biomol. Chem.,* **2012**, DOI: 10.1039/C2OB07025A

The work described in the above publication is discussed in Chapter 2 of this thesis. Chapter 2 contains the synthesis of the compounds featured in this publication, a discussion of their crystal structures, and a discussion of the anion binding properties of one of these compounds in solution. All the experimental work in this publication was performed by the candidate. The crystal structures were collected and solved by either Mr Colin A. Kilner or Dr Marc A. Little. The ^{1}H NMR titration experiments were performed by the candidate. The anion binding constants were calculated by Dr Charlotte Willans. Dr Charlotte Willans secured the funding and wrote the paper with the assistance of the candidate.

- Benjamin R.M. Lake, Emma K. Bullough, Thomas J. Willams, Adrian C. Whitwood, Marc A. Little and Charlotte E. Willans. **Simple and versatile selective synthesis of neutral and cationic copper(I) N-heterocyclic carbenes using an electrochemical procedure.** *Chem. Commun.,* **2012**, DOI: 10.1039/C2CC30862B

Work described in the above publication features in Chapter 4 of this thesis. Chapter 4 contains a discussion of the synthesis of one the ligands and complexes featured in the publication. Chapter 4 also contains a description of the electrochemical procedure that forms the basis of this publication. The synthesis of the aforementioned compound and complex was carried out by the candidate, which was a key contribution to the paper as it highlights that the electrochemical approach is effective for the generation of copper(I)-NHCs from imidazolium ligands that incorporate several acidic groups. The remainder of the experimental work in this publication was performed by Mr Benjamin R.M. Lake. Crystallography was performed by Mr Benjamin R.M. Lake, Dr Adrian C. Whitwood or Dr Marc A. Little. Dr Charlotte Willans secured the funding and wrote the paper.

- Emma K. Bullough, Marc A. Little, Charlotte E. Willans. **Electrochemical synthesis of a Tetradentate copper N-Heterocyclic carbene calix[4]arene and its transmetallation to Palladium: Activity of the complex in Suzuki-Miyaura Cross-coupling.** *Organometallics.,* **2013**, DOI: 10.1021/om301085s

Work described in the above publication features in Chapters 4 and 5 of this thesis. Chapter 4 contains the details of the synthesis of the compounds and complexes discussed in this publication, as well as the crystal structures. Chapter 5 contains the details of the activity of the reported complex in Suzuki-Miyaura cross-coupling reactions. All the experimental work in the publication was performed by the candidate, as were the Suzuki-Miyaura cross coupling reactions. The crystal structures were collected and solved by Dr Marc A. Little. Dr Charlotte Willans secured the funding and wrote the paper with the assistance of the candidate.

Acknowledgements

Firstly I would like to thank my supervisor Dr. Charlotte Willans for all her help and support throughout my PhD, for helping me put this thesis together, and for helping me get a job. I have really enjoyed being a part of your research group.

Secondly I would like the thank Ben Lake for his guidance in the Lab, reading all my chapters, and for keeping me company over the last three years! I would also like to thank all the past members of our group, in particular Diana Monterio for being an exceptional master student and a good friend.

I would also like to thank everyone who works (or has worked) in Labs 1.06 and 1.32 for their support and advice over the last three years. Especially, Marc Little for all his help with crystallography, James Henkelis, Flora Thorp Greenwood, Dave Bryant, Katie Marriot, and Chris Carruthers, for general advice and creating a good working environment. A special mention also goes to everyone in Lab 1.25, in particular Chris Pask for helping me out on many occasions, Ben Crossley and Stephanie Lucas for being good friends, and Jonathan Loughrey for all his help with the EPR work. I would also like to thank Jeff Plante for some great chemistry advice and Fraser Cunningham for being a good drinking partner.

Lastly I would like to thank James Mannion and my family for all their love and support. My dad who is to blame for my love of science, my mum for always listening to me and being so thoughtful, my brother James, and James Mannion for making me very happy.

This achievement is dedicated to my mum and dad.

Abstract

The synthesis and characterisation of novel multidentate N-heterocyclic carbene (NHC) ligand precursors built on calixarene, DOTA, and DTPA scaffolds is reported in this thesis. Several synthetic procedures to these imidazolium salts were attempted, and it was generally found that the best approach was to react a bromomethylated or chloromethylated reagent with an N-substituted imidazole, forming the imidazolium salt cleanly and in high yields.

Neutral tetrakis(methylimidazole) calix[4]arene (**2.4**) and cationic tetrakis(methylimidazolium) calix[4]arene (**2.5**) were prepared and their solid state and solution behaviour was examined. It was found that compound **2.4** forms a zwitterion at elevated temperatures, which was seen in both solution and in the solid state. The anion binding properties of compound **2.5** were probed through ^{1}H NMR titration experiments, combined with X-ray crystallography. It was found that compound **2.5** exhibits a large range of hydrogen bonding interactions with anions, interacting via acidic protons on both the upper and lower rim of the calixarene.

Propanol-tethered methyl-imidazolium mesityl-calix[4]arene (**3.4**) and acetate-tethered methyl-imidazolium mesityl calix[4]arene (**4.2**) were prepared and their structures examined through anion binding experiments and X-ray crystallography. It was found that the propanol tethers of compound **3.4** form the primary interaction with anions, of the type $[(O\text{-}H)^{+}\cdots X^{-}]$, over any other acidic protons in the compound. Different routes to form metal-NHC complexes using these imidazolium salts were explored. However, as these compounds contained several acidic protons, traditional routes to form metal-NHC complexes were unsuccessful, resulting in either the formation of a complicated mixture of products, or decomposition of the ligand.

It was found that an alternative novel electrochemical method of metal-NHC formation, developed in the Willans group, could be used to prepare metal-NHC complexes from compounds that incorporated several acidic protons. The electrochemical method was used to prepare tetrakis-p-(copper-N-heterocyclic carbene)mesityl calixarene (**4.6**), which was used as a ligand transfer agent to form tetrakis-p-(palladium-N-heterocyclic carbene) mesityl calix[4]arene (**4.7**). The activity of the palladium complex was probed in the Suzuki-Miyaura cross-coupling reaction, and was found to be active for the coupling of aryl bromides and phenylboronic acid.

An inverse correlation between activity and the concentration of the pre-catalyst (**4.7**) was observed, suggesting that the calix[4]arene does not offer any protection against aggregation of palladium to form palladium(0)-nanoclusters.

NHC-ligand precursor bis[2-imidazolium(3-*tert*-butylacetate)ethyl]amino benzyl (**6.5**) was prepared, which was inspired by the structure of DTPA. Using compound **6.5**, two bis-imidazolium amine salts were prepared that incorporated different potential donor groups (**6.6** and **6.11**). The electrochemical procedure was used to prepare a chelating copper(I)-NHC complex (**6.16**) from compound **6.5**.

NHC-ligand precursors were also prepared that were appended to a DOTA scaffold (compounds **7.15** and **7.16**). The electrochemical approach was explored with compound **7.15**, resulting in the formation of a mixed valence copper complex, where a copper(II) ion is coordinated inside the macrocycle, in addition to the formation a of copper(I)-NHC. Compound **7.16** was coordinated to gadolinium (**7.17**) and the potential of this complex as a contrast agent was examined by measuring the relaxivity. It was found that complex **7.17** has a relaxivity of (r1) = 5.70 mM^{-1} s^{-1} (0.5 T, 23.8 ± 0.5 °C), which is larger than the commercially available Gd-DOTA contrast agent Dotarem® (r1 = 3.3 mM^{-1} s^{-1} (1.5 T, 37 °C)).

Contents

List of Figures

List of Schemes

List of tables

List of Abbreviations

NHC	N-Heterocyclic Carbene
DTPA	Diethylenetriaminepentaacetic acid
DOTA	1, 4, 7, 10-Tetraazacyclododecane tetraacetic acid
δ	Chemical shift
ppm	Parts per million
m/z	Mass to charge ratio
ES	Electrospray
Hz	Hertz
g	Grams
°C	Degrees Celsius
Å	Angstrom
Deg	Degree
mg	Milligram
mol	Mole
mmol	Milli mole
M	Moles per litre
min	Minute
mL	Millilitre
µL	Microlitre
Calc.	Calculated
NMR	Nuclear magnetic resonance
VT	Variable temperature
K	Kelvin
$\{^1H\}$	^1H decoupled

DEPT	Distortion less enhancement by polarisation transfer
J	Spin-spin coupling constant
m	Multiplet
s	Singlet
d	Doublet
t	Triplet
q	Quartet
dd	Doublet of doublets
br	Broad multiplet
$[M^+]$	Parent molecular ion
DCM	Dichloromethane
THF	Tetrahydrofuran
$CHCl_3$	Chloroform
DMSO	Dimethylsulfoxide
MeCN	Acetonitrile
MeOH	Methanol
HBr	Hydrogen bromide
MeCN-d_3	Deuterated acetonitrile
DMSO-d_6	Deuterated dimethylsulfoxide
$CDCl_3$	Deuterated chloroform
D_2O	Deuterated water
MeOH-d_3	Deuterated methanol
^{n}BuLi	n-Butyllithium
Et al.	And others
e.g.	*Exempli gratia*, for example

Ar	Aromatic
Ph	Phenyl
^{i}Pr	Isopropyl
^{t}Bu	Tertiary butyl
Cp	Cyclopentadienyl
PCy_3	Tricyclohexylphosphine
PPh_3	Triphenylphosphine
Ln	Lanthanide
L_n	Ligand
R	General substituent
Bn	Benzyl
Me	Methyl
Mes	Mesityl
Dipp	2,6-Diisopropylphenolate
Et	Ethyl
IMes	1,3-bis-(2,4,6-trimethylphenyl)imidazol-2-ylidene
SIPr	N,N'-bis(2,6-diisopropylphenyl)-4,5-dihydroimidazol-2-ylidene
SIMes	1,3-bis(2,4,6-trimethylphenyl)imidazol-2-ylidine
Py	Pyridine
Bipy	bipyridine
NH_4	Tetrabutylammonium
X	Halide
2D	Two dimensional

SOFs	Site-occupation factor
UV	Ultraviolet

1 Introduction

1.1 Introduction

This thesis focuses on the synthesis, characterisation, and evaluation of novel multidentate N-heterocyclic carbene (NHC) ligand precursors and their coordination to metal centres. NHC ligand precursors have been designed that are appended to calixarene cores, as well as those that were inspired by the ligands DTPA and DOTA, which are used in contrast agents for magnetic resonance imaging. This chapter will introduce NHCs and present a review of their chemistry.

1.2 An Introduction to Carbenes

A carbene is a divalent carbon centre possessing six valence electrons and no charge.[1] The carbene centre itself can adopt one of two geometries, linear or bent. The linear geometry implies an *sp*-hybridised carbene centre, where the two non-bonding electrons occupy two degenerate *p*-orbitals (p_x and p_y) (Figure 1.1 **A**). The unpaired electrons are spin aligned following Hund's rule, where the electron configuration that gives the highest multiplicity has the lowest energy, giving linear carbenes triplet multiplicity. If the molecule is bent, this degeneracy is broken and the carbon centre adopts an sp^2-hybridised form.[2] The p_y orbital remains almost unchanged and is known as p_π, and the p_x orbital is stabilised and acquires some s-type orbital character so is referred to as σ. The ground state of a bent carbene therefore has four possible electronic configurations, being either singlet (Figure 1.1 **B**, **C**, **D**), or triplet (Figure 1.1 **E**) in nature. In a singlet carbene the σ- or p_π-orbital contains an electron pair (Figure 1.1 **B**, **C**), leaving the other orbital empty. The lowest energy configuration for a singlet carbene is displayed in Figure 1.1 **B**, where the stabilised σ-orbital contains the electron pair. In a triplet carbene, both the σ- and p_π-orbital contain a single unpaired electron with parallel spins (Figure 1.1 **E**). An excited state singlet carbene can also be envisaged, where a single electron is promoted from the σ-orbital to the p_π-orbital. Hence both the σ-orbital and p_π-orbital contain a single unpaired electron with opposing spins (Figure 1.1, **D**).

The linear geometry is an extreme case, with most carbenes having bent geometry. The electronic configuration, hence multiplicity of the carbene centre, is therefore strongly dependent upon the energy gap between the σ- and p_π-orbitals. A large energy gap favours the formation of a singlet carbene, where both electrons

occupy the stabilised σ-orbital. Conversely, a small energy gap favours the formation of a triplet carbene, where both the σ and p_π-orbitals contain one unpaired electron.

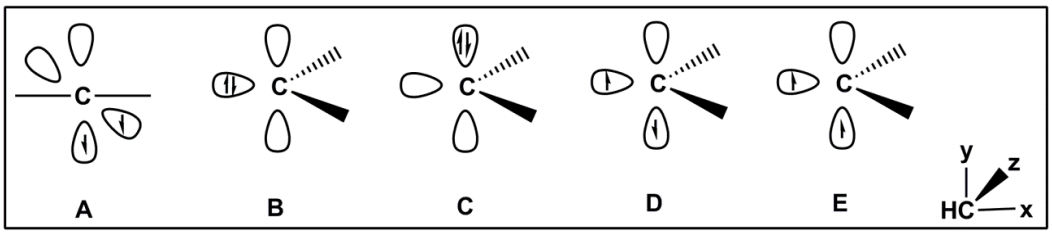

Figure 1.1 Possible electronic configurations of carbenes.[2]

The multiplicity of a bent carbene is strongly dependent upon the nature of the two α-substiuents, with inductive and mesomeric effects influencing the relative energies of the σ and p_π-orbitals. Electron withdrawing groups favour the singlet state by stabilising the filled non-bonding σ-orbital, which increases the σ-p_π gap (Figure 1.2, **A**).[3] π-Donating groups also favour the singlet state by destabilising the p_π-orbital, which again increases the σ-p_π gap.[4] The triplet carbene state (Figure 1.2, **B**) is favoured for π-withdrawing groups, where the p_π-orbital is stabilised so lowered in energy. σ-Donating groups also favour the triplet state by destabilising the σ-orbital, which decreases the σ-p_π gap (Figure 1.2, **B**).[5]

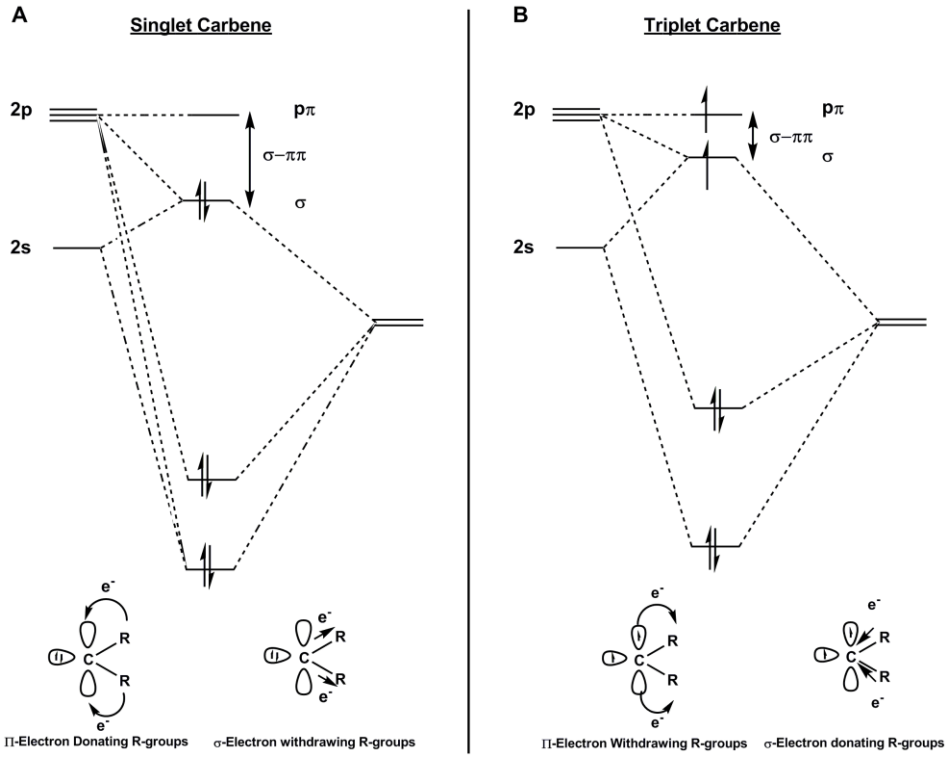

Figure 1.2 Orbital diagram showing the influence of the α-substituents on the multiplicity of the carbene centre.[1]

If electronic factors are negligible, then steric factors can influence the ground-state spin multiplicity of a carbene centre. The addition of large substituents forces the carbene to adopt a more linear geometry, which inherently favours the triplet ground-state.[1, 6]

1.3 An Introduction to N-Heterocyclic carbenes (NHCs)

N-heterocyclic carbenes (NHCs) are a type of diaminocarbene. They are typically five membered rings that incorporate two nitrogen atoms (Figure 1.3). The NHC ring can be fully saturated (imidazolidin-2-ylidenes, Figure 1.3, **B**) or contain an amount of unsaturation (imidazolin-2-ylidenes, Figure 1.3, **A**).[7] The carbenic carbon positioned between the two nitrogen atoms is referred to as the C2 carbon, and will be referenced as such throughout this thesis.

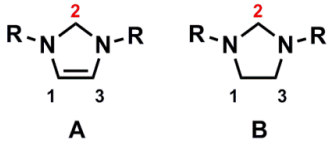

Figure 1.3 N-Heterocyclic carbenes

NHCs possess bent geometry, imposed by their cyclic nature, where the carbene centre is sp^2-hybridised and the singlet state dominates. Singlet multiplicity is achieved as a result of the constraints imposed by the geometry and nature of the α-nitrogen atoms. The α-nitrogen atoms are electron withdrawing which stabilises the non-bonding lone pair. In addition, they donate their lone pairs into the empty *p*-orbital which destabilises the empty orbital (Figure 1.4). This π-donor and σ-attractor relationship preserves the electroneutrality of the carbenic centre and ensures that the singlet state dominates.[1]

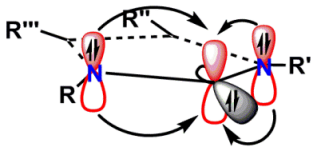

Figure 1.4 π-Donation from the α-nitrogen atoms into the p_π orbital, stabilising the NHC.

Consequently, NHCs act as Lewis base donors to metal ions, forming Fischer-type carbene complexes. The carbene donates an electron pair from the σ-orbital to the metal, and simultaneously accepts π-back donation from the metal d-orbitals into the empty p_π-orbital (Figure 1.5). However, the extent of π-back donation in metal-NHC complexes is usually considered to be small,[8] as the π-donating α-nitrogen atoms ensure that NHCs have no requirement for backbonding (Figure 1.4).[5] Therefore, unlike Fischer carbenes,

NHCs can be viewed as purely σ-donors. It should be noted here that the extent of π-back donation in metal-NHC complexes is an area that is still in dispute, with some research suggesting the extent of π-interaction in electron rich metal NHC-complexes is significant, forming 20-30 % of the overall orbital interaction.[9, 10]

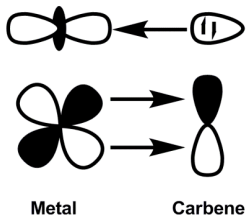

Figure 1.5 Metal bonding in Fischer type carbene complexes.[5]

As NHCs are strong σ-donors they are often compared to tertiary phosphine ligands. Indeed, a lot of early work in NHC chemistry involved replacing phosphine ligands in established transition metal complexes with NHCs and comparing the properties of the complexes. For example, a second generation Grubbs catalyst was prepared in which one of the tertiary phosphine ligands was replaced by an NHC group (Figure 1.6).[11] This was shown to have improved catalytic activity over the Grubbs first generation catalyst in olefin metathesis reactions.

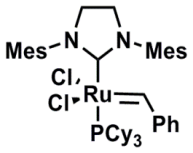

Figure 1.6 Second generation Grubbs catalyst.[11]

NHCs are now considered to be much more than just phosphine mimics, offering several advantages over phosphine ligands such as tighter binding, greater thermal stability, increased basicity, and easier synthesis.[12, 13] Furthermore, in contrast to aryl phosphines, NHCs have no requirement for backbonding, making them more suited to bind to a wider range of elements across the whole periodic table, including early transition metals and lanthanides ions.[14-16] It is these features that have prompted research groups to use NHCs as ligands to coordinate to a wide range of metals, either to replace phosphine ligands in established transition metal complexes or to design new organometallic species.

1.4 The Origins of NHC Chemistry

In 1969, the first examples of metal-NHC complexes were published independently by Wanzlick and Öfele. Wanzlick *et al.* treated an imidazolium salt with a basic metal precursor ($Hg(OAc)_2$) to generate a mercury-NHC complex *in situ* (Scheme 1.1, **A**).[17] Öfele *et al*. also used the *in situ* method with $[HCr(CO)_5]^-$ as the basic metal precursor to form a chromium-NHC complex (Scheme 1.1, **B**).[18]

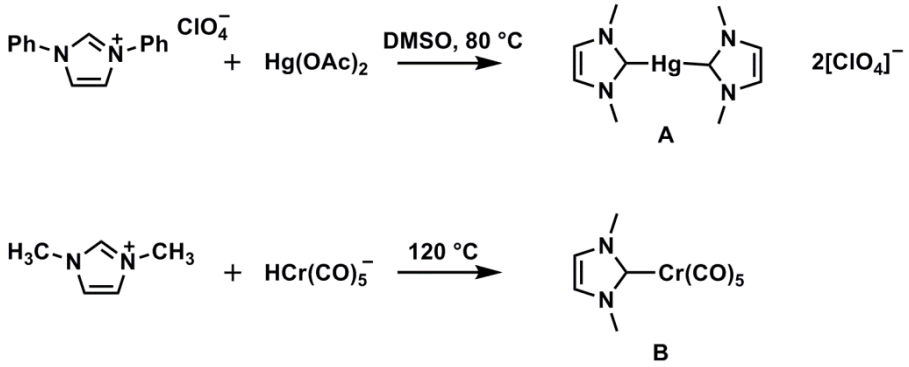

Scheme 1.1 Preparation of the first metal-NHC complexes synthesised by deprotonation of an imidazolium salt by a basic metal precursor.[17, 18]

Work in the field continued, and in 1991 the next major breakthrough was reported by Arduengo *et al*., who isolated the first uncoordinated NHC.[19] 1,3-Di-1-adamantylimidazolium chloride was deprotonated by DMSO / NaH in THF, which resulted in the formation of an NHC that was stable in anoxic conditions (Scheme 1.2). This procedure produced a 'bottle-able' carbene that could be used to prepare metal-NHC complexes directly from the free carbene, leading to a revival in the area.[20]

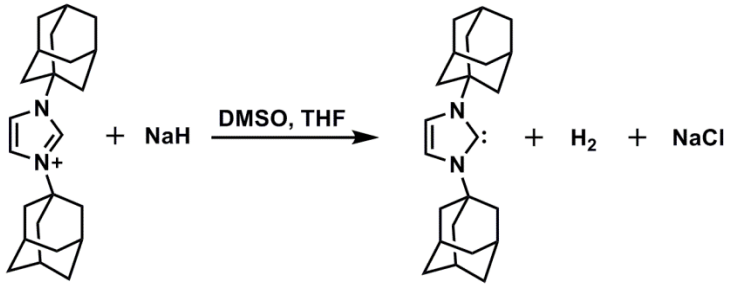

Scheme 1.2 Preparation of the first stable crystalline uncoordinated NHC.[19]

Since then, many different metal-NHC complexes have been prepared and characterised, with NHCs now recognised as very versatile ligands. They have tuneable steric and electronic properties that can be varied by changing the R-groups on the nitrogen atoms (Figure 1.3), or by changing the carbon backbone. They are also relatively easy to synthesise, with a range of synthetic methods being reported in the

literature.[1, 21-23] Hence, NHCs are now used widely as ligands in organometallic chemistry.

1.5 Synthesis of NHC ligand precursors

NHCs are usually formed *via* the deprotonation of an azolium salt precursor e.g. imidazolium, triazolium, benzimidazolium or imidazolinium salts. For this work we are interested in the preparation of NHCs from their imidazolium salt precursors. Generally, imidazolium salts are prepared following one of two synthetic procedures: a) the quaternization of a neutral N-substituted imidazole compound to form the imidazolium salt (Scheme 1.3);[24] or b) a multi-component reaction forming the heterocycle with the required substituents in one step, through the condensation of a primary amine with glyoxal and paraformaldehyde under acidic conditions (Scheme 1.4).[20] Notably, this second method can only be used to synthesise symmetrical imidazolium salts.

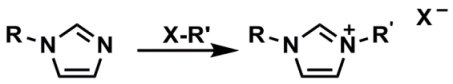

Scheme 1.3 Preparation of imidazolium salt from the N-substituted imidazole.

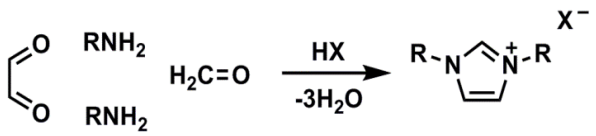

Scheme 1.4 Preparation of imidazolium salt by condensation of two equivalents of a primary amine with glyoxal and paraformaldehyde.

The C2 proton of imidazolium salts, which is on the carbon positioned between the two nitrogen atoms, has a characteristic low field resonance in ^{1}H NMR spectra. Imidazolium salts can be deprotonated at the C2 position to yield an NHC.

1.6 Synthesis of metal-NHC complexes

Most metal-NHC complexes are prepared either through the deprotonation of an azolium salt and formation of the metal-NHC complex *in situ*, or by adding the already formed NHC to a metal precursor. The typical methods used for the synthesis of metal-NHC complexes from imidazolium salts are discussed below.[12, 20]

1.6.1 Free carbene route

The free carbene is generated through the deprotonation of the imidazolium salt using a strong base (e.g. ^{n}BuLi, NaH, KO^{t}Bu). The uncoordinated NHC is then added to a metal precursor to form the metal-NHC complex (Figure 1.7, **A**).[25] This method is used if the free NHC is relatively stable, which is often the case for NHCs that have 'bulky' substituents on the nitrogen atoms that offer steric protection about the carbenic carbon, e.g. 1,3-di-1-adamantylimidazolium chloride, which was deprotonated by Arduengo *et al*., to form the free carbene, and was shown to coordinate to transition metals.[19]

1.6.2 The in situ formation of a metal-NHC complex

The imidazolium salt is deprotonated using a base (e.g. KH, KO^{t}Bu, NEt_3, K_2CO_3) in the presence of a metal precursor, with the metal-NHC complex being formed *in situ* (Figure 1.7, **D**). This procedure offers the advantage of not having to isolate the free carbene, which can be unstable and difficult to handle.

1.6.3 Transmetallation from silver

The imidazolium salt is reacted with a basic silver precursor (such as Ag_2O or Ag(OAc)), which deprotonates it and forms the silver-NHC complex *in situ* (Figure 1.7, **C**).[26] The silver-NHC complex can then be used as a ligand transfer agent to form other transition metal-NHC complexes.[23] This transmetallation route has been used extensively for the preparation of a range of transition metal-NHC complexes.[22]

1.6.4 Direct metallation

The desired transition metal-NHC complex is formed *in situ* using a basic metal precursor such as $Pd(OAc)_2$, $Rh(CO)_2(acac)$, Cu_2O (Figure 1.7, **B**).[27-30] This route is analogous to the silver oxide route, but forms the desired transition metal-NHC complex in one step.

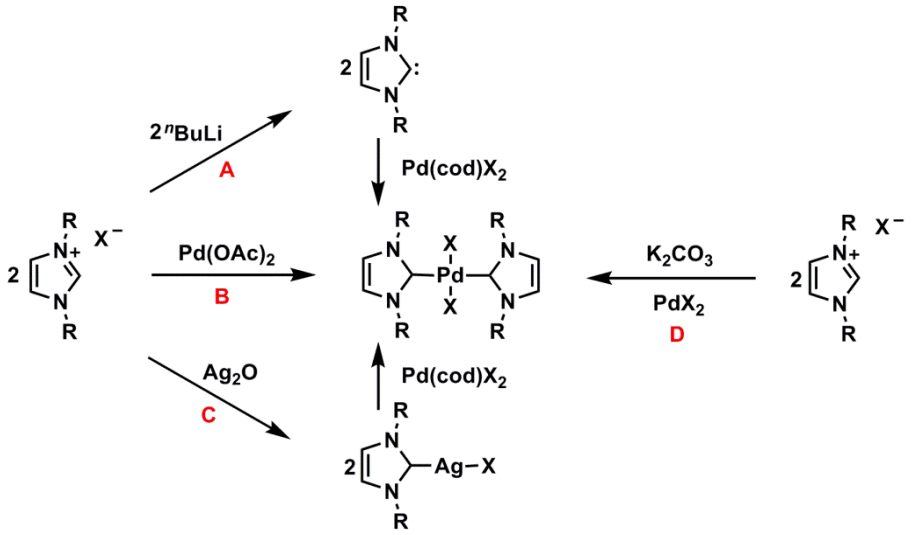

Figure 1.7 Different synthetic routes for the formation of a palladium(II)-NHC complex (X = Cl, Br, I).[31]

The methods discussed above have been used extensively for the preparation of metal-NHC complexes from their azolium salt precursors. However, other methods for NHC formation have been reported in the literature. For example, an NHC ligand precursor can be functionalised on the C2 carbon with a thermally labile group. This is then heated in the presence of a transition metal to form the metal-NHC complex.[32] This method was used by Grubbs *et al.* for the synthesis of a ruthenium-NHC complex from the alcohol azolium, or chloroform azolium adducts.[33]

Further examples include a templated approach, where an isocyanide ligand is used as the NHC building block. The isocyanide ligand is coordinated to a transition metal first, and then the NHC is formed. [34, 35] Also Lapperts' method, which involves the insertion of a metal into the electron rich carbon-carbon double bond of a bis(imidazolidin-2-ylidene)-dimer (Figure 1.8).[36, 37]

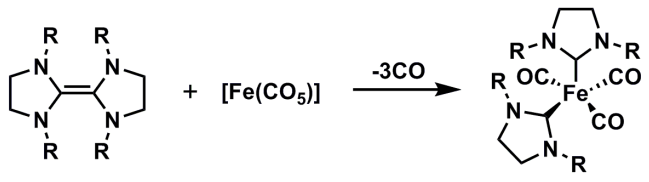

Figure 1.8 Synthesis of an iron(0)-NHC complex using the Lappert method (R = Me).[38]

The synthetic procedure that is used for the synthesis of a particular metal-NHC complex may be dependent on the nature of the metal and the ligand. For example, the transmetallation from silver is not a viable route for the synthesis of early transition metal- or lanthanide-NHC complexes. However, a synthetic route is often selected due to the preference of the researcher, or availability of starting materials.

1.7 Mid- to late-transition metal-NHC complexes

There are numerous examples of transition metal-NHC complexes in the literature, with NHCs being known to coordinate to all the d-block elements. As previously discussed, early work in the field concentrated on the replacement of phosphine ligands in established mid- to late-transition metal organometallic complexes with NHCs, and examining the catalytic potential of these new complexes. NHCs are known to form strong bonds to mid- to late-transition metals due to their soft nature, forming complexes with higher stability than their phosphine analogues.[39, 40] Research began with simple monodentate ligands, but soon expanded to multidentate and functionalised NHCs bearing donor groups such as amino, amido, ether, aryloxy and alkoxy groups.[41] There is now a wealth of literature available on mid- to late-transition metal NHC-complexes and their applications. In this section a few examples will be discussed.

Ruthenium(II)-NHC complexes have attracted wide interest due to their potential use as catalysts in olefin metathesis.[42] Grubbs second generation catalysts, in which the phosphine ligand has been replaced by an NHC, displayed higher activity and stability than the first generation Grubbs catalyst (Figure 1.9).[11, 43, 44] The observed increase in activity was originally thought to be a consequence of the strong *trans* effect of the NHC ligand increasing the rate of phosphine dissociation, hence the rate of formation of the catalytically active 14 electron species (Scheme 1.5). However, further studies by Grubbs *et al.*, showed that the rate of phosphine dissociation was actually slower in these complexes. Instead, it appeared that the greater affinity of the 14 electron species to bind the alkene substrates was most likely responsible for the increase in catalytic activity.[45, 46] Complex **D** remains one of the most successful ruthenium pre-catalysts for olefin metathesis, and is now commercially available.[47] Since then, many different ruthenium-NHC complexes have been synthesised and tested as catalysts in olefin metathesis.[48]

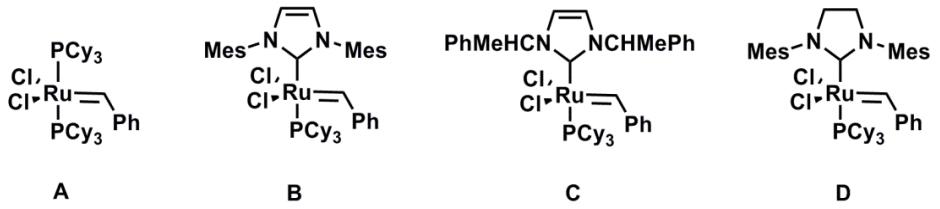

Figure 1.9 Grubbs first generation catalyst (**A**) and Grubbs second generation catalysts (**B**-**D**).[11, 43, 44]

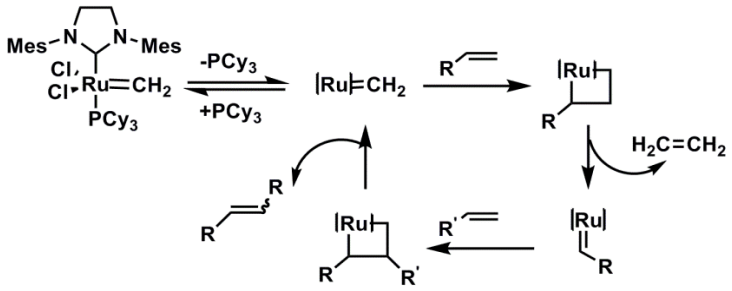

Scheme 1.5 Possible mechanism for olefin cross metathesis, where [Ru] = $Ru(NHC)Cl_2$.

The applications for ruthenium-NHCs extends well beyond olefin metathesis.[42] They have been used to promote reactions such as; polymerisations, olefin isomerisation, carbon-carbon bond forming reactions, and hydrogenation reactions.[49-53] An interesting report by Whittlesey *et al.* described the activation of carbon-fluorine bonds using a ruthenium-NHC complex (Figure 1.10).[54] The catalyst promoted the hydrodefluorination of hexafluorobenzene, pentafluorobenzene and pentafluoropyridine with alkylsilanes, with a good turnover (turnover number of up to 200), and frequency (0.86 h^{-1}) (Figure 1.10).

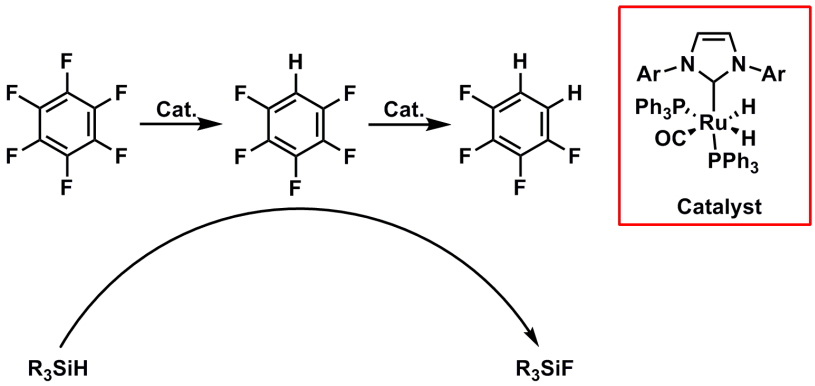

Figure 1.10 Catalytic C-F bond activation using a ruthenium(II)-NHC complex (Ar = IMes, IPr, SIMes, SIPr, and R = Et, *i*-Pr, Ph, EtO).[54]

Palladium-NHC complexes have also attracted a great deal of attention due to their use in carbon-carbon cross-coupling reactions. They have been found to be effective catalysts for Heck (M = aryl), Suzuki-Miyaura (M = $B(R'')_2$), Stille (M = SnR''_3), Negishi (M = ZnBr), Hiyama (M = $Si(OR'')_3$) and Kumada-Tamao-Corriu (M = MgBr) coupling reactions, which all differ in the choice of transmetallating agents (R'-M).[55] In general, the accepted mechanism follows the route outlined in Figure 1.11, where the difficulty of the reaction decreases in order R-Cl > R-Br > R-I. One of the most widely studied of these cross-coupling reactions is the Suzuki-Miyaura reaction, due to the low toxicity of the starting materials and good tolerance to different functional groups.

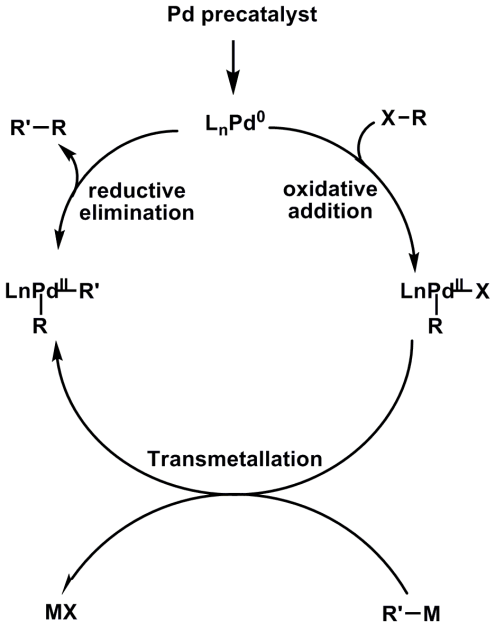

Figure 1.11 Proposed mechanism for palladium(II) cross-coupling reactions, where X = Cl, Br or I, and M = aryl, $B(R'')_2$, SnR''_3, ZnBr, $Si(OR'')_3$ or M = MgBr.[55]

The Suzuki-Miyaura reaction involves the coupling of an aryl or vinyl boronic acid / ester with an aryl or vinyl alkyl halide. The reaction is commonly catalysed by either a pre-formed palladium(II) complex,[56] or from the *in situ* formed catalyst generated from the ligand and a palladium precursor.[57] Elegant catalysts have been designed such as the complex in Figure 1.12, which allows for the coupling of sterically hindered aryl chlorides and aryl boronic acids to form di- and tri-substituted biaryls. The reaction can be performed at room temperature, and is complete in around one hour.[58]

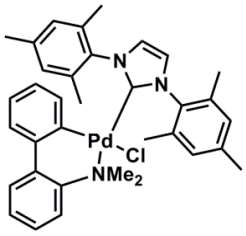

Figure 1.12 Palladium(II)-NHC catalyst for the Suzuki-Miyaura cross-coupling reaction.[58]

Nickel-NHC complexes are generally not as efficient as palladium-NHC complexes in cross-coupling reactions, and as a result are not as widely used. However, the use of nickel catalysts offers the advantage of lower cost, hence the design of efficient nickel catalysts is of interest. Chen *et al.*, prepared a mononuclear nickel(II) complex (Figure 1.13, **A**) and a binuclear nickel(II) complex (Figure 1.13, **B**), which were both found to be effective catalysts in the Negishi cross-coupling reaction, allowing for the coupling of unactivated aryl chlorides with organozinc reagents under mild conditions.[59] They

found the bimetallic complex (**B**) displayed higher activity than the mononuclear complex (**A**), which they postulate is due to a bimetallic cooperative effect.

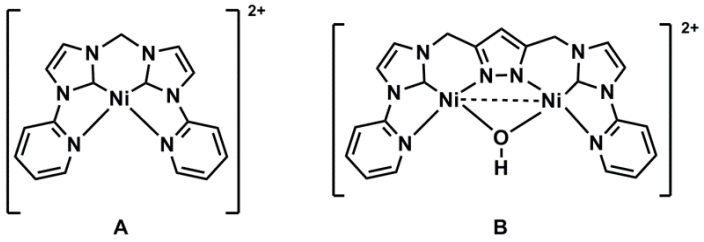

Figure 1.13 Nickel(II)-NHC catalysts for the Negishi cross coupling reaction.[59]

Rhodium-NHC and iridium-NHC complexes have attracted interest as catalysts for hydrogenation reactions. The cationic iridium complex (Figure 1.14, **A**) was reported to catalyse the hydrogenation of alkenes, under mild conditions (room temperature, 1atm H_2), with excellent enantioselectivity.[60] The cationic rhodium complex (Figure 1.14, **B**) was reported to catalyse the transfer hydrogenation of ketones and imines, via hydrogen transfer from *i*PrOH / KOH, with a low catalyst loading of 0.001 mol % being adequate to completely reduce the substrate.[61]

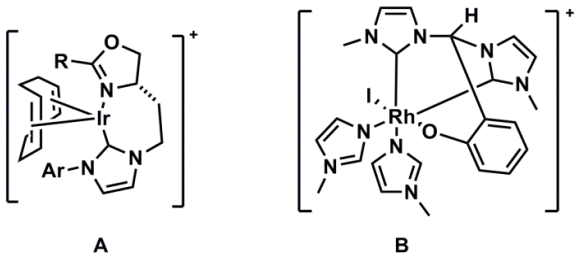

Figure 1.14 Iridium(I)-NHC and rhodium(III)-NHC for catalytic hydrogenation reactions.[60, 61]

Recently, gold-NHCs have emerged as interesting new catalysts, predominantly being used for the cycloisomerization of polyunsaturated substrates, and the hydration of alkynes.[62] An interesting report by Lin *et al.*, showed that gold(I)-NHC complexes of the type [Au(NHC)(Py)]PF_6 and [Au(Et_2-bimy)Cl] can catalyse the oxidation of benzyl alcohol to benzaldehyde, a reaction that gold complexes were previously seen to be barely active for.[63] In addition to showing catalytic potential, gold-NHCs have also attracted attention as potential drugs[64, 65] and luminescent complexes.[66]

Although transition metal-NHC chemistry has been somewhat dominated by catalysis, other potential applications for mid- to late-transition metal-NHC complexes have been reported in the literature. Work by Youngs *et al.* reported silver-NHCs that are water soluble and have antimicrobial properties comparable to silver nitrate.[67] NHC

complexes of silver(I), gold(I), palladium(II) and copper(I) have all been reported to be potential anticancer agents, with some displaying cytotoxicity values comparable to *cis*-platin.[68] A recent report by Santini, Dias *et al.* described the synthesis of amide and ester functionalised silver(I)-NHCs that are water soluble (Figure 1.15).[69] Complex **A** was shown to have cytotoxicity values similar to *cis*-platin against HCT-15 (colon) and A549 (lung) cancer cells, but had three times lower cytotoxity towards non-cancerous cells. A limitation for the application of metal-NHCs in biomedicine is likely to be complex stability in biomedical environments.

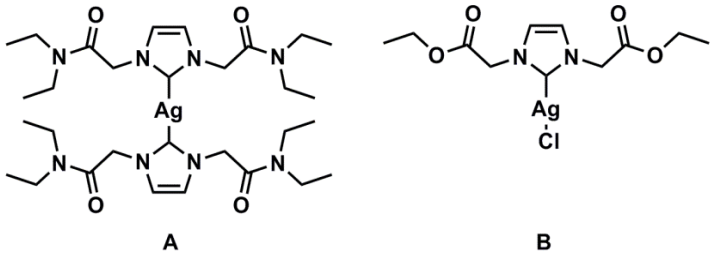

Figure 1.15 Ester and amide functionalised silver(I)-NHC complexes that display anticancer activity.[69]

1.8 NHC complexes of the early transition metals and f-elements

In contrast to their phosphine analogues, NHCs have no requirement for backbonding. Hence, they are more suited than phosphines to bind to hard, electropositive metals, such as the early transition metals and f-elements.[2] The first examples of these types of complexes had simple monodentate ligands, and were prepared through the substitution of weakly coordinating donor molecule(s) by a 'free' NHC (Scheme 1.6).[70] However, NHCs are relatively 'soft' ligands, so in order to synthesise stable metal-NHC complexes, functionalised NHC ligands were designed which incorporate an anionic tether.[2] The tether provides a form of covalent attachment between the metal ion and the ligand. Therefore, even if the metal-NHC interaction is broken, the NHC ligand will remain in close proximity to the metal. NHC ligands with alkoxide and amide tethers are most commonly used.

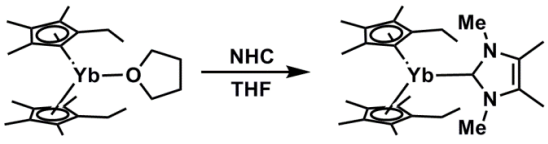

Scheme 1.6 Preparation of an ytterbium-NHC complex by substitution of a THF ligand by the NHC.[70]

The titanium(IV)-NHC complex (**A**), which incorporates an alkoxide tether, and the ytterbium(III)-NHC complex (**B**), which incorporates an amide tether, were prepared by

Arnold *et al*., and found to catalyse the polymerisation of lactide to polylactic acid (PLA) (Figure 1.16).[71] The complexes were prepared through the deprotonation of the functionalised imidazolium salt with an s-block base, to form the s-block-NHC adduct, in which the NHC acts as a donor to the alkali metal. The s-block-NHC adduct was then used as a transmetallation agent to prepare the desired complexes, *via* a salt metathesis reaction. In recent years, early transition metal-NHC and f-block-NHC complexes have often been prepared through this transmetallation route, rather than through the free NHC route.

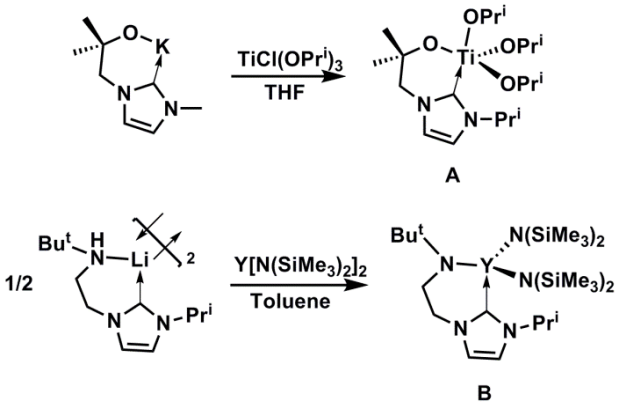

Figure 1.16 Synthesis of amido and alkoxy functionalised NHC complexes.[71, 72]

The suggested mechanism for the polymerisation of lactide using these complexes as catalysts is displayed in Scheme 1.7.[71] The lactide monomer coordinates to the metal centre, displacing the NHC. The 'free' NHC then attacks the lactide monomer, ring opening the lactide, and initiating polymerisation. Arnold *et al.* suggest that further chain growth occurs by monomer insertion at the metal centre. The anionic tether is crucial in this polymerisation reaction as it allows the NHC to be displaced from the metal centre but still be held in close proximity. This introduces the idea that an NHC could potentially act as a 'gatekeeper' which opens and closes at the active site, with the metal becoming involved in reactions such as atom abstraction and polymerisation. It should be noted that free NHCs are also reported as catalysts for this particular reaction, hence the metal centre may not be involved in polymersiation.[73]

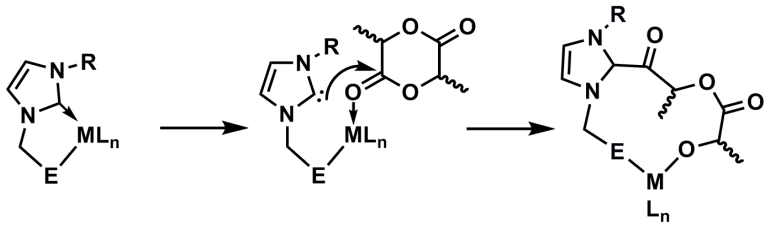

Scheme 1.7 Suggested mechanism for the polymerisation of lactide catalysed by ytterbium(III) or titanium(IV) anionic tethered metal-NHC complexes.[71]

Other types of anionic tethers have been reported that are not so widely used, such as indenyl and fluorenyl tethered NHC complexes (Figure 1.17). These complexes were found to be active catalysts for the living polymerisation of isopropene, with the fluorenyl substituted ligand (**B**) displaying the higher activity.[74, 75]

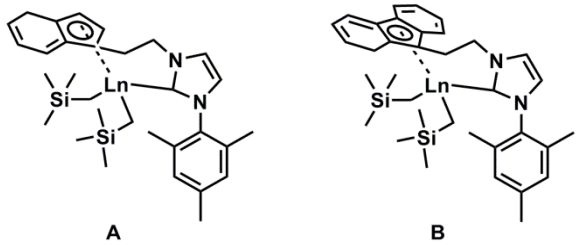

Figure 1.17 Indenyl and fluorenyl functionalised NHC complexes (Ln = Y, Ho, Lu).[75]

Multidentate NHC ligands have also been employed for the synthesis of stable early transition metal-NHC complexes. A pincer type titanium(III) complex was found to be active for the polymerisation of ethylene, following methylaluminoxane (MAO) activation, with a productivity of 790 kg mol^{-1} h^{-1} being reported (Figure 1.18). [76] The vanadium(III) complex of the same ligand was also synthesised and was found to be more active than the titanium analogue, with an activity of >1000 kg mol^{-1} h^{-1}.

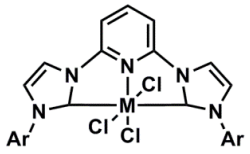

Figure 1.18 Pincer-type metal-NHC complexes that catalyse the polymerisation of ethylene (M = vanadium(III) or titanium(III), Ar = 2,6-$^{i}PrC_6H_3$).[76]

Examples of actinide-NHC complexes are rare, and consist primarily of uranium-NHC complexes.[77-81] Arnold *et al.* describe the synthesis of an alkoxide tethered uranium(IV)-NHC complex by treatment of the potassium alkoxide adduct with $UI_3(THF)_2$ (Scheme 1.8).[80] The outcome of the reaction was found to be dependent on the stoichiometry. If 3 equivalents of ligand are used in the reaction, a complex is

formed in which an NHC ligand remains uncoordinated. The free carbene can then be trapped by other reagents, demonstrating the possibility of complexes to participate in the bifunctional activation of small molecules.

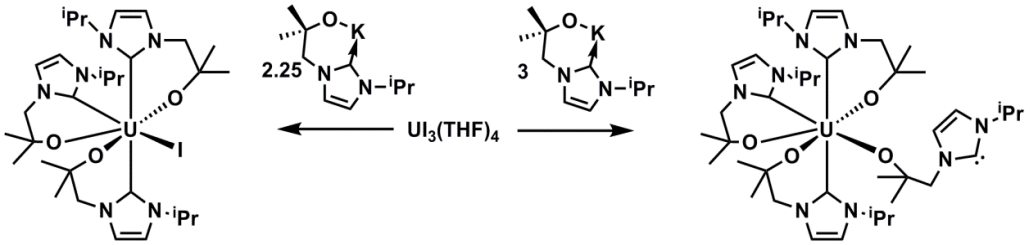

Scheme 1.8 Synthesis of alkoxide tethered uranium(IV)-NHC.[80]

To date, the applications of early transition metal and f-block NHC complexes are limited to polymerisation reactions. However, these complexes have potential to be used as bifunctional catalysts, and in the activation of small molecules. Another potential application of lanthanide-NHCs is in imaging. Gadolinium(III) coordination complexes have been used for a long time as imaging agents in magnetic resonance imaging (MRI), therefore it is possible that gadolinium-NHC complexes could find application in this field. As mentioned previously, the limitation for the application of metal-NHCs in biomedicine is likely to be complex stability in biomedical environments.

1.9 Abnormal NHCs

This thesis focuses on the synthesis of 'normal' NHCs, where the NHC coordinates to the metal ion through the C2 carbon (Figure 1.19, **A**). However, it is worth mentioning that unusual binding of a NHC to the metal ion can occur, where the NHC is instead coordinated to the metal through one of the backbone carbons (C4 / C5) and the C2 carbon remains protonated (**B**). These types of complexes are known as abnormal NHCs.

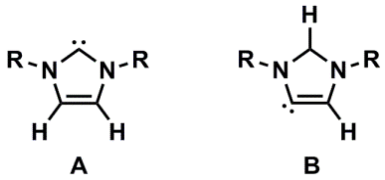

Figure 1.19 N-heterocyclic carbenes; (A) normal NHC, (B) abnormal NHC.[12]

The formation of an abnormal metal-NHC complex is favoured when steric strain is reduced at the metal centre.[82] Also, if the counter ion of the azolium salt is changed from a strongly coordinating anion (Br) to a weakly coordinating anion (PF_6) the

formation of the abnormal carbene becomes increasingly favourable ($Br < BF_4 < PF_6 < SbF_6$).[83, 84] A simple way to ensure that the abnormal carbene is formed exclusively is to introduce a substituent onto the C2 carbon of the azolium salt (e.g. a methyl group), forcing the NHC to coordinate to the metal in an abnormal fashion.[85]

Abnormal NHCs are not as widely explored as normal NHCs, but research in this field is growing. NHCs themselves are considered to be strong σ-donor ligands, but abnormal NHCs are known to be even stronger σ-donors, which can introduce some interesting properties.[86] Albrecht *et al.* synthesised a palladium complex (Figure 1.20) which, in the absence of other donor ions, could form an unusually short Pd-Ag interaction (2.8701(8) Å), highlighting the high electron density at the palladium centre.[87] Notably, the silver adduct could not be formed when the C2 bound carbene complex was synthesised using the same ligand (without the methyl groups on the C2 positions). The abnormal palladium-NHC complexes was found catalyse the hydrogenation of cyclooctene to cyclooctane under mild conditions (room temperature, 1 atm H_2), whereas the normal NHC complex was inactive. This suggests that the increased electron density at the metal centre was aiding the activation of the H_2 bond.

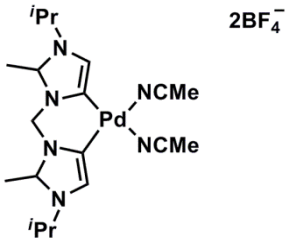

Figure 1.20 An abnormal palladium(II)-NHC complex which was found to be an effective catalyst precursor for the hydrogenation of cyclooctene to cyclooctane.[87]

In addition to displaying catalytic potential,[88] there are few other reported applications for abnormal metal-NHC complexes. A recent report by Brown *et al.*, describes the synthesis of a heteroleptic bis(tridentate) ruthenium(II) complex, that was found to have a microsecond excited-state lifetime (Figure 1.21). This is the highest lifetime that has been found for a unimolecular ruthenium(II) complex, being four times larger than $[Ru(II)(terpyridine)_2]^{2+}$.[89] Brown *et al.* propose that the long lived excited state lifetime is a consequence of the strongly σ-donating abnormal triazole carbene ligand.

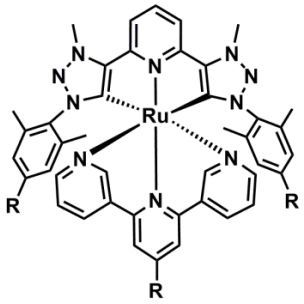

Figure 1.21 A heteroleptic bis(tridentate) ruthenium(II) complex bearing a terpyridine ligand and a tridentate abnormal carbene ligand.[89]

To the best of our knowledge, the only biomedical study on abnormal metal-NHC complexes examined the toxicity of abnormal ruthenium(II)-NHC complexes on zebrafish embryos.[90] The ruthenium(II)-NHC complexes were found to be non-toxic (LD_{50} > 100 mg L^{-1}), behaving as antioxidants at low concentrations, and pro-oxidants at higher concentrations.[91] The researchers suggest that these types of complexes may find application as antitumoral or neuroprotective drugs.

1.10 Multidentate and macrocyclic NHCs

The stability of metal-NHC complexes can be increased by using multidentate ligands. Indeed, one of the most stable palladium-NHC complexes reported to date is a bidentate pincer-type NHC-complex, which required prolonged heating at 140 °C before decomposing to form palladium(0) (Figure 1.22).[92] The enhanced stability of this complex is attributed to the chelate effect, which is generally thought to be an entropic effect resulting from the displacement of the non-chelating ligands around the metal centre, increasing the disorder within the system.

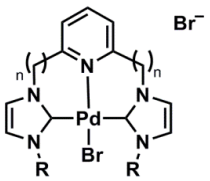

Figure 1.22 Bidentate palladium(II)-NHC complex where R= Me, Mes, ^{t}Bu, or Dipp, and n = 0 or 1.[92]

An interesting example of a tridentate NHC complex was reported by Meyer *et al.*, and was the first example of a thallium(I)-NHC complex (Scheme 1.9).[93] However, the complex was found to be highly temperature sensitive, and was only stable in THF at -35 °C. Tridentate NHC ligands have also been used to synthesise very stable metal-NHC complexes, such as an iron(III)-NHC complex (Figure 1.23) .[94]

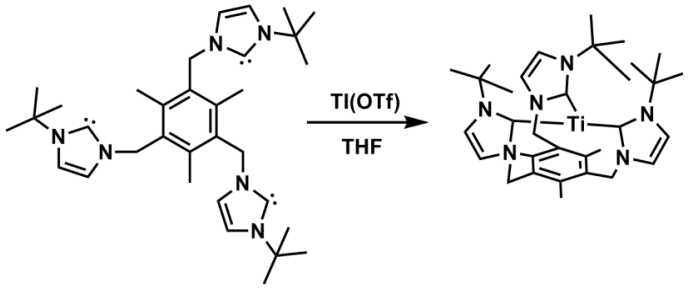

Scheme 1.9 Synthesis of the first thallium(I)-NHC complex from a tridentate NHC ligand.[93]

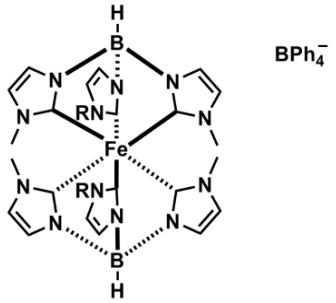

Figure 1.23 A stable iron(III)-complex bearing a tridentate NHC.[94]

The formation of macrocyclic metal-NHC complexes can be challenging, however, there are now a few examples reported in the literature.[95] They can be formed through a templated approach (Scheme 1.10),[96] or from the macrocyclic azolium salt (Scheme 1.11).[97]

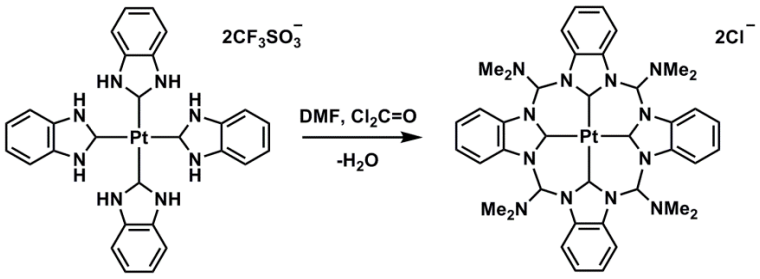

Scheme 1.10 Template synthesis of a macrocyclic tetracarbene platinum(II)-NHC complex.[96]

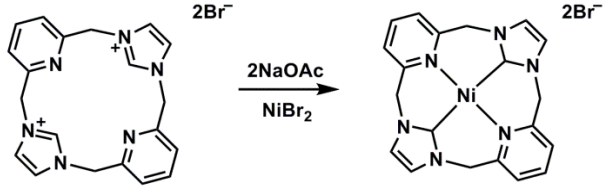

Scheme 1.11 Synthesis of a macrocyclic nickel(II)-NHC complex from the bisimidazolium salt.[97]

1.11 Conclusion

Over the last twenty years, the field of NHC chemistry has expanded. NHCs are no longer viewed as simply phosphine mimics and are now seen as versatile ligands with unique properties. By far the most widely reported application for NHCs is as ligands for the preparation of transition-metal catalysts. However, there are a growing number of reports of non-transition metal-NHC complexes, and NHCs are now finding potential application in the fields of biomedicine and materials. Although the field of NHC chemistry has reached a level of maturity, there is still much that remains to be discovered.

1.12 Project aims

This project seeks to prepare novel, multidentate, NHC ligand precursors, with a view to forming metal-NHC complexes with unique properties that can be exploited in catalytic and biomedical applications. Ligand precursors have been designed that are appended to calixarene cores, in addition to those that are inspired by the structural motifs of DTPA and DOTA. The target ligands all incorporate at least two potential NHC coordination sites, with some also incorporating anionic alkoxide binding sites. Hence, a combination of both soft (NHC) and hard (anionic tether) donor sites may help stabilise complexes that are not possible through a combination of monodentate ligands.

The calix[4]arene scaffold was selected as it provides a rigid platform that can be functionalised with up to four imidazolium groups. This presents the opportunity to prepare unique metal-NHC complexes that can incorporate up to four metal centres per ligand. These complexes can be monometallic or incorporate more than one type of metal (e.g. bimetallic systems). The project will firstly focus on synthesising two different types of calix[4]arenes, the cone type calix[4]arene and the 1,3-alternate calix[4]arene, that are functionalised with imidazolium groups. The synthetic routes will be obtimised where possible in order to produce compounds in high yield and purity. The N-substituent on the imidazolium nitrogen will be varied to include ligands that also incorporate anionic tethers, to extend the range of metals that the ligands can coordinate to. The coordination of these ligands to various metals will be explored, including silver, palladium, ruthenium, copper and rhodium, in order to generate complexes to examine in catalysis.

Ligands have also been designed that are inspired by the structural motifs of the acyclic chelating ligand DTPA, and the macrocyclic ligand DOTA, with a view to forming metal-NHC complexes with greater stability than traditional metal-NHC complexes. This may enable the application of metal-NHCs in biomedicine, an area that has not been widely studied. A synthetic route for the formation of these ligands will be determined and optimised. The coordination of these ligands to late-transition metals will be explored for potential application in catalysis. The ligands will also be coordinated to gadolinium(III) and their efficacy as contrasts agent examined through NMR experiments.

1.13 References

1. D. Bourissou, O. Guerret, F. P. Gabbaie and G. Bertrand, *Chem. Rev.*, 2000, **100**, 39-91.
2. S. T. Liddle, I. S. Edworthy and P. L. Arnold, *Chem. Soc. Rev.*, 2007, **36**, 1732-1744.
3. J. F. Harrison, R. C. Liedtke and J. F. Liebman, *J. Am. Chem. Soc.*, 1979, **101**, 7162-7168.
4. R. Gleiter and R. Hoffmann, *J. Amer. Chem. Soc.*, 1968, **90**, 5457-5460.
5. F. P. de, N. Marion and S. P. Nolan, *Coord. Chem. Rev.*, 2009, **253**, 862-892.
6. H. Tomioka, *Acc. Chem. Res.*, 1997, **30**, 315-321.
7. F. E. Hahn and M. C. Jahnke, *Angew. Chem., Int. Ed.*, 2008, **47**, 3122-3172.
8. J. C. Green, R. G. Scurr, P. L. Arnold and F. G. N. Cloke, *Chem. Commun.*, 1997, 1963-1964.
9. J. C. Green and B. J. Herbert, *Dalton Trans.*, 2005, **7**, 1214-1220.
10. D. Nemcsok, K. Wichmann and G. Frenking, *Organometallics*, 2004, **23**, 3640-3646.
11. J. Huang, E. D. Stevens, S. P. Nolan and J. L. Petersen, *J. Am. Chem. Soc.*, 1999, **121**, 2674-2678.
12. P. L. Arnold and S. Pearson, *Coord. Chem. Rev.*, 2007, **251**, 596-609.
13. H. Clavier and S. P. Nolan, *Annu. Rep. Prog. Chem., Sect. B: Org. Chem.*, 2007, **103**, 193-222.
14. C. Lorber and L. Vendier, *Dalton Trans.*, 2009, **0**, 6972-6984.
15. C. E. Willans, *Organomet. Chem.*, 2010, **36**, 1-28.
16. P. L. Arnold and I. J. Casely, *Chem. Rev.*, 2009, **109**, 3599-3611.
17. H. W. Wanzlick and Schonher.Hj, *Angew. Chem.-Int. Edit.*, 1968, **7**, 141-142.
18. K. Ofele, *J. Organomet. Chem.*, 1968, **12**, 42-43.
19. A. J. Arduengo, R. L. Harlow and M. Kline, *J. Am. Chem. Soc.*, 1991, **113**, 361-363.
20. T. Weskamp, V. P. W. Bohm and W. A. Herrmann, *J. Organomet. Chem.*, 2000, **600**, 12-22.
21. W. A. Herrmann and C. Kocher, *Angew. Chem., Int. Ed. Engl.*, 1997, **36**, 2162-2187.
22. I. J. B. Lin and C. S. Vasam, *Coord. Chem. Rev.*, 2007, **251**, 642-670.
23. C. E. Willans, K. M. Anderson, M. J. Paterson, P. C. Junk, L. J. Barbour and J. W. Steed, *Eur. J. Inorg. Chem.*, 2009, **7**, 2835-2843.
24. S. Guenal, N. Kaloglu, I. Oezdemir, S. Demir and I. Oezdemir, *Inorg. Chem. Commun.*, 2012, **21**, 142-146.
25. A. Caballero, E. Diez-Barra, F. A. Jalon, S. Merino and J. Tejeda, *J. Organomet. Chem.*, 2001, **617-618**, 395-398.
26. H. M. J. Wang and I. J. B. Lin, *Organometallics*, 1998, **17**, 972-975.
27. W. A. Herrmann, M. Elison, J. Fischer, C. Koecher and G. R. J. Artus, *Angew. Chem., Int. Ed. Engl.*, 1995, **34**, 2371-2374.
28. H. Lebel, M. K. Janes, A. B. Charette and S. P. Nolan, *J. Am. Chem. Soc.*, 2004, **126**, 5046-5047.
29. J. Chun, H. S. Lee, I. G. Jung, S. W. Lee, H. J. Kim and S. U. Son, *Organometallics*, 2010, **29**, 1518-1521.
30. W. A. Herrmann, M. Elison, J. Fischer, C. Koecher and G. R. J. Artus, *Chem.--Eur. J.*, 1996, **2**, 772-780.
31. O. Kühl, *Functionalised N-Heterocyclic Carbene Complexes*, John Wiley and sons Ltd. *(West Sussex, U. K.)*, 2010.
32. D. Enders, K. Breuer, G. Raabe, J. Runsink, J. H. Teles, J.-P. Melder, K. Ebel and S. Brode, *Angew. Chem., Int. Ed. Engl.*, 1995, **34**, 1021-1023.
33. T. M. Trnka, J. P. Morgan, M. S. Sanford, T. E. Wilhelm, M. Scholl, T.-L. Choi, S. Ding, M. W. Day and R. H. Grubbs, *J. Am. Chem. Soc.*, 2003, **125**, 2546-2558.
34. R. A. Michelin, A. J. L. Pombeiro and M. F. C. Guedes, *Coord. Chem. Rev.*, 2001, **218**, 75-112.
35. F. E. Hahn, C. G. Plumed, M. Muender and T. Luegger, *Chem.--Eur. J.*, 2004, **10**, 6285-6293.

36. D. J. Cardin, B. Cetinkaya, E. Cetinkaya and M. F. Lappert, *J. Chem. Soc., Dalton Trans.*, 1973, 514-522.
37. M. F. Lappert, *J. Organomet. Chem.*, 1988, **358**, 185-214.
38. M. F. Lappert and P. L. Pye, *J. Chem. Soc., Dalton Trans.*, 1977, 2172-2180.
39. L. Cavallo, A. Correa, C. Costabile and H. Jacobsen, *J. Organomet. Chem.*, 2005, **690**, 5407-5413.
40. A. M. Magill, K. J. Cavell and B. F. Yates, *J Am Chem Soc*, 2004, **126**, 8717-8724.
41. O. Kuhl, *Chem Soc Rev*, 2007, **36**, 592-607.
42. V. Dragutan, I. Dragutan, L. Delaude and A. Demonceau, *Coord. Chem. Rev.*, 2007, **251**, 765-794.
43. M. Scholl, T. M. Trnka, J. P. Morgan and R. H. Grubbs, *Tetrahedron Lett.*, 1999, **40**, 2247-2250.
44. L. Ackermann, A. Furstner, T. Weskamp, F. J. Kohl and W. A. Herrmann, *Tetrahedron Lett.*, 1999, **40**, 4787-4790.
45. M. S. Sanford, J. A. Love and R. H. Grubbs, *J. Am. Chem. Soc.*, 2001, **123**, 6543-6554.
46. M. S. Sanford, M. Ulman and R. H. Grubbs, *J. Am. Chem. Soc.*, 2001, **123**, 749-750.
47. C. Samojlowicz, M. Bieniek and K. Grela, *Chem. Rev.*, 2009, **109**, 3708-3742.
48. E. Colacino, J. Martinez and F. Lamaty, *Coord. Chem. Rev.*, 2007, **251**, 726-764.
49. J. C. Sworen, J. H. Pawlow, W. Case, J. Lever and K. B. Wagener, *J. Mol. Catal. A: Chem.*, 2003, **194**, 69-78.
50. H. M. Lee, D. C. Smith, Jr., Z. He, E. D. Stevens, C. S. Yi and S. P. Nolan, *Organometallics*, 2001, **20**, 794-797.
51. D. Banti and J. C. Mol, *J. Organomet. Chem.*, 2004, **689**, 3113-3116.
52. A. Nakazato, I. Saeed, T. Katsumata, M. Shiotsuki, T. Masuda, J. Zednik and J. Vohlidal, *J. Polym. Sci., Part A: Polym. Chem.*, 2005, **43**, 4530-4536.
53. W. Baratta, W. A. Herrmann, P. Rigo and J. Schwarz, *J. Organomet. Chem.*, 2000, **593-594**, 489-493.
54. S. P. Reade, M. F. Mahon and M. K. Whittlesey, *J. Am. Chem. Soc.*, 2009, **131**, 1847-1861.
55. G. C. Fortman and S. P. Nolan, *Chem. Soc. Rev.*, 2011, **40**, 5151-5169.
56. C. W. K. Gstottmayr, V. P. W. Bohm, E. Herdtweck, M. Grosche and W. A. Herrmann, *Angew. Chem., Int. Ed.*, 2002, **41**, 1363-1365.
57. A. C. Hillier, G. A. Grasa, M. S. Viciu, H. M. Lee, C. Yang and S. P. Nolan, *J. Organomet. Chem.*, 2002, **653**, 69-82.
58. O. Navarro, R. A. Kelly, III and S. P. Nolan, *J. Am. Chem. Soc.*, 2003, **125**, 16194-16195.
59. Z. Xi, Y. Zhou and W. Chen, *J. Org. Chem.*, 2008, **73**, 8497-8501.
60. M. T. Powell, D.-R. Hou, M. C. Perry, X. Cui and K. Burgess, *J. Am. Chem. Soc.*, 2001, **123**, 8878-8879.
61. E. Mas-Marza, M. Poyatos, M. Sanau and E. Peris, *Organometallics*, 2004, **23**, 323-325.
62. N. Marion and S. P. Nolan, *Chem. Soc. Rev.*, 2008, **37**, 1776-1782.
63. J. Y. Z. Chiou, S. C. Luo, W. C. You, A. Bhattacharyya, C. S. Vasam, C. H. Huang and I. J. B. Lin, *Eur. J. Inorg. Chem.*, 2009, 1950-1959.
64. S. Ray, R. Mohan, J. K. Singh, M. K. Samantaray, M. M. Shaikh, D. Panda and P. Ghosh, *J. Am. Chem. Soc.*, 2007, **129**, 15042-15053.
65. W. Liu, K. Bensdorf, M. Proetto, U. Abram, A. Hagenbach and R. Gust, *J. Med. Chem.*, 2011, **54**, 8605-8615.
66. P. J. Barnard, L. E. Wedlock, M. V. Baker, S. J. Berners-Price, D. A. Joyce, B. W. Skelton and J. H. Steer, *Angew. Chem., Int. Ed.*, 2006, **45**, 5966-5970.
67. A. Melaiye, R. S. Simons, A. Milsted, F. Pingitore, C. Wesdemiotis, C. A. Tessier and W. J. Youngs, *J. Med. Chem.*, 2004, **47**, 973-977.
68. M.-L. Teyssot, A.-S. Jarrousse, M. Manin, A. Chevry, S. Roche, F. Norre, C. Beaudoin, L. Morel, D. Boyer, R. Mahiou and A. Gautier, *Dalton Trans.*, 2009, **0**, 6894-6902.

69. M. Pellei, V. Gandin, M. Marinelli, C. Marzano, M. Yousufuddin, H. V. R. Dias and C. Santini, *Inorg. Chem.*, 2012, **51**, 9873-9882.
70. M. G. H. Schumann, J. Winterfeld, H. Hemling, N. Kuhn and T. Kratz, *Angew. Chem., Int. Ed.Engl.*, 1994, **33**, 1733-1734.
71. D. Patel, S. T. Liddle, S. A. Mungur, M. Rodden, A. J. Blake and P. L. Arnold, *Chem. Commun.*, 2006, 1124-1126.
72. P. L. Arnold, S. A. Mungur, A. J. Blake and C. Wilson, *Angew. Chem., Int. Ed.*, 2003, **42**, 5981-5984.
73. N. E. Kamber, W. Jeong, R. M. Waymouth, R. C. Pratt, B. G. G. Lohmeijer and J. L. Hedrick, *Chem. Rev.*, 2007, **107**, 5813-5840.
74. B. Wang, D. Wang, D. Cui, W. Gao, T. Tang, X. Chen and X. Jing, *Organometallics*, 2007, **26**, 3167-3172.
75. B. Wang, D. Cui and K. Lv, *Macromolecules*, 2008, **41**, 1983-1988.
76. D. S. McGuinness, V. C. Gibson and J. W. Steed, *Organometallics*, 2004, **23**, 6288-6292.
77. W. J. Oldham, Jr., S. M. Oldham, W. H. Smith, D. A. Costa, B. L. Scott and K. D. Abney, *Chem. Commun.*, 2001, 1348-1349.
78. H. Nakai, X. Hu, L. N. Zakharov, A. L. Rheingold and K. Meyer, *Inorg. Chem.*, 2004, **43**, 855-857.
79. T. Mehdoui, J.-C. Berthet, P. Thuery and M. Ephritikhine, *Chem. Commun.*, 2005, 2860-2862.
80. P. L. Arnold, A. L. Blake and C. Wilson, *Chem.-Eur. J.*, 2005, **11**, 6095-6099.
81. S. A. Mungur, S. T. Liddle, C. Wilson, M. J. Sarsfield and P. L. Arnold, *Chem Commun.*, 2004, 2738-2739.
82. B. Eguillor, M. A. Esteruelas, M. Olivan and M. Puerta, *Organometallics*, 2008, **27**, 445-450.
83. M. Baya, B. Eguillor, M. A. Esteruelas, M. Olivan and E. Onate, *Organometallics*, 2007, **26**, 6556-6563.
84. L. N. Appelhans, D. Zuccaccia, A. Kovacevic, A. R. Chianese, J. R. Miecznikowski, A. Macchioni, E. Clot, O. Eisenstein and R. H. Crabtree, *J. Am. Chem. Soc.*, 2005, **127**, 16299-16311.
85. A. R. Chianese, A. Kovacevic, B. M. Zeglis, J. W. Faller and R. H. Crabtree, *Organometallics*, 2004, **23**, 2461-2468.
86. R. H. Crabtree, *Coord. Chem. Rev.*, 2013, **257**, 755-766.
87. M. Heckenroth, E. Kluser, A. Neels and M. Albrecht, *Angew. Chem., Int. Ed.*, 2007, **46**, 6293-6296.
88. M. Albrecht and K. J. Cavell, *Organomet. Chem.*, 2009, **35**, 47-61.
89. D. G. Brown, N. Sanguantrakun, B. Schulze, U. S. Schubert and C. P. Berlinguette, *J. Am. Chem. Soc.*, 2012, **134**, 12354-12357.
90. J. M. Alfaro, A. Prades, M. d. C. Ramos, E. Peris, J. Ripoll-Gomez, M. Poyatos and J. S. Burgos, *Zebrafish*, 2010, **7**, 13-21.
91. A. Gautier and F. Cisnetti, *Metallomics*, 2012, **4**, 23-32.
92. E. Peris, J. Mata, J. A. Loch and R. H. Crabtree, *Chem. Commun.*, 2001, 201-202.
93. H. Nakai, Y. Tang, P. Gantzel and K. Meyer, *Chem. Commun.*, 2003, 24-25.
94. U. Kernbach, M. Ramm, P. Luger and W. P. Fehlhammer, *Angew. Chem., Int. Ed. Engl.*, 1996, **35**, 310-312.
95. P. G. Edwards and F. E. Hahn, *Dalton Trans.*, 2011, **40**, 10278-10288.
96. F. E. Hahn, V. Langenhahn, T. Luegger, T. Pape and V. D. Le, *Angew. Chem., Int. Ed.*, 2005, **44**, 3759-3763.
97. M. V. Baker, B. W. Skelton, A. H. White and C. C. Williams, *Organometallics*, 2002, **21**, 2674-2678.

2 Tetrakis(methylimidazole) and tetrakis(methylimidazolium) calix[4]arenes: competitive anion binding and deprotonation

Calixarene is the name given to a group of macrocyclic compounds that consist of linked phenol units. The term was originally conceived to describe the shape of the tetrakis phenol calixarene that is described in this chapter, but its use has been extended to include compounds that incorporate more or fewer phenol units, and those incorporating other aromatic groups. Calixarenes can adopt shapes from cones and baskets to wheels.[1] They contain hydrophobic cavities within the structure that are able to 'fit' other molecules, leading to them receiving wide attention in host-guest chemistry.[2-4] The design of these molecules can be varied by functionalising the phenolic (*lower*) and / or non-phenolic (*upper*) ring,[5] giving access to a range of compounds with interesting and useful properties.[6-8] Neutral tetrakis(methylimidazole) calix[4]arene (**2.4**) and the novel cationic tetrakis(methylimidazolium) calix[4]arene (**2.5**) have been prepared and their solid-state and solution behaviour examined. It was found that compound **2.4** forms a zwitterion at elevated temperatures, which was observed both in solution and in the solid-state. Compound **2.5** exhibits a range of hydrogen bonding interactions with anions, interacting *via* acidic protons on both the upper and lower rim of the calixarene. The anion binding properties of compound **2.5** were probed through ^{1}H NMR titration experiments combined with X-ray crystallography.

2.1 Synthesis of tetrakis(methylimidazole) and terakis(methylimidazolium) calix[4]arenes (2.4 and 2.5)

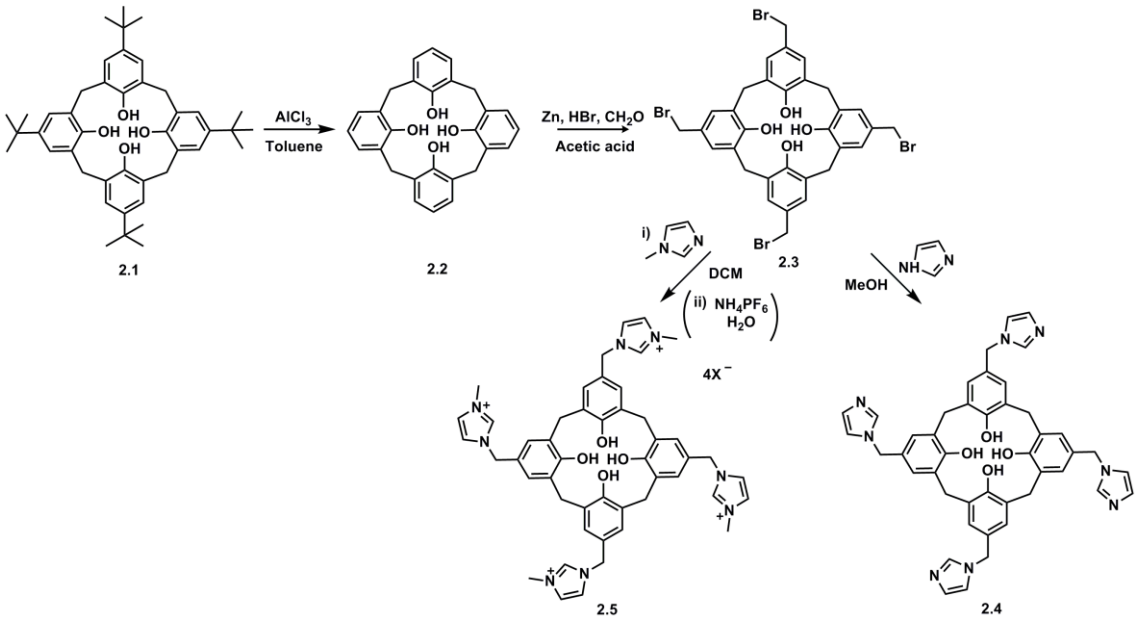

Scheme 2.1 Synthesis of tetrakis(methylimidazole) calix[4]arene **2.4** and tetrakis(methylimidazolium) calix[4]arene **2.5** (X = Br or PF_6).

The preparation of 4-hydroxy-*tert*-butyl calix[4]arene (**2.1**) was carried out *via* the base induced condensation of *para*-*tert*-butyl phenol and formaldehyde.[9] The procedure is well established, originally being reported by Zinke and later modified by Gutsche.[9, 10] The desired calixarene **2.1** is produced in moderate yields of 40-50 %, and isolated by recrystallisation from toluene. The removal of the *tert*-butyl groups using aluminium chloride generates 4-hydroxy calix[4]arene (**2.2**), a reagent suitable for functionalisation on the upper rim.[9, 11, 12] The bromomethylation of compound **2.2** was performed with HBr and paraformaldehyde in glacial acetic acid, isolating 1-bromomethyl-4-hydroxy calix[4]arene (**2.3**) as an off-white solid.[13] Compounds **2.1** and **2.3** were isolated and characterised by ^{1}H NMR and ^{13}C{^{1}H} NMR spectroscopy combined with mass spectrometry. The reaction of compound **2.3** with excess imidazole in methanol yields tetrakis(methylimidazole) calix[4]arene (**2.4**).[14] A base is not required due to the amphoteric nature of imidazole, which acts as a base in these types of nucleophilic substitution reactions. Although the compound is reported in the literature, we have developed a simpler synthetic procedure resulting in a product of similar purity and comparable yields.[15] Compound **2.4** was isolated as a colourless solid and characterised by ^{1}H NMR and ^{13}C{^{1}H} NMR spectroscopy, mass spectrometry and elemental

analysis. Colourless prism crystals were obtained by heating a saturated chloroform solution of compound **2.4** to 60 °C in a sealed vessel, then allowing the solution to cool slowly to room temperature. The molecular structure is displayed in Figure 2.1, and is the first time that the solid state structure has been reported.

The compound crystallised in the monoclinic *P* crystal system, and the structural solution was performed in the space group $P2_1/c$. To the best of our knowledge, this is the first calix[4]arene structure with methyl imidazole substituents on the upper rim (*para* positions with respect to the hydroxyl groups).

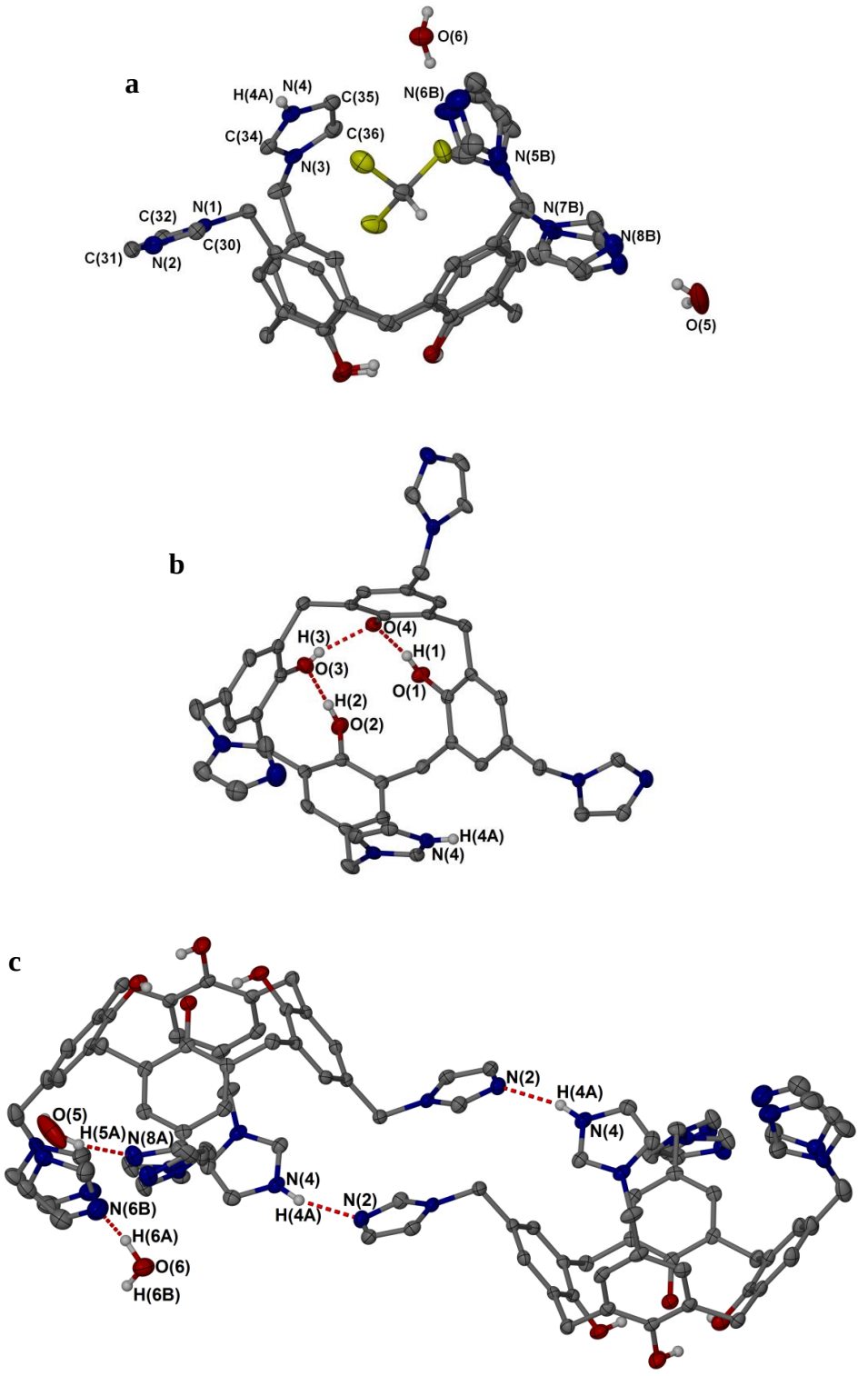

Figure 2.1 Molecular structure of compound **2.4**•CH_3Cl•$2H_2O$ illustrating a) cone conformation with a molecule of chloroform in the cavity, b) deprotonation of the hydroxyl group (O4) and protonation of the imidazole nitrogen (N4), c) hydrogen bonding network within the structure. The majority of the hydrogen atoms have been omitted for clarity. Ellipsoids are displayed at 50% probability.

N(4)-C(35)	1.383(3)	N(2)-C(30)-N(1)	112.25(19)
N(4)-C(34)	1.394(2)	C(30)-N(2)-C(31)	104.59(18)
O(2)-H(2)	0.857(1)		
O(2)-O(3)	2.704(2)		
O(6)-N(6B)	2.269		

Table 2.1 Selected bond distances (Å) and angles (deg) for compound **2.4**.

From the crystal structure it can be seen that compound **2.4** adopts the expected cone type conformation, where the imidazole groups project upwards with respect to the plane defined by the bridging methylene groups. The compound adopts the cone conformation due to the favourable hydrogen bonding network of the hydroxyl groups on the lower ring, as displayed in Figure 2.1b**.** Two of the imidazole groups orientate themselves with the carbon between the two nitrogen atoms (C2) protons pointing towards the centre of the ring, and two with the C2 protons pointing away, resulting in an unsymmetrical structure.

Compound **2.4** crystallises as a clathrate complex with a molecule of chloroform contained within the cavity. The inclusion of solvent in the solid state structures of calixarenes is often observed, with *para-tert*-butyl calix[4]arene being shown to form clathrate complexes with chloroform, toluene, xylene and anisole.[16-18] Parma *et al.* studied the factors that affect this complexation and found that it was dependent on the size of the calixarene, the substituents in the *para* position, and the conformational rigidity of the calixarene molecule.[17, 19, 20]

An interesting feature of the structure is that compound **2.4** exists as the mono-zwitterion in the solid state, with one of the hydroxyl groups deprotonated (**O4**), and one of the imidazole nitrogens protonated (**N4**). The protonated nitrogen (**N4**) on the imidazole of one calixarene hydrogen bonds with a non-protonated nitrogen (**N2**) on a neighbouring calixarene (Figure 2.1c). The remaining two imidazole groups interact with water molecules contained within the structure appearing to cause disorder, with the imidazole groups occupying two sites (**N6A / B**, **N8A / B**).

The formation of the mono-zwitterion was not entirely unexpected. The first deprotonation of a hydroxyl group of a calix[4]arene molecule has been shown to be

favourable by Grootenhuis *et al.*, with the reasons being twofold.[21] Firstly, the formation of a charged species dramatically increases the favourable electrostatic interactions of the calixarene with the solvent molecules. Secondly, from their calculations, it was shown that the hydrogen bonding interactions at the lower rim of the calixarene can be strengthened upon deprotonation of one of the hydroxyl groups. However, the deprotonation of the second, third and fourth hydroxyl group becomes progressively more unfavourable due to the repulsive interactions formed between the negatively charged oxygen atoms. As a result this mono-zwitterionic structure would be a favourable conformation for compound **2.4** to adopt.

A ^{1}H NMR spectrum of compound **2.4** in DMSO-d_6 at room temperature is displayed in Figure 2.2. The poor solubility of compound **2.4** in most organic solvents (it is only soluble in DMSO at room temperature and chloroform at elevated temperatures) made studying the solution-state properties of compound **2.4** a challenge. An interesting feature of the ^{1}H NMR spectrum is the appearance of the methylene proton signals of carbon **6** (Figure 2.2). At room temperature these appear as a broad set of doublets at δ = 3.13 ppm and δ = 4.21 ppm. This is attributed to the interconversion of the cone conformation that occurs slowly on the NMR timescale at room temperature, resulting in the signals broadening and unresolved coupling of the methylene protons. The remainder of the spectrum appears as expected, with the imidazole CH resonances as singlets at δ = 7.95 ppm (**1**), δ = 7.72 ppm (**2** / **3**) and δ = 7.06 ppm (**2 / 3**) (the ^{1}H NMR spectrum being too broad to show any coupling between the inequivalent backbone imidazole protons). The aromatic protons appear as a singlet at δ = 6.80 ppm (**5**), and a further singlet resonance at δ = 4.91 ppm is attributable to the CH_2 protons which tether the imidazole groups to the calixarene skeleton (**4**). We did not observe any signals for the hydroxyl protons in the ^{1}H NMR spectrum in DMSO-d_6.

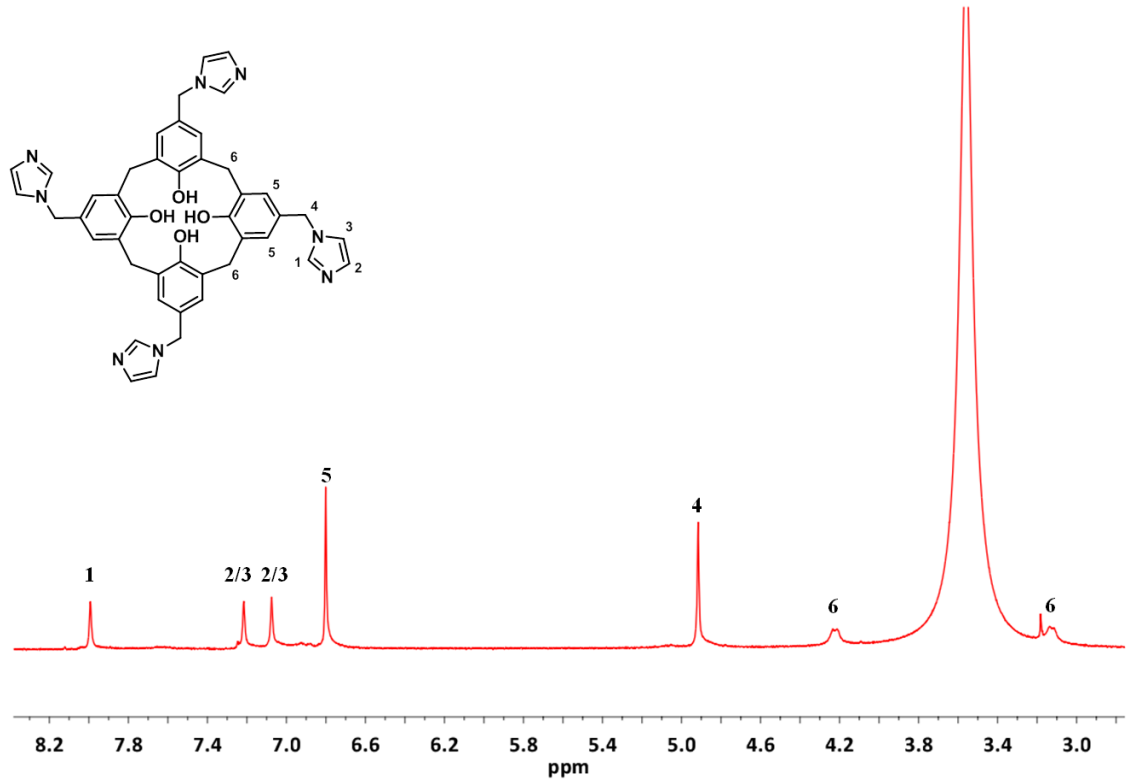

Figure 2.2 ^{1}H NMR (DMSO-d_6) spectrum of compound **2.4** at 298 K.

The ^{1}H NMR spectrum of compound **2.4** in DMSO-d_6 does not show any evidence for the formation of the mono-zwitterion. This would likely exhibit a low field resonance at around 9 ppm attributable to the imidazolium C2 proton. However, upon heating the DMSO-d_6 solution to 382 K, the ^{1}H NMR spectrum displays a lowering of symmetry and the appearance of a resonance at δ = 9.02 ppm, suggesting that the mono-zwitterion is formed at elevated temperatures (Figure 2.3). Upon cooling the NMR sample back to room temperature, the ^{1}H NMR spectrum remains unchanged rather than converting back to the original spectrum (Figure 2.4). This suggests that the mono-zwitterion is formed at elevated temperatures and is retained in solution upon cooling. We investigated this further by examining the conditions under which the crystals were prepared. Compound **2.4** was heated at 60 °C in chloroform for 18 hours in a sealed vessel. The solvent was removed *in vacuo* and the product examined by ^{1}H NMR spectroscopy in DMSO-d_6 at room temperature. Again, a high field resonance was observed at δ = 9.15 ppm that was attributed to the imidazolium C2 proton. We propose that the mono-zwitterion is formed on heating the molecule in chloroform, and crystallises when the solution is cooled.

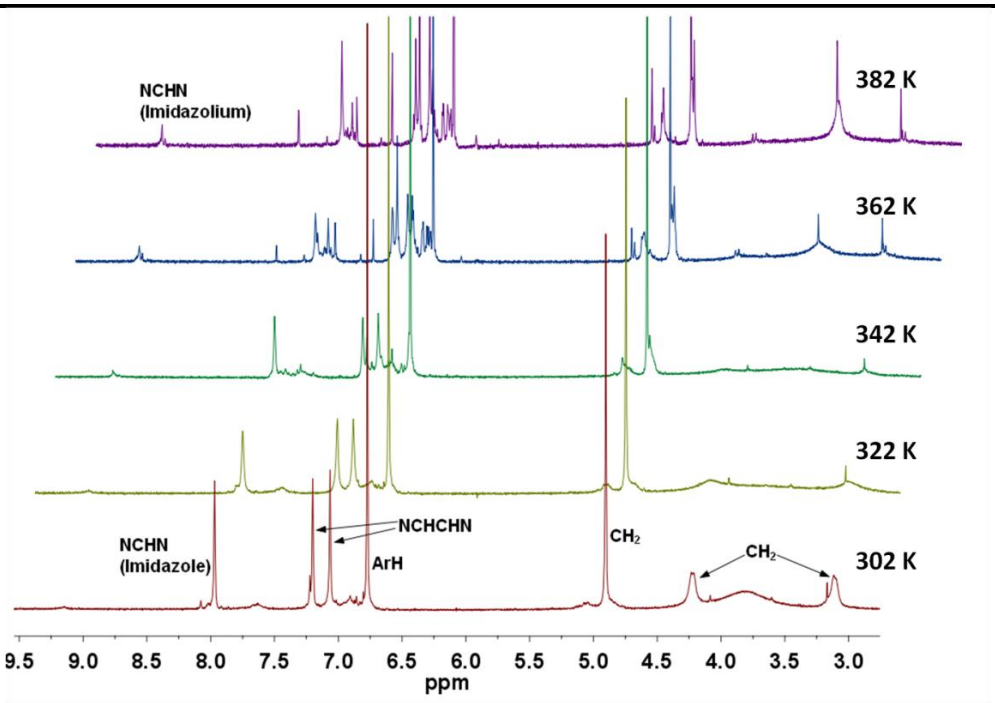

Figure 2.3 VT ^{1}H NMR spectra of compound **2.4** in DMSO-d_6.

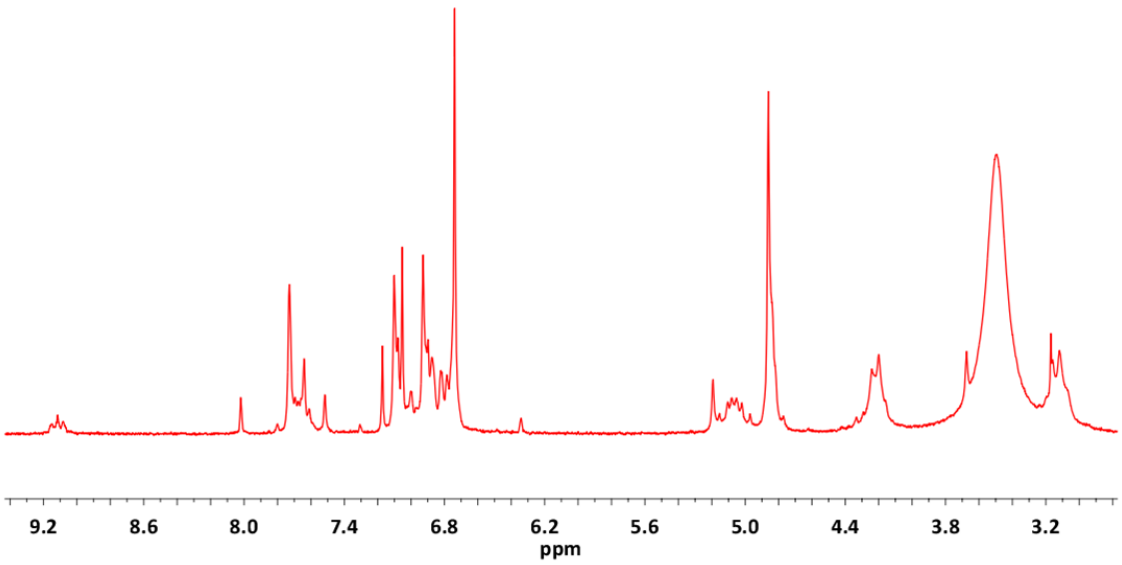

Figure 2.4 ^{1}H NMR spectrum of compound **2.4** after heating in DMSO-d_6 to 382 K, then allowing the NMR sample to cool to 302 K.

A further difference between the ^{1}H NMR spectra of compound **2.4** in DMSO-d_6 at room temperature and at elevated temperatures is the appearance of the methylene bridging protons (carbon **6**). As discussed previously, the methylene protons appear as a broad set of doublets at room temperature at δ = 3.13 ppm and δ = 4.21 ppm, attributed to the interconversion of the cone that occurs slowly on the NMR timescale at room

temperature. As the temperature is raised this interconversion becomes more rapid and therefore the resonances coalesce and appear as a broad singlet at 3.7 ppm (Figure 2.3, ^{1}H NMR spectrum recorded at 382 K). Upon closer examination of the spectra at elevated temperature, two sharp doublets at δ = 3.21 ppm and δ = 4.38 ppm can also be seen on either side of the singlet resonance. We propose that this is owing to restricted rotation on one side of the calixarene due to the formation of the mono-zwitterion and the resulting hydrogen bonding interactions. The formation of the zwitterion would also account for the lowering of symmetry that is observed in the ^{1}H NMR spectra at elevated temperatures.

Compound **2.4** was initially synthesised as a precursor to prepare the novel tetrakis(methylimidazolium) calix[4]arenes. The proposed synthetic route was to functionalise the uncoordinated nitrogen on the neutral imidazole of compound **2.4** to form an imidazolium species (Scheme 2.2). The quaternarisation of a neutral N-substituted imidazole is a method that is often used to prepare imidazolium salts.[22] The reaction of compound **2.4** with haloalkanes, haloalcohols and haloacetates was attempted as dry melts and in solution (THF / DCM). A complicated mixture of products was consistently formed which appeared to include imidazolium species, supported by the appearance of downfield resonances in the ^{1}H NMR spectra at between 8.5 ppm and 9.5 ppm. However, there were always multiple products and purification of the product mixtures proved unsuccessful.

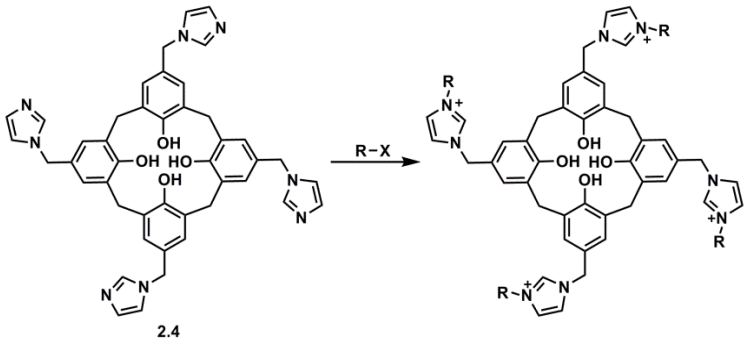

Scheme 2.2 Attempted synthesis of novel tetrakis methylimidazolium calix[4]arene molecules (R = alkyl, X = halide).

For the reaction to produce the desired tetrakis(methylimidazolium) calix[4]arene, all four uncoordinated nitrogen atoms on compound **2.4** would need to be alkylated. The product mixtures isolated from this set of reactions is likely due to the reaction forming the 4-, 3-, 2- and 1- substituted products in varying ratios (Figure 2.5). The desired 4-

tethered product (**A**) could not be isolated from the reaction mixture, which was most likely due to the similar properties that these molecules are expected to possess. There was also the possibility of the phenolic oxygens on the lower rim of compound **2.4** reacting with the alkylating agent to form the corresponding ester or ether. This would further complicate the product mixtures isolated from the reaction.

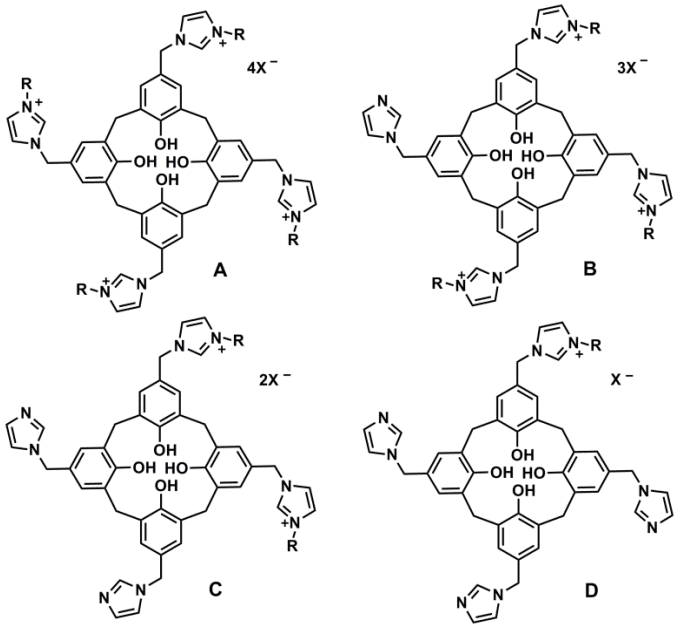

Figure 2.5 Suggested products from the reaction of compound **2.4** with haloalkanes, haloalcohols and haloacetate (R= alkyl group and X = halide).

The approach to the synthesis of the target imidazolium salts was therefore altered. 1-Bromomethyl-4-hydroxy calix[4]arene (**2.3**) was reacted with the already N-substituted imidazole to produce compound **2.5** directly (Scheme 2.1), rather than proceeding *via* compound **2.4**. The simplest imidazole, 1-methyl imidazole, was used as a starting point to test the synthetic method. 1-Methyl imidazole was added to a DCM solution of compound **2.3** and a white precipitate formed immediately. The mixture was stirred at room temperature, under a nitrogen atmosphere, for 12 hours. The white solid was isolated by filtration, and purified by washing further with DCM and was dried *in vacuo*. Compound **2.5 Br** was characterised by ^{1}H NMR and ^{13}C{^{1}H} NMR spectroscopy combined with mass spectrometry. The bromide anions were exchanged for hexafluorophosphate using ammonium hexafluorophosphate in water to afford the hexafluorophosphate salt of **2.5** as a white solid. Compound **2.5 PF_6** was characterised by ^{1}H NMR and ^{13}C{^{1}H} NMR spectroscopy, mass spectrometry and elemental analysis.

The ^{1}H NMR spectrum of compound **2.5 PF_6** in MeCN-d_3 is displayed in Figure 2.6, with the relevant peaks assigned in Table 2.2. At room temperature, the ^{1}H NMR spectrum appears as expected, with the resonance for the imidazolium C2 proton appearing at 8.47 ppm, which is a downfield shift compared to the neutral imidazole compound **2.5** at δ = 7.99 ppm. However, the signals for the methylene bridging protons (carbon **6**) were not observed. This was the case for both the bromide and the hexafluorophosphate salts in DMSO-d_6, MeCN-d_3 and MeOH-d_4. On cooling the MeCN-d_3 sample to 248 K, a pair of doublets appeared in the ^{1}H NMR spectrum at δ = 4.17 ppm and δ = 3.50 ppm, that were assigned as the methylene protons from carbon **6** (Figure 2.6). This is in contrast to the neutral imidazole compound **2.4**, where the signals from the methylene protons are observed as a broad set of doublets at room temperature. This suggests that the interconversion of the cone is faster in compound **2.5** than in compound **2.4** in the solvents studied, or alternatively another exchange process is occurring within the molecule. For example, the methylene protons could be exchanging with the acidic imidazolium protons in compound **2.5**.

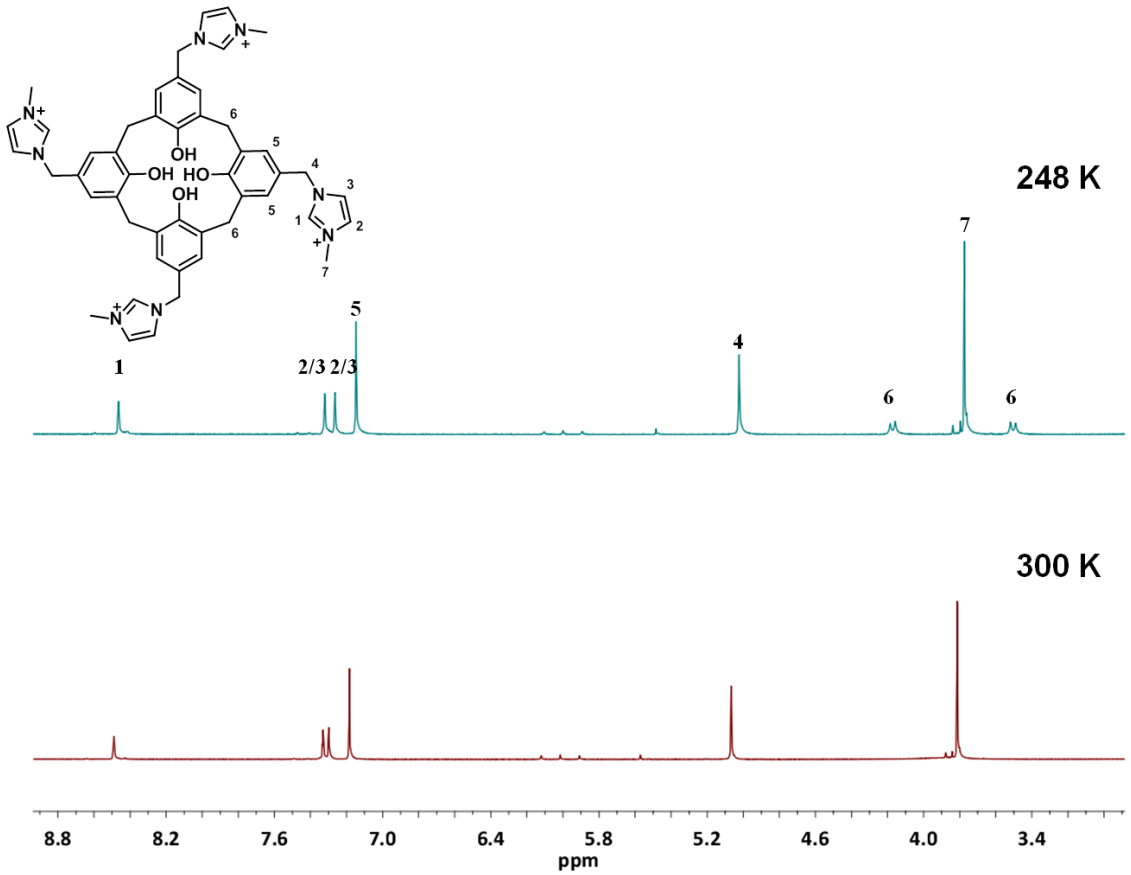

Figure 2.6 ^{1}H NMR spectra (MeCN-d_3) of compound **2.5 PF_6** at 300 K and 248 K.

Chemical shift (δ ppm) ^{1}H	**Assignment**
8.47 (s, 4H)	1
7.32 (s, 4H)	2 / 3
7.26 (s, 4H)	2 / 3
7.15 (s, 8H)	5
5.03 (s, 8H)	4
4.17 (d, 2H, $^{2}J_{HH}$ = 13.8 Hz)	6
3.78 (s, 12H)	7
3.50 (d, 2H, $^{2}J_{HH}$ = 13.8 Hz)	6

Table 2.2 ^{1}H NMR assignment for compound **2.5 PF_6** at 248 K.

Crystals were obtained by slow diffusion of diethyl ether into a methanol solution of compound **2.5 Br** (Figure 2.7). To the best of our knowledge, this is the first structure of a cationic calix[4]arene (bearing hydroxyl groups) in the absence of a metal. Once more, the structure shows the expected cone conformation, with the imidazolium groups projecting upwards with reference to the plane defined by the bridging methylene groups. Unlike compound **2.4**, the molecule is symmetrical, with the imidazolium groups pointing in the same direction on either side of the molecule (Figure 2.7a). The hydroxyl groups on the bottom of the ring interact with a bromide anion (**Br3**), illustrating that it is not just the imidazolium groups that interact with the anions (Figure 2.7b). The remaining bromide anions interact with the relatively acidic imidazolium protons within the structure. The calixarenes are arranged "back to back" with each aryl ring involved in π-π bonding with the neighbouring calixarene molecules (Figure 2.7c and d).

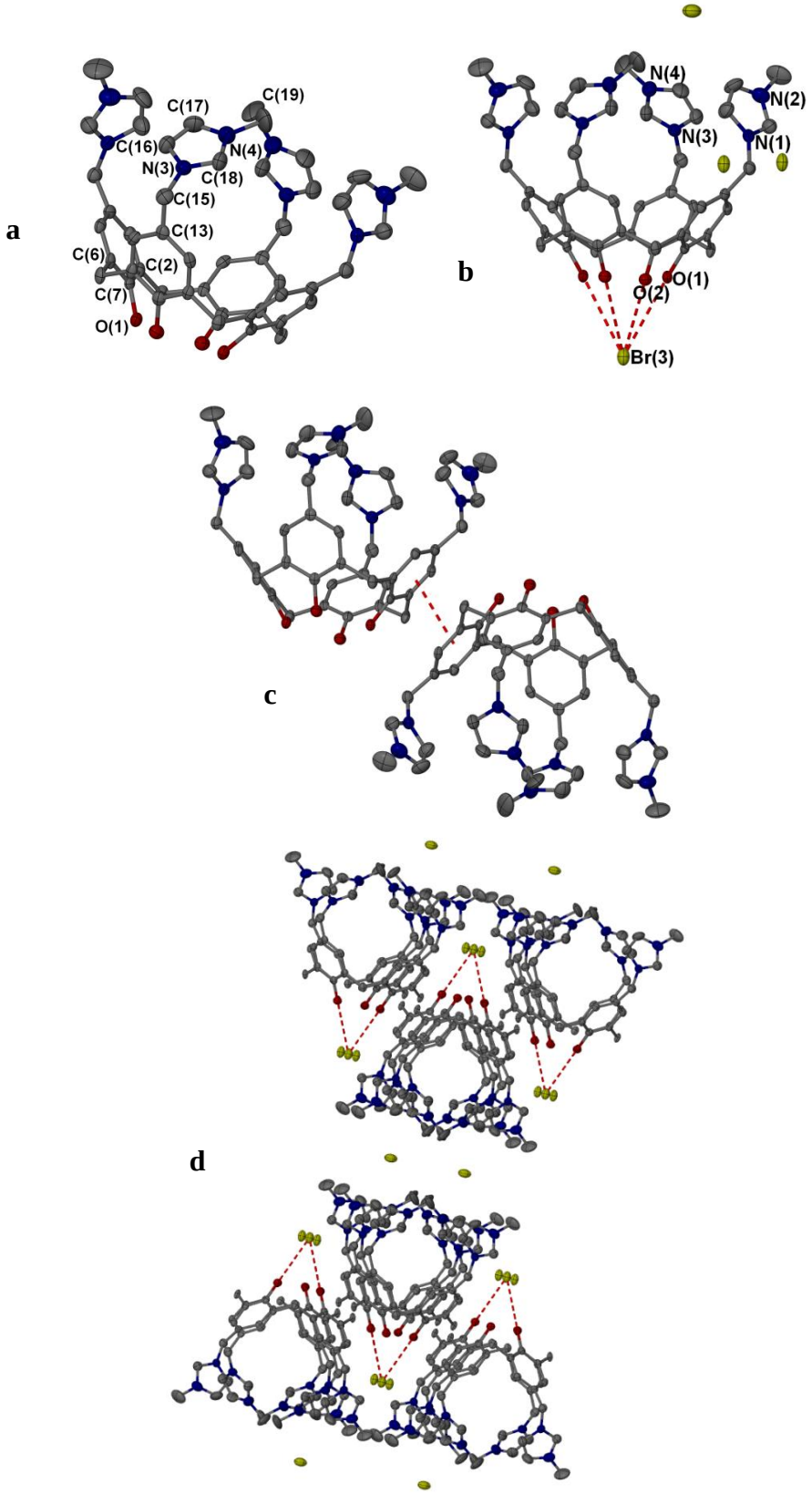

Figure 2.7 Molecular structure of **2.5 Br** illustrating a) the molecular structure of **2.5 Br**, b) OH···anion interactions, c) π-π interactions between neighbouring aromatic rings, d) packing of the molecule displaying the 2D layers. The hydrogen atoms and methanol molecules have been omitted for clarity. Ellipsoids are displayed at 50% probability.

N(4)-C(17)	1.362(10)	N(3)-C(18)-N(4)	109.1(6)
N(4)-C(18)	1.344(10)	N(3)-C(15)-C(13)	110.5(5)
N(3)-C(18)	1.327(9)	O(1)-C(7)-C(2)	120.9(5)
O(1)-C(7)	1.389(6)		

Table 2.3 Selected bond distances (Å) and angles (deg) for compound **2.5**.

The packing diagram for compound **2.5 Br** shows that the calixarene units are arranged in 2D layers, with the OH groups pointing inwards and the imidazolium groups pointing towards each other (Figure 2.8). The bromide anions that are interacting with the backbone C4 protons sit between the layers, with large pores between these bridging bromide ions. The distance between closest bridging bromide ions is 10.8 Å, and between OH-coordinating bromide ions is 9.8 Å. Disordered methanol molecules occupy the channels. The structure shows that several hydrogen bonding interactions with guest anions exist in this calixarene due to the range of acidic protons on both the upper and the lower rims. As the channels in the structure of compound **2.5 Br** are relatively large, and are lined by imidazolium moieties, the material offers distinct possibilities for use in both catalysis and gas storage.[23, 24]

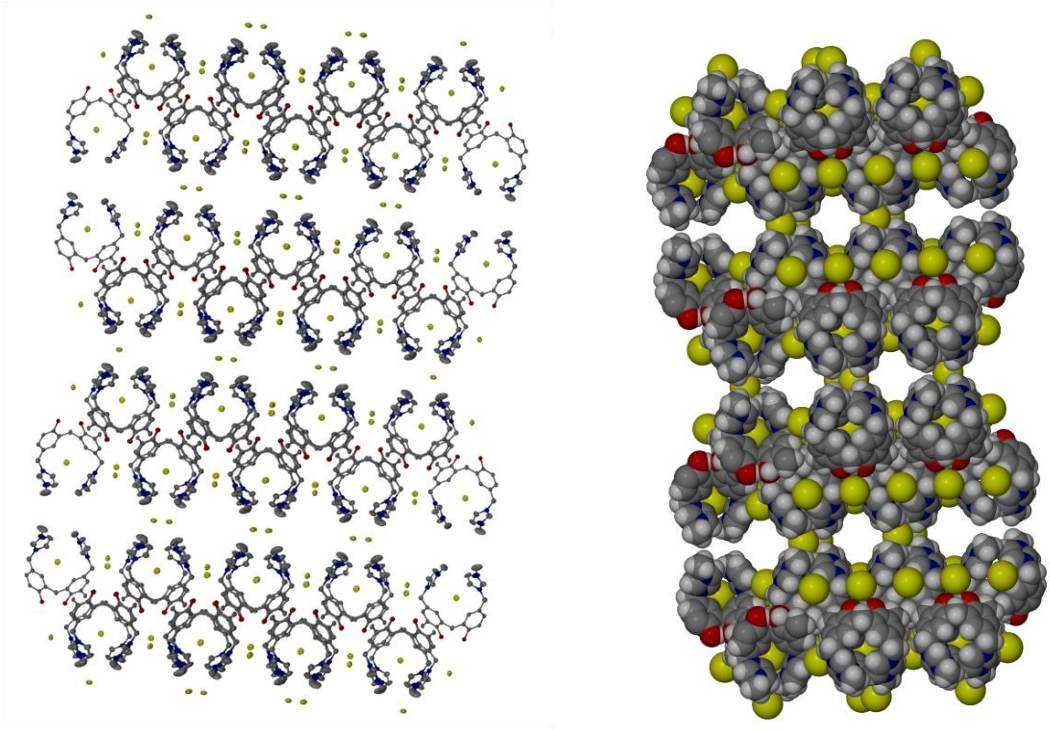

Figure 2.8 X-ray crystal packing diagrams of compound **2.5 Br** displaying 2D channels in the structure

2.2 Anion binding studies of tetrakis(methylimidazolium) calix[4]arene (2.5)

Anions play important roles in biological systems, medicine and the environment. Consequently, the design of anion binding and anion sensing systems is extremely topical.[25-29] Anion sensors usually rely on the presence of non-covalent interactions between the host and guest to allow for host-guest recognition. The range of interactions includes electrostatic interactions, hydrogen bonding interactions, dispersion interactions, coordination to a metal ion, or a combination of these non covalent interactions. Imidazolium units offer the potential of being effective anion receptors due to the strong hydrogen bonding interactions they are able to form with anions of the type $[(C\text{-}H)^{+}\cdots X^{-}]$.

A key challenge in anion recognition is the design of anion sensors that are selective. One way to achieve selectivity is the pre-organisation of the host molecule to 'fit' a guest based upon its size and charge distribution. Tripodal imidazolium, pyridinium and cryptand based systems, in addition to calixarenes, are examples of such pre-organised cavities.[30-32] With pre-organisation, even weak anion binding sites can act as effective anion receptors.[31, 33] In addition, many systems are highly dependent upon the location of the anion binding sites and can give an interesting response to anion binding. For example, an induced conformational change may bring about a photophysical, colourimetric or an electrochemical response.[34-39]

Calixarenes are versatile frameworks that can act as hosts for cations, anions and neutral molecules, depending upon their functionalisation. Calix[4]arenes can exist in four possible conformations; cone, partial cone, 1,2-alternate and 1,3-alternate. Each of these offers different advantages in terms of anion binding, with cone type structures acting as rigid scaffolds, whereas 1,2-alternate and 1,3-alternate calix[4]arenes have more flexible configurations. Studies on imidazolium calixarenes have shown that both cavity size and pre-organisation are important, with bis(imidazolium) calix[4]arenes showing selectivity for carboxylates, while tetrakis(imidazolium) calix[4]arenes are selective for dicarboxylates.[40, 41]Allosteric enhancement has also been shown to play a part in binding affinity.[42]

The anion binding properties of tetrakis(methylimidazolium) calix[4]arene (**2.5**) were probed by ^{1}H NMR spectroscopic titration with various tetrabutylammonium salts. As a precipitate formed during the titration experiments in MeCN-d_3, the spectroscopic data was obtained in DMSO-d_6. Compound **2.5 PF_6** was dissolved in 0.8 ml of DMSO-

d_6. The anions as their tetrabutylammonium salts were made up to 1 mL in DMSO-d_6, and were approximately 10 times the concentration of the host (Table 2.4). 20 µL aliquots of the guest were added to the NMR tube and the spectra recorded after each addition. Upon addition of chloride, bromide and nitrate anions, there is a downfield shift of the C2 proton of the imidazolium, clearly indicating $(C\text{-}H)^{+}\cdots X^{-}$ interactions. The downfield shift is most significant with chloride and least significant with nitrate, which reflects decreasing basicity, though size selectivity cannot be ruled out (Figure 2.9).

Guest as their $Bu_4N^+X^-$ salts	**Mass of 2.5 PF_6 (g)**	**Moles of 2.5 PF_6**	**Mass of Guest (g)**	**Moles of Guest**
Br^-	0.0201	1.45×10^{-5}	0.0637	1.98×10^{-4}
Cl^-	0.025	1.81×10^{-5}	0.0630	2.27×10^{-4}
CH_3COO^-	0.025	1.81×10^{-5}	0.0635	2.11×10^{-4}
$H_2PO_4^-$	0.023	1.66×10^{-5}	0.0629	1.85×10^{-4}
NO_3^-	0.025	1.81×10^{-5}	0.0630	2.07×10^{-4}

Table 2.4 Moles of host (**2.5 PF_6**) and guest (Bu_4NX, X = Cl, Br, CH_3COO, PO_4, NO_3) used in the ^1H NMR titration experiments.

The equivalents of guest that had been added were calculated by taking the ratio of host: guest concentration after each 20 µL addition, hence taking into account the change in volume. The equivalents of guest were plotted against the chemical shift of the C2 proton and the results are displayed in Figure 2.9. Figure 2.9 illustrates that as the tetrabutylammonium chloride and bromide salts were titrated into the DMSO-d_6 solution of **2.5 PF_6**, there is a significant change in the chemical shift up to the point where four equivalents of the anion has been added. The largest change in the chemical shift of the C2 proton occurs between 0-1 equivalents of guest. Above four equivalents, the graph begins to level off, with the chemical shift only changing slightly between four and six equivalents. During the addition of the tetrabutylammonium nitrate salt, there is less of a change in the chemical shift, with only a slight increase observed up to the point where 2 equivalents of the nitrate anion has been added, then the graph begins to level off.

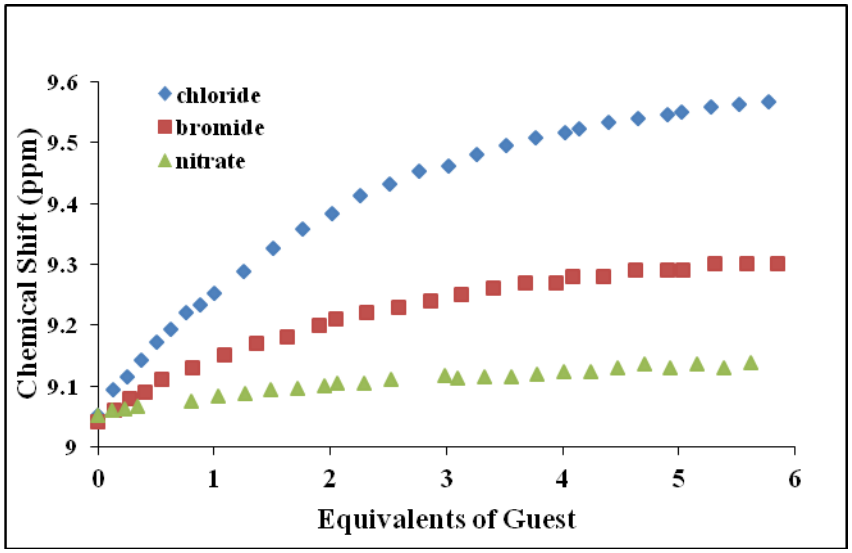

Figure 2.9 ^{1}H NMR spectroscopic titration data for binding of Cl^-, Br^- and NO_3^- by compound **2.5 PF_6** in DMSO-d_6.

The stoichiometry of the chloride and bromide binding was examined by the Job's method. The plot maximum falls at 0.5, suggesting 1:1 binding for both chloride and bromide (Figure 2.10). The binding of nitrate was also probed by the Job's method but showed no correlation, suggesting that binding was less selective for nitrate than for chloride and bromide anions. The data obtained from these experiments was used to calculate the anion binding constants. Using HypNMR, fits were obtained manually for anion binding constants based upon a 1:1 stoichiometry (Table 2.5).

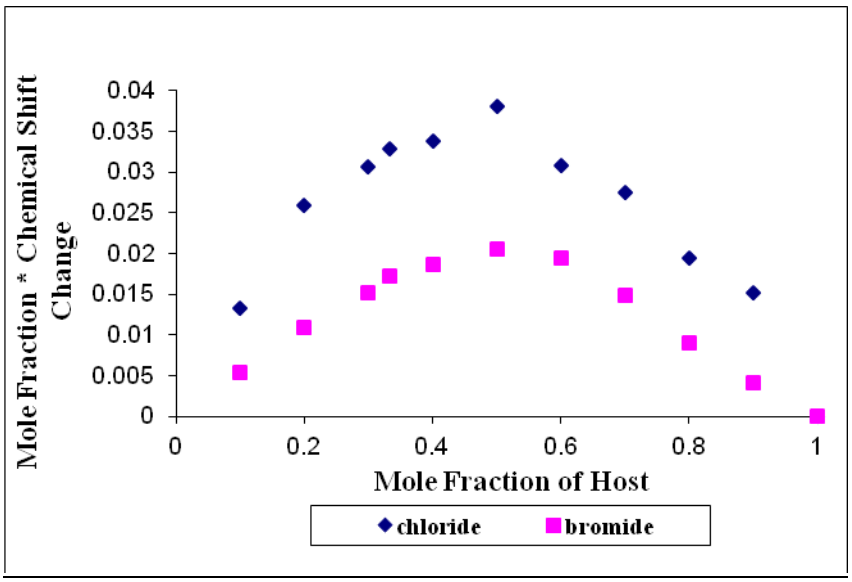

Figure 2.10 Job plot in DMSO-d_6 for the interaction of compound **2.5 PF_6** with Bu_4NBr and Bu_4NCl.

Anion	$\log\beta_{11}$	$\Delta\delta$ at 1 equivalent
Cl^-	1.45	0.201
Br^-	1.40	0.110
NO_3^-	1.06	0.026

Table 2.5 Anion binding constants of **2.5 PF_6** with tetrabutylammonium salts.

The calculated binding constants show, as expected, that chloride has the highest stability constant for 1:1 binding, and nitrate the lowest. Automatic refinement was not possible, likely due to the broad range of CH hydrogen bonding interactions involving not just the acidic NC*H*N units but also the backbone imidazolium protons and the lower rim hydroxyl groups. Evidence for this is in the ^{1}H NMR spectra, where a chemical shift change occurs for the backbone imidazolium protons as well as for the C2 proton. In compound **2.5 PF_6**, the backbone resonances appear as a singlet at δ = 7.65 ppm and, upon addition of anions, split into two singlets, with one moving further downfield (Figure 2.11). The downfield shift is most pronounced for chloride and least for nitrate. Further evidence of a broad range of anion interactions is seen in the crystal structure discussed previously (Figure 2.7). The bromide anions form several different hydrogen bonding interactions with the acidic protons on both the upper and lower rims of the calix[4]arene.

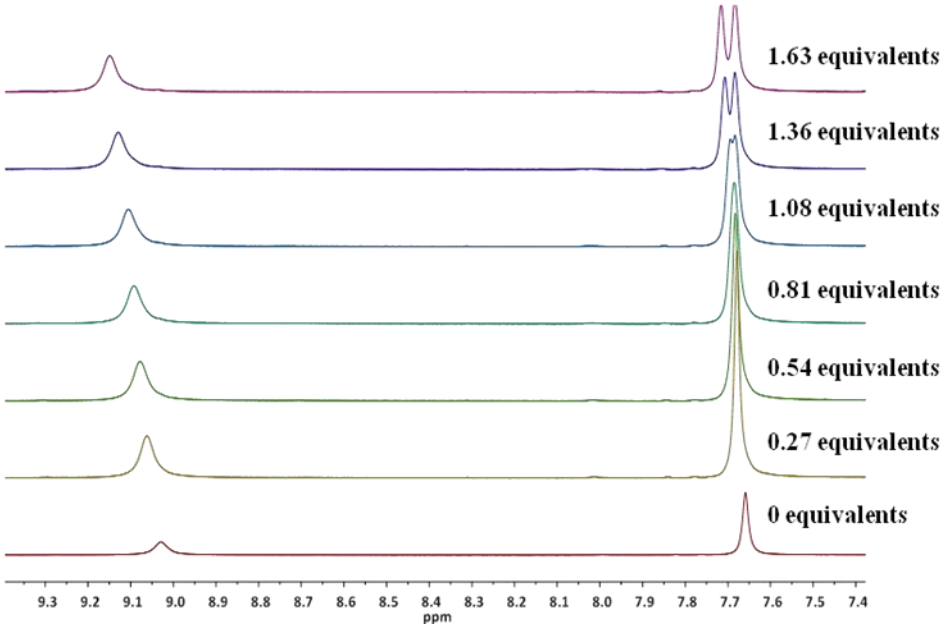

Figure 2.11 ^{1}H NMR (DMSO-d_6) spectroscopic titration data for compound **2.5 PF_6** on addition of Bu_4NBr.

The anion binding of compound **2.5 PF_6** was also probed with tetrabutylammonium acetate and tetrabutylammonium dihydrogen phosphate, both of which show unusual behaviour. A downfield shift of the C2 proton resonance is observed up to the addition of one equivalent of guest. Following this, there is a slight upfield shift of the C2 proton resonance to about 1.5 equivalents of guest, before the resonance continues to move downfield upon further addition of guest (Figure 2.12). As acetate and phosphate are basic anions, they also have the potential to deprotonate acidic protons and, as discussed previously, compound **2.5** has a broad range of acidic protons. It appears that the first equivalent of these guests interacts with the imidazolium C2 protons at the upper rim, resulting in the downfield shift of the proton resonance for these protons. Following this the anions interact with a different part of the calixarene, with a change in molecular shape being the likely cause of the slight upfield chemical shift of the C2 protons. It is probable that the second equivalent of these basic anions are interacting with the acidic lower rim, causing (partial) deprotonation of one of the hydroxyl groups, which will result in a slight change in the shape of the calixarene. The anions then continue to interact with the C2 protons of the upper rim. This behaviour would lead to the unusual appearance of the titration curves.

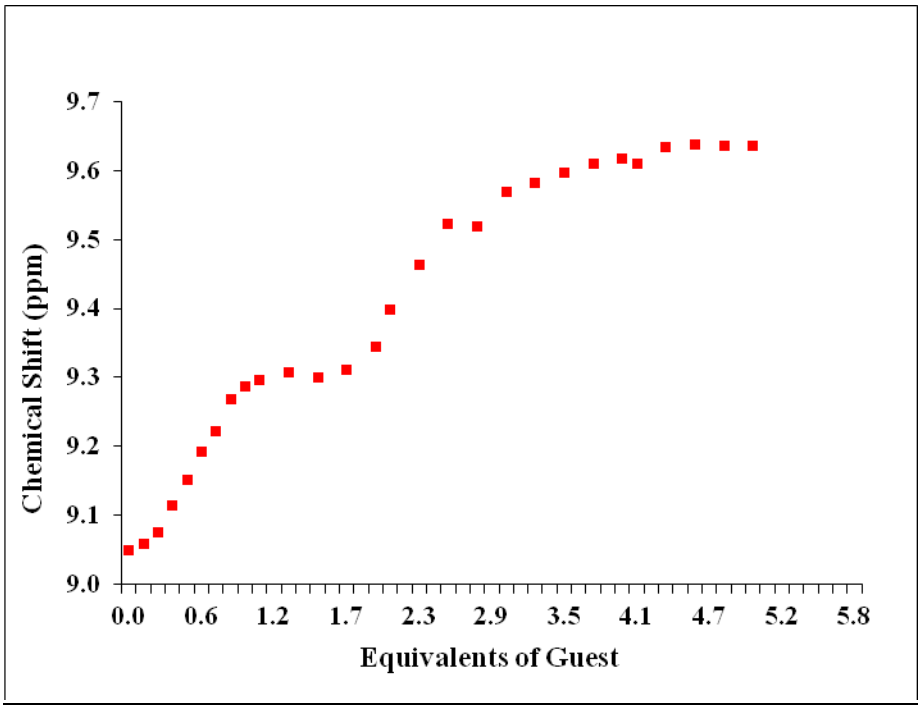

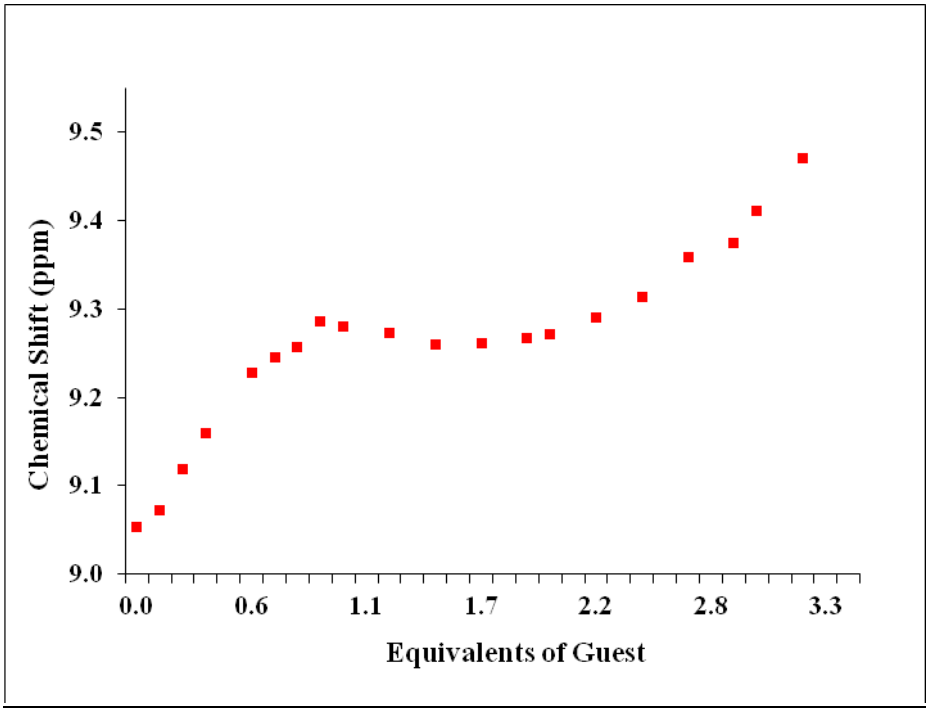

Figure 2.12 ^{1}H NMR spectroscopic titration data for binding of acetate (top) and dihydrogen phosphate (bottom) by compound **2.5 PF_6** in DMSO-d_6.

2.3 Conclusion

In conclusion, a synthetic procedure has been developed for the synthesis of neutral tetrakis(methylimidazole) calix[4]arene (**2.4**) and the novel cationic tetrakis(methylimidazolium) calix[4]arene (**2.5**). The properties of these compounds in solution and the solid state have been thoroughly investigated.

It was found that the neutral compound **2.4** can exist as the mono-zwitterion, both in solution and the solid state. The zwitterion has the potential to bind cations on the lower rim through electrostatic interactions e.g. alkali metals, or in the cavity engaging in cation-π interactions. The compound could also bind anions on the non-phenolic upper rim through hydrogen bonding to the acidic protons of the imidazole. The solubility of compound **2.4** is the limiting factor in studying these applications. The project could be extended by looking into the synthesis of soluble imidazole calixarenes, with the potential to act as hosts for salts. The solubility would most likely be improved by adding a functional group to the phenolic oxygen of the lower rim.

The novel cationic tetrakis(methylimidazolium) calix[4]arene **2.5** has also been prepared and fully characterised. Compound **2.5** shows increased solubility compared to the neutral tetrakis(methylimidazole) calixarene **2.4**, allowing the binding properties of this molecule to be studied. The studies on compound **2.5** have shown that it contains a plethora of acidic CH groups which take part in hydrogen bonding interactions with anions, observable both in solution and in the solid-state. The location of the interaction site with basic anions appears to be selective depending upon the concentration of anions relative to calixarene. This offers the possibility of sensing, or communication between the different binding regions, which is dependent upon anion concentration.

2.4 Future work

The tetrakis(methylimidazolium) calix[4]arene has been prepared using the simplest N-substituted imidazole (1-methyl imidazole) as a precursor. This has allowed the development of a synthetic procedure, and the opportunity to study the properties of this molecule in comparison to the neutral tetrakis(methylimidazole) calix[4]arene. As the molecule has been shown to display interesting interactions with anions, the project has the potential to be developed further. The N-substituent on the imidazole could easily be changed from methyl to another more complex substituent such as propanol, acetate, aromatic, or even a biologically relevant group e.g. peptide. It would be expected that

the desired product could be synthesised following the same synthetic procedure. This may introduce further anion binding possibilities or even fluorescent properties to the molecule, depending on the substituent that was selected.

The introduction of the imidazolium functionality to the tetrakis calix[4]arene molecule also offers the potential to prepare metal-NHC complexes of this ligand. This has not been investigated to date as it is anticipated that the hydroxyl groups on the lower rim would make the formation of the desired carbene complex problematic. However, if the hydroxyl groups were protected, the formation of the metal-NHC complex should be possible and would be an interesting extension to this work.

2.5 References

1. C. D. Gutsche, *Accounts Chem. Res.*, 1983, **16**, 161-170.
2. N. Basilio, V. Francisco and L. Garcia-Rio, *J. Org. Chem.*, 2012, **77**, 10764-10772.
3. D. Diamond and K. Nolan, *Anal. Chem.*, 2001, **73**, 22A-29A.
4. J. Rebek, Jr., *Chem. Commun.*, 2000, 637-643.
5. A. Ikeda and S. Shinkai, *Chem. Rev.*, 1997, **97**, 1713-1734.
6. B. Mokhtari, K. Pourabdollah and N. Dalali, *J. Inclusion Phenom. Macrocyclic Chem.*, 2011, **69**, 1-55.
7. F. Perret and A. W. Coleman, *Chem. Commun.*, 2011, **47**, 7303-7319.
8. D. T. Schuehle, J. A. Peters and J. Schatz, *Coord. Chem. Rev.*, 2011, **255**, 2727-2745.
9. C. D. Gutsche, M. Iqbal and D. Stewart, *J. Org. Chem.*, 1986, **51**, 742-745.
10. A. Zinke and E. Ziegler, *Berichte Der Deutschen Chemischen Gesellschaft*, 1941, **74**, 1729-1736.
11. C. D. Gutsche, J. A. Levine and P. K. Sujeeth, *J. Org. Chem.*, 1985, **50**, 5802-5806.
12. C. D. Gutsche and L. G. Lin, *Tetrahedron*, 1986, **42**, 1633-1640.
13. L.-M. Yang, Y.-S. Zheng and Z.-T. Huang, *Synth. Commun.*, 1999, **29**, 4451-4460.
14. C. E. Willans, K. M. Anderson, P. C. Junk, L. J. Barbour and J. W. Steed, *Chem. Commun.*, 2007, 3634-3636.
15. C. D. Gutsche and K. C. Nam, *J. Am. Chem. Soc.*, 1988, **110**, 6153-6162.
16. C. D. Gutsche, B. Dhawan, K. H. No and R. Muthukrishnan, *J. Am. Chem. Soc.*, 1981, **103**, 3782-3792.
17. M. Coruzzi, G. D. Andreetti, V. Bocchi, A. Pochini and R. Ungaro, *J. Chem. Soc.-Perkin Trans. 2*, 1982, 1133-1138.
18. G. D. Andreetti, R. Ungaro and A. Pochini, *J. Chem. Soc.-Chem. Commun.*, 1979, 1005-1007.
19. R. Ungaro, A. Pochini, G. D. Andreetti and P. Domiano, *J. Chem. Soc.-Perkin Trans. 2*, 1985, 197-201.
20. R. Ungaro, A. Pochini, G. D. Andreetti and V. Sangermano, *J. Chem. Soc.-Perkin Trans. 2*, 1984, 1979-1985.
21. S. Shinkai, K. Araki, P. D. J. Grootenhuis and D. N. Reinhoudt, *J. Chem. Soc.-Perkin Trans. 2*, 1991, 1883-1886.
22. S. Guenal, N. Kaloglu, I. Oezdemir, S. Demir and I. Oezdemir, *Inorg. Chem. Commun.*, 2012, **21**, 142-146.
23. H. C. Cho, H. S. Lee, J. Chun, S. M. Lee, H. J. Kim and S. U. Son, *Chem. Commun.*, 2011, **47**, 917-919.
24. J. Zhu, J. Zhou, H. Zhang and R. Chu, *J. Polym. Res.*, 2011, **18**, 2011-2015.
25. S. Kubik, *Chem. Soc. Rev.*, 2009, **38**, 585-605.
26. P. A. Gale, *Chem. Soc. Rev.*, 2010, **39**, 3746-3771.
27. C. Caltagirone and P. A. Gale, *Chem. Soc. Rev.*, 2009, **38**, 520-563.
28. J. W. Steed, *Chem. Soc. Rev.*, 2009, **38**, 506-519.
29. J. W. A. Steed, J.L., *Supramolecular chemistry*, 2009.
30. V. Amendola, M. Boiocchi, B. Colasson, L. Fabbrizzi, D. M.-J. Rodriguez and F. Ugozzoli, *Angew. Chem., Int. Ed.*, 2006, **45**, 6920-6924.
31. K. J. Wallace, W. J. Belcher, D. R. Turner, K. F. Syed and J. W. Steed, *J. Am. Chem. Soc.*, 2003, **125**, 9699-9715.
32. C. A. Ilioudis, D. A. Tocher and J. W. Steed, *J. Am. Chem. Soc.*, 2004, **126**, 12395-12402.
33. Y. Li and A. H. Flood, *Angew. Chem., Int. Ed.*, 2008, **47**, 2649-2652.
34. Y. Bai, B.-G. Zhang, J. Xu, C.-Y. Duan, D.-B. Dang, D.-J. Liu and Q.-J. Meng, *New J. Chem.*, 2005, **29**, 777-779.
35. D. R. Turner, M. J. Paterson and J. W. Steed, *Chem. Commun.*, 2008, **12**, 1395-1397.

36. M. H. Filby, S. J. Dickson, N. Zaccheroni, L. Prodi, S. Bonacchi, M. Montalti, M. J. Paterson, T. D. Humphries, C. Chiorboli and J. W. Steed, *J. Am. Chem. Soc.*, 2008, **130**, 4105-4113.
37. J. W. Steed and K. J. Wallace, *Adv. Supramol. Chem.*, 2003, **9**, 219-260.
38. S. J. Dickson, E. V. B. Wallace, A. N. Swinburne, M. J. Paterson, G. O. Lloyd, A. Beeby, W. J. Belcher and J. W. Steed, *New J. Chem.*, 2008, **32**, 786-789.
39. T. Gunnlaugsson, M. Glynn, G. M. Tocci, P. E. Kruger and F. M. Pfeffer, *Coord. Chem. Rev.*, 2006, **250**, 3094-3117.
40. S. K. Kim, B.-G. Kang, H. S. Koh, Y. J. Yoon, S. J. Jung, B. Jeong, K.-D. Lee and J. Yoon, *Org. Lett.*, 2004, **6**, 4655-4658.
41. I. Dinares, d. M. C. Garcia, N. Mesquida and E. Alcalde, *J. Org. Chem.*, 2009, **74**, 482-485.
42. C. E. Willans, K. M. Anderson, L. C. Potts and J. W. Steed, *Org. Biomol. Chem.*, 2009, **7**, 2756-2760.

3 Propanol tethered methylimidazolium mesityl calix[4]arene: Ligand synthesis and metal complexation

As discussed in chapter two, calixarene is a name given to a group of macrocyclic molecules that consist of four or more linked aromatic units. Calix[4]arenes can adopt four possible conformations; cone, partial cone, 1,2-alternate and 1,3-alternate, with the conformation of the calixarene being dependent on the rotation about the CH_2-aromatic bond. The previous chapter focused on calix[4]arenes that adopt the cone-type conformation, which is favoured due to the hydrogen bonding network formed between the hydroxyl groups on the lower rim. In this chapter we are concerned with the synthesis of the 1,3-alternate calix[4]arene, where two of the functional groups project upwards, and two project downwards, in reference to the plane defined by the bridging methylene groups. In this scenario, the conformation of the molecule is no longer restricted by the hydrogen bonding of the hydroxyl groups, since mesityl moieties replace the phenol groups. The steric bulk of the mesityl groups forces the molecule to adopt the 1,3-alternate conformation.

Propanol tethered methylimidazolium mesityl calix[4]arene (**3.4**) has been prepared and examined through ^{1}H NMR spectroscopy and X-ray crystallography. Compound **3.4** was used as an NHC ligand precursor to prepare metal-NHC complexes through a range of experimental techniques. A silver-NHC complex of the ligand was prepared following the well-documented Ag_2O route.[1-3] A copper(I)-NHC complex was prepared using Cu_2O, following a similar procedure to the Ag_2O reaction.[4] The use of the silver-NHC and copper-NHC complexes as transmetallation agents to form palladium-NHC complexes was explored.[5-7] The palladium-NHC complex is expected to find application in catalysis e.g. cross-coupling reactions.[8]

3.1 Synthesis of propanol tethered methylimidazolium mesityl calix[4]arene (compound 3.4)

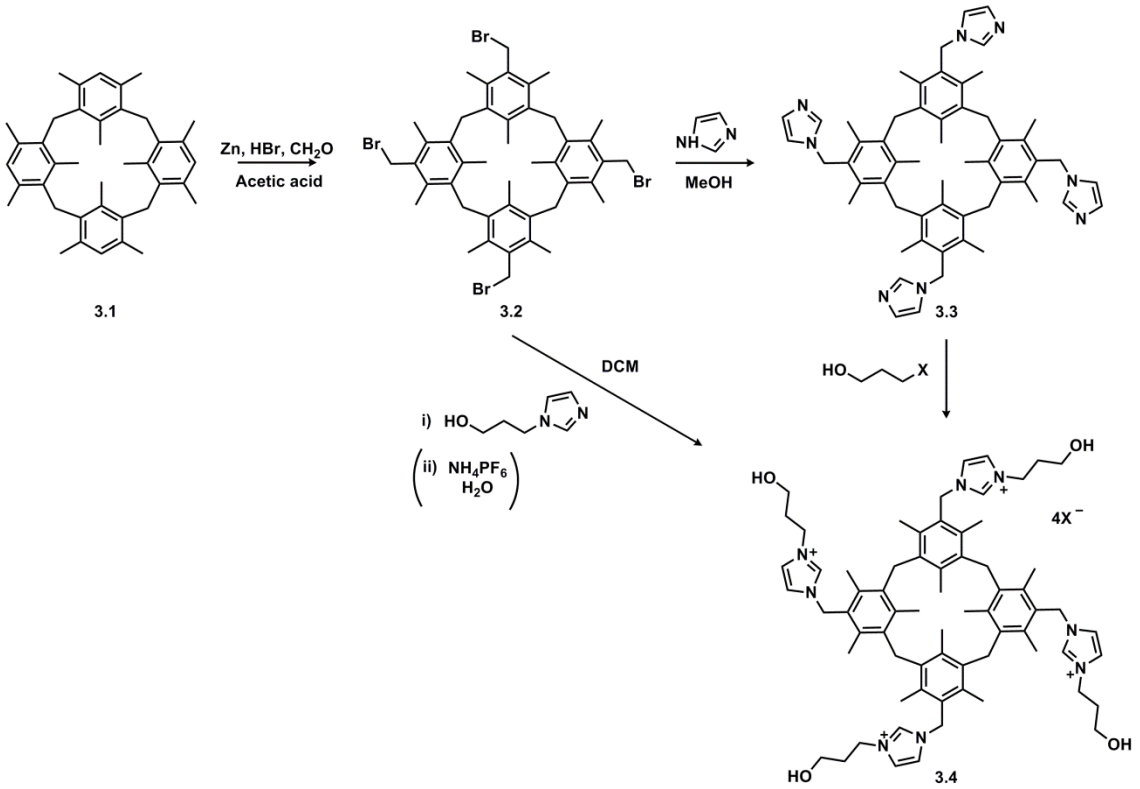

Scheme 3.1 Proposed synthetic routes for the preparation of propanol tethered methylimidazolium mesityl calix[4]arene **3.4** (X = Br, Cl, I or PF_6).

The preparation of mesityl calix[4]arene (**3.1**) was carried out *via* the $SnCl_4$ catalysed cyclisation of α-chloroisodurene.[9] The product was isolated in moderate yields of 40-50 % and purified by extraction into DCM from water. The molecule is locked in the 1, 3-alternate conformation, and can be used as a platform to support functional groups such as organometallic anion binding groups, or anion receptor groups.[10, 11]

The bromomethylation of compound **3.1** was performed using HBr and paraformaldehyde in glacial acetic acid, isolating the bromo-methylated mesityl calix[4]arene (**3.2**), a reagent that is suitable for functionalisation by nucleophiles.[12] The reaction of **3.2** with excess imidazole in methanol affords methylimidazole mesityl calix[4]arene (**3.3**).[13] As previously discussed, a base is not required in these types of nucleophilic substitution reactions as imidazole itself acts as a base. Compound **3.3** was isolated as a cream coloured solid and characterised by ^{1}H NMR and $^{13}C\{^{1}H\}$ NMR spectroscopy combined with mass spectrometry. The compound is reported in the literature, however, we report a simplified synthetic procedure that results in a product of similar purity and comparable yield.[14] Compound **3.3** was initially prepared as a

precursor to synthesise the novel propanol tethered methylimidazolium mesityl calix[4]arene (**3.4**). The synthetic route attempted was the quaternization of the neutral imidazole compound (**3.3**) as described in Chapter 2 (Chapter 2, Scheme 2.2). Compound **3.3** was reacted with four equivalents of bromopropanol as a dry melt. The mixture was heated at 60 °C for 24 hours, under a nitrogen atmosphere. A yellow oil formed which, when washed with acetone, became a white solid. Low field resonances were observed in the ^{1}H NMR spectrum between δ = 8.5 ppm and δ = 9.5 ppm, suggesting that the reaction was forming imidazolium species. However, there were multiple products formed, and the purification of the product mixture proved unsuccessful. We propose that the reaction was forming the 4-, 3-, 2-, and 1-substituted products in varying ratios (Chapter 2, Figure 2.5), and as these molecules are likely to have very similar properties they were not easily separable from each other. The reaction was repeated using iodopropanol, as iodide is a better leaving group than bromide, but the same result was observed. Increasing the reaction time or increasing the reaction temperature did not force the reaction to completion, and multiple imidazolium species were always observed.

Due to the mixture of products formed in the above reactions, the approach to the synthesis of compound **3.4** was altered. Bromo-methylated mesityl calix[4]arene (**3.2**) was reacted with 1-propanol imidazole, rather than proceeding through compound **3.3**. 1-Propanol imidazole was added to a DCM solution of compound **3.2** and the solution was stirred at room temperature, under a nitrogen atmosphere, for 12 hours. During this time, a white solid precipitated from solution. The solvent was decanted from the solid and the compound was purified by washing with DCM, and was dried *in vacuo*. Compound **3.4 Br** was characterised by ^{1}H NMR and ^{13}C{^{1}H} NMR spectroscopy combined with mass spectrometry. The bromide counter ions were exchanged for hexafluorophosphate using ammonium hexafluorophosphate in water to afford the hexafluorophosphate salt of **3.4** as a white solid. Compound **3.4 PF_6** was characterised by ^{1}H NMR and ^{13}C{^{1}H} NMR spectroscopy, mass spectrometry and elemental analysis.

The ^{1}H NMR spectrum of compound **3.4 Br** in DMSO-d_6 is displayed in Figure 3.1, with the relevant peaks assigned in Table 3.1. The ^{1}H NMR spectrum appears as expected, with a characteristic resonance for the imidazolium C2 proton downfield at δ = 8.93 ppm. The hydroxyl group protons are seen in the ^{1}H NMR spectrum as a triplet at δ = 4.70 ppm, coupling to the neighbouring methylene protons. Notably, the methyl

groups of the mesityl moieties appear as two separate resonances at δ = 1.12 ppm and δ = 2.34 ppm, with those that are shielded by the aromatic flux shifted upfield by 1.22 ppm.

The ^{1}H NMR spectrum of compound **3.4 PF$_6$** (DMSO-d$_6$) is consistent with the ^{1}H NMR data reported for compound **3.4 Br** (DMSO-d$_6$). A slight change in chemical shift is observed for the C2 proton, which is shifted upfield by 0.1 ppm, to δ = 8.83 ppm. This is expected due to the change from a coordinating anion (Br) to a non-coordinating anion (PF$_6$). Notably, the resonance for the hydroxyl protons no longer appears as a sharp triplet, but is observed as a broad singlet resonance at δ = 4.69 ppm.

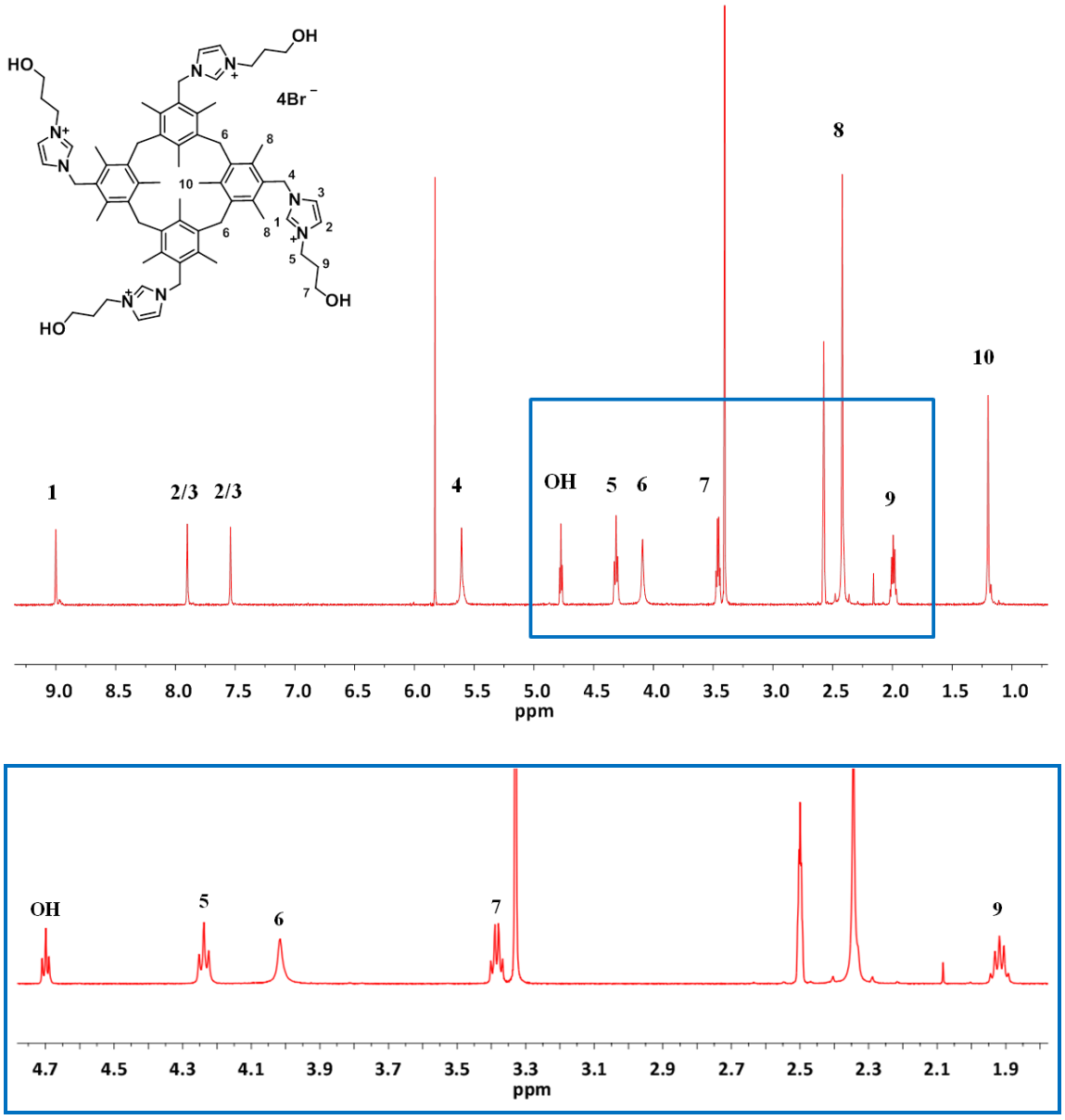

Figure 3.1 ^{1}H NMR spectrum (DMSO-d$_6$) of compound **3.4 Br** at 298 K (top). Expansion of the region δ = 1.9 ppm to δ = 4.7 ppm (bottom).

Chemical shift (δ ppm) ^{1}H	Assignment
8.93 (s, 4H)	1
7.83 (s, 4H)	2 / 3
7.46 (s, 4H)	2 / 3
5.53 (s, 8H)	4
4.70 (t, 4H, $^3J_{HH}$ = 4.9 Hz)	OH
4.24 (t, 8H, $^3J_{HH}$ = 6.9 Hz)	5
4.02 (s, 8H)	6
3.38 (q, 8H, $^3J_{HH}$ = 5.3 Hz)	7
2.34 (s, 24H)	8
1.92 (quintet, 8H, $^3J_{HH}$ = 6.3 Hz)	9
1.12 (s,12H)	10

Table 3.1 ^{1}H NMR assignments for compound **3.4 Br**.

Colourless needle crystals of compounds **3.4 3Cl.PF$_6$** and **3.4 4Br** were obtained by slow evaporation of saturated acetonitrile solutions of **3.4 PF$_6$** with four equivalents of NBu_4^+ X^- salts (where X = Cl or Br). These were structurally characterised using single crystal X-ray diffraction analysis and the molecular structures are displayed in Figure 3.2. Both compounds crystallised in the triclinic crystal system and structural solutions were obtained in the space group *P*-1. Interestingly, although four equivalents of the NBu_4^+ X^- salts were added to both crystallisations, the chloride anion only replaced three of the PF_6 anions, whereas the bromide anion replaced all four. Several crystals were removed from the **3.4 PF$_6$** and NBu_4^+ Cl^- solution, and analysed by single crystal X-ray diffraction, and they all showed the same structure with the 3:1 anion ratio.

Both **3.4 3Cl.PF$_6$** and **3.4 4Br** show the expected 1,3-alternate conformation of the calixarene core, with two imidazolium groups projecting upwards, and two projecting downwards (Figure 3.2). The molecules are locked in this conformation due to the steric effects of the mesityl groups. However, the tethered imidazoles can freely rotate within that constraint and orientate themselves with different geometries.[11] Steed *et al*. reported a comparable crystal structure of an imidazolium calixarene that has the 1,3-alternate calixarene framework, with methyl groups as the substituents on the imidazolium nitrogen atoms.[11] They describe how the molecule can exist in two different conformations, either *in-out* or *out-out* conformers, depending on whether the imidazolium C2 proton is orientated towards the calixarene axis or away. It is reported

that the *in-in* conformation is never observed, which they propose is due to steric constraints. In both our structures we observe the *out-out* conformation, with all four imidazolium groups orientated away from the calixarene core.

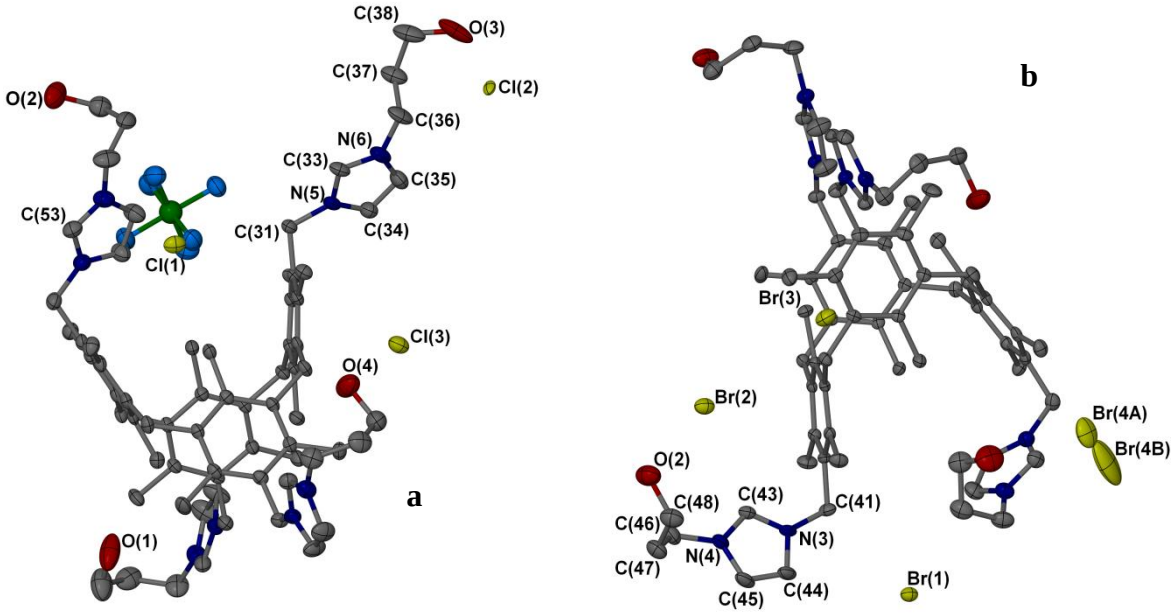

Figure 3.2 Molecular structure of (a) **3.4 3Cl.PF$_6$**, and (b) **3.4 4Br** . Hydrogen atoms and solvent molecules are omitted for clarity. Ellipsoids are displayed at 50% probability**.**

O(3)-C(38)	1.430(8)	N(6)-C(33)-N(5)	108.6(4)
C(38)-C(37)	1.510(6)	C(33)-N(6)-C(35)	108.7(3)
N(6)-C(33)	1.334(5)	C(33)-N(5)-C(34)	108.2(3)
C(35)-C(34)	1.356(6)		
N(5)-C(31)	1.486(4)		

Table 3.2 Selected bond distances (Å) and angles (deg) for compound **3.4 3Cl.PF$_6$** (Figure 3.2a).

O(2)-C(48)	1.427(5)	N(4)-C(43)-N(3)	109.1(3)
C(48)-C(47)	1.529(5)	C(43)-N(4)-C(45)	108.2(3)
N(4)-C(43)	1.335(4)	C(43)-N(3)-C(44)	108.1(3)
C(45)-C(44)	1.354(5)		
N(3)-C(41)	1.489(4)		

Table 3.3 Selected bond distances (Å) and angles (deg) for compound **3.4 4Br** (Figure 3.2b).

Imidazolium groups have the potential of being effective anion binders due to the hydrogen bonding interactions they form with anions of the type [(C-H)$^{+}$····X^{-}]. Steed *et*

al. report that the imidazolium calixarene molecule, discussed previously, binds to anions within the structure through a broad range of hydrogen bonding interactions. Interactions exist not only through the imidazolium NC*H*N protons, but also through the backbone protons on the imidazolium groups and through the methyl groups.[11] We also observed similar behaviour with the tetrakis(methylimidazolium) calix[4]arene (**2.5**) reported in Chapter 2 (Figure 2.7). The solid state structure of compound **2.5** displays a broad range of hydrogen bonding interactions with anions through acidic protons on both the upper and lower rim of the calixarene molecule.[15] An interesting feature of compound **3.4** is that the molecule interacts with anions primarily through hydrogen bonding with the hydroxyl groups on the propanol substituents, forming interactions of the type $[(O\text{-}H)^{+}\cdots X^{-}]$, rather than through the acidic imidazolium protons, or other acidic protons contained within the structure.

Upon closer examination of the X-ray crystal structure of compound **3.4 3Cl.PF$_6$**, it can be seen that the hydroxyl groups interact with two of the chloride anions (**Cl2 / Cl3**), with the length of the $[(O\text{-}H)^{+}\cdots Cl^{-}]$ bonds being 3.113-3.168 Å (O$\cdots$Cl distance), which is typical for this type of interaction (Figure 3.3).[16] The remaining chloride anion (**Cl1**) interacts with two enclathrated water molecules, and does not form any interaction with the calixarene atoms. There is no evidence that any of the other acidic protons of compound **3.4 3Cl.PF$_6$** interact with the anions.

The molecule packs as a 1D ladder, propagated through a three coordinate hydrogen bond from the hydroxyl groups to **Cl3** (Figure 3.4). **Cl2** forms a single terminal hydrogen bond with one hydroxyl group (**O3-H3**), and does not influence the hydrogen bonding network.

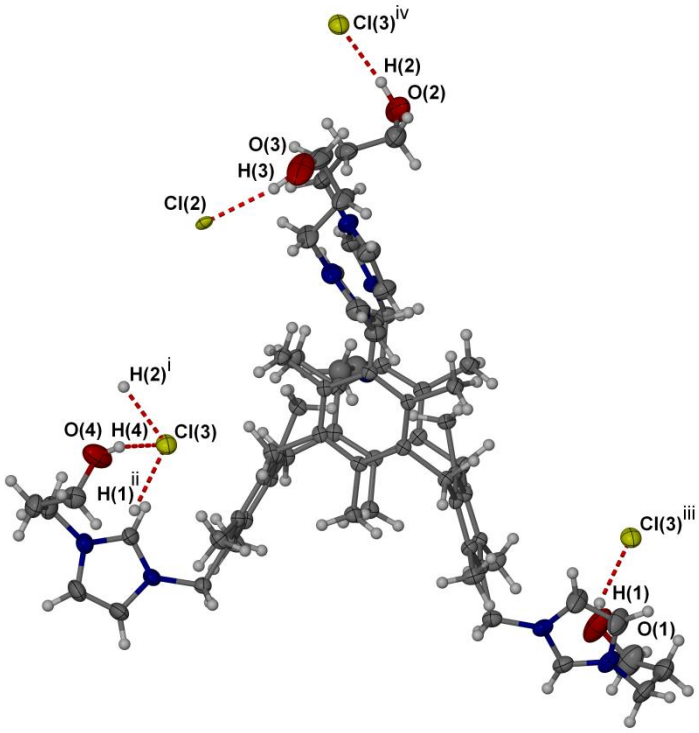

Figure 3.3 X-ray crystal structure displaying the hydrogen bonding interactions observed in the solid state structure of **3.4 3Cl.PF$_6$**. Symmetry operations for symmetry generated atoms i: -x, 1-y, 1-z; ii: x, y-1, z; iii: x, 1+y, z; iv: -x, 1-y, 1-z. Solvent atoms and anions not involved in hydrogen bonding to the calixarene (Cl1 and PF_6) have been omitted for clarity. Ellipsoids are displayed at 50% probability.

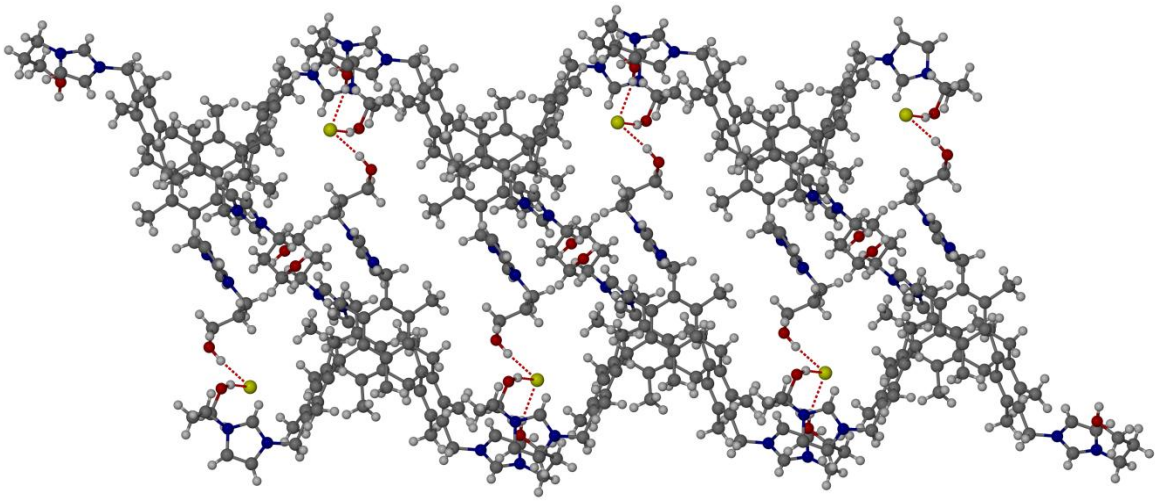

Figure 3.4 X-ray crystal packing diagram of compound **3.4 3Cl.PF$_6$** displaying the 1D hydrogen bonding ladder. Solvent atoms and anions not involved in the hydrogen bonding network (Cl1, Cl2 and PF_6) have been omitted for clarity.

The X-ray crystal structure of compound **3.4 4Br** shows similar bonding patterns to compound **3.4 3Cl.PF$_6$**, with the primary interactions to the bromide anions being through the hydroxyl groups on the propanol substituents (Figure 3.5). In this structure the hydroxyl groups interact with three bromide anions (**Br3 / Br2 / Br4A**), with the hydrogen bond lengths of [(O-H)$^+$····Br$^-$] being 3.166-3.341 Å (O····Br distance), which is typical for this type of bond.[16] This is slightly longer than the [(O-H)$^+$····Cl$^-$] bonds in **3.4 3Cl.PF$_6$**, which would be expected due to the relative basicity of the anions and size. **Br1** does not appear to form any close interactions with the calixarene.

Upon closer examination of the crystal structure of **3.4 4Br** it can be seen that, in this case, an acidic imidazolium proton (**H63**) does form an interaction with one of the bromide anions (**Br4B**). The occupancy of **Br4** is disordered over two positions (**Br4A / B**), interacting with either the hydroxyl proton (**H4**) or the imidazolium proton (**H63**) (Figure 3.5). The two parts have SOFs of 85 % (**Br4A**) and 15 % (**Br4B**) respectively. Therefore, it is predominantly in position **Br4A**, where it interacts with the hydroxyl proton (**H4**). Again, this highlights the preferred binding of **3.4** to anions through the hydroxyl protons over the other acidic protons present in the compound. There is no further evidence of the other acidic protons in compound **3.4 4Br** interacting with the bromide anions.

The molecule packs as a 1D chain, propagated through a two coordinate hydrogen bond from the hydroxyl groups to **Br3** (Figure 3.6). The hydrogen bonds from the hydroxyl groups to **Br2** and **Br4** are terminal, and do not influence the hydrogen bonding network.

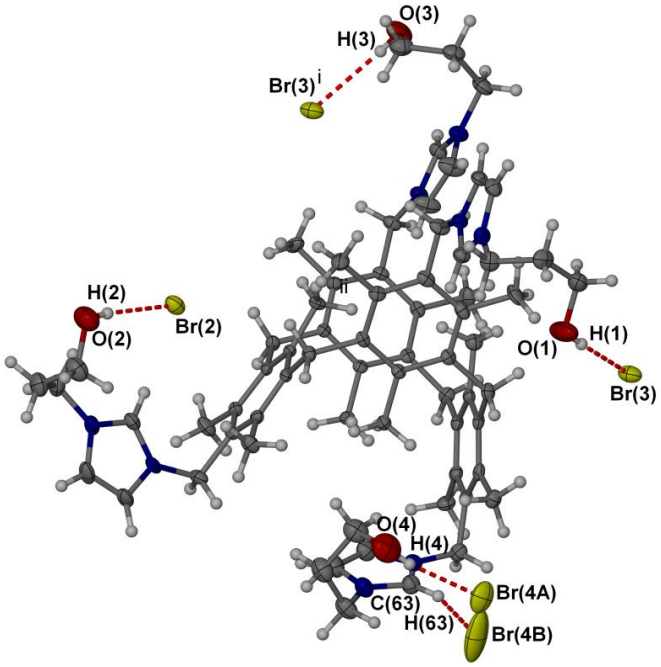

Figure 3.5 X-ray crystal structure of compound **3.4 4Br** displaying the hydrogen bonding interactions observed in the solid state structure. Symmetry operations for symmetry generated atoms i: -x, 2-y, 1-z. Solvent atoms and anions not involved in hydrogen bonding to the calixarene (Br1) have been omitted for clarity. Ellipsoids are displayed at 50% probability.

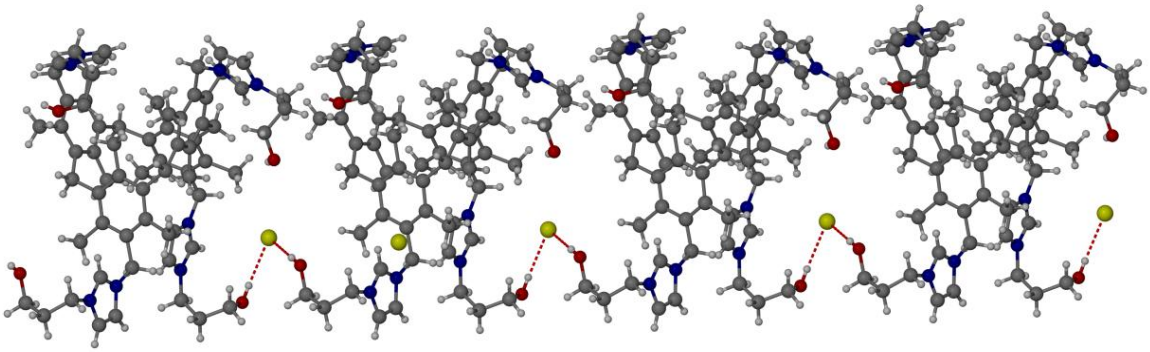

Figure 3.6 X-ray crystal packing diagram of compound **3.4 4Br** displaying the 1D hydrogen bonding chain. Solvent atoms and anions not involved in the hydrogen bonding network (Br1, Br2 and Br4) have been omitted for clarity.

Both crystal structures of compound **3.4** reveal that it is not the acidic imidazolium protons (C2 protons) that form the primary interactions with the anions in the solid state, but it is the hydroxyl groups of the propanol substituents. In order to investigate if this behaviour is also evident in solution, the anion binding properties of **3.4 PF_6** were probed. The changes in the ^{1}H NMR spectra of compound **3.4 PF_6** were monitored as aliquots of tetrabutylammonium bromide were added, exchanging the non-coordinating

PF_6 anion for the coordinating bromide anion. Compound **3.4** PF_6 (0.01 g, 6.02×10^{-6} moles) was dissolved in 0.5 ml of MeCN-d_3. Tetrabutylammonium bromide (0.0234 g, 7.25×10^{-5} moles) was dissolved in 1 mL of MeCN-d_3, approximately 10 times the concentration of the host. 10 µL aliquots of the guest (tetrabutylammonium bromide solution) were added to the NMR tube and the spectra recorded following each addition. The equivalents of guest that had been added were calculated, taking the ratio of host: guest concentration after each 10 µL addition. The equivalents of guest added was then plotted against the chemical shift of the C2 proton, and against the chemical shift of the hydroxyl proton. The results are displayed in Figures 3.7 and 3.8 respectively. The graphs are plotted up to the point where just over two equivalents of guest had been added, as at this point the compound precipitated from solution

Figure 3.7 shows the change in the chemical shift of the C2 proton as the tetrabutylammonium bromide solution was added. Initially the signal shifts downfield, from δ = 8.14 ppm when no guest is present, to δ = 8.37 ppm when one equivalent of guest has been added. After this point, there is an upfield shift in the C2 proton resonance, up to the addition of 1.3 equivalents of guest (δ = 8.30 ppm). The signal then moves downfield again until the product precipitated from solution, with the final recorded shift for the C2 proton being δ = 8.41 ppm. Unsurprisingly, there is also a significant change observed in the chemical shift of the hydroxyl group protons as the tetrabutylammonium bromide solution was added (Figure 3.8). The change in the chemical shift for the hydroxyl protons mirrors the change in the chemical shift observed for the C2 protons, with the signal moving downfield from δ = 2.86 ppm to δ = 3.20 ppm between 0-1 equivalents of guest. Following this there is an upfield change in chemical shift until 1.3 equivalents of the guest has been added (δ = 3.17 ppm). Then the signal moves downfield again to δ = 3.30 ppm, at the point before the product precipitated from solution.

These observations infer that the first equivalent of guest binds to both the C2 and the hydroxyl group protons, resulting in a downfield shift of the proton resonances for both groups. Following this there is an upfield change in the chemical shift of both these signals, which is most likely due to the anions interacting with a different part of the calixarene molecule. Other acidic protons that are likely to take part in the hydrogen bonding are those of the imidazolium backbone. This interaction presumably results in a slight conformational change of the calixarene molecule, accounting for the upfield chemical shifts observed in the ^{1}H NMR spectra for the C2 and hydroxyl protons

between 1–1.3 equivalents of guest. Following this the anions continue to interact with the C2 protons and the hydroxyl group protons. The overall change in the chemical shift is more significant for the hydroxyl group protons (0.44 ppm), than for the C2 imidazolium protons (0.27 ppm), which supports observations made in the solid state that it is the hydroxyl group protons that form the primary interaction to the anions. However, the ^{1}H NMR data does suggest that when the molecule is in solution, and able to rotate freely, other acidic protons of **3.4** interact with the anions.

Figure 3.9 shows the change in the chemical shift of one of the imidazolium backbone protons (Figure 3.1, **H2 / H3**) as tetrabutylammonium bromide solution was added. Interestingly, the observed change in the chemical shift for the imidazolium backbone protons follows the opposite trend of that observed for the C2 and hydroxyl group protons. Initially the signal shifts upfield, from δ = 7.11 ppm when no guest is present to δ = 7.06 ppm when one equivalent of guest has been added. Following this, there is a downfield change in the chemical shift until the point where 1.3 equivalents of guest has been added (δ = 7.09 ppm). The signal then shifts upfield again to δ = 7.07 ppm, at the point before the product precipitated from solution. The overall change in the chemical shift of the imidazolium backbone protons is less significant than for the C2 and hydroxyl protons (0.05 ppm). However, the data supports the theory that the upfield change in the chemical shifts of the C2 and hydroxyl protons observed between 1-1.3 equivalents of guest was due to the anions interacting with the acidic imidazolium backbone protons, as there is a simultaneous downfield shift in the imidazolium backbone protons chemical shift at this point.

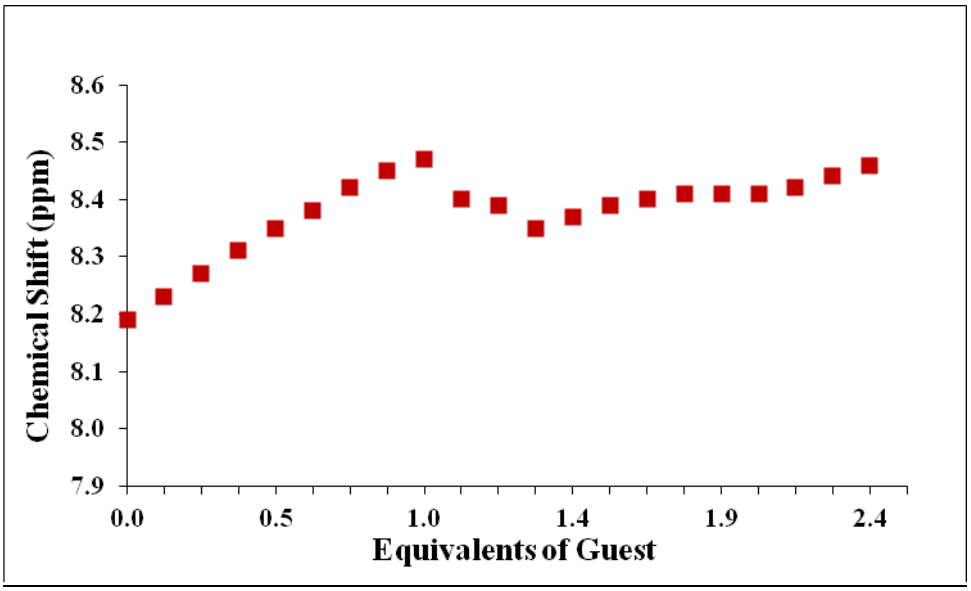

Figure 3.7 ^{1}H NMR spectroscopic titration data for the shift in the C2 imidazolium protons of compound **3.4** $\mathbf{PF_6}$ upon addition of tetrabutylammonium bromide (MeCN-d_3).

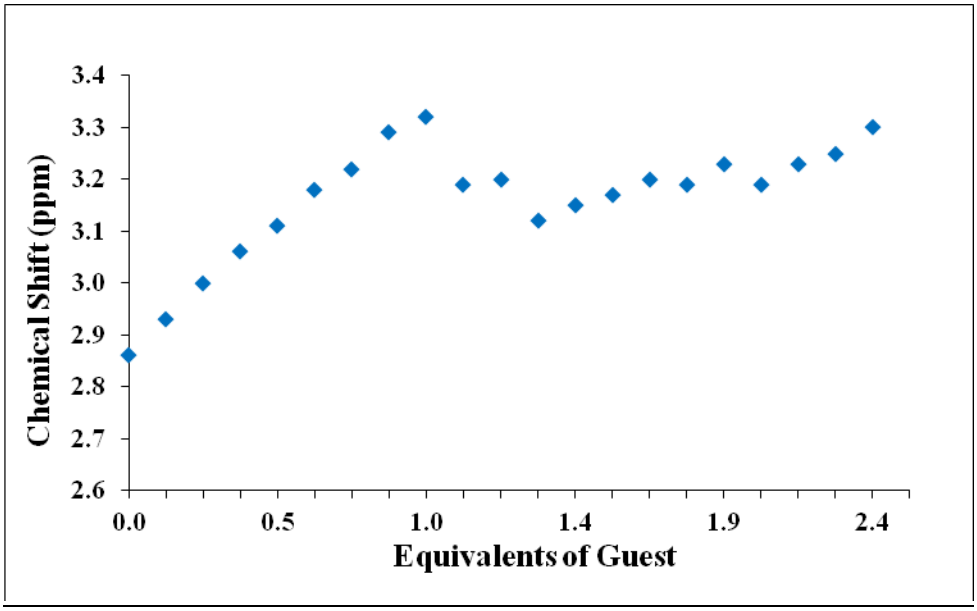

Figure 3.8 ^{1}H NMR spectroscopic titration data for the shift in the hydroxyl protons of compound **3.4** $\mathbf{PF_6}$ upon addition of tetrabutylammonium bromide (MeCN-d_3).

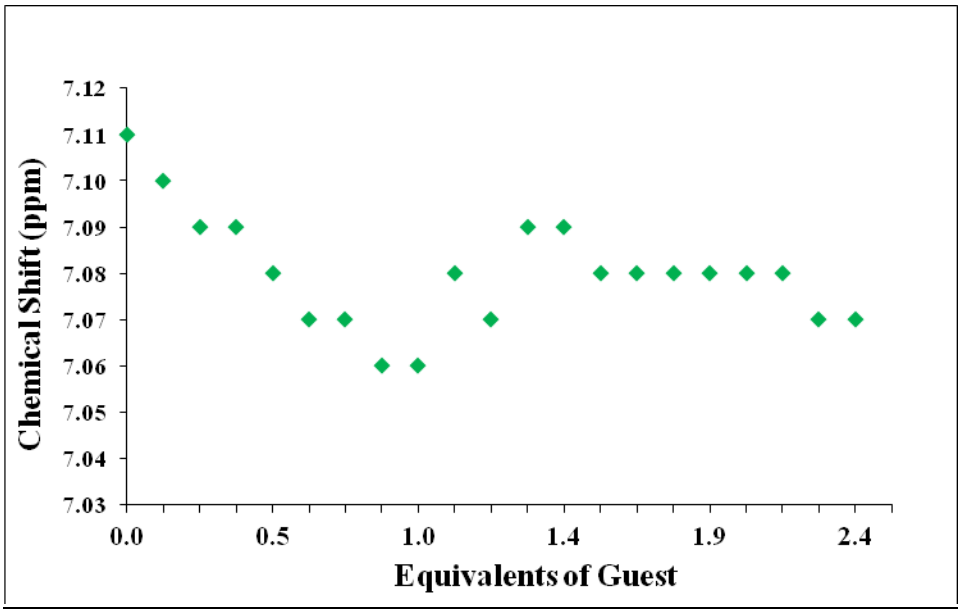

Figure 3.9 ^{1}H NMR spectroscopic titration data for the shift in one of the backbone imidazolium protons (Figure 3.1, H2 / H3) of compound **3.4 PF_6** upon addition of tetrabutylammonium bromide (MeCN-d_3).

3.2 Formation of metal-NHC complexes using NHC-ligand precursor 3.4 Br

NHC-substituted calixarenes is an area that remains relatively unexplored, with only a few reported examples in the literature.[17-21] Compound **3.4** offers the potential of forming a unique metal-NHC complex as, to the best of our knowledge, all NHC substituted calixarenes reported to date are functionalised with only one or two NHC groups, forming monodentate or bidentate metal-NHC complexes.[17-21] Compound **3.4** is functionalised with four imidazolium groups and, as a result, has the potential to form four metal-NHC bonds, forming a bidentate or monodentate metal-NHC complex that can incorporate two or four metal centres respectively. The propanol substituents in compound **3.4** offer the potential of forming an anionic interaction to the metal centre which, if formed, can be expected to increase the stability of the metal-NHC complex.[22] The use of compound **3.4** as an NHC-ligand precursor was investigated through its reaction with basic metal precursors (Ag_2O, Cu_2O, $Pd(OAc)_2$), to form the metal-NHC complexes *in situ*. The products from these reactions were analysed using ^{1}H NMR and $^{13}C\{^{1}H\}$ NMR spectroscopy combined with mass spectrometry.

Silver-NHCs are of particular interest as they are easily synthesised, and it is well established that they can be used as carbene transfer agents, which can allow the formation of a wide range of transition metal-NHC complexes.[1, 2, 5] In addition, silver-NHCs are known to have exploitable properties themselves, and have found application as antimicrobial agents and as anticancer agents.[23, 24] There are two methods that are routinely used to prepare silver-NHCs; a) the deprotonation of an imidazolium precursor (using a strong base such as BuLi or KO^{t}Bu) to form the free carbene, followed by addition of a silver salt (e.g. $AgBF_4$),[25] b) the reaction of an imidazolium salt with a basic silver reagent, such as Ag_2O, which deprotonates the imidazolium salt and forms the silver-NHC *in situ*.[1, 3] The use of a basic silver reagent is often preferred as it avoids the need to isolate the free carbene intermediate, which is often extremely unstable, and circumvents the need for strict inert conditions. It also negates the need for a strong base which can react with other acidic protons in the ligand and cause undesirable side reactions.

Compound **3.4 Br** was reacted with two equivalents of silver oxide in anhydrous methanol at room temperature, in the dark, under a nitrogen atmosphere, for 1.5 hours (Scheme 3.2). The reaction was stopped once the solution appeared light brown, indicating the consumption of Ag_2O and the formation of AgBr. 3Å molecular sieves

were added to absorb the water formed in the reaction, as it has been reported that the addition of molecular sieves decreases the reaction time, as well as improving the purity of the product.[1, 26, 27] The mixture was filtered through celite and the solvent removed *in vacuo* to yield a white solid that was analysed by ^{1}H NMR and $^{13}C\{^{1}H\}$ NMR spectroscopy combined with mass spectrometry. The formation of a silver-NHC was indicated by the absence of the low field resonance in the ^{1}H NMR spectrum (DMSO-d_6) at δ = 8.93 ppm, indicating the removal of the C2 imidazolium proton (Figure 3.10). However, no low field resonance was seen in the $^{13}C\{^{1}H\}$ NMR spectrum for the C2 carbon bound to silver, usually observed at around 180 ppm. Also, the mass spectrometry data was very weak and inconclusive. Despite repeated attempts, a crystal structure could not be obtained, which would have assisted in the analysis. Colourless crystals were grown from methanol / diethyl ether, but they decomposed as soon as they were removed from solution and exposed to the air. This is likely due to the loss of solvent from the crystal lattice.

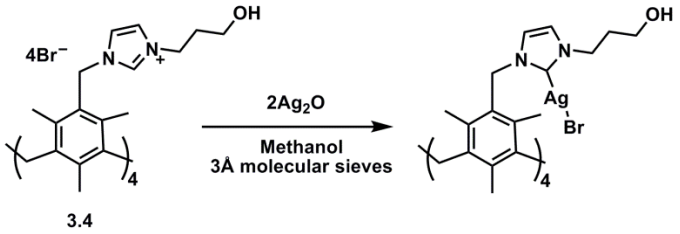

Scheme 3.2 Proposed product from the reaction of compound **3.4 Br** with Ag_2O.

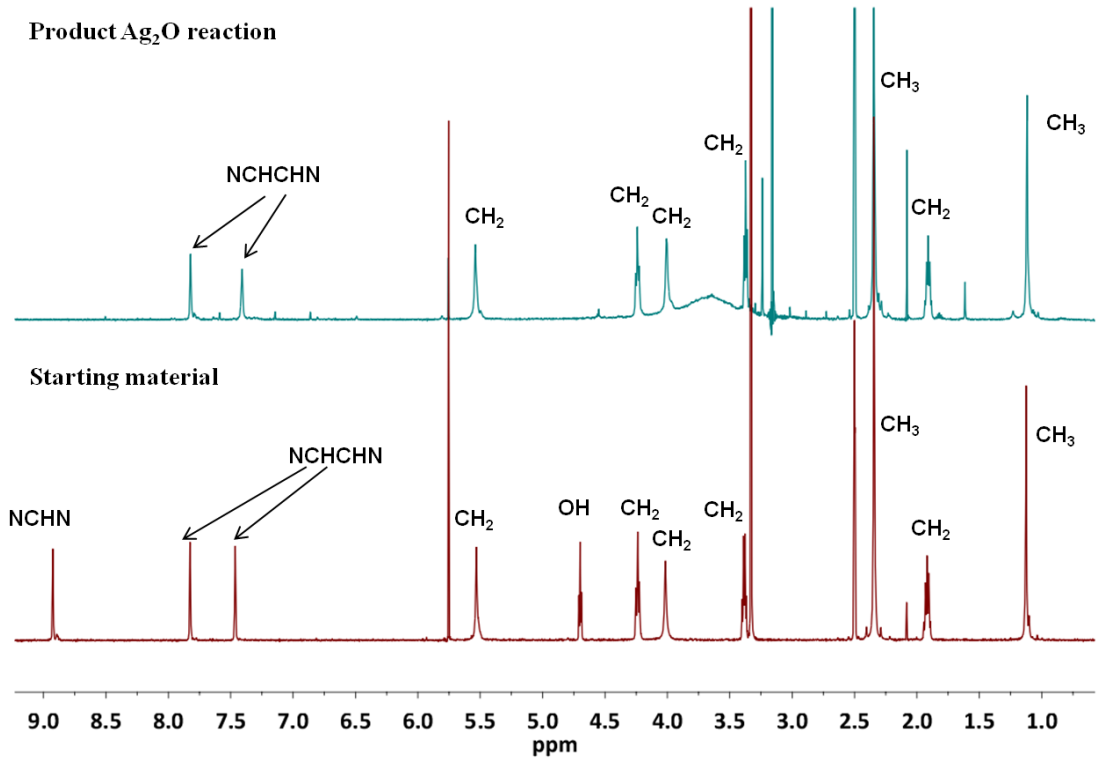

Figure 3.10 ^{1}H NMR spectra (DMSO-d_6) displaying **3.4 Br** (bottom) and the product formed in the reaction between **3.4 Br** and Ag_2O in methanol (top).

It has been observed within our group that some silver-NHC complexes synthesised in methanol tend to be unstable, becoming brown over time and depositing a dark brown solid. These compounds were found to contain a large excess of silver bromide, which could have been incorporated into the structure through a halide bridging system.[28] When the reaction was performed in DCM or DCM / methanol (7:1), the silver-NHCs formed were found to be more stable and appeared not to contain any excess AgBr.[23] This was attributed to the low solubility of silver salts in DCM, resulting in the silver bromide formed precipitating from solution.

The reaction of compound **3.4 Br** with Ag_2O was therefore investigated in a range of solvents to see if this increased the stability of the silver-NHC complex, enabling more characterisation data to be obtained. Using the same reaction conditions in anhydrous DCM at room temperature, or with heating (30 °C), no reaction occurred, and only starting material was isolated from the reaction. This was thought to be due to the poor solubility of compound **3.4 Br** in DCM. A mixture of DCM / methanol (2:1) was therefore used, with enough methanol added to solubilise the compound. The reaction produced the same result as when using only methanol in the reaction, with the ^{1}H NMR spectrum indicating the presence of a silver-NHC complex by the absence of

the low field resonance attributed to the C2 proton (Figure 3.10).$^{13}C\{^{1}H\}$ NMR spectroscopy and mass spectrometry provided no further evidence for the formation of the desired silver-NHC complex. The reaction was also attempted in THF / methanol (1:1) and worked up in the same way as previously, but this time yielded a yellow film. The ^{1}H NMR spectrum obtained was the same as that from the previous methanol reaction, though in this case the $^{13}C\{^{1}H\}$ NMR spectrum displayed evidence for the C2 carbon coordinating to silver, with a resonance observed at δ = 182.4 ppm. Again the mass spectrometry data did not provide further insight into the structure of the silver-NHC complex. Crystallisations were attempted in a range of solvents / solvent mixtures, but no crystals were obtained that were suitable for single crystal X-ray diffraction analysis.

Due to the nature of compound **3.4**, there are numerous possibilities for the structure of the silver-NHC complex. Firstly, there is the potential to form either the neutral monodentate NHC complex 4Ag(NHC)Br, or the cationic bidentate silver-NHC complex $2[Ag(NHC)_2]^{+}2Br^{-}$, incorporating four or two silver centres respectively. The formation of the neutral complex, 4Ag(NHC)Br, would be expected due to the coordinating nature of the bromide anion. Conversely, if the reaction was performed with compound **3.4 PF_6** and Ag_2O, the charged $2[Ag(NHC)_2]^{+}2PF_6^{-}$ complex would be the expected product due to the non-coordinating nature of the PF_6 anion.[28]

Another consideration is that the propanol substituents of compound **3.4** are likely to be deprotonated under the basic reaction conditions, leading to a mixed binding complex, with the alkoxy groups forming an anionic interaction to the silver metal centre in addition to the silver-NHC bond. The hydroxyl groups were shown to have the most acidic protons in compound **3.4** in the solution studies. Their relative acidity also suggests that they would be deprotonated during the reaction, with the pK_a of a primary alcohol being around 16 compared to the C2 imidazolium proton pK_a that is in the region of 20-25. Arnold *et al.* reported an alcohol functionalised imidazolium that, when reacted with Ag_2O, lead to deprotonation of both the C2 proton and hydroxyl group, in this case generating the halide free alkoxy bound silver-NHC complex (Figure 3.11).[29] Notably, this is a tertiary alcohol not a primary alcohol, with tertiary alcohols having a higher pK_a of around 19.

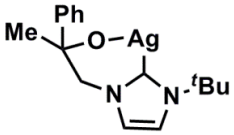

Figure 3.11 Reported product from the reaction of an alcohol functionalised imidazolium with Ag_2O.[29]

If the alkoxy groups in compound **3.4** do interact with silver, either a discrete complex (as in Figure 3.11) or a polymeric complex may form. The tendency of silver to form silver-silver and / or silver-halide interactions could also aid the formation of a polymeric species.[30] The analysis obtained of the silver-NHC complexes does not provide any confirmation as to whether the alkoxy tethers are interacting with the silver centres. In the ^{1}H NMR spectrum of the product formed from the reaction of Ag_2O and compound **3.4 Br** (Figure 3.10), the hydroxyl protons are no longer present (they were observed as a triplet resonance at δ = 4.70 ppm in compound **3.4 Br**). This could be an indication that the hydroxyl groups have remained deprotonated during the reaction and formed an interaction with silver, but this evidence is not conclusive.

Although we were unable to fully characterise the silver-NHC complex formed, we are confident that the reaction of **3.4 Br** with Ag_2O generated a silver-NHC of some description. This was confirmed by the ^{1}H NMR spectra which, under all the different reaction conditions investigated, had no evidence of the resonance attributed to the C2 proton. The use of this silver-NHC complex as a ligand transfer agent was therefore explored. Silver-NHCs are often used as intermediate species for the formation of other transition metal-NHC complexes, and it is not always necessary to isolate the silver intermediate.[31] We were interested to see if we could use this silver-NHC complex in this way.

The product formed in the reaction of **3.4 Br** with Ag_2O (in methanol) was reacted with $PdCl_2(MeCN)_2$ in anhydrous DCM at room temperature, in the dark, for 12 hours (Scheme 3.3).[2, 32] The reaction was filtered and the solvent removed from the filtrate *in vacuo* to yield a yellow oil, which was analysed by ^{1}H NMR and $^{13}C\{^1H\}$ NMR spectroscopy (in both $CDCl_3$ and MeCN-d_3) combined with mass spectrometry. The ^{1}H NMR spectrum was indicative of a reaction occurring, as the starting material was not present, though the identity of the product was not clear. There was no C2 imidazolium proton resonance in the ^{1}H NMR spectrum (MeCN-d_3), but there was also no evidence of the C2 carbon coordinating to palladium in the ^{13}C NMR spectrum (MeCN-d_3), which appears in the region of δ = 140 ppm to 170 ppm. The mass

spectrometry data indicated that palladium species were present due to the observed splitting patterns. However, these signals could not be attributed to a desirable product. Crystallisations were attempted (MeCN / diethyl ether), but unfortunately no crystals were suitable for analysis by single crystal X-ray diffraction.

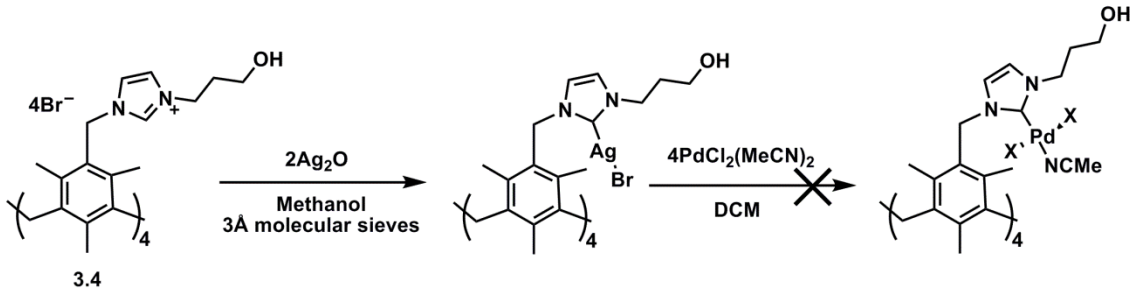

Scheme 3.3 Proposed product from the attempted carbene transfer reaction from silver(I) (reaction of compound **3.4 Br** with Ag_2O) to palladium(II) (X = Cl, Br).

As the transmetallation reaction was inconclusive, compound **3.4 Br** was reacted with $Pd(OAc)_2$ to try and form the palladium species directly (Scheme 3.4). Reaction conditions reported by Dinares *et al*. were used, where a bidentate palladium-NHC supported by a calixarene scaffold was synthesised.[33] Compound **3.4 Br** was reacted with $Pd(OAc)_2$ in anhydrous dioxane at 50 °C for 1 hour, then at reflux (110 °C) for 12 hours, under a nitrogen atmosphere. The solution became black, indicative of palladium(II) being reduced to form palladium(0). The solvent was removed *in vacuo* and the resulting solid dissolved in DCM and filtered through celite. The solvent was removed from the filtrate *in vacuo* and the yellow solid was analysed by ^1H NMR spectroscopy ($CDCl_3$) combined with mass spectrometry, but there was no evidence that the palladium product had formed. The reaction was also attempted under milder conditions in anhydrous acetonitrile (80 °C), in the presence of a base (K_2CO_3). Again, the reaction appeared to form palladium(0) and no desired product was isolated from the reaction solution. It appeared that $Pd(OAc)_2$ was being reduced in the reaction rather than forming the palladium-NHC complex. This is likely due to the hydroxyl tether of **3.4**, which itself can be oxidised to an aldehyde as the palladium(II) is reduced to palladium(0).

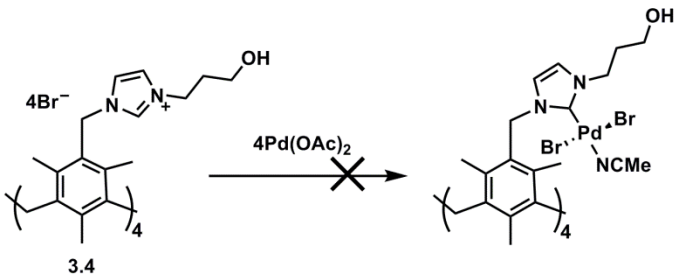

Scheme 3.4 Reaction of compound **3.4 Br** with $Pd(OAc)_2$ in dioxane or MeCN.

The reaction of **3.4 Br** with Cu_2O was explored, with the route being analogous to the Ag_2O route (Scheme 3.5).[4, 34, 35] Compound **3.4 Br** was reacted with six equivalents of Cu_2O, in anhydrous acetonitrile at reflux (80 °C), for 120 hours, under a nitrogen atmosphere. 3Å molecular sieves were added to remove the water formed in the reaction. The solvent was removed *in vacuo* and the resultant red solid dissolved in anhydrous acetone. The solution was filtered and the solvent removed *in vacuo*, to yield a pale yellow solid, which was analysed by ^{1}H NMR spectroscopy ($(CD_3)_2CO$) combined with mass spectrometry. The product had very limited solubility and was not soluble in chloroform, THF, DCM or acetonitrile. The ^{1}H NMR spectrum ($(CD_3)_2CO$) shows the formation of new products, however, there is still a small resonance at δ = 8.65 ppm in the imidazolium C2 proton region (Figure 3.12). The ^{1}H NMR spectrum was also complicated, suggesting the formation of more than one species. Mass spectrometry data confirmed the formation of multiple copper(I) containing species, namely the 1-, 2-, 3- and 4-copper-NHC complexes (Figure 3.13, **A**, **B**, **C** and **D**) with *m/z*; 1678.1 [**D**+Na]$^+$; 1593.2 [**C**+H]$^+$; 1449.3 [**B**-Br]$^+$; 1385.4 [**A**-Br]$^+$. This explains the presence of the C2 imidazolium proton peak in the ^{1}H NMR spectrum, as all four imidazolium groups on **3.4 Br** have not formed the copper carbene in all cases, and a product mixture was generated. In an attempt to form the 4-copper-NHC complex selectively the reaction was repeated, increasing the reaction time (168 hours), and increasing the volume of acetonitrile used. However, a product mixture was always observed. Due to the poor solubility of the copper(I)-NHC complexes, combined with their air sensitivity, the reaction mixture could not be purified.

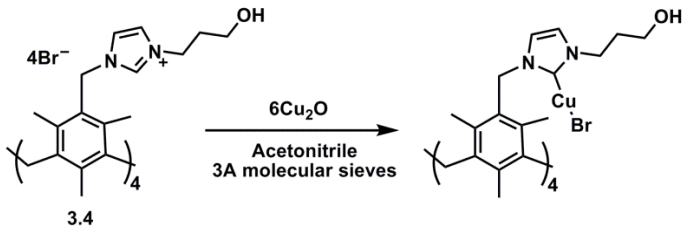

Scheme 3.5 Reaction of compound **3.4 Br** with Cu_2O.

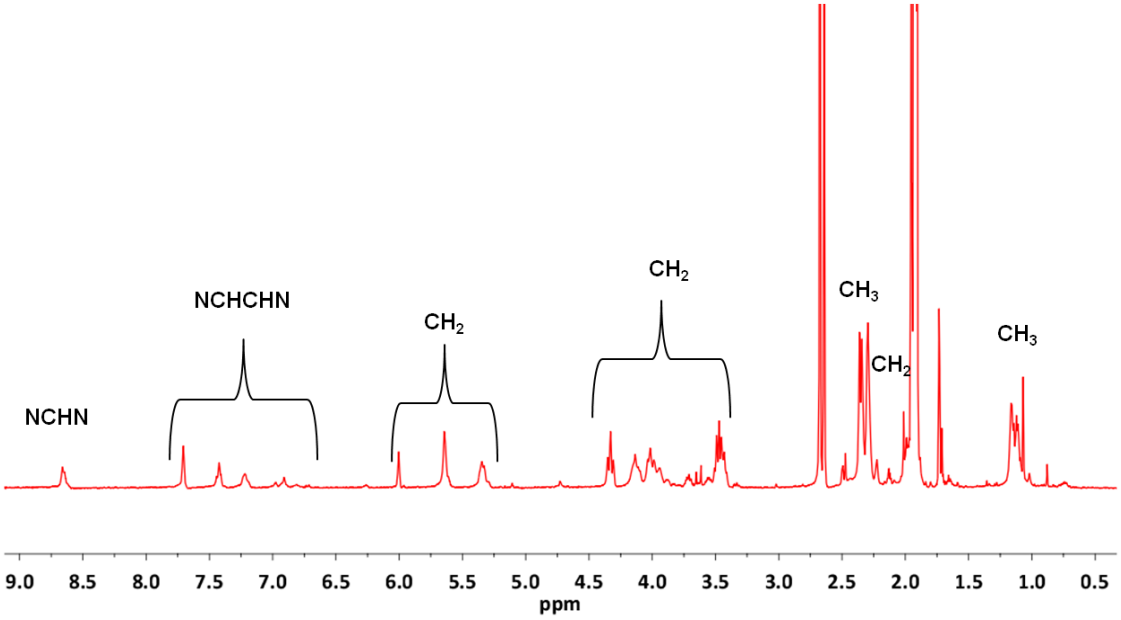

Figure 3.12 ^{1}H NMR spectrum ($(CD_3)_2CO$**)** displaying the products formed in the reaction between compound **3.4 Br** and Cu_2O.

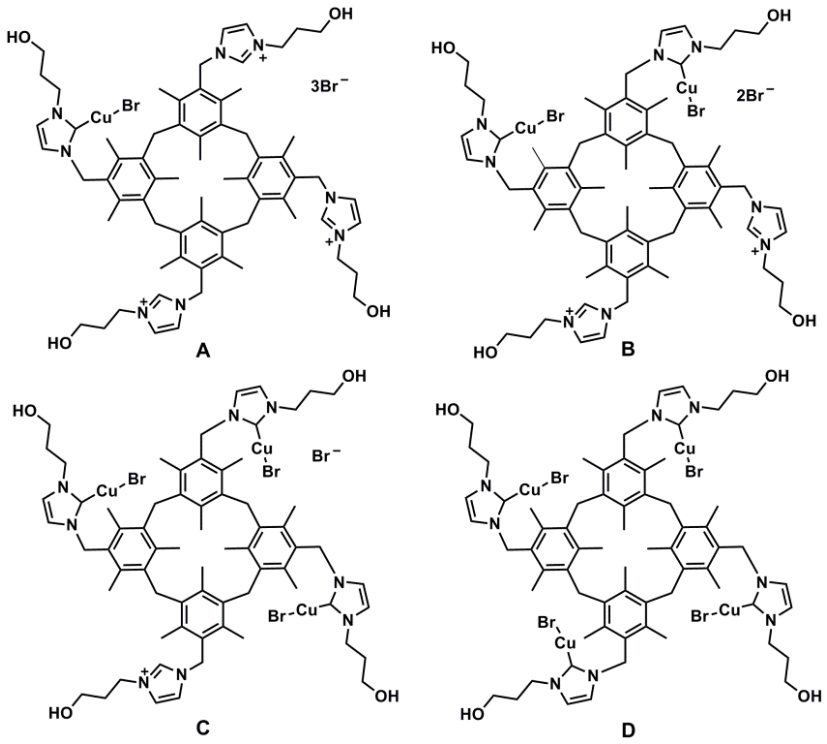

Figure 3.13 Proposed products from the reaction between compound **3.4 Br** and Cu_2O.

A reaction was performed with these copper-NHC products (Figure 3.13, **A**, **B**, **C** and **D**) to see if the copper-NHC could be used as a ligand transfer agent to form other transition metal-NHCs, with the aim of forming more stable / soluble metal complexes that could be purified. It has been reported that copper(I)-NHCs can be used as ligand transfer agents in the same ways as silver-NHCs. Cazin *et al*. reported that copper(I)-NHCs could be used as ligand transfer agents to form gold(I)- and palladium(II)-NHC complexes.[6] Albrecht *et al.* reported copper(I)-NHCs as ligand transfer agents to form a ruthenium(II)-NHC complex.[36]

The product mixture formed from the reaction of **3.4 Br** with Cu_2O was reacted with $PdCl_2(MeCN)_2$ in acetone, at room temperature, for 12 hours (Scheme 3.6). A precipitate formed almost immediately, indicating the formation of CuBr. The solvent was removed *in vacuo* and the red solid was dissolved in acetonitrile and filtered. The ^1H NMR spectrum (MeCN-d_3) was complicated, but showed the formation of new products. As expected, small resonances were observed in the region for the imidazolium C2 proton, at δ = 8.41 ppm and δ = 8.31 ppm. The $^{13}C\{^1H\}$ NMR spectrum (MeCN-d_3) displayed high field resonances at δ = 153.86 ppm and δ = 197.85 ppm, attributed to the C2 carbon bound to the palladium centre in two different geometries, $Pd(NHC)(MeCN)X_2$ and $Pd(NHC)_2X_2$. The mass spectrometry data

strongly suggests that a polymeric species had been formed, with the peaks all being separated by a mass of 75. The peaks were, however, unable to be assigned to a desired product. Single crystals suitable for analysis by single crystal X-ray diffraction were obtained from MeCN / diethyl ether. However, they were found to be a polymeric copper(I) chloride acetonitrile complex. It should be noted that the mass of this did not match any of the mass spectrometry data. Although we were unable to characterise the products formed in this reaction, obtaining a CuCl structure strongly suggests that palladium had displaced the copper in the complex, and a transfer had occurred. This supports the potential of the copper(I)-NHC being used as a ligand transfer agent to form other transition metal-NHC complexes of compound **3.4**.

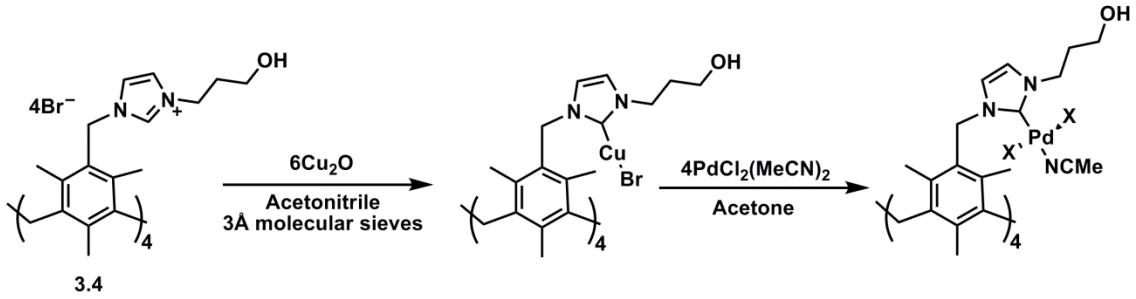

Scheme 3.6 Carbene transfer reaction from copper(I) (reaction of compound **3.4 Br** with Cu_2O) to palladium(II) (X = Cl, Br).

3.3 Conclusion

In conclusion, a synthetic procedure has been developed for the synthesis of the novel propanol tethered methyl-imidazolium mesityl calix[4]arene (**3.4**), and the compound has been fully characterised. The properties of the compound in the solid state and in solution have been examined. The studies on compound **3.4** have shown that the hydroxyl groups on the propanol tether form the primary hydrogen bonding interaction with anions, of the type $[(O\text{-}H)^{+}\cdots X^{-}]$, over any other acidic protons in the molecule. This was observed in the solid state and in solution studies.

The use of compound **3.4** as an NHC ligand precursor to form metal-NHC complexes was explored. Compound **3.4** was reacted with basic metal precursors, in an attempt to form the metal-NHC complexes *in situ*. This avoided the need for strong bases and strict inert conditions.

The formation of a silver-NHC by reaction of compound **3.4** with Ag_2O appeared to be successful, inferred by the absence of the C2 proton in the ^{1}H NMR spectra. However, the complex could not be fully characterised and the exact coordination of the silver to the ligand is unknown. The use of the silver-NHC as a ligand transfer agent to palladium did not proceed cleanly and the desired product was not identified.

The reaction of compound **3.4** with $Pd(OAc)_2$ did not form the desired palladium species and instead the palladium(II) was reduced to palladium(0), suggesting that it may have been reacting with another part of the molecule other than the imidazolium group, most likely the hydroxyl groups. The formation of a copper-NHC by reaction of compound **3.4** with Cu_2O appeared to be successful, with the mass spectrometry data indicating mixtures of copper(I)-NHCs (Figure 3.13). Due to the poor solubility of the copper(I)-NHC complexes, combined with their air sensitivity, the reaction mixture could not be purified. The copper(I)-NHC complexes were shown to have potential as carbene transfer agents, as it appeared that palladium could displace the copper metal. The exact nature of the resultant product could not be identified.

Due to the acidic nature of the propanol substituents of compound **3.4**, a predication of the products formed from the metal complexation reactions was not straightforward. There are numerous possibilities as to what the structures of these complexes could be, and the structure will vary based on the preferred coordination geometry of the metal. To date, as no crystal structures of the metal-NHC complexes

have been obtained, there is no evidence as to whether the deprotonated hydroxyl groups on the propanol tether form any interaction with the metal centres.

3.4 Future work

The use of compound **3.4** as an NHC-ligand precursor has been explored through its reaction with basic metal precursors. Further work should be done to explore different synthetic routes to form metal-NHC complexes of compound **3.4**, with the aim of isolating discrete metal-complexes that can be fully characterised. The next approach should be the reaction of compound **3.4** with a strong base (such as ^{n}BuLi), followed by the coordination of the free NHC to a metal centre. Following this synthetic route the hydroxyl groups are likely to remain deprotonated, and form an interaction with the metal centre. Following structure and stability studies, the applications of the metal-NHC complexes can then be explored to evaluate the influence of the calixarene core and propanol tethers on the properties of the metal-NHC complexes.

3.5 References

1. H. M. J. Wang and I. J. B. Lin, *Organometallics*, 1998, **17**, 972-975.
2. C. E. Willans, K. M. Anderson, M. J. Paterson, P. C. Junk, L. J. Barbour and J. W. Steed, *Eur. J. Inorg. Chem.*, 2009, **7**, 2835-2843.
3. I. J. B. Lin and C. S. Vasam, *Coord. Chem. Rev.*, 2007, **251**, 642-670.
4. C. A. Citadelle, N. E. Le, F. Bisaro, A. M. Z. Slawin and C. S. J. Cazin, *Dalton Trans.*, 2010, **39**, 4489-4491.
5. J. C. Garrison and W. J. Youngs, *Chem. Rev.*, 2005, **105**, 3978-4008.
6. M. R. L. Furst and C. S. J. Cazin, *Chem. Commun.*, 2010, **46**, 6924-6925.
7. C. Chen, H. Qiu and W. Chen, *J. Organomet. Chem.*, 2011, **696**, 4166-4172.
8. G. C. Fortman and S. P. Nolan, *Chem. Soc. Rev.*, 2011, **40**, 5151-5169.
9. T. T. Wu and J. R. Speas, *J. Org. Chem.*, 1987, **52**, 2330-2332.
10. M. Staffilani, G. Bonvicini, J. W. Steed, K. T. Holman, J. L. Atwood and M. R. J. Elsegood, *Organometallics*, 1998, **17**, 1732-1740.
11. C. E. Willans, K. M. Anderson, L. C. Potts and J. W. Steed, *Org. Biomol. Chem.*, 2009, **7**, 2756-2760.
12. L.-M. Yang, Y.-S. Zheng and Z.-T. Huang, *Synth. Commun.*, 1999, **29**, 4451-4460.
13. C. E. Willans, K. M. Anderson, P. C. Junk, L. J. Barbour and J. W. Steed, *Chem. Commun.*, 2007, 3634-3636.
14. J. Ehrhart, J. M. Planeix, N. Kyritsakas-Gruber and M. W. Hosseini, *Dalton Trans.*, 2009, 2552-2557.
15. E. K. Bullough, C. A. Kilner, M. A. Little and C. E. Willans, *Org. Biomol. Chem.*, 2012, **10**, 2824-2829.
16. T. Steiner, *Angew. Chem., Int. Ed.*, 2002, **41**, 48-76.
17. E. Brenner, D. Matt, M. Henrion, M. Teci and L. Toupet, *Dalton Trans.*, 2011, **40**, 9889-9898.
18. T. Fahlbusch, M. Frank, G. Maas and J. Schatz, *Organometallics*, 2009, **28**, 6183-6193.
19. D. Qin, X. Zeng, Q. Li, F. Xu, H. Song and Z.-Z. Zhang, *Chem. Commun.*, 2007, 147-149.
20. T. Brendgen, M. Frank and J. Schatz, *Eur. J. Org. Chem.*, 2006, 2378-2383.
21. M. Frank, G. Maas and J. Schatz, *Eur. J. Org. Chem.*, 2004, 607-613.
22. S. T. Liddle, I. S. Edworthy and P. L. Arnold, *Chem. Soc. Rev.*, 2007, **36**, 1732-1744.
23. D. C. F. Monteiro, R. M. Phillips, B. D. Crossley, J. Fielden and C. E. Willans, *Dalton Trans.*, 2012, **41**, 3720-3725.
24. A. Kascatan-Nebioglu, M. J. Panzner, C. A. Tessier, C. L. Cannon and W. J. Youngs, *Coord. Chem. Rev.*, 2007, **251**, 884-895.
25. A. J. Arduengo, III, H. V. R. Dias, J. C. Calabrese and F. Davidson, *Organometallics*, 1993, **12**, 3405-3409.
26. P. L. Arnold, *Heteroat. Chem.*, 2002, **13**, 534-539.
27. A. A. D. Tulloch, A. A. Danopoulos, S. Winston, S. Kleinhenz and G. Eastham, *Dalton*, 2000, 4499-4506.
28. I. J. B. Lin and C. S. Vasam, *Coord. Chem. Rev.*, 2007, **251**, 642-670.
29. P. L. Arnold, A. C. Scarisbrick, A. J. Blake and C. Wilson, *Chem. Commun.*, 2001, 2340-2341.
30. P. L. Chiu, C. Y. Chen, J. Y. Zeng, C. Y. Lu and H. M. Lee, *J. Organomet. Chem.*, 2005, **690**, 1682-1687.
31. C. Gandolfi, M. Heckenroth, A. Neels, G. Laurenczy and M. Albrecht, *Organometallics*, 2009, **28**, 5112-5121.
32. H. Turkmen, O. Sahin, O. Buyukgungor and B. Cetinkaya, *Eur. J. Inorg. Chem.*, 2006, 4915-4921.
33. I. Dinares, M. C. Garcia, M. Font-Bardia, X. Solans and E. Alcalde, *Organometallics*, 2007, **26**, 5125-5128.

34. A. A. D. Tulloch, A. A. Danopoulos, S. Kleinhenz, M. E. Light, M. B. Hursthouse and G. Eastham, *Organometallics*, 2001, **20**, 2027-2031.
35. S. Simonovic, A. C. Whitwood, W. Clegg, R. W. Harrington, M. B. Hursthouse, L. Male and R. E. Douthwaite, *Eur. J. Inorg. Chem.*, 2009, 1786-1795.
36. G. Venkatachalam, M. Heckenroth, A. Neels and M. Albrecht, *Helv. Chim. Acta*, 2009, **92**, 1034-1045.

4 Acetate ester and acetic acid tethered methylimidazolium mesityl calix[4]arene: Ligand synthesis and metal complexation

This chapter discusses the synthesis of a novel 1,3-alternate calix[4]arene, where two of the functional groups project upwards, and two project downwards, in reference to the plane defined by the bridging methylene groups. Acetate ester tethered methylimidazolium mesityl calix[4]arene (**4.2**) has been prepared and examined through ^{1}H NMR spectroscopy and X-ray crystallography. The *tert*-butyl protecting groups were removed from the ester by heating the compound in excess HCl, to form the acid (**4.3**). Acetic acid tethered methylimidazolium mesityl calix[4]arene (**4.3**) offers the potential of forming a bidentate chelating metal-NHC complex, through coordination to the metal *via* both the NHC group and the carboxylate ion upon deprotonation of the acid.[1]

The use of compound **4.2** as an NHC ligand precursor was explored. It was found that the most common approaches reported in the literature for the formation of metal-NHC complexes were not suitable for the formation of metal NHC-complexes when using compound **4.2** as a ligand precursor.[2-5] Under the basic conditions that are required, it appeared that the base reacted with another part of the compound instead of, or in addition to, the C2 proton.

An alternative electrochemical method of metal-NHC formation that has been developed in the Willans group was attempted, that did not require the need for a strong base or a basic metal precursor.[6] This novel synthetic method was used to prepare a copper(I)-NHC complex of our calix[4]arene (**4.6**). It was found that this copper(I)-NHC complex could be used as a ligand transfer agent for the formation of a palladium(II)-NHC complex (**4.7**), the structure of which was confirmed by X-ray crystallography.[7] The use of complex **4.6** as a ligand transfer agent to form other transition metal NHCs was also explored, resulting in the synthesis of a rhodium(I)-NHC complex (**4.8**). To the best of our knowledge, this is the first example of a copper(I)-NHC being used as a ligand transfer agent to prepare a rhodium-NHC complex.

The use of the acetic acid tethered compound **4.3** as an NHC ligand precursor was also explored following the well documented Ag_2O route.[8-10] From analysis by ^{1}H NMR spectroscopy it appeared that Ag_2O reacted with the carboxylic acid functionality, and did not form a silver-NHC. Compound **4.3** was also tested in the electrochemical synthetic procedure but this was not successful. It is likely that the poor solubility of

compound **4.3**, as it is only soluble in DMSO, combined with the side reactions involving the carboxylic acid functionality, resulted in decomposition of the ligand.

4.1 Synthesis of acetate ester and acetic acid tethered methylimidazolium mesityl calix[4]arene (compounds 4.2 and 4.3)

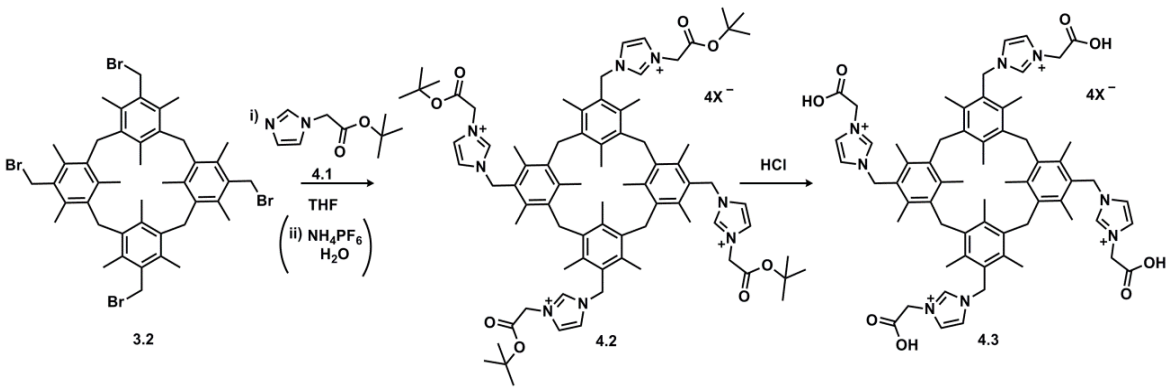

Scheme 4.1 Synthesis of acetate ester (**4.2**) and acetic acid (**4.3**) tethered methylimidazolium mesityl calix[4]arenes (X = Br, Cl or PF_6).

The preparation of bromomethylated mesityl calix[4]arene (**3.2**) was carried out as described in Chapter 3. *Tert*-butyl acetate substituted imidazole (**4.1**) was synthesised from the reaction of *tert*-butyl chloroacetate with imidazole, and the product was purified by column chromatography (Silica gel, 10 % MeOH / chloroform, I_2 active by TLC).[11] The purification of compound **4.1** by column chromatography was found to be necessary to remove any imidazolium species formed *via* further reaction of *tert*-butyl chloroacetate with the second nitrogen of compound **4.1**. This was found to occur even when excess imidazole was used. The product was characterised by ^{1}H NMR and $^{13}C\{^{1}H\}$ NMR spectroscopy, mass spectrometry and elemental analysis.

A THF solution of compound **4.1** was added to a THF solution of compound **3.2**, and the resultant solution was stirred at room temperature for 12 hours under an atmosphere of nitrogen. During this time a white solid precipitated from solution. The solvent was decanted from the solid, and the solid washed with THF and dried *in vacuo*. Compound **4.2 Br** was characterised by ^{1}H NMR and $^{13}C\{^{1}H\}$ NMR spectroscopy combined with mass spectrometry. A ^{1}H NMR spectrum of compound **4.2 Br** in DMSO-d_6 is displayed in Figure 4.1, with the relevant peaks assigned in Table 4.1.

The ^{1}H NMR spectrum of compound **4.2 Br** appears as expected, with a characteristic resonance for the imidazolium C2 proton at δ = 8.92 ppm. The backbone imidazolium protons appear as two separate resonances at δ = 7.81 ppm and δ = 7.57

ppm, with the resonances being too broad to show any coupling between the inequivalent backbone protons. The methylene bridging protons (**H5**) were assigned using 2D HMBC NMR spectroscopy, which showed the two bond coupling of the methylene protons on the acetate tether (**H5**) to the quaternary acetate carbon, which has a characteristic low field resonance in the $^{13}C\{^{1}H\}$ NMR spectrum at δ = 166.1 ppm. Notably the methyl groups on the calix[4]arene framework (**H7** and **H9**) appear as two separate resonance, with those shielded by the aromatic flux being downfield at δ = 1.14 ppm (**H9**), compared to δ = 2.34 ppm for the unshielded methyl groups (**H7**).

The bromide counter ions were exchanged for hexafluorophosphate ions using ammonium hexafluorophosphate in water to afford the hexafluorophosphate salt of **4.2** as a white solid. Compound **4.2 PF_6** was characterised by ^{1}H NMR and $^{13}C\{^{1}H\}$ NMR spectroscopy, mass spectrometry and elemental analysis. The ^{1}H NMR spectrum (DMSO-d_6) of compound **4.2 PF_6** was consistent with the ^{1}H NMR data reported for compound **4.2 Br**. A slight change in the chemical shift was observed for the C2 proton, shifting upfield by 0.13 ppm to δ = 8.80 ppm. This is expected due to the change from a coordinating anion (Br) to a non-coordinating anion (PF_6).

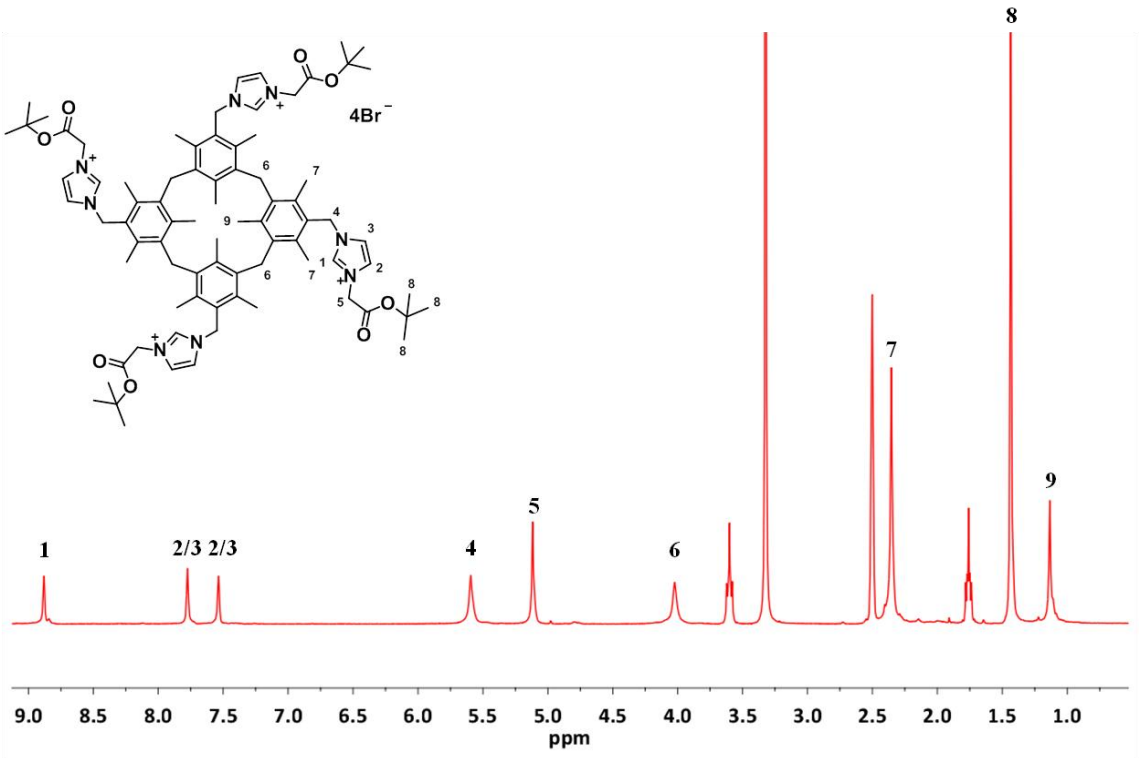

Figure 4.1 ^{1}H NMR spectrum (DMSO-d_6) of **4.2 Br** at 298 K.

Chemical shift (δ ppm) ^{1}H	Assignment
8.92 (s, 4H)	1
7.81 (s, 4H)	2 / 3
7.57 (s, 4H)	2 / 3
5.62 (s, 8H)	4
5.13 (s, 8H)	5
4.01 (s, 8H)	6
2.34 (s, 24H)	7
1.43 (s, 36H)	8
1.14 (s, 12H)	9

Table 4.1 ^{1}H NMR assignments of compound **4.2 Br**.

Colourless crystals of compound **4.2 Br** were obtained by slow diffusion of ethyl acetate into a DMSO solution. These were analysed by single crystal X-ray diffraction and the molecular structure is displayed in Figure 4.2. The compound crystallised in the triclinic crystal system and the structural solution was performed in the space group *P*-1. Two calixarene molecules are contained within the asymmetric unit, with one being removed for clarity in Figure 4.2. The structure displays the expected 1,3-alternate conformation of the calixarene core, with two imidazolium groups projecting upwards, and two projecting downwards. The molecule is locked in this conformation due to the steric constraints of the mesityl groups. However, the tethered imidazoles can freely rotate within that constraint and orientate themselves with different geometries. Compound **4.2 Br** displays the *out-out* conformation, with all four imidazolium groups orientated away from the calixarene core.[9]

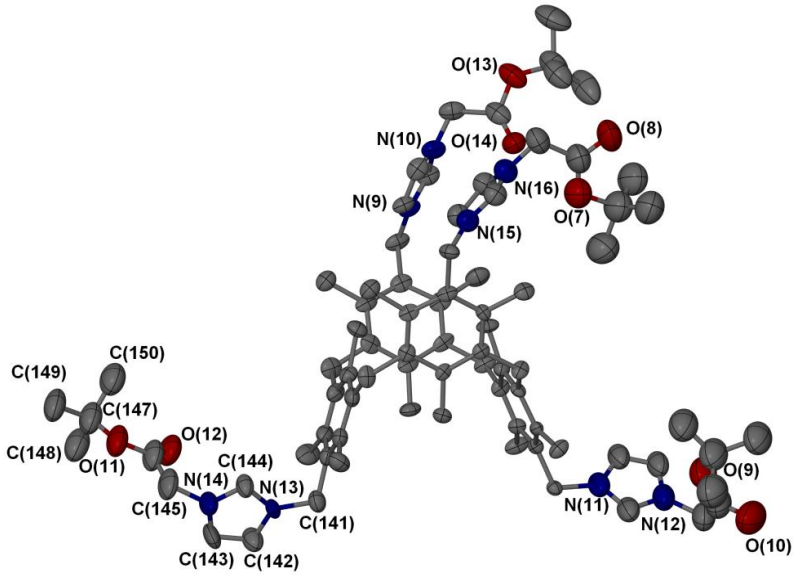

Figure 4.2 Molecular structure of compound **4.2 Br**. One molecule in the asymmetric unit has been omitted. The hydrogen atoms, solvent molecules and 8 bromide counter anions are omitted for clarity. Ellipsoids are displayed at 50% probability.

N(14)-C(144)	1.341(8)	N(14)-C(143)-C(142)	104.1(7)
N(14)-C(143)	1.385(10)	N(14)-C(144)-N(13)	106.3(6)
C(143)-C(142)	1.385(12)		
O(11)-C(147)	1.452(15)		

Table 4.2 Selected bond distances (Å) and angles (deg) for compound **2.4 Br**.

The interactions of compound **4.2** with the bromide anions in the asymmetric unit are displayed in Figure 4.3. **Br1** does not form any interaction with the calixarene and has been removed for clarity. It can be seen from the structure that the bromide anions interact with various acidic imidazolium protons within the structure, not just the C2 protons but also the imidazolium backbone protons. The length of the $[(C\text{-}H)^{+}\cdots Br^{-}]$ interactions range from 2.612 Å (**H112-Br7**) to 2.862 Å (**C93-Br4**), with the full range of $[(C\text{-}H)^{+}\cdots Br^{-}]$ bond lengths being reported in Table 4.3. The interactions are weaker than typical $[H^{+}\cdots Br^{-}]$ hydrogen bonds, which are reported to have a mean bond length of 2.415 Å and a range of 2.24-2.66 Å.[12] The only $[(C\text{-}H)^{+}\cdots Br^{-}]$ interaction in compound **4.2 Br** falling within the reported range is **H112-Br7** with a length of 2.612 Å. The remaining bonds are best described as weak interactions rather than hydrogen bonds. It should be noted that the hydrogen atoms in this structure were not located in the diffraction map and were placed in calculated position using a riding model. However, the distance between the bromide anions and the calculated hydrogen atoms gives an indication of the interactions between the calixarene and the bromide anions.

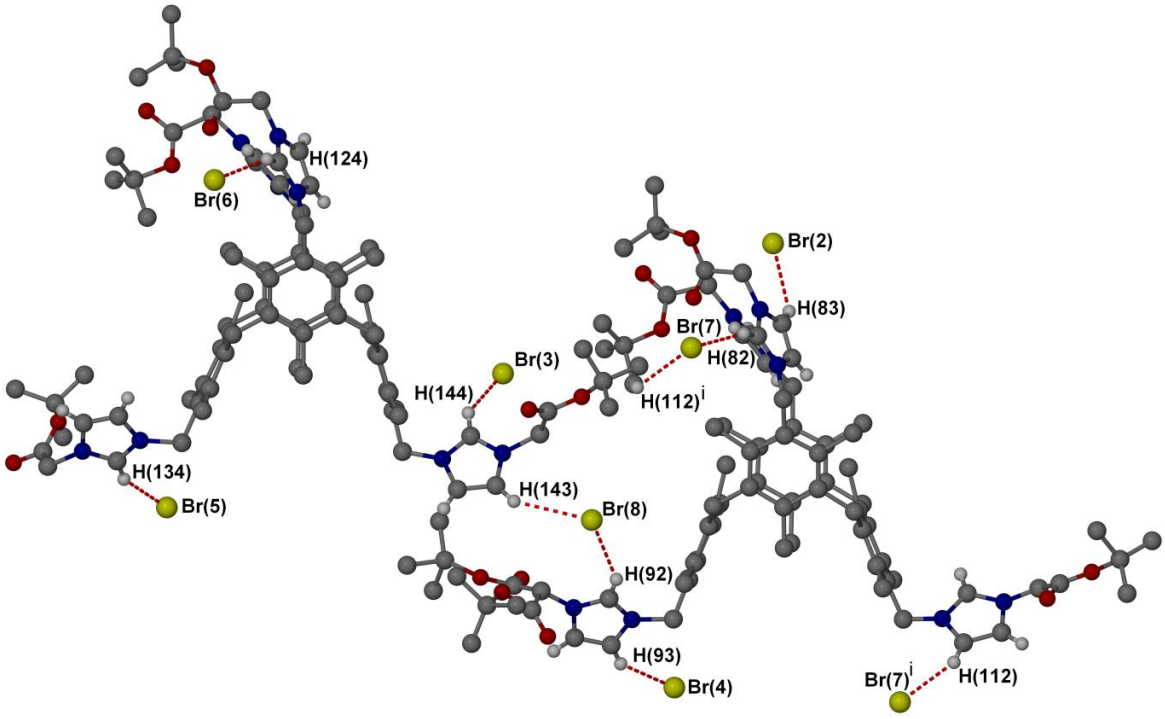

Figure 4.3 X-ray crystal structure displaying the interactions observed in the solid state structure of compound **4.2 Br**. Symmetry operations for symmetry generated atoms i: 1-x, 2-y, -z. The solvent molecules, anions not bonding to the calixarene (Br1), and the hydrogen atoms not involved in the bonding network have been omitted for clarity.

H(112)-Br(7)	2.612	C(112)-Br(7)	3.468
H(82)-Br(7)	2.613	C(82)-Br(7)	3.499
H(92)-Br(8)	2.813	C(92)-Br(8)	3.588
H(143)-Br(8)	2.866	C(143)-Br(8)	3.703
H(114)-Br(3)	2.683	C(114)-Br(3)	3.484
H(83)-Br(2)	2.884	C(83)-Br(2)	3.662
H(134)-Br(5)	2.750	C(134)-Br(5)	3.625
H(124)-Br(6)	2.642	C(124)-Br(6)	3.500
H(93)-Br(4)	2.862	C(93)-Br(4)	3.723

Table 4.3 Interatomic distances (Å) for $[(C\text{-}H)^{+}\cdots Br^{-}]$ interactions.

The *tert*-butyl groups of the ester were removed by dissolving compound **4.2 Br** in excess HCl (aq) and heating at reflux (110 °C) for 1 hour. The solvent was removed *in vacuo*, and the resultant solid was purified by washing with acetone and diethyl ether, and was dried *in vacuo*. Compound **4.3 Br** was analysed by ^{1}H NMR and $^{13}C\{^{1}H\}$ NMR spectroscopy combined with mass spectrometry. The bromide counter ions were exchanged for hexafluorophosphate using ammonium hexafluorophosphate ions in water to afford the hexafluorophosphate salt of **4.3** as a white solid. Compound **4.3 PF_6** was characterised by ^{1}H NMR and $^{13}C\{^{1}H\}$ NMR spectroscopy, along with mass spectrometry. A ^{1}H NMR spectrum of compound **4.3 PF_6** in DMSO-d_6 is displayed in Figure 4.5, with the relevant peaks assigned in Table 4.4.

The ^{1}H NMR spectrum of compound **4.3 PF_6** appears as expected, with the only difference between this and the ^{1}H NMR spectrum of compound **4.2 PF_6** being the loss of the signal for the *tert*-butyl groups at δ = 1.43 ppm. The protons of the hydroxyl groups were not observed in the ^{1}H NMR spectrum in DMSO-d_6 at room temperature. Crystallisations of compound **4.3** were attempted from a range of solvents / solvent systems, but unfortunately no crystals were obtained that were suitable for analysis by single crystal X-ray diffraction. It should be noted that compound **4.3** has the potential to exist as a zwitterion at basic pH, with the carboxylic acid groups being deprotonated (Figure 4.4). However, deliberate attempts to form the zwitterions of **4.3 Br** using

triethylamine did not appear to be successful. Addition of $AgNO_3$ to the product always generated a white precipitate, presumably AgBr, indicating the presence of bromide ions.[13] It is likely that compound **4.3** exists in equilibrium in solution between the hydroxyl groups being protonated and deprotonated, and is dependent on the pH of the solution and the choice of solvent.

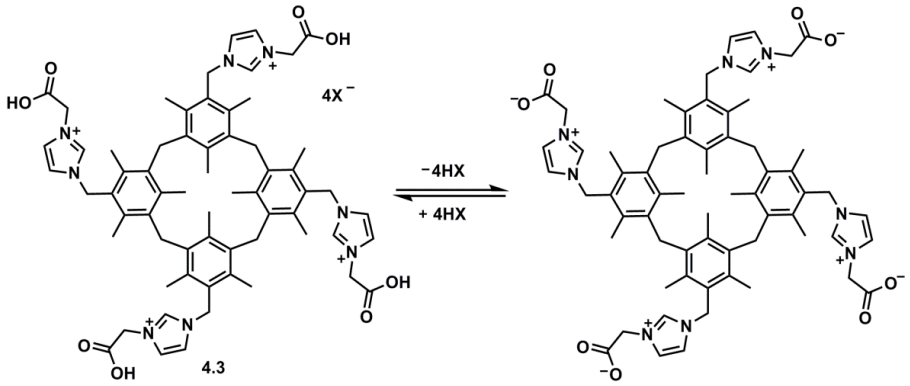

Figure 4.4 Equilibrium between compound **4.3** and the potential zwitterion.

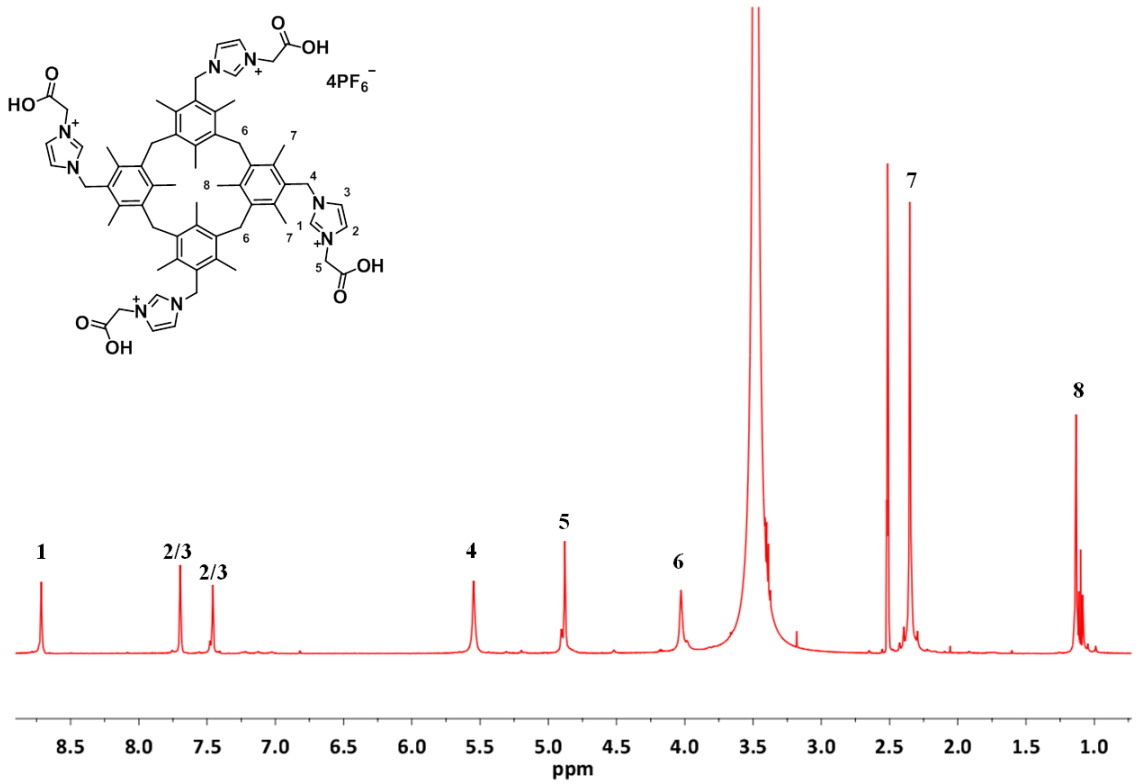

Figure 4.5 ^{1}H NMR spectrum (DMSO-d_6) of **4.3 PF_6** at 298 K.

Chemical shift (δ ppm) ^{1}H	Assignment
8.71 (s, 4H)	1
7.69 (s, 4H)	2 / 3
7.45 (s, 4H)	2 / 3
5.54 (s, 8H)	4
4.87 (s, 8H)	5
4.02 (s, 8H)	6
2.35 (s, 24H)	7
1.13 (s, 12H)	8

Table 4.4 ^{1}H NMR assignments of compound **4.3 PF_6**.

.

4.2 Formation of metal-NHC complexes from acetate ester and acetic acid tethered methylimidazolium mesityl calix[4]arenes (ligand precursors 4.2 and 4.3)

NHC-substituted calixarenes is an area that remains relatively unexplored, with only a few examples reported in the literature.[14-18] As discussed in chapter three, the inclusion of four imidazolium groups onto the 1,3-alternate calix[4]arene scaffold introduces the potential to form four metal-NHC bonds, affording a unique metal-NHC complex. The acetic acid tether was of particular interest (compound **4.3**) as it offers the additional advantage of forming an anionic interaction to the metal centre through the carboxylate ion upon deprotonation of the acid.[19] It was decided that, in order to simplify the number of potential products formed, we would initially explore the formation of metal-NHC complexes using the acetate ester imidazolium **4.2**, where the acetate groups are protected by *tert*-butyl groups.

4.2.1 Traditional routes attempted for the preparation of metal-NHC complexes using NHC-ligand precursor 4.2 Br

Two of the most common methods for the preparation of metal-NHCs are; a) deprotonation of an imidazolium salt and formation of the metal-NHC *in situ*, using a basic metal precursor and b) deprotonation of the imidazolium salt using a base to form the free carbene followed by coordination to a metal centre. Both these routes were investigated using compound **4.2 Br** (Figure 4.6).[2-5]

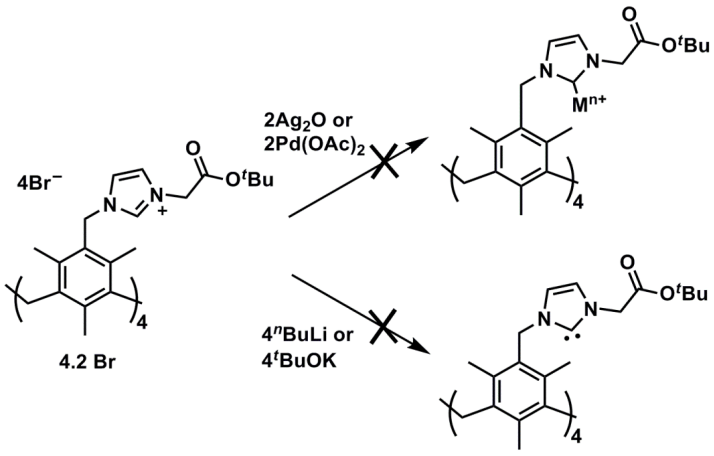

Figure 4.6 Routes attempted to prepare an NHC complex from ligand precursor **4.2**.

The route using a basic metal precursor is often preferred as it negates the need for strong bases and strict inert conditions. The reaction of **4.2 Br** with Ag_2O was

investigated under a range of experimental conditions.[10] However, starting material was always isolated from these reactions, with the C2 proton still present in the ^{1}H NMR spectra. There are examples in the literature where the Ag_2O route has been used to synthesise silver-NHC complexes using functionalised NHC ligand precursors, some of which incorporate acetate ester groups.[20, 21] However, under the range of experimental conditions we explored, we found no evidence for the formation of a silver-NHC. The reaction of compound **4.2 Br** with $Pd(OAc)_2$ was also investigated, but again starting material was isolated from the reaction mixture.[22]

Deprotonation of the imidazolium salt **4.2 Br** to form the free carbene, followed by coordination to a metal centre was explored. The formation of the free carbene was investigated first in an attempt to find a suitable base for the deprotonation step. These reactions were conducted under an atmosphere of argon in anhydrous solvents. Compound **4.2 Br** was dissolved in THF and the solution was cooled to -78 °C. 4.2 equivalents of ^{n}BuLi (1.6 M in hexane) was added and the solution stirred for 1 hour whilst being allowed to warm to room temperature slowly. The ^{1}H NMR spectrum (anhydrous DMSO-d_6) exhibited a low field resonance attributed to the C2 proton, indicating that the free carbene had not been formed. It was not, however, simply starting material that was isolated from the reaction, as the ^{1}H NMR spectrum was more complicated than this (Figure 4.7). The reaction of compound **4.2 Br** with KO^{t}Bu was also conducted using the same experimental procedure, but again the C2-carbon remained protonated, and the ^{1}H NMR spectrum appeared more complex than the starting material, with additional resonances.

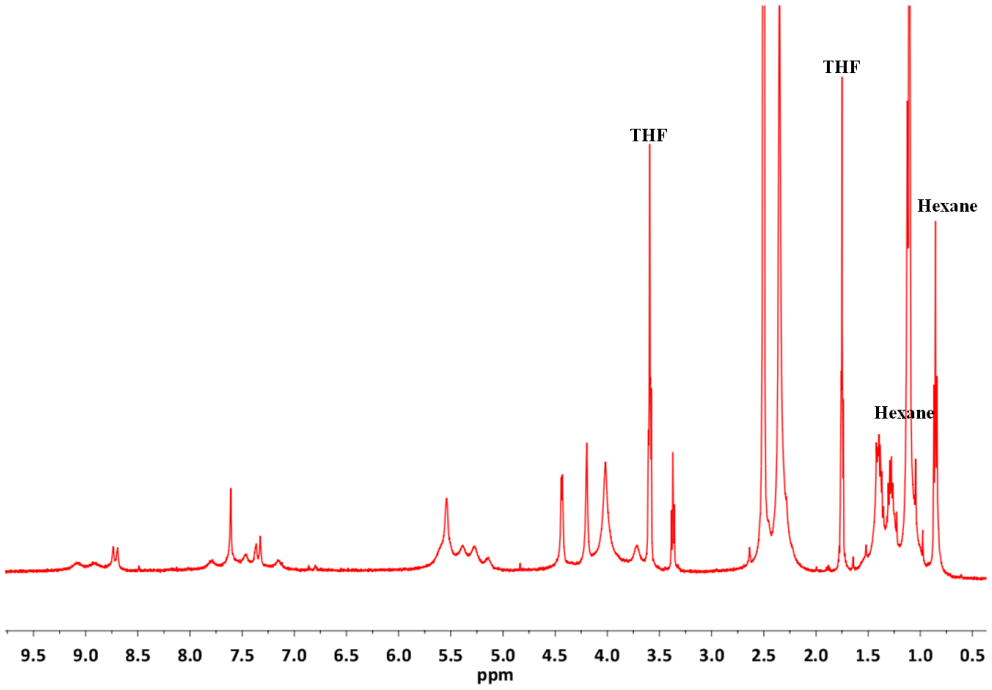

Figure 4.7 ^{1}H NMR spectrum (DMSO-d_6) of the product isolated from the reaction of compound **4.2 Br** with ^{n}BuLi at 298 K.

The reaction was also attempted with the aim of generating the free carbene and coordinating to a metal *in situ*. This removed the possibility that the free carbene was generated in the reaction and was too unstable to be isolated and observed by ^{1}H NMR spectroscopy. Compound **4.2 Br** was dissolved in anhydrous THF and the solution was cooled to 0 °C. 4.2 equivalents of KO^{t}Bu was added and the solution was stirred for 2 hours, whilst slowly warming to room temperature. 4 equivalents of $AgBF_4$ were added and the resultant mixture was stirred at room temperature, in the dark, for 12 hours. The mixture was filtered through celite and the solvent removed *in vacuo*, yielding an off white solid. The ^{1}H NMR spectrum (DMSO-d_6) was complicated, but showed no evidence for the formation of a silver-NHC, with the C2 proton being observed in the ^{1}H NMR spectrum at δ = 8.93 ppm. The reaction was repeated using $PdCl_2(MeCN)_2$ as the metal source under the same reaction conditions, which resulted in a brown solid being isolated from the reaction mixture. The ^{1}H NMR spectrum (DMSO-d_6) was again complicated, but showed no evidence for the formation of the desired palladium-NHC, with the C2 proton being observed at δ = 9.73 ppm. The shift in the signal of the C2 proton, in addition to the increased complication in the ^{1}H NMR spectrum, was indicative of a new compound or compounds being formed.

From these reactions it was evident that, under basic conditions, the imidazolium C2 carbons of compound **4.2 Br** were not being deprotonated, and the increased complication in the ^{1}H NMR spectra suggests that the base was reacting with another part of the compound. It is likely that the methylene groups of the acetate ester substituents have a similar acidity to the imidazolium C2 protons (Figure 4.8). We estimate the pK_a of these protons to be in the region of 20-24, with the pK_a of the imidazolium proton being reported in the region of 20-25.[23] We propose that a base may react with the methylene protons over the C2 protons, resulting in undesired reactions rather than the formation of an NHC.

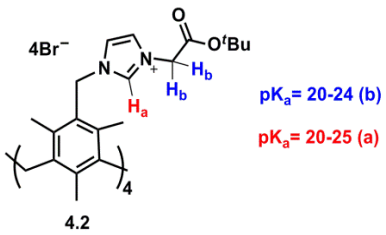

Figure 4.8 Relative acidity of the protons in compound **4.2**.

In order to confirm this theory, 1-methyl-3-*tert*-butylacetate imidazolium chloride (**4.4**) was synthesised. Compound **4.4** has a methyl group in place of the calixarene scaffold, enabling the acetate ester functionality to be investigated thoroughly, without potential interference or complication from the calixarene group. Compound **4.4** was synthesised from the reaction of 1-methylimidazole with *tert*-butyl 2-chloroacetate. The mixture was stirred at room temperature under an atmosphere of nitrogen for 12 hours, during which time the mixture solidified. The product was recrystallised from DCM / hexane and purified further by washing with diethyl ether and dried in *vacuo*, affording compound **4.4** as a white solid. This was characterised by ^{1}H NMR and ^{13}C{^{1}H} NMR spectroscopy, mass spectrometry and elemental analysis. A ^{1}H NMR spectrum of compound **4.4** in DMSO-d_6 is displayed in Figure 4.9, with the relevant peaks assigned in Table 4.5.

The ^{1}H NMR spectrum appears as expected, with the resonance for the C2 proton appearing downfield at δ = 9.31 ppm. Interestingly, the resonances for the imidazolium backbone protons appear as one resonance at δ = 7.78 ppm, suggesting that the protons are coincidently in the same environment.

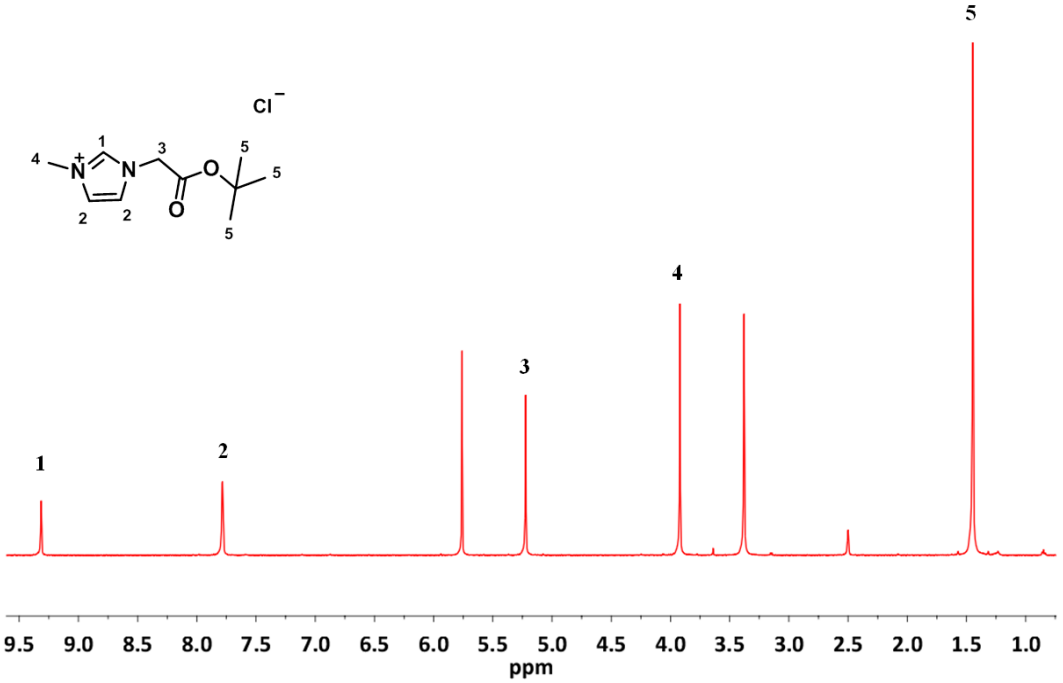

Figure 4.9 ^{1}H NMR spectrum (DMSO-d_6) of compound **4.4** at 298 K.

Chemical shift (δ ppm) ^{1}H	Assignment
9.31 (s, 1H)	1
7.78 (s, 2H)	2
5.22 (s, 2H)	3
3.91 (s, 3H)	4
1.44 (s, 9H)	5

Table 4.5 ^{1}H NMR assignments of compound **4.4**.

As with compound **4.2 Br**, the traditional routes for forming metal-NHC complexes using ligand precursor **4.4** proved unsuccessful (Figure 4.10). The reaction of compound **4.4** with Ag_2O yielded starting material, with the C2 proton still being present in the ^{1}H NMR spectrum. Reactions of compound **4.4** with a base, in an attempt to form the free carbene, showed increased complication in the ^{1}H NMR spectra, with multiple resonances being observed in the CH, CH_2 and CH_3 regions. Furthermore, a characteristic low field resonance was observed for the C2 proton, indicating that the NHC had not been formed. This confirmed that it was the acetate ester functionality that

was causing problems in the synthesis of metal-NHC complexes using compound **4.2 Br**, rather than the calixarene moiety.

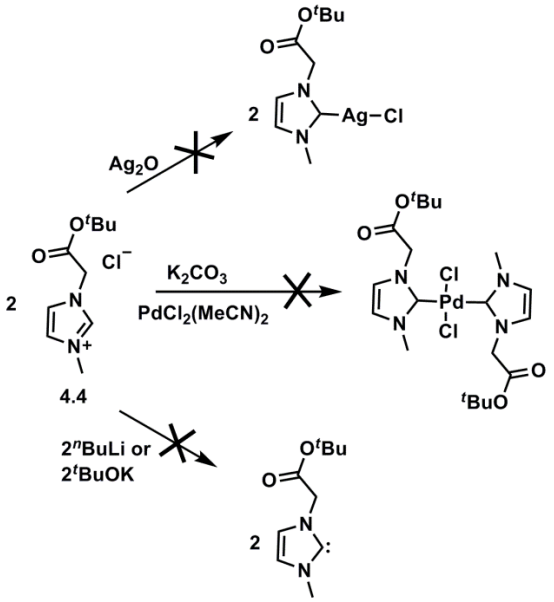

Figure 4.10 Routes attempted to prepare metal-NHC complexes using ligand precursor **4.4**.

4.2.2 Electrochemical synthesis of copper(I)-NHC complexes using NHC-ligand precursor 4.2 Br

In 2011, Liu *et al*. reported an electrochemical procedure for the synthesis of metal-NHC complexes.[24] The electrochemical approach relies upon the redox-active nature of imidazoliums in order to generate free NHCs *in situ*. During the electrochemical reaction the imidazolium is reduced at the cathode, releasing molecular hydrogen, and forming the free NHC (Figure 4.11a). Concomitantly, at the anode the metal is oxidised releasing metal ions into solution (Figure 4.11b). The NHC(s) and metal ion(s) then combine in solution and form the metal-NHC complex (Figure 4.11c). Lin *et al.* describe the synthesis of Cu(I), Cu(II), Ni(II), and Fe(II) metal-NHC complexes of ligands bearing N-pyridine or N-pyrimidine groups using this electrochemical approach.[24] To the best of our knowledge this is the first report of transition metal-NHC complexes being synthesised electrochemically, despite the electrochemical reduction of imidazoliums to form free NHCs having been previously reported.[25-27]

The electrochemical procedure was developed further within the Willans group, and has been successful for the synthesis of a wide range of copper(I)-NHC complexes of monodentate and bidentate ligands that do not contain pendant donor arms.[6] A major advantage of this procedure is that it does not rely on the relative acidity of the

imidazolium proton, only upon the redox potential, making this a viable synthetic route for the synthesis of metal-NHC complexes using imidazolium salts that contain acidic functionalities.

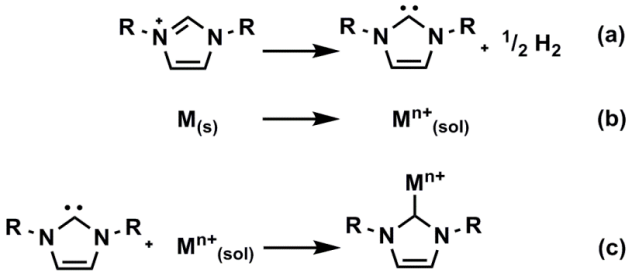

Figure 4.11 Process occurring at the (a) cathode, (b) anode and (c) in solution, during the electrochemical synthesis of metal-NHC complexes.[6]

Compound **4.4** was used in the electrochemical method to investigate if it could be used to generate copper(I)-NHC complexes from imidazolium salts that incorporate nitrogen substituents with acidic protons (Scheme 4.2).

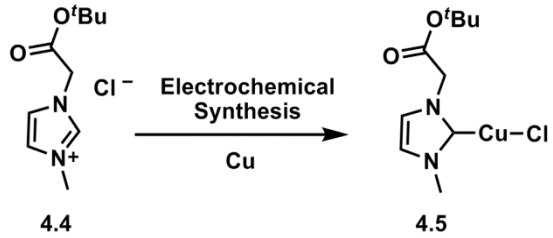

Scheme 4.2 Electrochemical synthesis of complex **4.5**.

Copper plates were used as both the sacrificial anode and the cathode (1 × 3 cm), and the reaction was performed in anhydrous acetonitrile, as this is known to stabilise copper(I) species. Compound **4.4** was added to the flask and degassed. Anhydrous acetonitrile was added (15 ml) and the solution was degassed for 1 hour by bubbling argon through. The electrodes were inserted into the solution and a potential applied such as to maintain a constant current of 50 mA. The reaction was monitored using ^{1}H NMR spectroscopy, and stopped when the resonance attributed to the C2 proton was no longer present. The theoretical reaction time can be calculated using Faraday's law (Figure 4.12), based upon maintaining a constant current throughout the course of the reaction. The solution containing compound **4.4** was electrolysed for 50 minutes, which was calculated to be 2 Q. After this time, the mixture was filtered to remove suspended copper particles, and the solvent removed *in vacuo* to yield complex **4.5** as an off-white solid, which was characterised by ^{1}H NMR and ^{13}C{^{1}H} NMR spectroscopy, mass

spectrometry and elemental analysis. A ^{1}H NMR spectrum ($CDCl_3$) of compound **4.5** is displayed in Figure 4.13, with the relevant peaks assigned in Table 4.6.

$$Q = nFN$$

$$t = \frac{Q}{I}$$

Q = total charge (C or A)
n = number of electrons transferred
F = Faraday's constant (C mol^{-1})
N = moles of starting material (mol)
I = current (A)
t = time (s)

Figure 4.12 Faraday's law

From the ^{1}H NMR spectrum it is evident that a copper-NHC complex has been formed, due to the disappearance of the resonance attributed to the C2 proton that was observed at δ = 9.15 ppm (DMSO-d_6) in the imidazolium starting material. Markedly, the backbone imidazolium protons (**1** / **2**) now appear as two separate resonances at δ = 6.98 ppm and δ = 6.93 ppm. This could be a result of metal complexation, or it could be a solvent effect, as the starting material is not soluble in chloroform so the ^{1}H NMR spectra of compound **4.4** and complex **4.5** (Figures 4.9 and 4.13) cannot be directly compared in this case. The ^{13}C{^{1}H} NMR spectrum also displays a low field resonance at δ = 178 ppm that corresponds to the carbenic carbon atom coordinating to copper.

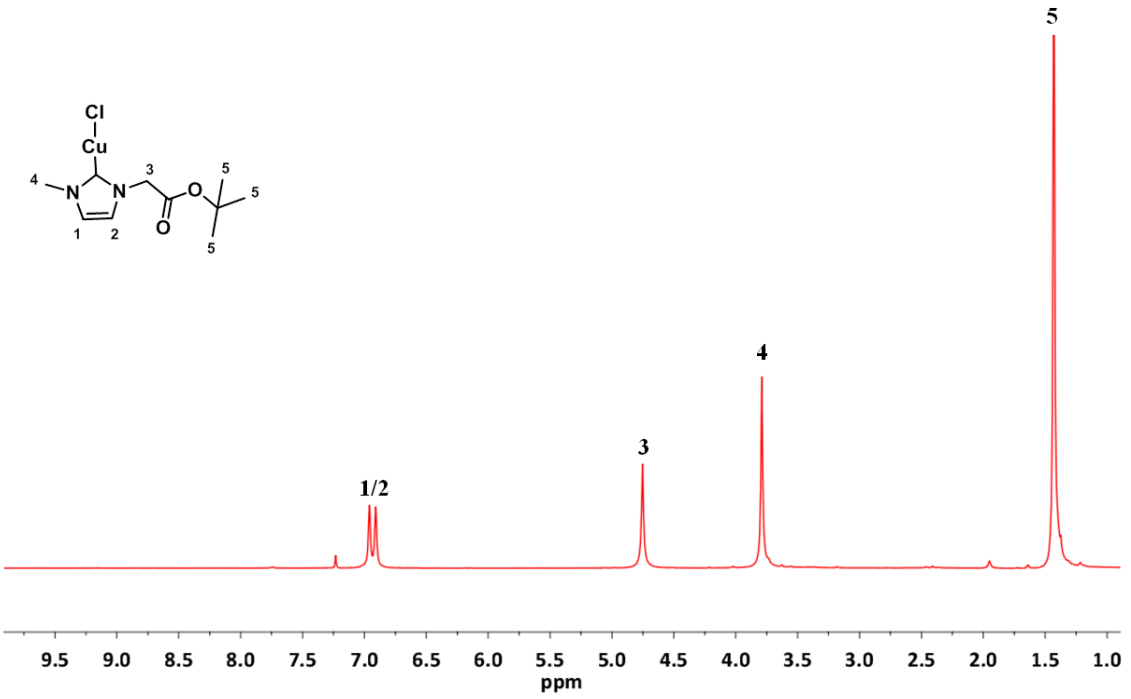

Figure 4.13 ^{1}H NMR spectrum ($CDCl_3$) of complex **4.5** at 298 K.

Chemical shift (δ ppm) ^{1}H	**Assignment**
6.98 (s, 1H)	1 / 2
6.93 (s, 1H)	1 / 2
4.78 (s, 2H)	3
3.81 (s, 3H)	4
1.45 (s, 9H)	5

Table 4.6 ^{1}H NMR assignments of complex **4.5**.

The mass spectrometry data confirmed the presence of a copper(I)-NHC complex with an *m/z* observed for [**4.5**-Cl+MeCN]$^{+}$ at 300.1. It has been established by the Willans group that, when using the electrochemical synthetic method, imidazoliums that contain a coordinating anion (such as chloride or bromide) form a neutral complex of the type Cu(NHC)X, whereas, imidazoliums with a non coordinating anion (such as PF_6) form a cationic complex of the type $[Cu(NHC)_2]^{+}X^{-}$.[6] Consequently the neutral copper(I)-NHC was the expected structure for complex **4.5**. However, the cationic $[Cu(NHC)_2]^{+}$

complex was also observed in the mass spectrometry data with *m/z* at 455.2. Fluxional behaviour between the cationic and neutral complexes is known, and has been observed for d^{10} metals previously, with silver complexes [Ag(NHC)X] and $[Ag(NHC)_2]^+AgX_2^-$ being observed in equilibrium in solution.[4] However, the ^1H NMR and $^{13}C\{^1H\}$ NMR spectrum of complex **4.5** suggest the formation of one species in acetonitrile, which is the solvent used in the mass spectrometry experiments. Therefore it is likely that the cationic complex is formed during the mass spectrometry analysis as the complex is ionised. A mass is also observed for the imidazolium starting material, suggesting that the complex is fragmented during the ionisation process. The formation of the neutral complex of the type Cu(NHC)Cl was confirmed by elemental analysis. Complex **4.5** was found to be extremely air / moisture sensitive, which is often observed for 'non bulky' NHCs, where the nitrogen substituents do not provide sufficient steric protection around the carbenic centre.

As the electrochemical synthetic method proved to be compatible using ligand precursor **4.4**, it was explored using our calixarene compound **4.2 Br** (Scheme 4.3).

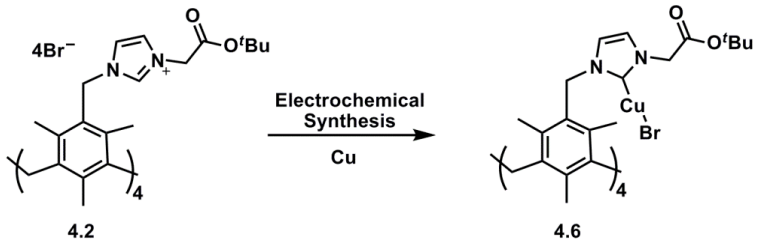

4.2 4.6

Scheme 4.3. Electrochemical procedure for the synthesis of complex **4.6.**

The reaction was carried out as described previously, using compound **4.2 Br** in place of compound **4.4** and monitoring the reaction using ^1H NMR spectroscopy. The mixture was electrolysed for 32 hours, (6 Q), at a current of 10 mA. Compound **4.2 Br** is a poorer electrolyte than compound **4.4** and a current of 10 mA was the highest that could be achieved during the reaction. Complete disappearance of the C2 proton resonance after 6 Q indicated that the reaction was complete. The reaction time was considerably longer than that of the monodentate imidazolium precursor (compound **4.4**), which had a reaction time of 2 Q. We have not yet determined why these electrochemical reactions take longer than the predicated time (i.e. Q).

Figure 4.14 shows the ^1H NMR spectra of the reaction as it progressed. It can be seen that, as the mixture was electrolysed, multiple products were formed. For example, if we examine the resonance for the C2 imidazolium proton between 0 Q and 6 Q we

can see that the signal moves upfield and splits, with multiple resonances being observed before disappearing at 6 Q. It is likely that a mixture of the 1-, 2-, 3- and 4-copper-NHC complexes form as the reaction proceeds, until the reaction is driven to completion and the desired 4-copper-NHC complex is formed (**4.6**).

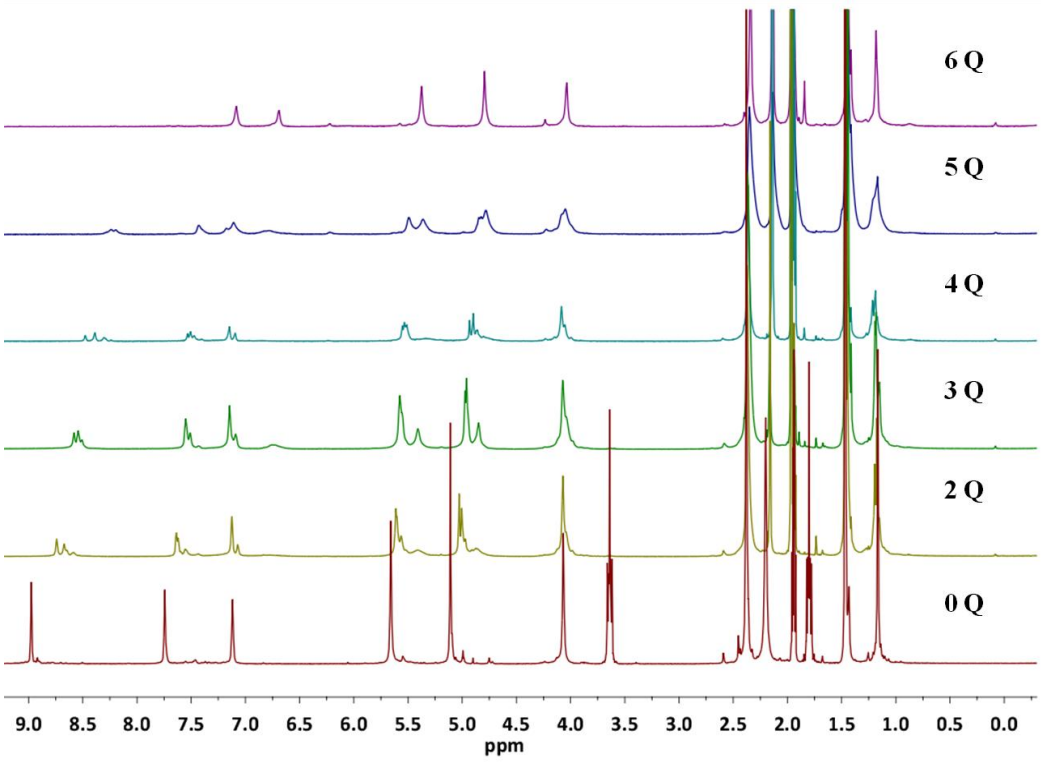

Figure 4.14 ^{1}H NMR spectra (MeCN-d_3) taken during the electrolysis of compound **4.2 Br**, from starting material (0 Q), to product **4.6** (6 Q) recorded at 298 K.

Following the completion of the above reaction the solvent was removed *in vacuo*, and the resultant solid was dissolved in DCM and filtered to remove suspended metal particles. The solvent was removed from the filtrate *in vacuo* to yield complex **4.6** as a pale yellow solid, which was characterised by ^{1}H NMR and ^{13}C{^{1}H} NMR spectroscopy combined with mass spectrometry. The ^{1}H NMR spectrum is displayed in Figure 4.15 with the relevant peaks assigned in Table 4.7. From the ^{1}H NMR spectrum (MeCN-d_3) it is evident that the copper(I)-NHC complex has formed due to the disappearance of the resonance attributed to the C2 proton, that was observed at δ = 8.92 ppm in the starting imidazolium material (**4.2 Br**). The ^{13}C{^{1}H} NMR spectrum displays a low field resonance at δ = 178. 6 ppm attributed to the C2 carbon bound to copper. The mass spectrometry data is consistent with the formation of complex **4.6**, with the *m/z* observed at 1879.2 for [**4.6**+H]$^{+}$.

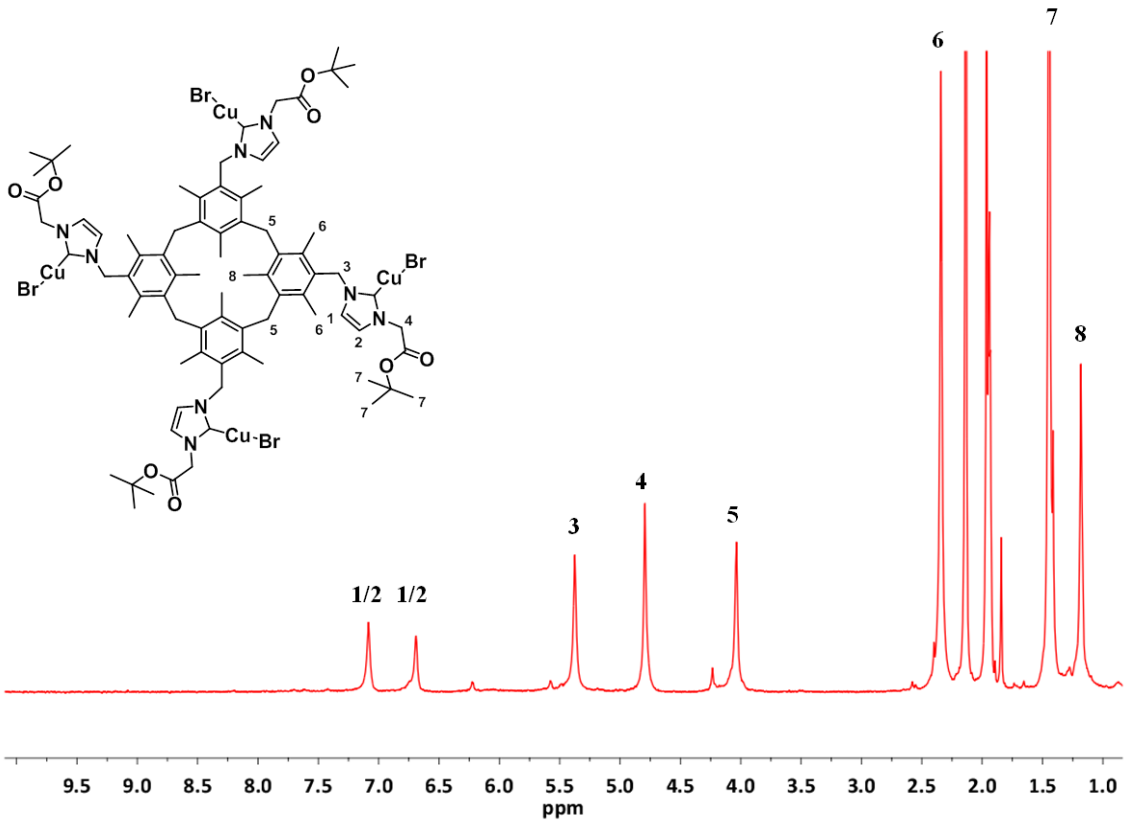

Figure 4.15 ^{1}H NMR spectrum (MeCN-d_3) of complex **4.6** at 298 K.

Chemical shift (δ ppm) ^{1}H	Assignment
7.08 (s, 4H)	1 / 2
6.69 (s, 4H)	1 / 2
5.37 (s, 8H)	3
4.79 (s, 8H)	4
4.03 (s, 8H)	5
2.34 (s, 24H)	6
1.44 (s, 36H)	7
1.18 (s, 12H)	8

Table 4.7 ^{1}H NMR assignments of complex **4.6**.

Complex **4.6** appears more stable than complex **4.5**, however it was still found to be air / moisture sensitive. If exposed to air, the complex degrades over a few hours in

solution, and over a few days in the solid state. Although the calixarene is a large molecule it does not provide a large degree of steric protection around the carbenic centre, therefore this would still be considered a 'non-bulky' NHC, accounting for the relative instability. Crystallisations of complex **4.6** were attempted in a range of solvents / solvent mixtures, however no crystals were obtained that were suitable for analysis by single crystal X-ray diffraction.

4.2.3 Transmetallation from Cu(I)-NHC complex 4.6 to palladium(II)

An attractive route for the synthesis of a range of transition metal-NHC complexes is to use ligand transfer from one metal to another. The most widely used NHC transfer agents are silver(I)-NHC complexes, which have been shown to transfer NHC-ligands to a wide range of transition metals (Pd(II), Ru(II), Ru(III), Ru(IV), Rh(I), Rh(III), Ir(I), Ir(III), Au(I), Ni(II), Cu(I), Cu(II)).[10, 28] Silver(I)-NHC complexes are widely used due to their relative ease of synthesis. The reaction of an imidazolium salt with a basic silver reagent forms the silver-NHC *in situ*, and the procedure circumvents the need for anoxic conditions.[8] Other transition metal-NHC complexes have also been reported as transmetallation agents; gold(I)-NHCs have been used to prepare palladium(II)-NHC complexes, and nickel(II)-NHCs have recently been used to prepare palladium(II)-, platinum(II)-, cobalt(III)- and ruthenium(II)-NHC complexes.[29, 30] Conveniently, copper(I)-NHCs have also been reported as carbene transfer agents and, to the best of our knowledge, the transmetallation from copper(I)-NHCs has been limited to ruthenium(II), palladium(II), nickel(II) and gold(I).[7, 31, 32]

Until recently, the most widely reported method of forming copper(I)-NHC complexes was through using a strong base to form the free NHC, then adding a CuX salt (where X = halide).[33-35] These reactions require strict anoxic conditions and generate undesirable inorganic salts as by-products. With the development of new methodologies for the synthesis of Cu(I)-NHC complexes such as a) using Cu_2O in analogy to Ag_2O or b) the electrochemical synthesis of copper(I)-NHCs, the use of copper(I)-NHC complexes as ligand transfer agents is becoming more attractive.[6, 36] Cu(I)-NHC complex **4.6** was investigated as a transmetallation agent to prepare a palladium(II)-NHC complex.

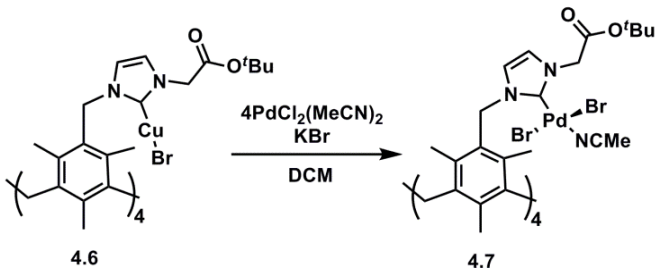

4.6 4.7

Scheme 4.4 Synthesis of palladium-NHC complex **4.7**.

Complex **4.6** was reacted with four equivalents of $PdCl_2(MeCN)_2$, in the presence of excess KBr, in anhydrous DCM (Scheme 4.4). The addition of KBr ensured that all the halide atoms in the resulting complex were bromide atoms rather than generating a mixed chloride / bromide complex. After 12 hours the solvent was removed *in vacuo* and the resulting dark red solid was dissolved in acetonitrile and filtered through celite. The product was precipitated from acetonitrile by the addition of diethyl ether, collected by gravity filtration, and purified by column chromatography (silica gel, MeCN). Complex **4.7** was collected as a dark red solid and analysed by ^{1}H NMR and ^{13}C{^{1}H} NMR spectroscopy, mass spectrometry and elemental analysis. The ^{1}H NMR spectrum is displayed in Figure 4.16 with the relevant peaks assigned in Table 4.8.

The ^{1}H NMR spectrum (MeCN-d_3) is indicative of a metal-NHC complex, as there is no high field resonance attributed to the C2 proton. The remaining signals have shifted compared to the starting copper(I)-NHC complex, suggesting that transfer to palladium has occurred. The ^{13}C{^{1}H} NMR spectrum (MeCN-d_3) no longer displays the resonance for the C2-carbon bound to copper at δ = 178.6 ppm, and instead displays a low field resonance at δ = 147.3 ppm. This is consistent with palladium(II)-NHC complexes that have a *trans*-coordinating two electron donor ligand such as PdX_2(NHC)(py) or PdX_2(NHC)(MeCN).[37, 38] This provides evidence that the monodentate NHC complex PdX_2(NHC)(MeCN) has been formed, rather than the bidentate palladium-NHC complex $PdX_2(NHC)_2$, which would display a resonance for the C2 carbon bound to palladium further downfield at δ = 160 - 170 ppm.[14] Mass spectrometry data further confirms the presence of the expected palladium-NHC complex, with a signal at *m/z* 992.8 for [**4.7**-4^{t}Bu-2Br-4MeCN]$^{2+}$ (Figure 4.17).

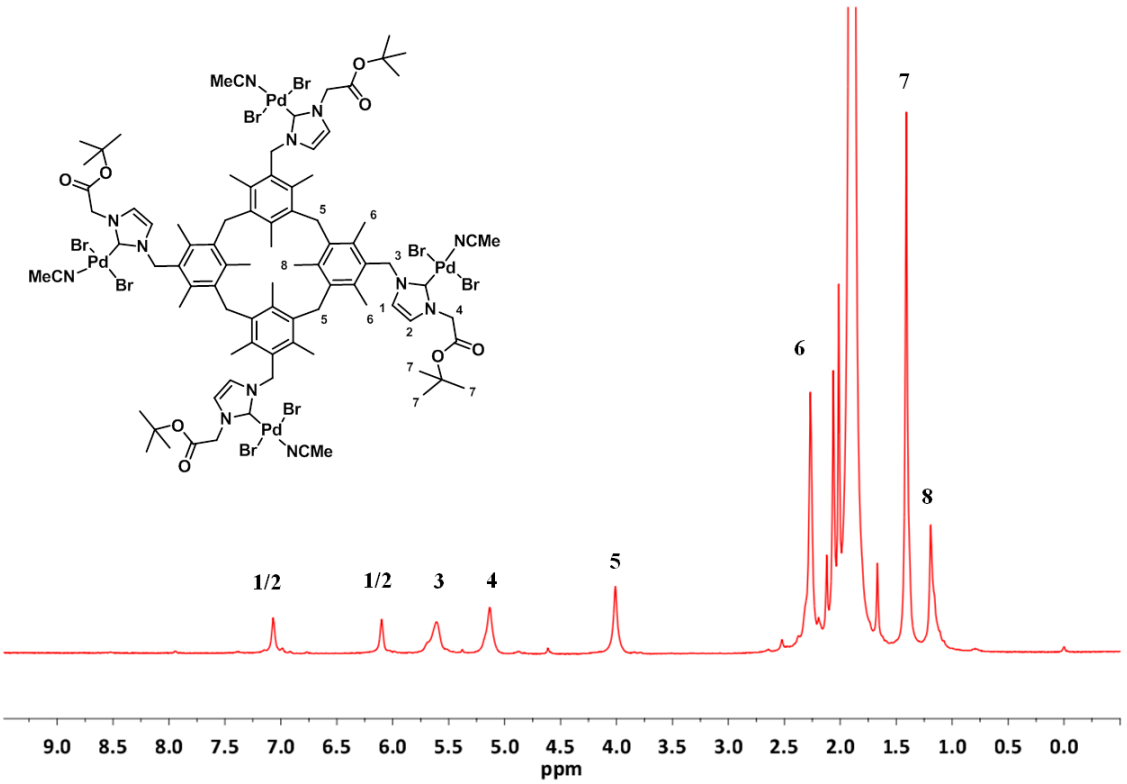

Figure 4.16 ^{1}H NMR spectrum (MeCN-d_3) of complex **4.7** at 298 K.

Chemical shift (δ ppm) ^{1}H	**Assignment**
7.11 (s, 4H)	1 / 2
6.14 (s, 4H)	1 / 2
5.6 (s, 8H)	3
5.2 (s, 8H)	4
4.05 (s, 8H)	5
2.3 (s, 24H)	6
1.46 (s, 36H)	7
1.24 (s, 12H)	8

Table 4.8 ^{1}H NMR assignments of complex **4.7**.

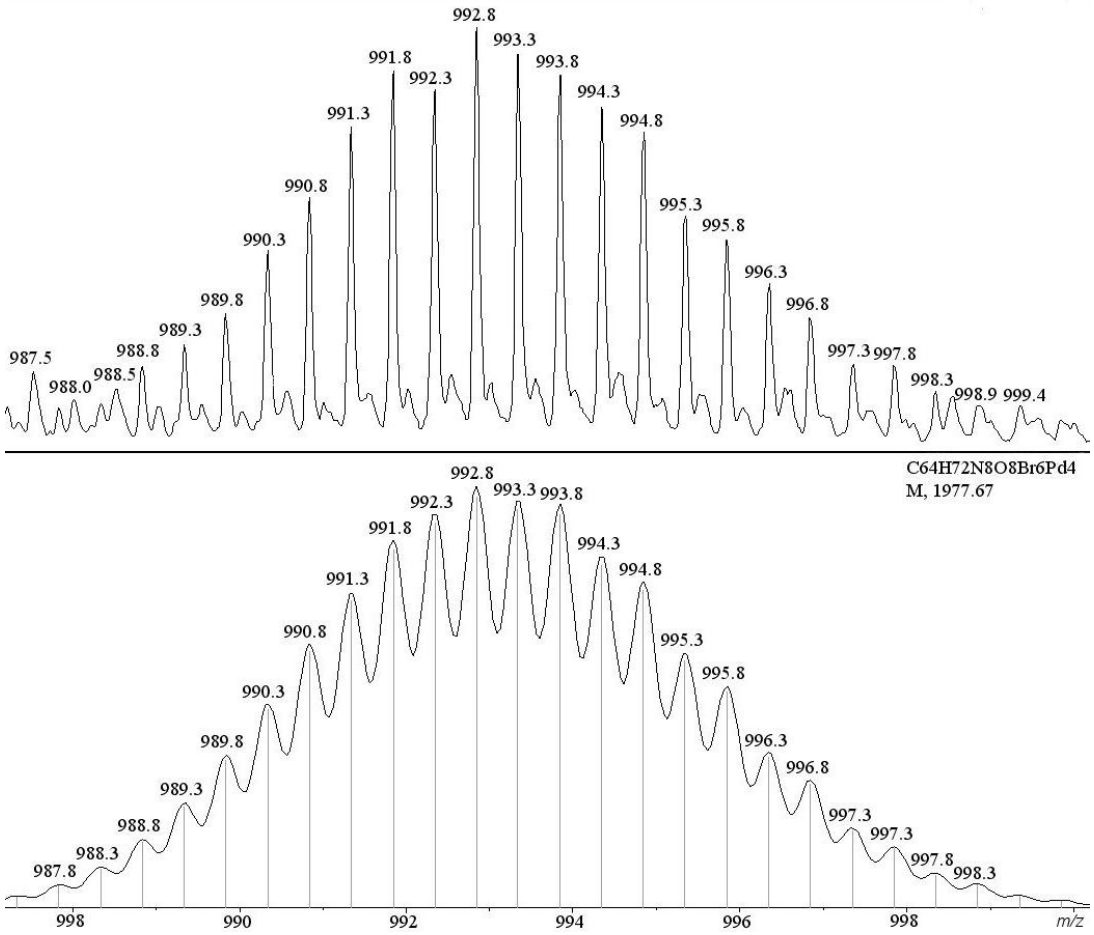

Figure 4.17 Mass spectrometry data of complex **4.7** (top): calculated for [**4.7**-4^{t}Bu-2Br-4MeCN]$^{2+}$ (bottom).

The structure of the palladium-NHC complex was confirmed using single crystal X-ray diffraction analysis. Yellow plate crystals were obtained by the slow diffusion of pentane into an acetonitrile solution of complex **4.7**. The molecule crystallised in the monoclinic crystal system, and the structural solution was performed in the space group *C*2/*c*. Only half the calixarene molecule is contained within the asymmetric unit. The crystals were highly sensitive to de-solvation and were weakly diffracting. There was significant void space and diffuse electron density which could not be accurately modelled, hence the routine SQUEEZE in the interface PLATON was employed.[39] The molecular structure is displayed in Figure 4.18 with selected bond lengths and angles in Table 4.9.

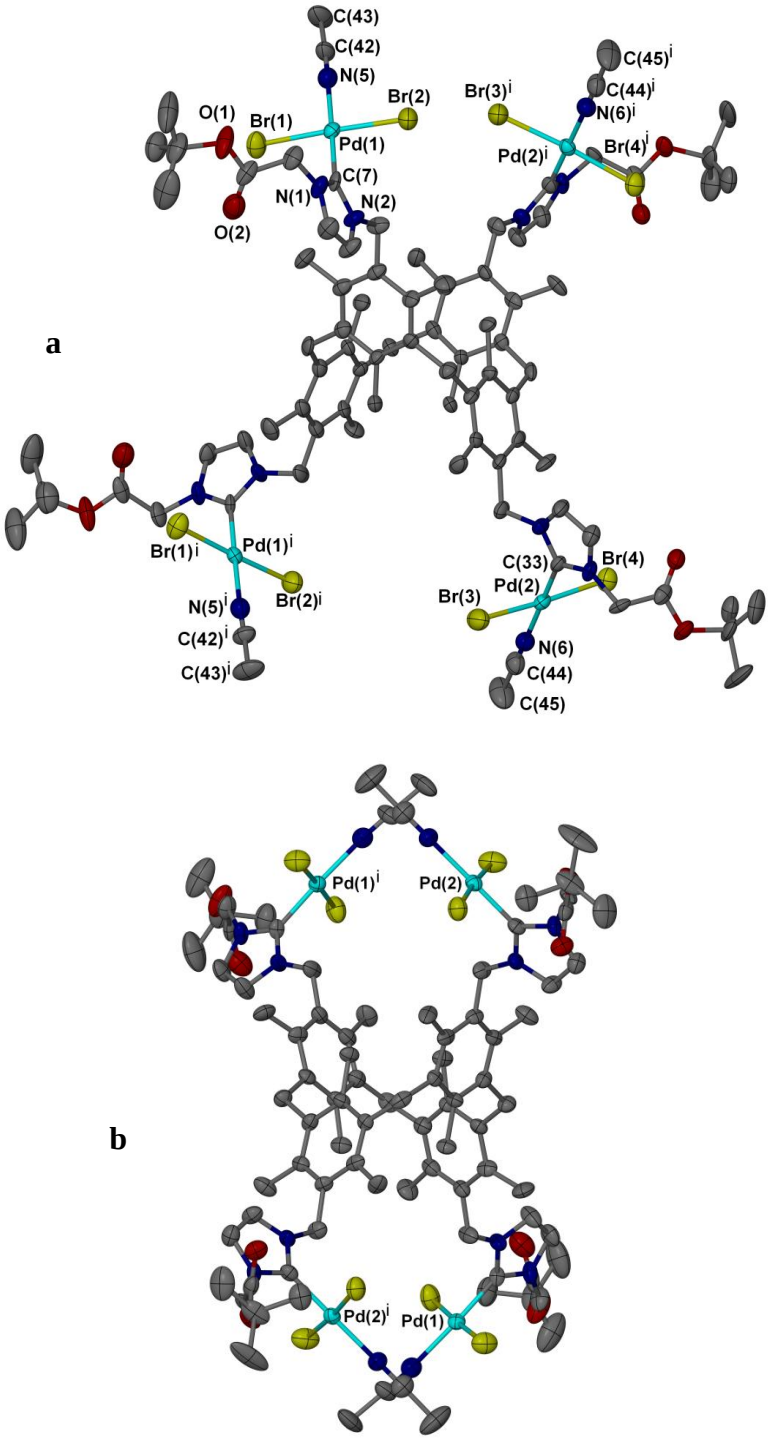

Figure 4.18 X-ray crystal structure of complex **4.7**. Symmetry operations for symmetry generated atoms i: 1-x, y, 3/2-z. The acetonitrile molecules not coordinating to the palladium atoms and hydrogen atoms have been omitted for clarity. Ellipsoids are displayed at 50 % probability.

Pd(1)-C(7)	1.972(10)	C(7)-Pd(1)-N(5)	177.5(4)
Pd(1)-N(5)	2.103(11)	C(7)-Pd(1)-Br(1)	86.8(3)
Pd(1)-Br(1)	2.4412(16)	N(5)-Pd(1)-Br(1)	92.0(3)
Pd(1)-Br(2)	2.4481(16)	C(7)-Pd(1)-Br(2)	91.0(3)
Pd(2)-C(33)	1.973(11)	N(5)-Pd(1)-Br(1)	90.2(3)
Pd(2)-N(6)	2.079(10)	Br(1)-Pd(1)-Br(2)	177.73(6)
Pd(2)-Br(3)	2.4353(17)	C(33)-Pd(2)-Br(4)	87.1(3)
Pd(2)-Br(4)	2.4461(16)	N(6)-Pd(2)-Br(3)	91.1(3)
N(1)-C(7)	1.375(13)	N(6)-Pd(2)-Br(3)	92.9(3)
N(5)-C(42)	1.129(16)	C(33)-Pd(2)-Br(3)	88.8(3)
		N(2)-C(7)-N(1)	105.2(9)

Table 4.9 Selected bond distances (Å) and angle (deg) for complex **4.7**.

The structure displays the expected 1,3-alternate conformation of the calixarene core, with two NHC groups projecting upwards and two projecting downwards. As implied by the $^{13}C\{^{1}H\}$ NMR spectroscopy and mass spectrometry data, the monodentate palladium-NHC complex of the type $PdBr_2(NHC)(MeCN)$ was formed, incorporating four palladium(II) centres per calixarene molecule. The coordination geometry around the palladium is square planar, with two coordinating bromide atoms and an acetonitrile molecule *trans* to the NHC ligand (max deviation from the square planar geometry **C7-Pd1-Br1** angle 86.8 °). The acetonitrile molecule is weakly bound owing to the *trans* effect of the NHC ligand, with the bond length of **Pd1-N5** being 2.103(10) Å, and **Pd2-N6** being 2.079(10) Å. The Pd-C bond lengths, **Pd1-C7** 1.972(10) Å and **Pd2-C33** 1.973(11) Å, are in the range of the literature values for palladium-NHC complexes of the type $PdX_2(NHC)(MeCN)$.[5, 38]

Each palladium atom is orientated towards one side of the cavity, with opposite palladium atoms positioned on opposite sides (Figure 4.18b). The packing diagram for complex **4.7** shows that the calixarene molecules are arranged in 2D layers, with acetonitrile groups positioned between the layers (Figure 4.19). The 2D channels

between the acetonitrile molecules measure approximately 9 Å by 11 Å, and the smaller channels observed between the neighbouring calixarene molecules measure approximately 3 Å by 11 Å. The structure shows that the palladium centres are buried within the molecule and are not very exposed. This may be advantageous for the use of the complex as a catalyst, as it may stabilise the active species (Chapter 5).

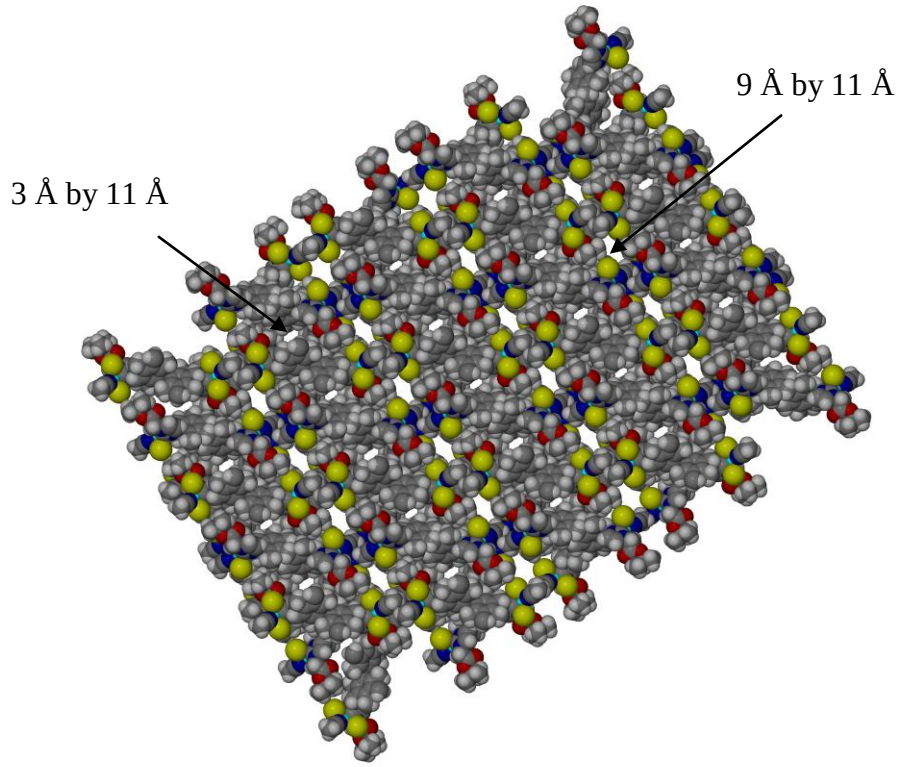

Figure 4.19 X-ray crystal packing diagram of complex **4.7** showing the palladium atoms are buried within the molecule.

4.2.4 Transmetallation from Cu(I)-NHC complex 4.6 to other transition metals

The transmetallation of the NHC ligand in complex **4.6** to Ru(II) was explored following a procedure outlined by Albrecht *et al.*[31] Complex **4.6** was reacted with two equivalents of $[RuCl_2(cymene)]_2$, in the presence of KBr, in anhydrous DCM (Scheme 4.5). The solution was filtered through celite and the solvent removed *in vacuo* to yield a red solid that was analysed by ^1H NMR and $^{13}C\{^1H\}$ NMR spectroscopy combined with mass spectrometry. The ^1H NMR and $^{13}C\{^1H\}$ NMR spectra (DCM-d_2 / $CDCl_3$) were broad and gave no insight as to the identity of the product. The mass spectrometry data showed the presence of ruthenium containing species from the observed splitting pattern, but the *m/z* signals were not large enough to incorporate the calixarene framework. Crystallisations were attempted in a range of solvents / solvent mixtures,

but only the ruthenium precursor, $[RuCl_2(cymene)]_2$ or $RuCl_2(MeCN)_4$ (crystallisations set in up MeCN) crystallised from solution, suggesting that the ligand was not transferred. The reaction was repeated in a sealed ampoule with the temperature raised to 40 °C, in an attempt to promote the transmetallation reaction. The same result was observed as previously, with $[RuCl_2(cymene)]_2$ crystallising from solution (DCM / diethyl ether).

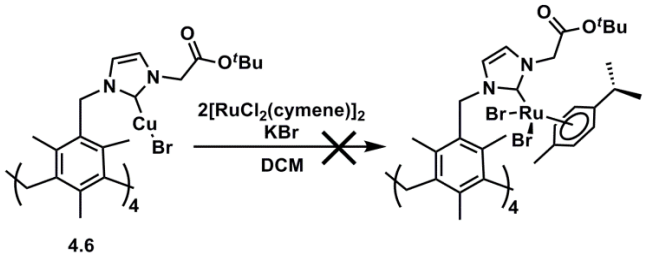

4.6

Scheme 4.5 Reaction Scheme for the attempted carbene transfer reaction from copper(I) (complex **4.6**) to ruthenium(II).

The transmetallation of the NHC ligand in complex **4.6** to nickel(II) was explored. Complex **4.6** was reacted with four equivalents of $NiBr_2(PPh_3)$ in anhydrous DCM (Scheme 4.6). The solution was filtered through celite and the solvent removed *in vacuo* to yield a yellow solid. The solid was washed with diethyl ether, dried *in vacuo*, and the product analysed by ^{1}H NMR and $^{13}C\{^1H\}$ NMR spectroscopy combined with mass spectrometry. There was no evidence from the analytical data that any product had formed, with only simple nickel salts being identified by X-ray crystallography (e.g. $NiBr(PPh_3)_3$). The reaction was repeated in a range of solvents, but a nickel-NHC complex was never identified.

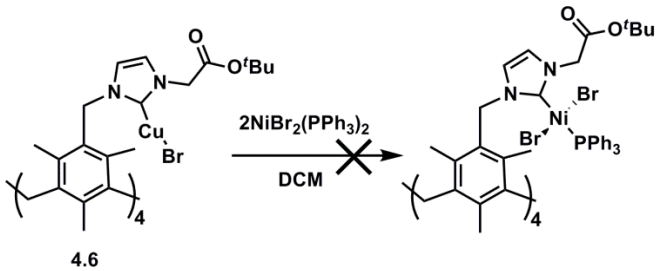

4.6

Scheme 4.6 Reaction scheme for the attempted carbene transfer reaction from copper(I) (complex **4.6**) to nickel(II).

The transmetallation of the NHC ligand in complex **4.6** to rhodium(I) was also explored. To the best of our knowledge a transmetallation reaction from copper(I) to rhodium(I) has not been previously reported. Complex **4.6** was reacted with two

equivalents of $[Rh(COD)Cl]_2$ in anhydrous chloroform (Scheme 4.7). The solution was filtered and the solvent removed from the filtrate *in vacuo* to yield a yellow solid. The product was analysed by ^{1}H NMR and $^{13}C\{^{1}H\}$ NMR spectroscopy combined with mass spectrometry.

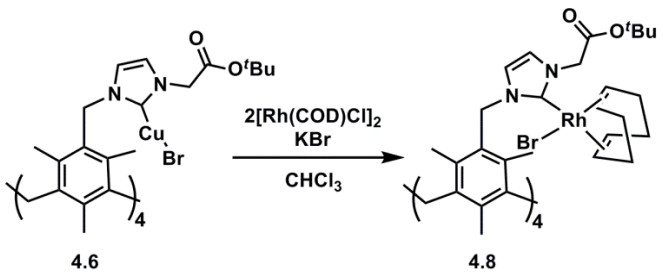

4.6 4.8

Scheme 4.7 Proposed product from the attempted carbene transfer reaction from copper(I) (complex **4.6**) to rhodium(I).

Figure 4.20 displays the ^{1}H NMR spectra ($CDCl_3$) starting from the Cu(I)-NHC complex **4.6** (**A**), 10 minutes after addition of $[Rh(COD)Cl]_2$ (**B**), and after 12 hours of reaction (**C**). The spectrum of the final product (**C**) is too broad to be fully assigned, though signals can be observed in the correct regions for the CH, CH_2 and CH_3 groups, and no low field resonance for the C2 imidazolium proton is present suggesting the formation of a new carbene complex.

The $^{13}C\{^{1}H\}$ NMR spectrum of the product does not exhibit the resonance at δ = 178.6 ppm attributed to the C2 carbon bound to copper in complex **4.6**, and instead displays a low field doublet resonances at δ = 182.15 ppm. This can be assigned to the C2 carbon coordinated to rhodium(I), with a Rh-C coupling constant of 50.1 Hz, which is typical for rhodium(I)-NHC complexes.[40] The formation of the rhodium(I) complex (**4.8**) was confirmed by mass spectrometry, which displays a signal at *m/z* 2389.4 assigned to [**4.8**-Br]$^{+}$ and at *m/z* 1154.8 assigned to [**4.8**-2Br]$^{2+}$ (Figure 4.21).

Crystallisations of complex **4.8** were attempted from a range of solvents / solvent systems but no crystals were obtained that were suitable for analysis by single crystal X-ray diffraction. However, the analytical data obtained strongly indicates the synthesis of the Rh(I)-NHC complex **4.8**, and confirms that copper(I)-NHC complexes can be used as ligand transfer agents to form rhodium(I)-NHC complexes.

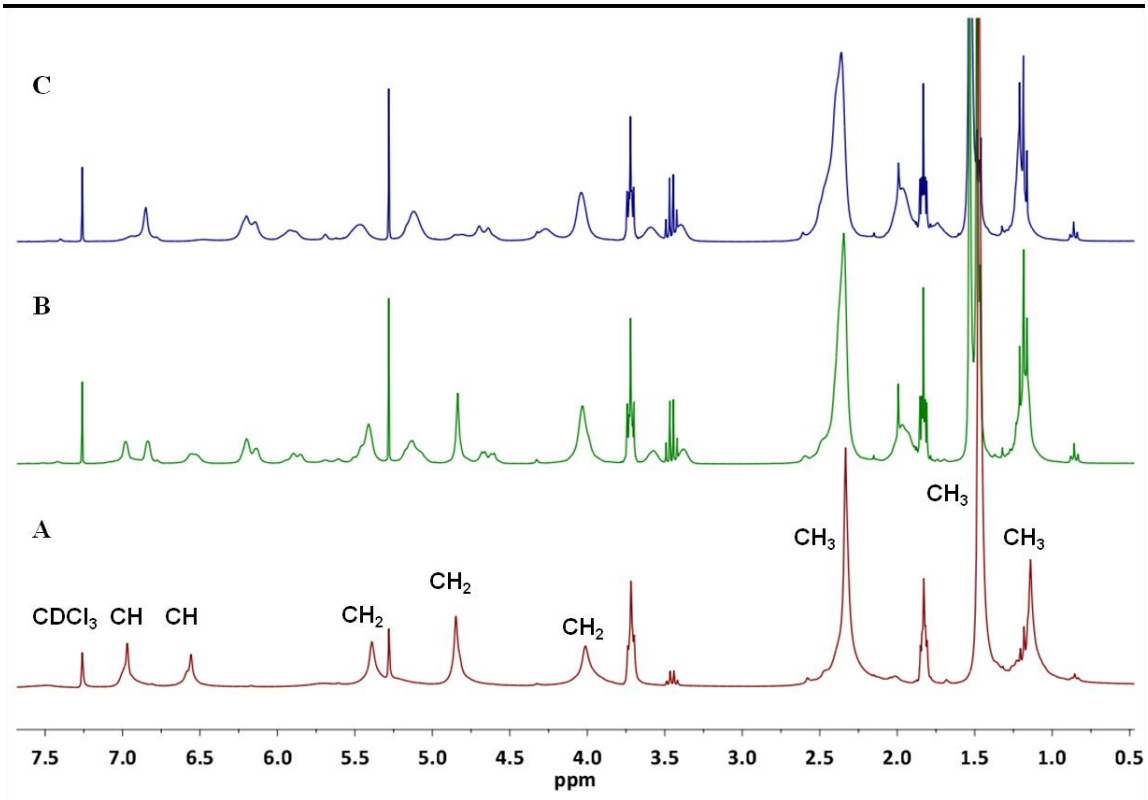

Figure 4.20 ^{1}H NMR spectra ($CDCl_3$) from the reaction of complex **4.6** with $[Rh(COD)Cl]_2$; (A) Cu(I)-NHC complex **4.6**, (B) complex **4.6** 10 minutes after the addition of $[Rh(COD)Cl]_2$, (C) complex **4.6** 12 hours after addition of $[Rh(COD)Cl]_2$.

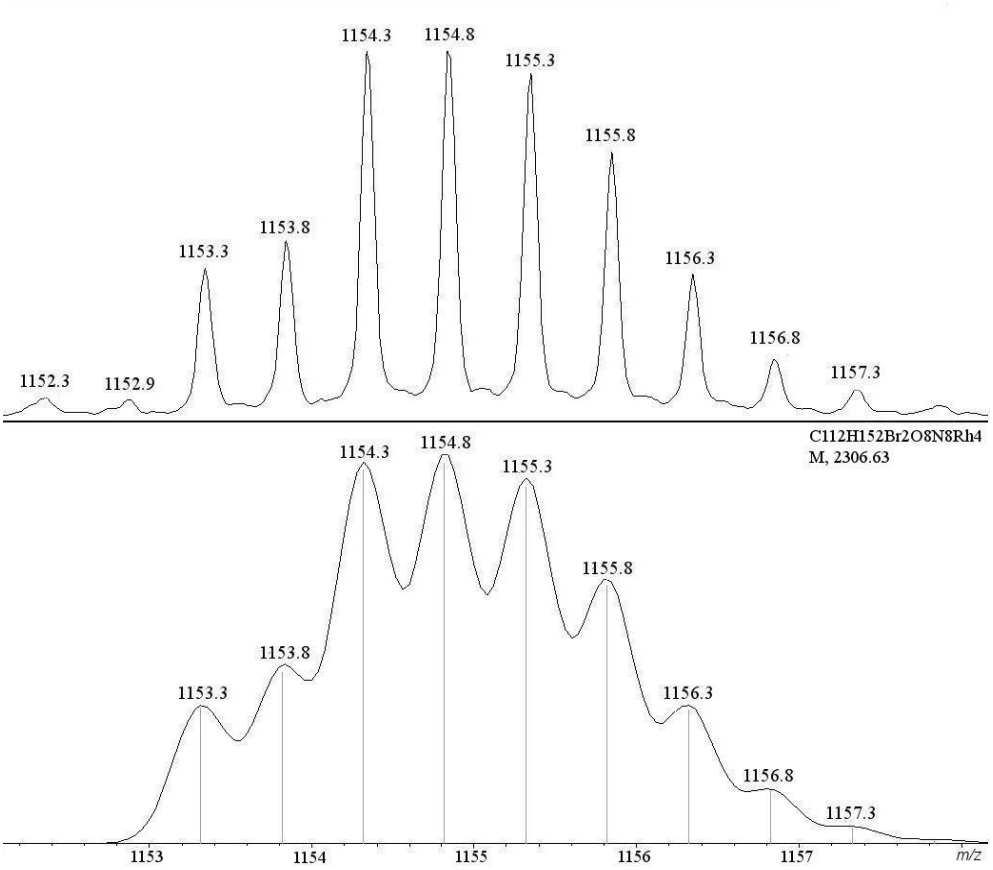

Figure 4.21 Mass spectrometry data of complex **4.8** (top), and calculated for [**4.8**-2Br]$^{2+}$ (bottom).

4.2.5 Formation of metal-NHC complexes using acetic acid tethered NHC-ligand precursor 4.3

Compound **4.3** (Scheme 4.1) is functionalised with acetic acid substituents, which offers the potential of forming a bidentate chelating metal-NHC complex, through coordination to the metal *via* both the NHC groups and the carboxylate groups.[1] The methylene protons of the acetic acid tethers are less acidic than those of the acetate tethers in compound **4.2**. Therefore, under basic reaction conditions, the methylene protons would not be deprotonated as readily. However, the hydroxyl groups are very acidic due to the short alkyl chain length of the carboxylic acid, with the pK_a expected to be in the region of 1.90-2.50 depending on the counter anion, and would be expected to deprotonate under basic reaction conditions.[13]

As discussed previously, an attractive route for the synthesis of a wide range of transition metal-NHC complexes is through transmetallation from a silver-NHC complex.[8, 28] Albrecht *et al.* have reported the synthesis of a ruthenium(II)-NHC

complex with a tethered carboxylate donor that was synthesised through the *in situ* formation of the silver-NHC complex, followed by transmetallation from silver(I) to ruthenium(II) using [RuCl(Cp)(PPh_3)$_2$] (Figure 4.22).[1]

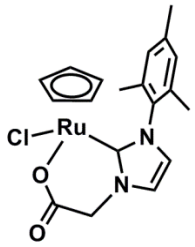

Figure 4.22 Reported product from the reaction of a carboxylate functionalised imidazolium zwitterion with Ag_2O, followed by transmetallation from Ag(I) to Ru(II) using [RuCl(Cp)(PPh_3)$_2$] precursor.[1]

The reaction of compound **4.3 Br** with two equivalents of Ag_2O was investigated in different solvents (MeOH, DCM), varying the temperature of the reaction (from room temperature to 70 °C), and varying the reaction time (24-72 hours). Analysis by ^{1}H NMR spectroscopy of the products formed in the reactions revealed that, in all cases, the imidazolium C2 carbon remained protonated, indicating that a silver-NHC complex had not been formed. Notably, the resonance for the methylene protons of the acetic acid tether had shifted upfield from δ = 5.15 to δ = 4.39 ppm. To investigate this more thoroughly, 1-methyl-3-acetic acid imidazolium chloride (**4.9**) was synthesised. Compound **4.9** has a methyl group in place of the calixarene scaffold, enabling the acetic acid functionality to be investigated thoroughly without potential interference or complications from the calixarene group.

Compound **4.9** was synthesised by heating compound **4.4** in excess HCl (aq) at reflux (110 °C). The product was purified by washing with acetone and diethyl ether, and was dried *in vacuo*, affording compound **4.9** as an off white solid which was analysed by ^{1}H NMR and ^{13}C{^{1}H} NMR spectroscopy combined with mass spectrometry. A ^{1}H NMR spectrum of compound **4.9** (DMSO-d_6) is displayed in Figure 4.23 with the relevant peaks assigned in Table 4.10. The ^{1}H NMR spectrum appears as expected, with the resonance for the C2 imidazolium proton appearing downfield at δ = 9.33 ppm. The backbone imidazolium protons now appear as two separate resonances at δ = 7.80 ppm and δ = 7.78 ppm, whereas in compound **4.4** these protons appeared as one resonance at δ = 7.78 ppm. Notably, the residual water peak is not observed in the ^{1}H NMR spectrum of compound **4.9**, even though the spectrum was recorded in DMSO-d_6. Any water protons in solution will most likely be exchanging with the hydroxyl

group protons of the acetic acid tethers, which would cause the water signal to broaden, and is likely to account for the absence of the water peak. However, a water peak was observed in the ^{1}H NMR spectrum of the calixarene that incorporates the acetic acid substituents (compound **4.3**, Figure 4.4). Adding 10 µL aliquots of D_2O to the NMR sample of compound **4.9** (DMSO-d_6) resulted in the proton signals shifting upfield. For example, the C2 proton resonance shifted from δ = 9.33 ppm to δ = 9.16 ppm after 40 µL of D_2O was added. This evidence suggests that compound **4.9** may be interacting with water molecules in solution.

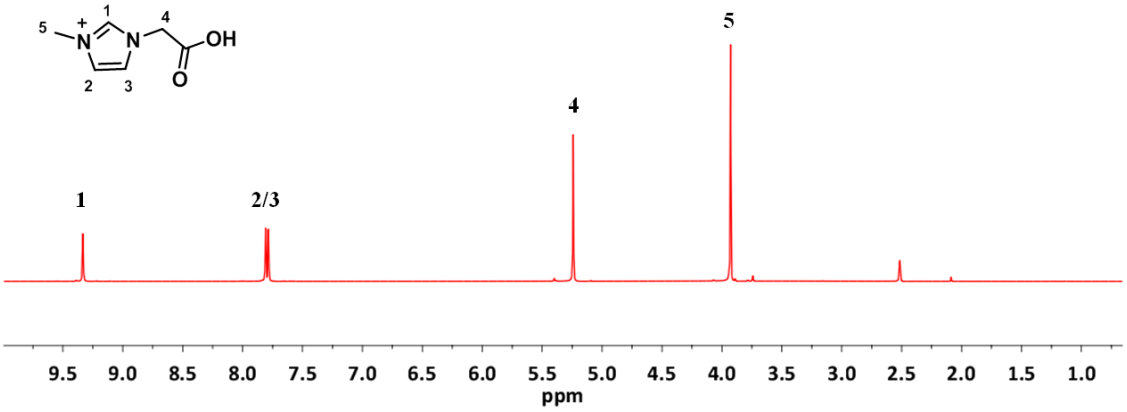

Figure 4.23 ^{1}H NMR spectrum (DMSO-d_6) of compound **4.9** at 298 K.

Chemical shift (δ ppm) ^{1}H	Assignment
9.33 (s, 1H)	1
7.80 (s, 1H)	2 / 3
7.78 (s, 1H)	2 / 3
5.24 (s, 2H)	4
3.93 (s, 3H)	5

Table 4.10 ^{1}H NMR assignment of compound **4.9**.

Compound **4.9** was reacted with two equivalents of Ag_2O in anhydrous DCM, at 40 °C for 12 hours. 4 Å molecular sieves were added to the reaction to remove the water formed in the reaction. The mixture was filtered through celite and the solvent removed *in vacuo*, but only a few mgs of solid was isolated. This was most likely due to the poor

solubility of compound **4.9** in DCM.

The reaction was repeated in a DCM / methanol mixture (2:1), with enough methanol added to solubilise compound **4.9**, and the mixture was heated at reflux (70 °C). The isolated product was analysed by ^{1}H NMR and ^{13}C{^{1}H} NMR spectroscopy combined with mass spectrometry. The ^{1}H NMR spectrum (MeOD-d_4) does not exhibit a low field resonance attributed to the C2 proton, suggesting the formation of a silver-NHC complex (Figure 4.24). It should be noted that in protic solvents, such as methanol, imidazolium compounds do not always exhibit a resonance for the C2 proton. This is attributed to the exchange of the acidic C2 proton with the deuterium atoms of the solvent. However, a ^{1}H NMR spectrum of compound **4.9** taken in methanol displays a resonance at δ = 9.03 ppm, attributed to the C2 proton. This suggests that proton exchange does not account for the absence of the C2 proton resonance in Figure 4.24. The ^{13}C{^{1}H} NMR spectrum (MeOD-d_4) does not display a resonance attributed to the C2 carbon bound to silver, which is usually observed at around 180 ppm. Intriguingly, there is also no resonance observed for the methylene carbons on the acetic acid group (at δ = 49.8 ppm in compound **4.9**), even though the methylene protons can be seen in the ^{1}H NMR spectrum at δ = 4.74 ppm (MeOD-d_4) (Figure 4.24). The mass spectrometry data does not show evidence for the formation of a silver-NHC complex, with the major signal seen at *m/z* 141.1 assigned to the starting imidazolium ligand (**4.9**).

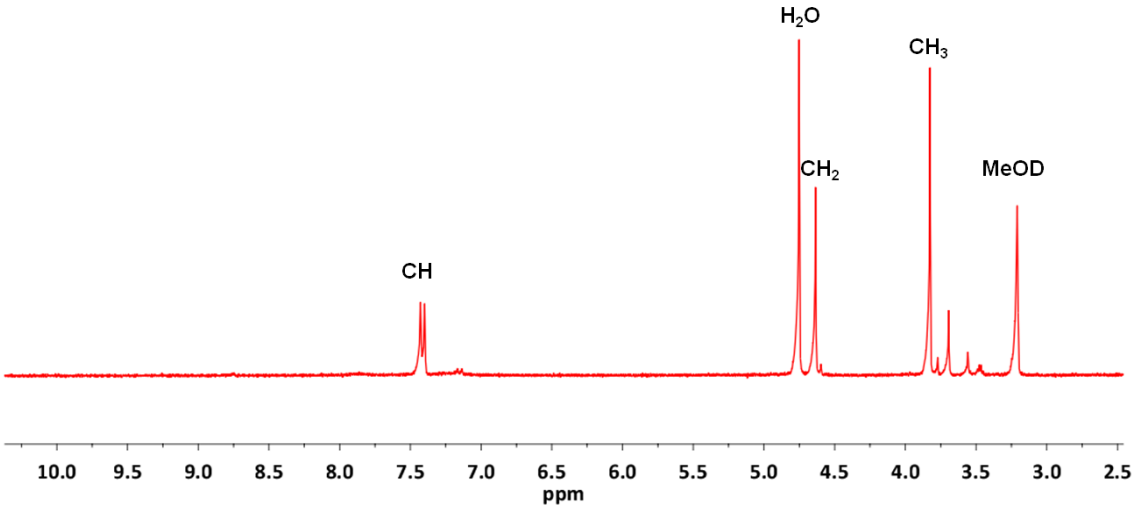

Figure 4.24 ^{1}H NMR spectrum (MeOD-d_4) of the product formed in the reaction of compound **4.9** with Ag_2O in DCM at 298 K.

The reaction of compound **4.9** with Ag_2O was repeated in methanol alone. Again, a low field resonance was not observed for the C2 imidazolium proton in the ^1H NMR spectrum (MeOD-d_4), and at least two products appeared to be present in a ratio of ~3:1 (blue triangle: green circle, Figure 4.25). Upon closer examination of the ^1H NMR spectrum, additional smaller resonances can be seen in the region of these peaks, suggesting further minor products have also formed. Again, the $^{13}C\{^1H\}$ NMR spectrum does not display evidence for the C2 carbon bound to silver. The mass spectrometry data displays a signal at *m/z* 141.1, assigned to the starting imidazolium salt (**4.9**), in addition to some larger mass peaks that appeared to incorporate silver(I) by the observed splitting patterns at *m/z* 433.9, 492.0, 566.9. These signals could not be assigned to a desirable product. From the mass spectrometry data it did not appear that a simple monodentate or bidentate silver-NHC complex, or a mixture of the two, had been formed in the reaction.

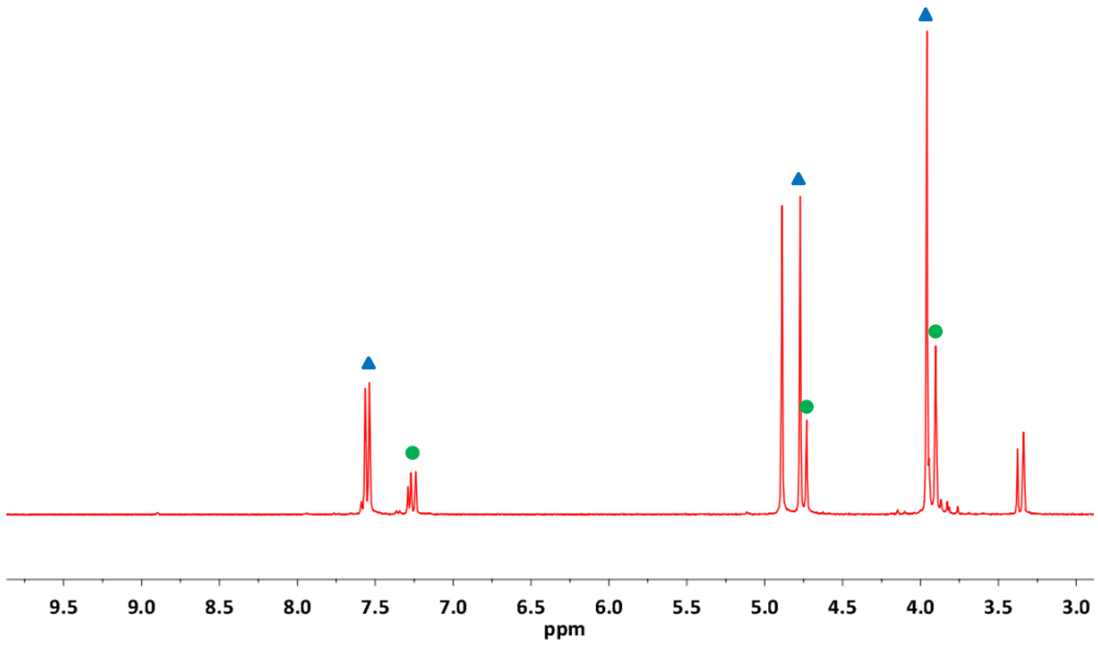

Figure 4.25 ^1H NMR spectrum (MeOD-d_4) of the products formed in the reaction of compound **4.9** with Ag_2O in methanol at 298 K.

Single crystals suitable for analysis by single crystal X-ray diffraction were grown by slow diffusion of diethyl ether into a methanol solution of the product from the reaction of compound **4.9** with Ag_2O in methanol. The X-ray crystal structure revealed a zwitterion, with the hydroxyl group deprotonated (compound **4.10**, Figure 4.26). The carbon to oxygen bond lengths, **O1-C6** and **O2-C6**, are identical (1.268 Å), showing the electron density is delocalised across the **O(1)-C(6)-O(2)** bonds. The carbon to oxygen

bond lengths are shorter than a C-O single bond (1.318 Å) and longer than a C=O bond (1.206 Å) providing further evidence that the electron density is delocalised.[13] The molecule packs as a 1D chain, propagated through a hydrogen bond from the deprotonated hydroxyl group (**O2**) to one of the backbone imidazolium protons (**H2**), with the length of the [$O^{-}\cdots C$] bonds being 3.147 Å (Figure 4.27).

It has not been confirmed as to whether a silver-NHC complex was formed in the reaction of compound **4.9** with Ag_2O and decomposed in solution, liberating silver chloride and reprotonating the C2 carbon, or if the zwitterion was formed during the reaction. However, the ^{1}H NMR spectrum does not show any evidence for the presence of the C2 imidazolium proton, which would be expected to appear downfield at around 9 ppm in the zwitterion, suggesting that the zwitterion was not the major product of the reaction (Figure 4.25). It is likely that the silver-NHC, or silver adduct, was formed in the reaction and decomposed in solution to form the zwitterion that crystallised from solution.

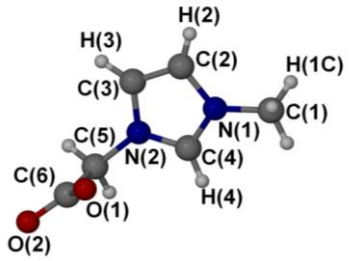

Figure 4.26 Molcular structure of compound **4.10**. Ellipsoids are displayed at 50 % probability.

C(4)-H(4)	0.9500	C(4)-N(1)-C(2)	109.1(2)
C(3)-H(3)	0.9500	O(2)-C(6)-O(1)	126.9(2)
N(2)-C(4)	1.341(3)	O(1)-C(6)-C(5)	118.9(2)
C(6)-O(1)	1.268(3)	N(2)-C(4)-N(1)	108.3(2)
C(6)-O(2)	1.268(3)		

Table 4.11 Selected bond distances (Å) and angles (deg) for compound **4.10**.

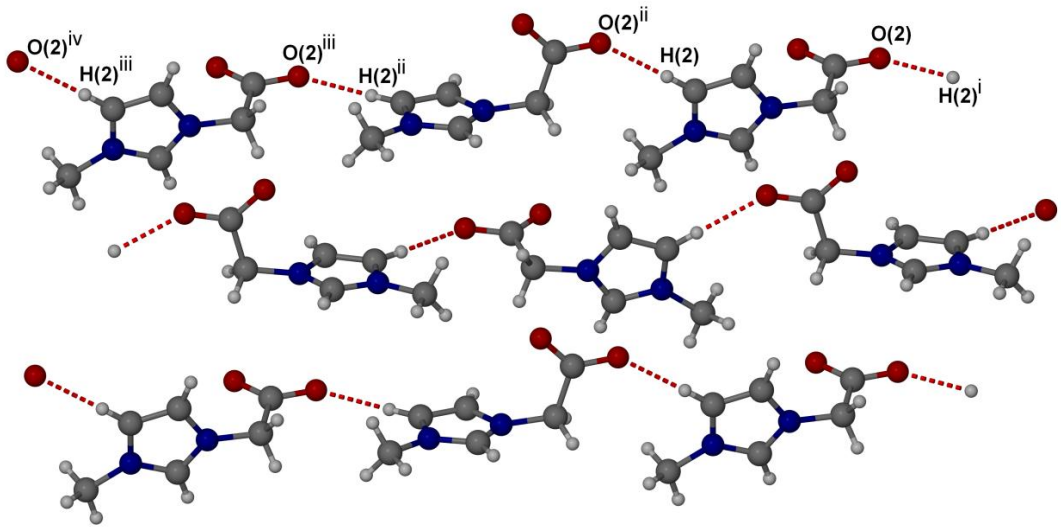

Figure 4.27 X-ray crystal structure displaying the bonding interactions observed in the solid state structure of **4.10**. Symmetry operations for symmetry generated atoms i: x-1/2, 1-y, z; ii: 1/2+x, 1-y, z; iii: 1+x, y, z; iv: 3/2+x, 1-y, z. Ellipsoids are displayed at 50 % probability.

The *in situ* transmetallation of the product formed in the reaction between compound **4.9** and Ag_2O to ruthenium(II) (using $[RuCl_2(cymene)]_2$) and palladium(II) (using $PdCl_2(MeCN)_2$) was explored, to see if a stable product could be isolated from the reaction. Neither reaction was successful.

From this investigation it is clear that Ag_2O is reacting with the carboxylic acid group of compound **4.9** as well as, or instead of, reacting with the imidazolium C2 proton. The ^1H NMR spectroscopy data suggests that, in methanol / DCM or in just methanol, the reaction between compound **4.9** and Ag_2O forms a silver-NHC complex due to the absence of the resonance assigned to the C2 imidazolium proton in the ^1H NMR spectrum. However, no desirable product could be identified by mass spectrometry. When compound **4.3 Br** was reacted with Ag_2O, analysis of the products formed by ^1H NMR spectroscopy revealed that the imidazolium C2 carbon remained protonated and that the acetic acid methylene protons had shifted upfield from $\delta = 5.15$ to $\delta = 4.39$ ppm. It is likely that, in this reaction, the Ag_2O has reacted with the carboxylic acid group and not the C2 imidazolium proton, deprotonating the hydroxyl groups and forming the zwitterion, or forming a silver network structure bonded through the carboxylate groups.

4.2.6 Electrochemical synthesis of copper(I)-NHC complexes using NHC-ligand precursor 4.3

The electrochemical synthesis of Cu(I)-NHC complexes was explored using compound **4.9** (Scheme 4.8).

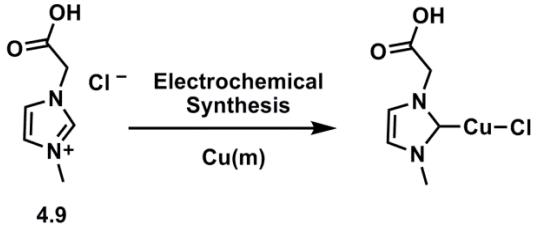

Scheme 4.8 Electrochemical reaction using NHC-ligand precursor **4.9**.

Copper plates were used as both the sacrificial anode and cathode (1 × 3 cm), and the reaction was performed in anhydrous acetonitrile. Compound **4.9** was added to the flask and degassed. Anhydrous acetonitrile was added (15 ml) and the solution was degassed for 1 hour by bubbling argon through. The electrodes were inserted into the solution and a potential applied such to maintain a constant current of 30 mA. The reaction was monitored by ^{1}H NMR spectroscopy and the theoretical reaction time was calculated using Faraday's law (Figure 4.12). The mixture was electrolysed for 106 minutes, calculated as 2 Q. The mixture was filtered to remove suspended copper particles and the solvent was removed *in vacuo*. The product was analysed by ^{1}H NMR and ^{13}C{^{1}H} NMR spectroscopy combined with mass spectrometry. A ^{1}H NMR spectrum (DMSO-d_6) of the product formed in the reaction is displayed in Figure 4.28, and compared with the starting imidazolium ligand **4.9**.

The product formed in the electrochemical reaction using ligand precursor **4.9** displays a low field resonance attributed to the C2 proton at δ = 8.92 ppm in the ^{1}H NMR spectrum. This resonance has broadened and shifted slightly upfield compared to compound **4.9**. Electrolysing the mixture for a further 2 Q did not result in any further change in the ^{1}H NMR spectrum. The most striking difference between the ^{1}H NMR spectrum of the starting imidazolium ligand and that of the product is the absence of the methylene protons signal of the acetic acid tether, that were observed at δ = 5.24 ppm in the spectrum of compound **4.9**. The ^{1}H NMR spectrum of the product was recorded in MeCN-d_3 to allow low temperature studies to be conducted. However, at 263.2 K a resonance for the methylene protons was still not observed. The ^{13}C{^{1}H} NMR spectrum (MeCN-d_3) displays resonances at δ = 36.95 ppm (CH_3), 123.62 ppm (CH),

124.74 ppm (CH), 138.10 ppm (CH) and 172.9 ppm (quaternary), with the resonances being assigned with the assistance of $^{13}C\{^{1}H\}$ DEPT 135 NMR spectroscopy. As observed in the ^{1}H NMR spectrum there is no CH_2 resonance attributed to the methylene carbons of the acetic acid tether, which was observed at δ = 49.8 ppm in the $^{13}C\{^{1}H\}$ NMR spectrum of the starting imidazolium ligand. The low field resonance at δ = 172.9 ppm was assigned as a quaternary carbon and could be the quaternary carbon of the acetic acid substituent (COOH), or the C2 carbon coordinating to copper. As the C2 carbon appeared to remain protonated, suggested by the ^{1}H NMR spectrum, it is likely that the low field resonance is attributed to the quaternary acetic acid carbon (COOH). However, this would suggest that the acetic acid group was not eliminated during the reaction and would not account for the absence of the CH_2 resonance for the methylene protons of the acetic acid tether.

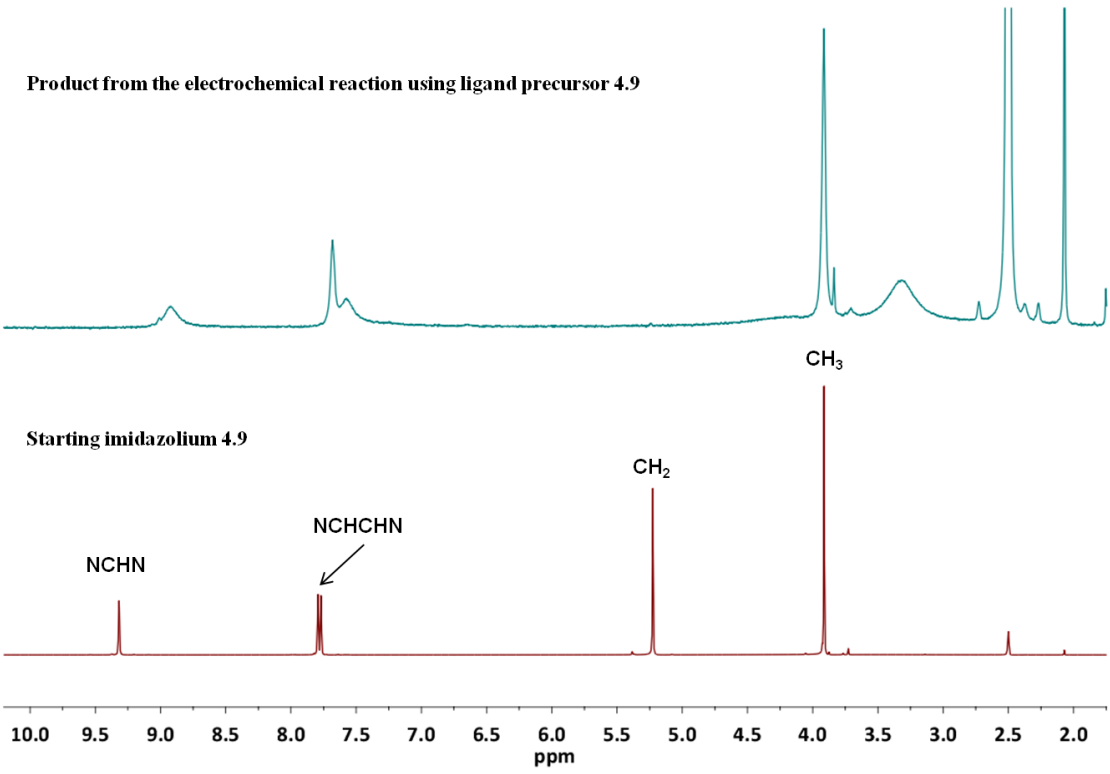

Figure 4.28 ^{1}H NMR spectra (DMSO-d_6) displaying compound **4.9** (bottom) and the product formed in the electrochemical reaction using ligand precursor **4.9** (top).

Unexpectedly the mass spectrometry data suggests the presence of the monodentate copper complex [**4.9**-H+Cu-Cl+NCMe]$^{+}$ at *m/z* 244.0, and the bidentate copper complex [(2×**4.9**)-2H+Cu-2Cl]$^{+}$ at 343.0. However, decomposition products were also observed in the mass spectrum at *m/z* 145.0 and at *m/z* 132.0, with the suggested structures of

these compounds being displayed in Figure 4.29 (*m/z* 145.0 **A** and **B**; *m/z* 132.0 **C** and **D**). Both of these decomposition products have two possible structures, either coordinating to copper(I) through the C2 proton to form the carbene (**B** and **D**), or coordinating through the nitrogen leaving the C2 carbon protonated (**A** and **C**). In both of these scenarios it appears that decomposition has occurred through loss of the acetic acid group.

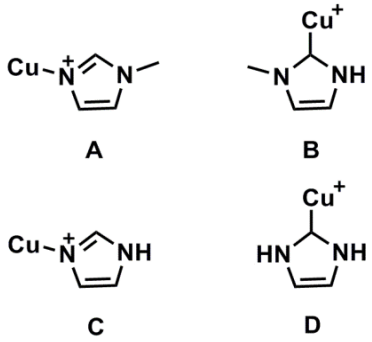

Figure 4.29 Suggested structures for the decomposition compounds seen in the mass spectrum following the electrochemical procedure using ligand precursor **4.9**.

The ^{1}H NMR, $^{13}C\{^{1}H\}$ NMR and mass spectrometry data appeared to contradict each other, but it is clear that the electrochemical route did not produce the desired copper(I)-NHC complex selectively, and it appears that more than one product has been formed. Examination of the literature shows that when an acetate ion is electrolysed it breaks down to CO_2 and C_2H_6, with the half-reactions for this and H^+ being displayed in Figure 4.30.[41, 42] In our electrochemical reaction, the acetic acid may deprotonate to form the acetate and decompose in a similar manner, which would account for the moiety not being observed in the ^{1}H NMR spectrum.

$$2CH_3COO^- \longrightarrow 2CO_2 + C_2H_6 + 2e^- \quad (1)$$

$$2H^+ + 2e^- \longrightarrow H_2 \quad (2)$$

Figure 4.30 Overall electrode reactions of an acetate ion and its corresponding proton.[42]

The electrochemical reaction was explored using the acetic acid tethered calixarene **4.3 Br** (Scheme 4.9), with the experimental procedure being repeated as described previously.

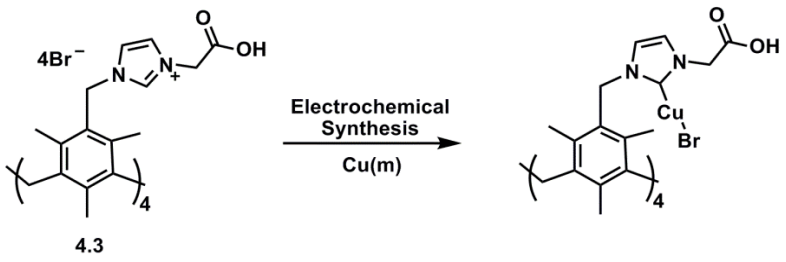

4.3

Scheme 4.9 Proposed product in the electrochemical reaction using compound **4.3**.

The highest current that could be achieved when using compound **4.3 Br** as the ligand precursor was 10 mA, with the current falling below 10 mA at intervals during the reaction. Complex **4.3 Br** formed a suspension in acetonitrile and it is likely that the poor solubility resulted in a low current. After 2 Q an aliquot of the reaction mixture was removed and the isolated product examined by ^{1}H NMR spectroscopy (DMSO-d_6). The ^{1}H NMR spectrum displayed only starting material, with no reduction observed in the integral for the C2 proton. The reaction was electrolysed for a further 2 Q but no change in the ^{1}H NMR spectrum was observed. The use of another electrolyte was not desirable as it is likely that this would cause complications in the purification of the final product. The reaction was repeated using compound **4.3 PF_6** in the hope that this would have increased solubility in acetonitrile. However, the product was still not sufficiently soluble for a good current to be achieved.

The electrochemical reaction was repeated with **4.3 PF_6**, with anhydrous DMSO added to the reaction to solubilise the compound (5 ml). The reaction was electrolysed at 20 mA for 270 minutes (3 Q). The solution was filtered to remove suspended copper particles, and the product precipitated from solution by the addition of DCM (30 ml). The precipitate was isolated by filtration and dried *in vacuo*. The isolated solid was analysed by ^{1}H NMR and ^{13}C{^{1}H} NMR spectroscopy, combined with mass spectrometry. The ^{1}H NMR spectrum (DMSO-d_6) is very broad (Figure 4.31), with the resonance assigned to the C2 proton being observed at δ = 8.65 ppm, suggesting that a copper-NHC complex did not form. The C2 proton resonance has broadened and shifted slightly upfield when compared with compound **4.3 PF_6**. A CH_2 peak is absent, with only two CH_2 resonances seen in the ^{1}H NMR spectrum of the product. However, as the spectrum is very broad this resonance may be in the baseline. The ^{13}C{^{1}H} NMR spectrum displays no low field resonances, with no resonance being attributed to the

quaternary acetic acid carbon (COOH), which was observed at δ = 167.7 ppm in compound **4.3 PF_6**. In addition, there is no evidence of any copper containing species in the mass spectrum, with the major signal seen at *m/z* 1103.6 assigned to the zwitterion $[4.3\text{-}4Br\text{-}4H+Na]^+$. It is clear that the copper(I)-NHC complex displayed in Scheme 4.9 was not formed during the electrochemical reaction, and the acetic acid substituent may have been eliminated, or altered, during the reaction.

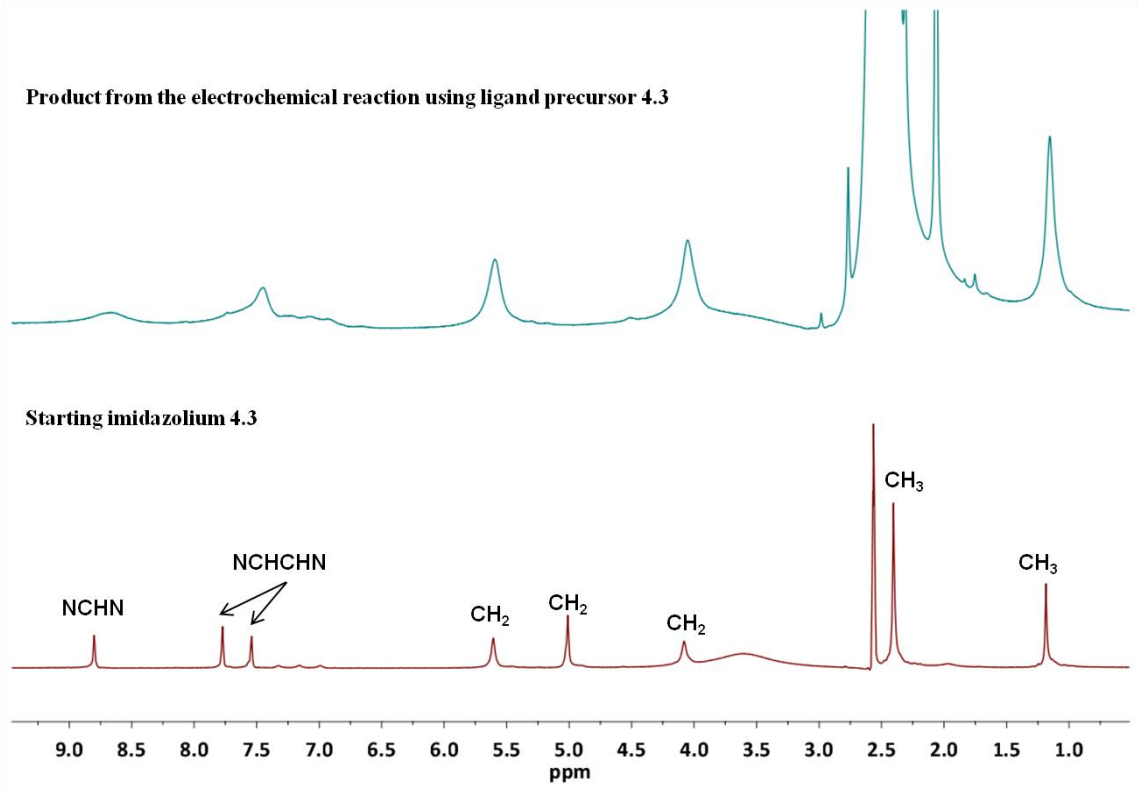

Figure 4.31 ^{1}H NMR spectra (DMSO-d_6) displaying compound **4.3 PF_6** (bottom) and the product formed in the electrochemical reaction of **4.3 PF_6** (top).

From this study it can be concluded that the electrochemical reaction is not a viable route for the synthesis of copper(I)-NHCs using ligand precursor **4.3**. The acetic acid functionality limits the solubility of compound **4.3**, with it only being soluble in DMSO, and it appears that the carboxylic acid group is eliminated or altered during the electrochemical reaction, which results in decomposition of the ligand.

4.3 Conclusion

In conclusion, a synthetic method has been developed for the synthesis of the novel acetate ester tethered methylimidazolium calix[4]arene (**4.2**), and the compound has been fully characterised. The solid state properties of **4.2 Br** were examined by single crystal X-ray diffraction. It was found that the bromide anions form weak interactions with both the C2 imidazolium protons and the imidazolium backbone protons of the calix[4]arene. The *tert*-butyl ester groups of **4.2** were removed by heating at reflux in acid, to form the acetic acid tethered methylimidazolium mesityl calix[4]arene (**4.3**). Compound **4.3** was fully characterised.

The use of compound **4.2 Br** as an NHC ligand precursor to form metal-NHC complexes was explored. It was found that the most widely reported synthetic routes for the formation of metal-NHC complexes were not compatible with this ligand. When using a basic metal precursor a reaction was not observed. Under basic conditions, the C2 carbon remained protonated and the base reacted with other acidic protons in the ligand. Further investigation showed that the base was most likely reacting with the methylene protons of the acetate substituent, resulting in decomposition of the ligand. An alternative electrochemical method was explored that did not require the need for basic conditions.[6] It was found that the electrochemical method is compatible for the synthesis of copper(I)-NHC complexes from imidazolium ligands that incorporate base sensitive groups. The electrochemical method was used to synthesise two copper(I)-NHC complexes (**4.5** and **4.6**). Complex **4.6** was used as a carbene transfer agent for the formation of a palladium(II)-NHC complex (**4.7**) and a rhodium(I)-NHC complex (**4.8**). Both of these complexes are expected to have application as catalysts. Other transmetallation reactions (Ru(II), Ni(II)) were explored but these were unsuccessful, most likely due to the steric constraints imposed by the calix[4]arene framework.

The use of compound **4.3** as an NHC ligand precursor to form metal-NHC complexes was explored. Compound **4.3** offers the potential of forming a bidenate chelating metal-NHC complex coordinated to the metal through the NHC groups and the carboxylate donors. The reaction of **4.3** with Ag_2O was unsuccessful, inferred by the C2 proton remaining in the ^{1}H NMR spectrum. However, a shift was observed in the ^{1}H NMR spectrum for the resonance assigned to the methylene protons of the acetic acid substituents. Following further investigation, it was found to be highly likely that Ag_2O reacts with the carboxylic acid substituents of **4.3** over the C2 imidazolium protons,

deprotonating the hydroxyl groups and forming the zwitterion, or forming a silver network structure through the carboxylate. Either of these scenarios would account for the shift observed in the methylene protons. The electrochemical reaction was explored with compound **4.3**, but was found not to be compatible with the acetic acid substituent. It appeared the acetic acid group was eliminated or altered during the reaction.

4.4 Future work

Future work in this area should involve extending the electrochemical method to other transition metals. This would allow a range of transition-metal NHC complexes to be synthesised from imidazolium ligands that incorporate base sensitive groups, such as compound **4.2**. The applications of the resulting metal-NHC complexes in catalysis can then be explored, to determine if having four metal centres per calix[4]arene ligand improves their performance as a catalyst, or if a macrocyclic / cavity effect aids in the catalysis. The palladium-NHC complex synthesised (**4.7**) is expected to be an effective catalyst in cross coupling reactions, which is discussed in Chapter 5. The carbene transfer reaction from complex **4.6** to other transition metals can be explored, using metal precursors that do not contain bulky groups, as another approach to synthesising a range of metal-NHC complexes.

Further work can involve different synthetic routes to forming metal-NHC complexes using ligand precursor **4.3**, with the aim of isolating discrete metal complexes that can be fully characterised. The next approach taken should be the reaction of **4.3** with a base, followed by the coordination of the free NHC to a metal centre. Further work can also be done to determine if the acetic acid tether is lost during the electrochemical reaction. This could be done by probing the composition of the gas that is produced during the experiment to see if CO_2 and C_2H_6 are detected as well as H_2.

4.5 References

1. C. Gandolfi, M. Heckenroth, A. Neels, G. Laurenczy and M. Albrecht, *Organometallics*, 2009, **28**, 5112-5121.
2. W. A. Herrmann and C. Kocher, *Angew. Chem., Int. Ed. Engl.*, 1997, **36**, 2162-2187.
3. D. Bourissou, O. Guerret, F. P. Gabbaie and G. Bertrand, *Chem. Rev.*, 2000, **100**, 39-91.
4. I. J. B. Lin and C. S. Vasam, *Coord. Chem. Rev.*, 2007, **251**, 642-670.
5. C. E. Willans, K. M. Anderson, M. J. Paterson, P. C. Junk, L. J. Barbour and J. W. Steed, *Eur. J. Inorg. Chem.*, 2009, **7**, 2835-2843.
6. B. R. M. Lake, E. K. Bullough, T. J. Williams, A. C. Whitwood, M. A. Little and C. E. Willans, *Chem. Commun.*, 2012, **48**, 4887-4889.
7. M. R. L. Furst and C. S. J. Cazin, *Chem. Commun.*, 2010, **46**, 6924-6925.
8. H. M. J. Wang and I. J. B. Lin, *Organometallics*, 1998, **17**, 972-975.
9. C. E. Willans, K. M. Anderson, L. C. Potts and J. W. Steed, *Org Biomol Chem*, 2009, **7**, 2756-2760.
10. I. J. B. Lin and C. S. Vasam, *Coord. Chem. Rev.*, 2007, **251**, 642-670.
11. S. K. Singh, N. Manne, P. C. Ray and M. Pal, *Beilstein J. Org. Chem.*, 2008, **4**, 42.
12. T. Steiner, *Angew. Chem., Int. Ed.*, 2002, **41**, 48-76.
13. Z. Fei, D. Zhao, T. J. Geldbach, R. Scopelliti and P. J. Dyson, *Chem.--Eur. J.*, 2004, **10**, 4886-4893.
14. E. Brenner, D. Matt, M. Henrion, M. Teci and L. Toupet, *Dalton Trans.*, 2011, **40**, 9889-9898.
15. T. Fahlbusch, M. Frank, G. Maas and J. Schatz, *Organometallics*, 2009, **28**, 6183-6193.
16. D. Qin, X. Zeng, Q. Li, F. Xu, H. Song and Z.-Z. Zhang, *Chem. Commun.*, 2007, 147-149.
17. T. Brendgen, M. Frank and J. Schatz, *Eur. J. Org. Chem.*, 2006, 2378-2383.
18. M. Frank, G. Maas and J. Schatz, *Eur. J. Org. Chem.*, 2004, 607-613.
19. S. T. Liddle, I. S. Edworthy and P. L. Arnold, *Chem. Soc. Rev.*, 2007, **36**, 1732-1744.
20. D. S. McGuinness and K. J. Cavell, *Organometallics*, 2000, **19**, 741-748.
21. M. Pellei, V. Gandin, M. Marinelli, C. Marzano, M. Yousufuddin, H. V. R. Dias and C. Santini, *Inorg. Chem.*, 2012, **51**, 9873-9882.
22. I. Dinares, M. C. Garcia, M. Font-Bardia, X. Solans and E. Alcalde, *Organometallics*, 2007, **26**, 5125-5128.
23. E. M. Higgins, J. A. Sherwood, A. G. Lindsay, J. Armstrong, R. S. Massey, R. W. Alder and A. C. O'Donoghue, *Chem. Commun.*, 2011, **47**, 1559-1561.
24. B. Liu, Y. Zhang, D. Xu and W. Chen, *Chem. Commun.*, 2011, **47**, 2883-2885.
25. B. Gorodetsky, T. Ramnial, N. R. Branda and J. A. C. Clyburne, *Chem. Commun.*, 2004, 1972-1973.
26. M. Orsini, I. Chiarotto, G. Sotgiu and A. Inesi, *Electrochim. Acta*, 2010, **55**, 3511-3517.
27. M. Feroci, I. Chiarotto, M. Orsini, G. Sotgiu and A. Inesi, *Adv. Synth. Catal.*, 2008, **350**, 1355-1359.
28. J. C. Garrison and W. J. Youngs, *Chem. Rev.*, 2005, **105**, 3978-4008.
29. B. Liu, X. Liu, C. Chen, C. Chen and W. Chen, *Organometallics*, 2012, **31**, 282-288.
30. S.-T. Liu, C.-I. Lee, C.-F. Fu, C.-H. Chen, Y.-H. Liu, C. J. Elsevier, S.-M. Peng and J.-T. Chen, *Organometallics*, 2009, **28**, 6957-6962.
31. G. Venkatachalam, M. Heckenroth, A. Neels and M. Albrecht, *Helv. Chim. Acta*, 2009, **92**, 1034-1045.
32. C. Chen, H. Qiu and W. Chen, *J. Organomet. Chem.*, 2012, **696**, 4166-4172.
33. S. Diez-Gonzalez and S. P. Nolan, *Synlett*, 2007, 2158-2167.
34. N. P. Mankad, D. S. Laitar and J. P. Sadighi, *Organometallics*, 2004, **23**, 3369-3371.
35. N. Schneider, V. Cesar, S. Bellemin-Laponnaz and L. H. Gade, *J. Organomet. Chem.*, 2005, **690**, 5556-5561.
36. C. A. Citadelle, N. E. Le, F. Bisaro, A. M. Z. Slawin and C. S. J. Cazin, *Dalton Trans.*, 2010, **39**, 4489-4491.

37. K.-T. Chan, Y.-H. Tsai, W.-S. Lin, J.-R. Wu, S.-J. Chen, F.-X. Liao, C.-H. Hu and H. M. Lee, *Organometallics*, 2010, **29**, 463-472.
38. H. V. Huynh, Y. Han, J. H. H. Ho and G. K. Tan, *Organometallics*, 2006, **25**, 3267-3274.
39. S. P. Van and A. L. Spek, *Acta Crystallogr., Sect. A: Found. Crystallogr.*, 1990, **A46**, 194-201.
40. C. S. Straubinger, N. B. Jokic, M. P. Hoegerl, E. Herdtweck, W. A. Herrmann and F. E. Kuehn, *J. Organomet. Chem.*, 2011, **696**, 687-692.
41. C. L. Wilson and W. T. Lippincott, *J. Am. Chem. Soc.*, 1956, **78**, 4290-4294.
42. S. D. Ross, M. Finkelstein and R. C. Petersen, *J. Am. Chem. Soc.*, 1964, **86**, 4139-4143.

5 Activity of tetrakis-(*p*-palladium-NHC) mesityl calix[4]arene in the Suzuki-Miyaura cross-coupling reaction

This chapter focuses on the study of tetrakis-(*p*-palladium-NHC) mesityl calix[4]arene (compound **4.7**), reported in Chapter four, in the Suzuki-Miyaura cross-coupling reaction. The Suzuki-Miyaura reaction is a cross-coupling process between an organoboron reagent and an aryl halide, catalysed by a palladium complex (or source), to form a new carbon-carbon bond.[1] Cross-coupling reactions play an important part in the synthesis of a wide range of drugs, natural products, and industrially important starting materials.[2] Therefore, the development of more efficient and selective catalysts is of industrial importance.[3] The scientific importance of the cross-coupling reaction was recognised in 2010 when Heck, Negishi and Suzuki were jointly awarded the Nobel Prize in chemistry for their work on cross-coupling reactions.[4]

Schatz *et al.* were the first group to report that imidazolium salts tethered to a calix[4]arene framework were promising ligand precursors in palladium catalysed Suzuki-Miyaura reactions.[5] They synthesised a calix[4]arene in the cone conformation, functionalised with two imidazolium groups on the 1,3-positions of the upper rim. The reaction of this ligand with $Pd(OAc)_2$ in dioxane formed a chelating bis-NHC complex, with *cis* geometry around the palladium centre. They investigated the catalytic activity of this ligand using an *in situ* protocol and reported reasonable activity. Dinarès *et al*. later compared the activity of a well defined, pre-formed complex, with an *in situ* generated catalyst.[6] They found the catalytic activity to be significantly different at the same catalyst loadings, and highlighted the need to be careful when postulating the nature of the active species from *in situ* formed systems. Schatz *et al.* found that catalytic activity was independent of whether the bis-NHC units are *cis* or *trans* with respect to each other on a palladium centre, suggesting that a mono-ligated NHC complex is the catalytically active species in these cross-coupling reactions.[7] They also reported that the activity of a pre-formed catalyst was superior to an *in situ* generated catalyst. The aforementioned catalysts all consist of two NHC moieties at the 1,3-positions on the upper rim of a cone-type calix[4]arene.

Brenner et al. synthesised a calix[4]arene in the cone conformation that was functionalised with a single imidazolium group on the upper rim. They prepared a palladium-NHC complex from this ligand, with the palladium centre bearing one NHC group, two bromide atoms, and a pyridine molecule (Figure 5.2).[8] They also synthesised

a bis-NHC complex with the NHC groups on the 1,2-positions of the upper rim of the calix[4]arene, with *trans* geometry about the palladium centre. They found that the mono-NHC complex displayed good activity in the Suzuki-Miyaura reaction, whereas the bis-NHC complex showed poor activity. This evidence again suggests that a mono-ligated palladium complex is the catalytically active species, with the poor activity of the bis-NHC complex being attributed to the difficulty of forming catalytically active species from the rigid chelating complex. Comparison of the activity of a related mono-NHC palladium complex without the calix[4]arene core suggested that no supramolecular effect was involved in this calix[4]arene system.

Tetrakis-(*p*-palladium-NHC) mesityl calix[4]arene (**4.7**) has been prepared and the structure examined through single crystal X-ray crystallography. The structure shows a tetrakis-NHC complex, incorporating four palladium(II) centres per calix[4]arene molecule, with the calix[4]arene adopting the 1,3-alternate conformation. The coordination geometry around each palladium is square planar, with two coordinating bromide atoms and an acetonitrile molecule *trans* to the NHC. As a monodentate palladium-NHC is thought to be the active species in several palladium-NHC catalysts, we were keen to test our mono-ligated complex **4.7** in the Suzuki-Miyuara cross-coupling reaction of p-tolyl halides with phenyl boronic acid to yield 4-methyl-biphenyl. We were interested in looking at the effect of having four palladium centres per calix[4]arene molecule, as this has not been previously explored, in addition to the effect of having a 1,3-alternate conformation. The conditions were varied (catalyst loading, solvent, reaction time) and the results compared. In addition, other palladium sources ($Pd_2(dba)_3$ and $Pd(OAc)_2$) and an *in situ* generated catalyst ($4Pd(OAc)_2$ + Ligand **4.2**) were tested. The reactions were conducted in parallel in a carousel reactor to ensure the conditions were kept constant.

5.1 Suzuki-Miyaura cross-coupling reaction catalysed by complex 4.7

The conditions applied for the catalytic reactions were the same as those reported by Brenner *et al.* and Dinarès *et al*., allowing for direct comparison of our results with those reported.[8,6] Phenylboronic acid was reacted with either 4-chlorotoluene or 4-bromotoluene, with Cs_2CO_3 used as the base. The yields were determined by ^{1}H NMR spectroscopy using 1,4-dimethoxybenzene as a standard (Scheme 5.1).

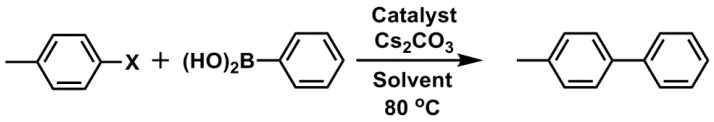

Scheme 5.1 Cross-coupling reaction of phenylboronic acid and aryl halide to yield 4-methyl-biphenyl (X = Cl, Br).

Phenylboronic acid (1.5 mmol), Cs_2CO_3 (2 mmol) and an acetonitrile solution of complex **4.7** (or a palladium source with ligand precursor **4.2**) were added to a carousel reactor and the solvent removed *in vacuo*. The reaction solvent was added (3 ml) followed by the aryl halide (1 mmol). The mixture was stirred vigorously at 80 °C for 2 hours, under an atmosphere of nitrogen. The hot mixture was filtered through a pad of celite, and the celite washed with the reaction solvent (2 ml). 1,4-dimethoxybenzene (0.5 mmol) was added to the filtrate and the solvent removed *in vacuo*. The mixture was analysed by ^{1}H NMR spectroscopy, comparing the intensity of the methyl signal of the product (δ = 2.41 ppm) with that of 1,4-dimethoxybenzene (δ = 3.78 ppm) (Figure 5.1).

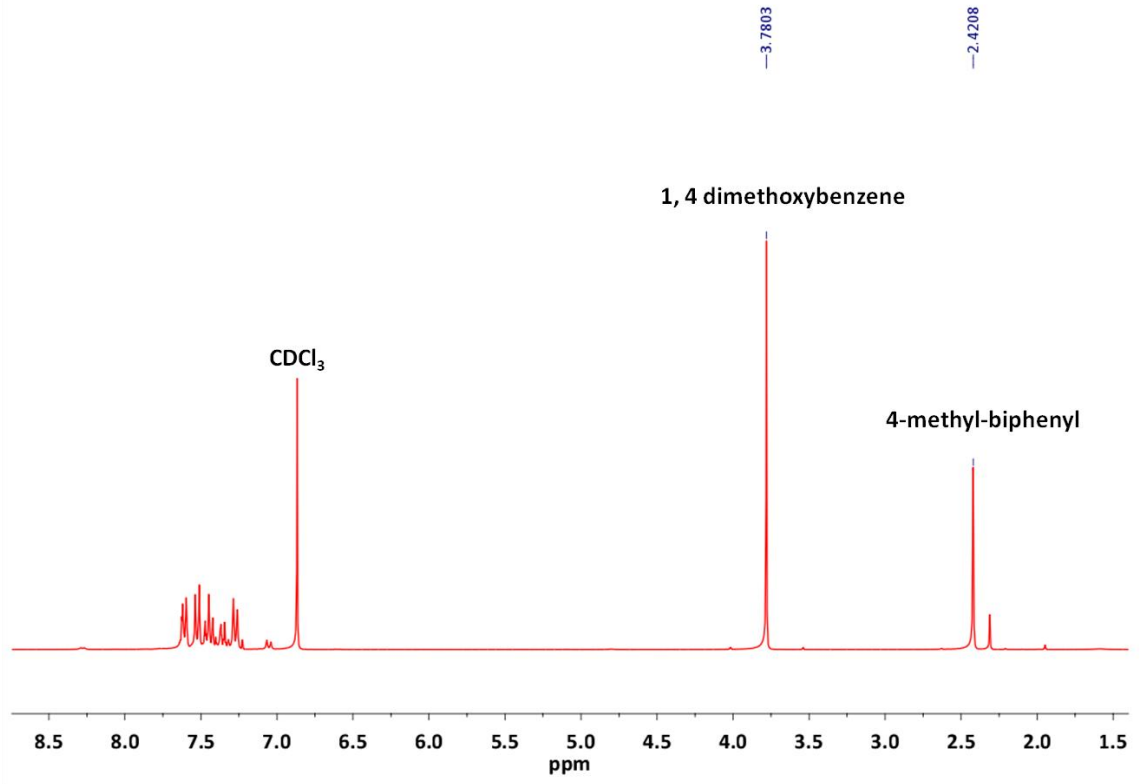

Figure 5.1 ^{1}H NMR spectrum ($CDCl_3$) of the products formed in the Suzuki-Miyaura cross-coupling reaction between 4-bromotoluene and phenylboronic acid, catalysed by complex **4.7** at a Pd loading of 0.25 mol %, in acetonitrile, with 1,4-dimethoxybenzene added as a standard.

The results for the coupling of aryl bromide and phenylboronic acid catalysed by complex **4.7** are displayed in Table 5.1. The table shows the catalyst loading used in each run, and the palladium mol % which is four times the catalyst loading, taking into account that complex **4.7** has four palladium centres per ligand. The results show that complex **4.7** displays good activity for the coupling reaction with aryl bromide.

In dioxane, the yield increases as the catalyst concentration is decreased (Entries 1-5), with a maximum yield of 89 % at a catalyst loading of 0.0625 mol %. The yield then decreases as the catalyst loading is lowered further, to 74 % at 0.03125 mol % of catalyst (Entry 6). The increased yield with decreasing catalyst concentration is attributed to the 'homeopathic palladium' effect, which is thought to be due to the reduced palladium forming palladium(0)-nanoclusters which, at higher concentrations, aggregate to form inactive palladium black.[9-11] By lowering the palladium concentration, the oxidative addition of the aryl bromide can compete against cluster formation, resulting in an improved yield. This indicates that the catalytically active species is unstable, and the calix[4]arene does not offer any protection against aggregation. The same trend is also observed when the reaction was performed in

acetonitrile, with the yield increasing as the catalyst loading was decreased (Entries 7-9). The maximum yield of 73 % was observed at 0.03125 mol % of catalyst. The reaction was also carried out in more environmentally friendly solvents, and found to give moderate yields in ethanol and in a mixture of H_2O / dioxane (1:1) (Entries 10 and 11). However, when the catalytic reaction was performed in H_2O alone, the cross-coupled product was not formed.

Entry	Catalyst	X	Solvent	Catalyst loading (mol %)	Pd loading (mol %)	Yield (%)
1	Complex **4.7**	Br	Dioxane	2.5	10	40
2	Complex **4.7**	Br	Dioxane	1.25	5	59
3	Complex **4.7**	Br	Dioxane	0.25	1	64
4	Complex **4.7**	Br	Dioxane	0.125	0.5	80
5	Complex **4.7**	Br	Dioxane	0.0625	0.25	89
6	Complex **4.7**	Br	Dioxane	0.03125	0.125	73
7	Complex **4.7**	Br	Acetonitrile	0.125	0.5	49
8	Complex **4.7**	Br	Acetonitrile	0.0625	0.25	60
9	Complex **4.7**	Br	Acetonitrile	0.03125	0.125	73
10	Complex **4.7**	Br	Ethanol	0.125	0.5	53
11	Complex **4.7**	Br	H_2O / Dioxane	0.125	0.5	42

Table 5.1 4-bromotoluene (1 mmol), phenylboronic acid (1.5 mmol), Cs_2CO_3 (2 mmol), solvent (3 ml), reaction time 2 hours. Yields determined by ^{1}H NMR spectroscopy using 1,4-dimethoxybenzene as an internal standard.

Comparison of the catalytic activity of complex **4.7** with the mono-NHC palladium calix[4]arene complex reported by Brenner *et al.*, (Figure 5.2, complex **5.1**), shows that the opposite trend in activity was observed.[8] In dioxane, the yield increases as the catalyst loading is increased, with a 100 % yield being observed at 0.1 mol % catalyst (Table 5.2). This suggests that the catalytically active species formed from complex **5.1** is more stable, and the calix[4]arene ligand helps prevent the aggregation of inactive palladium(0)-nanoclusters. However, it should be noted that they do not increase the

catalyst loading above 0.1 mol %, which is where we observe the largest effect of palladium aggregation on yield.

Upon comparison of Tables 5.1 and 5.2, it can be seen that at lower catalyst loadings complex **4.7** shows comparable activity to complex **5.1**. At 0.03125 mol % of complex **4.7**, a yield of 73 % is achieved, and at 0.05 mol % of complex **5.1** a yield of 85 % is achieved. However, if we include the fact that our complex has four palladium centres per calix[4]arene, at 0.03125 mol % of catalyst there is 0.125 mol % of palladium. At a similar catalyst loading (0.1 mol %) Brenner et al. report a 100 % yield compared to our 73 % yield.[8]

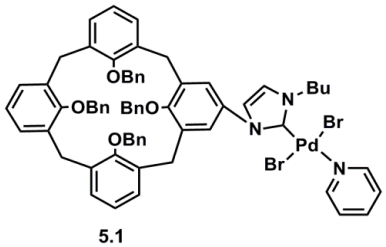

5.1

Figure 5.2 Palladium complex **5.1** synthesised by Brenner et al.[8]

X	Catalyst	Catalyst loading (mol %)	Yield (%)
Br	Complex **5.1**	0.1	100
Br	Complex **5.1**	0.05	84
Br	Complex **5.1**	0.01	2

Table 5.2 Catalytic results reported by Brenner *et al*. 4-bromotoluene (1 mmol), phenylboronic acid (1.5 mmol), Cs_2CO_3 (2 mmol), dioxane (3 ml), reaction time 2 hours. Yields determined by ^{1}H NMR spectroscopy using 1,4-dimethoxybenzene as an internal standard.[8]

Metal-free catalytic pathways were ruled out by performing the reaction with imidazolium compound **4.2** and no metal source, which did not result in any cross-coupled product. A palladium(0) source ($Pd_2(dba)_3$) and a palladium(II) source ($Pd(OAc)_2$) were also tested and were found to be less active than complex **4.7**, showing that the NHC group enhances catalytic activity (Table 5.3).

Entry	X	Catalyst	Catalyst loading (mol %)	Pd Loading (mol %)	Yield (%)
12	Br	Compound **4.2**	0.0025	0	0
13	Br	$Pd_2(dba)_3$	0.5	1	10
14	Br	$Pd(OAc)_2$	1	1	57
15	Br	$Pd(OAc)_2$	0.25	0.25	72

Table 5.3 4-bromotoluene (1 mmol), phenylboronic acid (1.5 mmol), Cs_2CO_3 (2 mmol), dioxane (3 ml), reaction time 2 hours. Yields determined by ^{1}H NMR spectroscopy using 1,4-dimethoxybenzene as an internal standard.

The catalytic reaction was carried out for the coupling of aryl chloride and phenylboronic acid. Aryl chlorides are known to be more difficult to activate than aryl bromides due to the stronger carbon-chloride bond. However, some palladium-NHC complexes have been shown to be very active catalysts for the coupling of aryl chlorides.[12-14] The catalytic results for the coupling of aryl chloride and phenylboronic acid, catalysed by complex **4.7**, are displayed in Table 5.4. As expected, the reactivity towards the chloride is lower than the reactivity towards the bromide, with the reported yields for the reactions carried out in dioxane for 2 hours (Entries 16-18) being negligible (3-13 %). $Pd(OAc)_2$ was investigated under these conditions and was also shown to be fairly inactive, giving a 16 % yield at 1 mol % of catalyst. It was found that increasing the reaction time from 2 hours to 24 hours dramatically improved the yield, and a 39 % yield was obtained at 1 mol % catalyst loading after 24 hours (Entry 19), compared to a 13 % yield after 2 hours (Entry 17).

The formation of the active Pd(0) species from the Pd(II) pre-catalyst is an essential step in the catalytic reaction. The choice of solvent and base has been reported to aid the formation of the active species, and improve the efficiency of the reaction. It has previously been reported that alcoholic solvents can improve the yield of Suzuki-Miyaura cross-coupling reactions when using NHC ligand precursors, presumably the change to a more polar solvent aids the formation of the active species.[14] We found that changing the solvent to ethanol (from dioxane) increased the yield when using chlorotoluene, and a 39 % yield was obtained at a catalyst loading of 0.125 mol %, after

2 hours (Entry 20). $Pd(OAc)_2$ was also investigated under these conditions and was shown to be inactive.

Entry	X	Catalyst	Solvent	Catalyst loading (mol %)	Pd Loading (mol %)	Yield (%)
16	Cl	Complex **4.7**	Dioxane	2.5	10	7
17	Cl	Complex **4.7**	Dioxane	1	4	13
18	Cl	Complex **4.7**	Dioxane	0.25	1.0	3
19	Cl	Complex **4.7**	Dioxane	1	4	39[a]
20	Cl	Complex **4.7**	Ethanol	0.125	0.5	39

Table 5.4 4-chlorotoluene (1 mmol), phenylboronic acid (1.5 mmol), Cs_2CO_3 (2 mmol), solvent (3 ml), reaction time 2 hours. Yields determined by ^1H NMR spectroscopy using 1,4-dimethoxybenzene as an internal standard.[a] Reaction time 24 hours.

As discussed previously, it has been reported by Schatz *et al.* that an *in situ* generated catalyst did not always give the same catalytic activity as a pre-formed catalyst, when using a calix[4]arene scaffold.[7] We wanted to investigate the activity of an *in situ* generated catalyst, formed from compound **4.2** and $Pd(OAc)_2$ (Table 5.5). It was found that the catalytic activity of the *in situ* formed catalyst was higher than that of the pre-formed catalyst, with the highest yield of 97 % being achieved at 0.25 mol % catalyst loading in dioxane (Entry 22). The *in situ* reaction was also carried out in the more economical solvent mixture of dioxane / H_2O (1:1), giving a 58 % yield. As the pre-formed and *in situ* generated catalysts do not display the same catalytic activity under the same experimental conditions, it is likely that the structure of the catalytically active species, generated from these two pre-catalysts, is different.

Entry	X	Catalyst	Solvent	Catalyst loading (mol %)	Pd Loading (mol %)	Yield (%)
21	Br	$Pd(OAc)_2$ + compound **4.2**	Dioxane	1	1	93
22	Br	$Pd(OAc)_2$ + compound **4.2**	Dioxane	0.25	0.25	97
23	Br	$Pd(OAc)_2$ + compound **4.2**	H_2O / Dioxane	1	1	58

Table 5.5 4-bromotoluene (1 mmol), phenylboronic acid (1.5 mmol), Cs_2CO_3 (2 mmol), solvent (3 ml), reaction time 2 hours. Yields determined by ^1H NMR spectroscopy using 1,4-dimethoxybenzene as an internal standard.

5.2 Conclusion

In conclusion, the catalytic activity of tetrakis-(*p*-palladium-NHC) mesityl calix[4]arene (complex **4.7**) has been investigated in the Suzuki-Miyaura cross-coupling reaction. Complex **4.7** was shown to be active for the coupling of aryl bromides and phenylboronic acid, with the best yields of the cross-coupled product being obtained at lower catalyst loadings. Complex **4.7** was shown to be more active for the coupling of aryl bromides than aryl chlorides. However, moderate yields of the cross-coupled product could be obtained from aryl chloride and phenylboronic acid when performing the reaction in ethanol. The catalytic activity of complex **4.7** was compared with $Pd(OAc)_2$, and $Pd_2(dba)_3$. Complex **4.7** was shown to be more active, confirming that the NHC group improved the activity of the catalyst.

The cross-coupling reaction with an *in situ* generated catalyst (compound **4.2** and $Pd(OAc)_2$) was also explored. It was found that the *in situ* generated catalyst had improved activity over complex **4.7**, suggesting that the active species generated from these two pre-catalysts was different.

5.3 Future work

Following the preparation of the palladium complexes of propanol-tethered methylimidazolium mesityl calix[4]arene (compound **3.4**) and acetic acid tethered

methylimidazolium mesityl calix[4]arene (compound **4.3**), the catalytic activity of these complexes should be explored, and the results compared. This will indicate if the nitrogen substituent of the imidazolium group has any effect on the catalytic activity of the complex. If the nitrogen substituent on the imidazolium groups of compound **3.4** or compound **4.3** form an interaction with the palladium centre, this could help stabilise the catalytically active species, and improve the catalytic activity.

Further work should also been done to probe the nature of the catalytically active species from the well defined, pre-formed catalyst, and the *in situ* protocol. This may help the design of more efficient catalyst systems.

5.4 References

1. A. Suzuki, *J. Organomet. Chem.*, 1999, **576**, 147-168.
2. G. C. Fortman and S. P. Nolan, *Chem. Soc. Rev.*, 2011, **40**, 5151-5169.
3. J.-P. Corbet and G. Mignani, *Chem. Rev.*, 2006, **106**, 2651-2710.
4. *Nobelprize.org. http://nobelprize.org/nobel_prizes/chemistry/laureates/2010/press.html*
5. M. Frank, G. Maas and J. Schatz, *Eur. J. Org. Chem.*, 2004, 607-613.
6. I. Dinares, M. C. Garcia, M. Font-Bardia, X. Solans and E. Alcalde, *Organometallics*, 2007, **26**, 5125-5128.
7. T. Fahlbusch, M. Frank, G. Maas and J. Schatz, *Organometallics*, 2009, **28**, 6183-6193.
8. E. Brenner, D. Matt, M. Henrion, M. Teci and L. Toupet, *Dalton Trans.*, 2011, **40**, 9889-9898.
9. C. E. Willans, J. M. C. A. Mulders, A. H. M. de Vries and J. G. de Vries, *J. Organomet. Chem.*, 2003, **687**, 494-497.
10. A. Alimardanov, V. L. Schmieder-van, A. H. M. de Vries and J. G. de Vries, *Adv. Synth. Catal.*, 2004, **346**, 1812-1817.
11. V. F. Slagt, A. H. M. de Vries, J. G. de Vries and R. M. Kellogg, *Org. Process Res. Dev.*, 2010, **14**, 30-47.
12. I. Ozdemir, S. Yasar, S. Demir and B. Cetinkaya, *Heteroat. Chem.*, 2005, **16**, 557-561.
13. Y.-Q. Tang, J.-M. Lu and L.-X. Shao, *J. Organomet. Chem.*, 2011, **696**, 3741-3744.
14. O. Diebolt, P. Braunstein, S. P. Nolan and C. S. J. Cazin, *Chem. Commun.*, 2008, 3190-3192.

6 Synthesis of NHC ligand precursors that are inspired by the structural motif of DTPA: Ligand synthesis and metal complexation

Diethylenetriaminepentaacetic acid (DTPA) is a linear octadentate ligand that incorporates three tertiary nitrogen atom donors, and five carboxylic acid donor groups (Figure 6.1, **A**).[1] The ligand chelates to metals, forming complexes with enhanced stability over similar complexes with non-chelating ligands. This enhanced stability is a consequence of the chelate effect, which is attributed to an increase in entropy upon chelation.[2] A major application for the DTPA ligand is in MRI (magnetic resonance imaging), where DTPA is coordinated to gadolinium and the complex is used as a contrast agent. Gadolinium-DTPA, commercially known as Magnevist® (Bayer Heathcare), was the first example of a contrast agent used to aid medical diagnostics in MRI, and is still used in practice today. Contrast agents consist of a paramagnetic metal ion (usually Gd^{3+}) bound by an organic ligand. The paramagnetic metal ion accelerates the relaxational properties of surrounding water molecules, which enhances the image produced in MRI. The organic ligand encases the gadolinium and allows for the complex to be easily excreted from the body following the procedure.[3] Ligands that bind to Gd^{3+} and form stable complexes are vital, as dechelation of the metal has been linked to a disease called nephrogenic systemic fibrosis (NSF), which can lead to serious complications or in some cases death.[4, 5] The DTPA ligand has also been used in chelation therapy, where it has been used to remove actinides from the body after contamination.[6, 7]

An NHC-ligand precursor was designed that is inspired by the structural motif of DTPA, with a view to forming metal-NHC complexes with enhanced stability (Figure 6.1, **6.3**). In the target DTPA-type ligand, two of the tertiary nitrogen atoms have been replaced by imidazolium groups, offering the potential to prepare metal-NHC complexes using this type of ligand. The synthesis of the ligand, which incorporates two imidazolium groups and three carboxylic acid groups, was unsuccessful. However, three novel bis-imidazolium amine salts based upon a similar structure were prepared (compounds **6.5**, **6.6**, **6.11**). The coordination of compound **6.5** to copper was explored using an electrochemical synthetic procedure to prepare complex **6.16**. The use of complex **6.16** as a transmetallation agent to form a palladium-NHC complex was investigated.

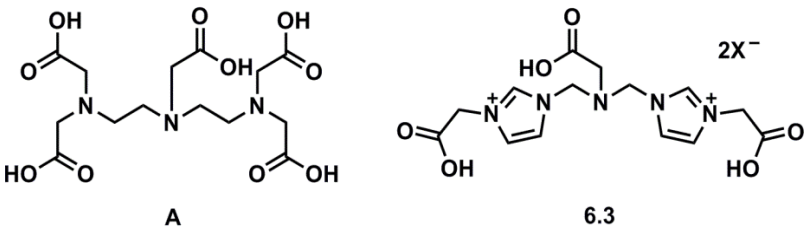

Figure 6.1 Structure of (A) DTPA, and (**6.3**) the novel DTPA-inspired NHC-ligand precursor, (X = Cl or Br).

6.1 Synthesis of DTPA-inspired NHC ligand precursors

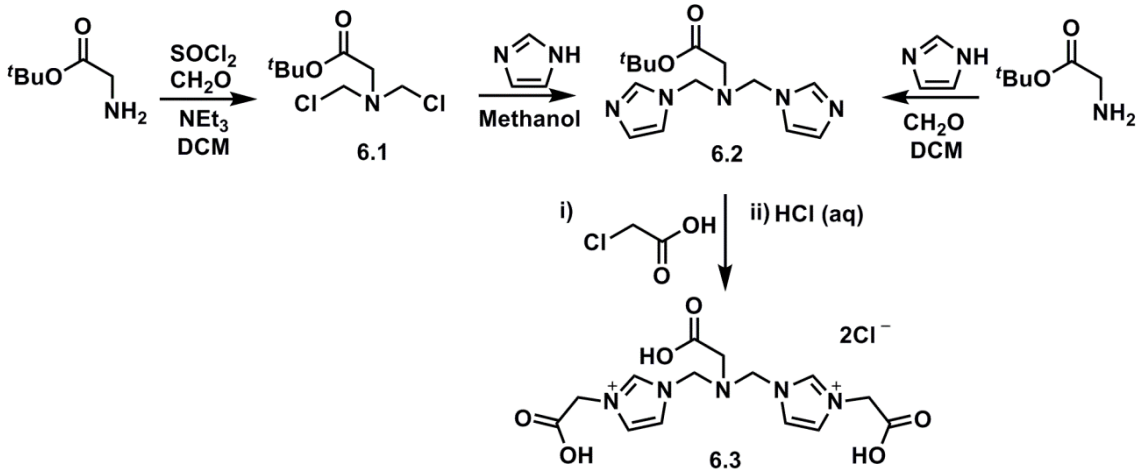

Scheme 6.1 Proposed synthesis of DTPA-inspired NHC ligand precursor **6.3**.

The preparation of amino(dichloromethyl) *tert*-butyl acetate (**6.1**) was achieved through the reaction of glycine *tert*-butyl ester hydrochloride, paraformaldehyde, and thionyl chloride.[8] Triethylamine was added to the reaction to neutralise the eliminated HCl, and protect the *tert*-butyl group. Compound **6.1** was characterised by ^{1}H NMR and ^{13}C{^{1}H} NMR spectroscopy and mass spectrometry.

Compound **6.1** was reacted with excess imidazole in methanol at reflux (75 °C). A base is not usually required in these nucleophilic reactions as imidazole itself acts as a base.[9] The reaction was unsuccessful, with none of the desired product being identified from the reaction mixture. The reaction was repeated in different solvents (CH_3Cl, THF), but still none of the desired product was obtained. Compound **6.1** is a type of nitrogen mustard and, as expected, was found to be unstable, requiring careful handling and storage at 4 °C. It has the potential to decompose, with the lone pair on the tertiary nitrogen attacking the adjacent carbon to generate an imine (Figure 6.2).

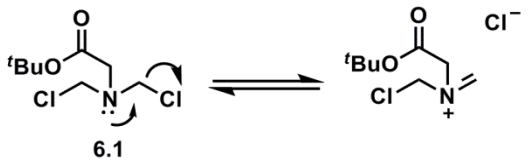

Figure 6.2 Possible degradation pathway for compound **6.1**.

The analytical data for compound **6.1** was re-examined and a signal was observed in the mass spectrum at 192.1 ($[C_8H_{15}NO_2Cl]^+$), which could be an indication that the imine had formed. However, it is also possible that compound **6.1** could have fragmented during the mass spectrometry experiment. An infrared spectrum of compound **6.1** was collected and a signal was observed at 1600 cm^{-1}, which is in the reported range for an imine bond (around 1480-1690 cm^{-1}).[10] This was not present in the infrared spectrum of the starting material (glycine *tert*-butyl ester hydrochloride) and implies that compound **6.1** degrades to form the imine.

The synthesis of compound **6.2** was therefore attempted directly from glycine *tert*-butyl ester hydrochloride with two equivalents of formaldehyde and excess imidazole. The product was purified by recrystallisation from diethyl ether (4 °C) to yield compound **6.2** as a white solid. Compound **6.2** was analysed by ^{1}H NMR and $^{13}C\{^1H\}$ NMR spectroscopy, mass spectrometry and elemental analysis. The ^{1}H NMR spectrum appears as expected, with the resonance for the imidazole proton at δ = 7.63 ppm. The two backbone imidazole protons appear as two separate resonance at δ = 7.12 ppm and δ = 6.97 ppm, with the resonances being too broad to show any coupling between the inequivalent backbone protons (Figure 6.6, **A**).

Colourless needle crystals were obtained by slow evaporation of a saturated chloroform solution of compound **6.2**. These were analysed by single crystal X-ray diffraction and the molecular structure is displayed in Figure 6.3. The compound crystallised in the monoclinic crystal system, and the structural solution was performed in the space group $P2_1/c$. The structure displays the expected compound, with a tertiary amine bearing two methyl imidazoles and a *tert*-butyl acetate group.

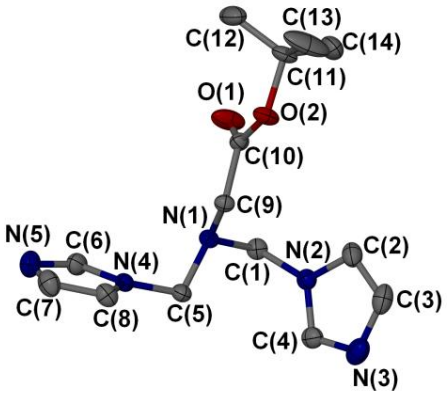

Figure 6.3 Molecular structure of compound **6.2**. The hydrogen atoms have been omitted for clarity. Ellipsoids are displayed at 50 % probability.

N(1)-C(1)	1.459(6)	N(1)-C(1)-N(2)	114.63(11)
N(5)-C(6)	1.325(2)	N(4)-C(5)-N(1)	110.90(11)
C(7)-C(8)	1.362(2)	C(8)-N(4)-C(5)	126.58(12)
C(2)-N(2)	1.381(2)	C(4)-N(2)-C(1)	126.79(13)
C(1)-N(2)	1.4781(19)	O(1)-C(10)-O(2)	125.77(13)

Table 6.1 Selected bond distances (Å) and angles (deg) for compound **6.2**.

The next step in the synthesis of the DTPA-type ligand (compound **6.3**) was the quaternization of the neural imidazole in compound **6.2** to form the imidazolium species. Compound **6.2** was reacted with a small excess of chloroacetic acid as a dry melt. The mixture was heated at 60 °C for 12 hours under a nitrogen atmosphere. A brown oil formed which, when washed with acetone, became a yellow solid. Low field resonances were observed in the ^{1}H NMR spectrum between δ = 7.45 ppm and δ = 8.82 ppm, which suggests the presence of imidazolium species. However, there were multiple products that, owing to their similar chemical properties, could not be easily separated. Attempts were made to improve the selectivity of the reaction by altering the reaction conditions. Initially, the same dry melt procedure was employed with the temperature being varied between 40-110 °C. Analysis by ^{1}H NMR spectroscopy of the product(s) formed again showed low field resonances, indicative of imidazolium salts, but no increased purity was observed at either lower or higher temperatures. The

reaction was carried out in solution (DCM / THF) both at reflux and at room temperature. No reaction occurred in solution and analysis by ^{1}H NMR spectroscopy showed only starting material.

A study was conducted to aid in the assignment of the different species that were formed in the reaction. A similar reaction was investigated following a literature procedure by Yi *et al.*, where the simpler 1-methylimidazole is reacted with chloroacetic acid as a dry melt to form the acetic acid tethered imidazolium salt, which they isolate as the BF_4 salt (Scheme 6.2).[11]

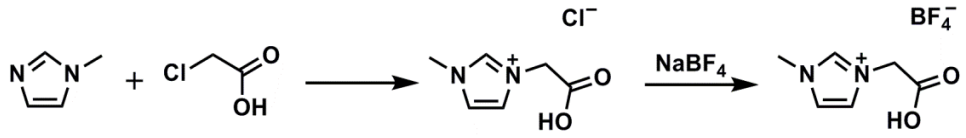

Scheme 6.2 Synthesis of 1-methyl acetic acid imidazolium tetrafluoroborate.[11]

The reaction was repeated following the procedure outlined in the literature, and the product was analysed by ^{1}H NMR spectroscopy combined with mass spectrometry. The ^{1}H NMR spectrum (DMSO-d_6) shows the formation of multiple imidazolium salts which include 1-methyl acetic acid imidazolium tetrafluoroborate and at least two other major imidazolium products (Figure 6.5). The mass spectrometry data confirmed the formation of multiple imidazolium species, namely; **A**; 1-methylimidazolium chloroacetate, **B**; 1-methyl-3-acetic acid imidazolium tetrafluoroborate, **C**; 1-methyl-3-acetyloxy acetic acid imidazolium tetrafluoroborate, the structures of which can be seen in Figure 6.4. Mass spectrometry data also showed evidence for the presence of **D** where n = 2-6.

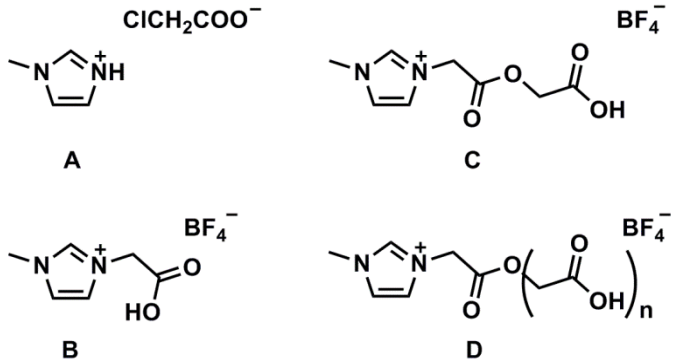

Figure 6.4 Products formed in the reaction of N-methyl imidazole and chloroacetate.

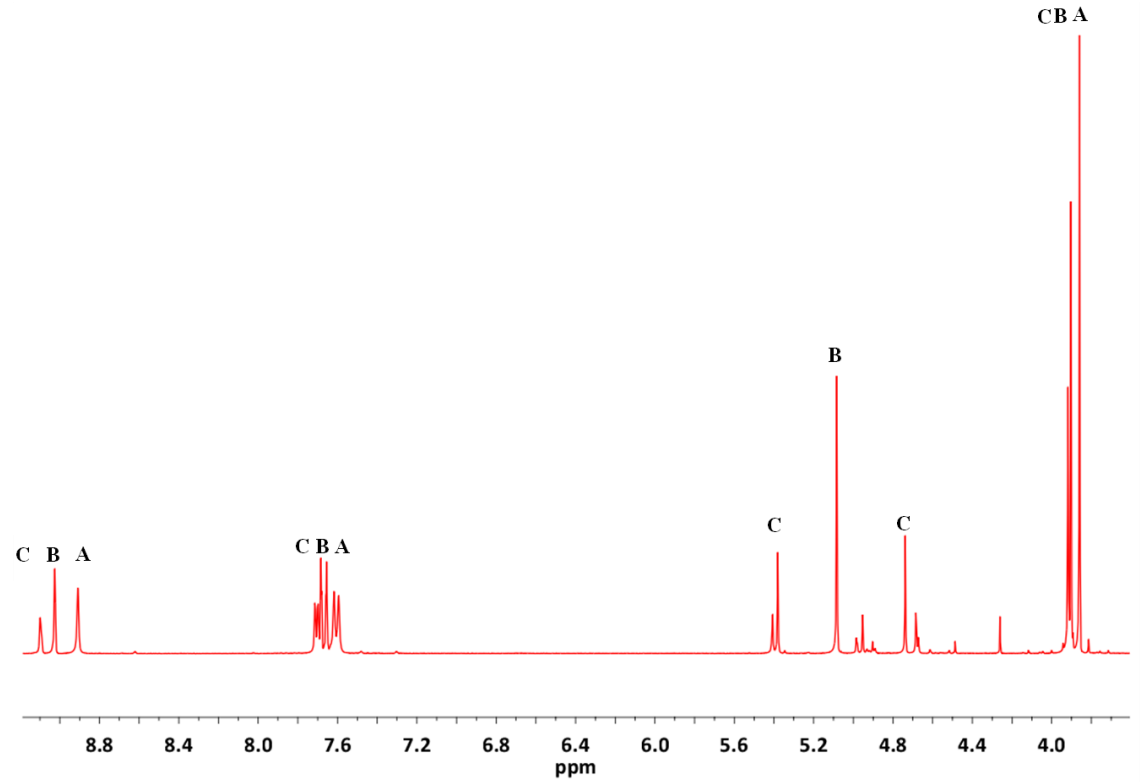

Figure 6.5 ^{1}H NMR spectrum (DMSO-d_6) displaying the products formed in the reaction of 1-methyl imidazole and chloroacetate at 298 K. **A**; 1-methylimidazolium chloroacetate, **B**; 1-methyl-3-acetic acid imidazolium tetrafluoroborate, **C**; 1-methyl-3-acetyloxy acetic acid imidazolium tetrafluoroborate.

The analytical data collected from the reaction of compound **6.2** with chloroacetate was re-examined to determine if similar species could be identified. The data was not as straight forward due to the complexity of the starting material and the presence of two imidazole moieties. However, it is likely that similar species were formed. In order to try and prevent these side reactions occurring, the same procedure was followed using *tert*-butyl chloroacetate, hence removing the acidic proton and protecting the oxygen from undergoing further reactions (Scheme 6.3). This reaction had already been successful with the simpler 1-methylimidazole, allowing for the selective synthesis of 1-methyl-3-*tert*-butylacetate imidazolium chloride (compound **4.4**), reported in Chapter 4. The *tert*-butyl protecting could then be removed to form the target compound **6.3**

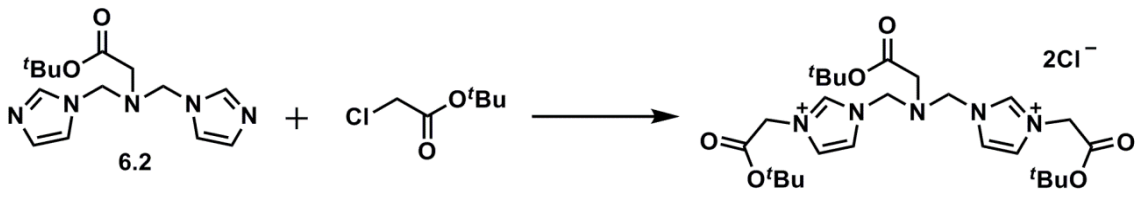

Scheme 6.3 Proposed product from the reaction of compound **6.2** with *tert*-butyl chloroacetate.

Compound **6.2** was reacted with an excess of *tert*-butyl chloroacetate (2.2 equivalents) as a dry melt. The mixture was heated at 45 °C for 12 hours, under a nitrogen atmosphere. A brown oil formed which, when washed with acetone, became an off-white solid. Low field resonances were observed in the ^{1}H NMR spectrum (DMSO-d_6), indicative of the formation of imidazolium species (Figure 6.6, **B**). However, a mixture of products still formed which appear to include imidazolium species and potentially some neutral imidazole species. The mass spectrometry data was complicated, and the signals could not be assigned to a desirable product.

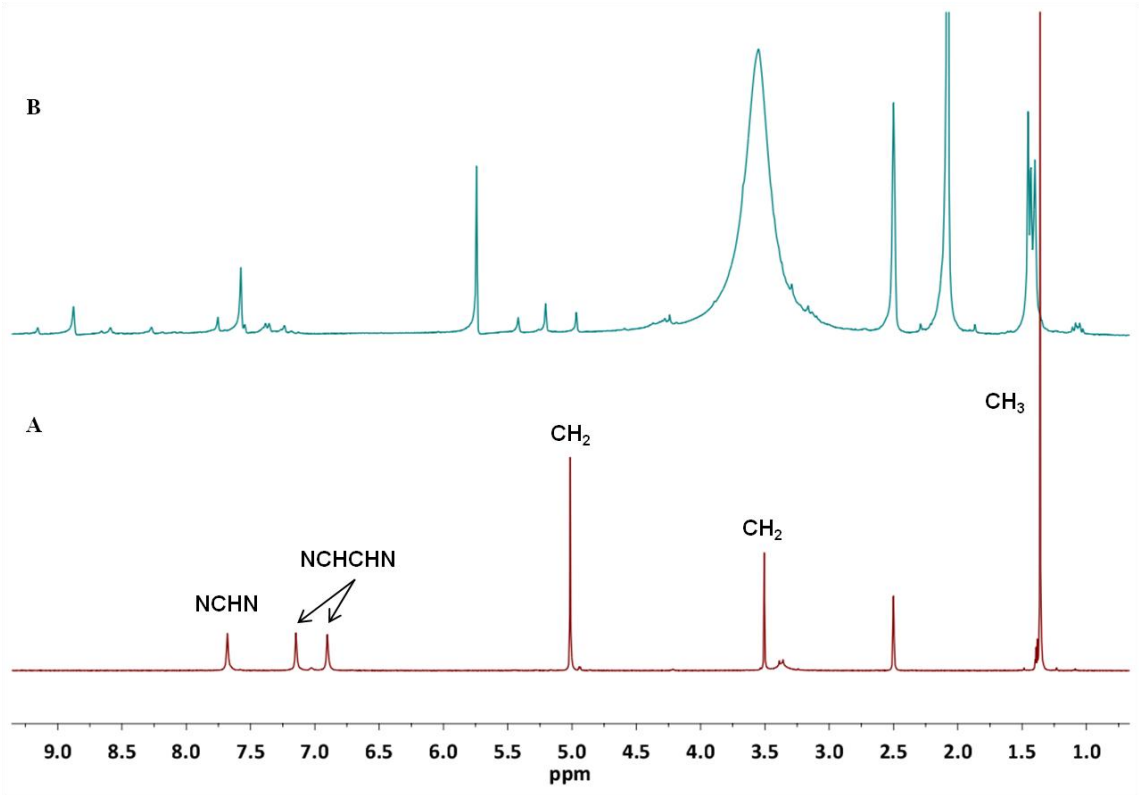

Figure 6.6. ^{1}H NMR spectra (DMSO-d_6) of (A) compound **6.2**, and (B) the products formed in the reaction of compound **6.2** with *tert*-butyl chloroacetate as a dry melt.

This result was somewhat surprising, as the reaction of 1-methylimidazole with *tert*-butyl chloroacetate had been found to proceed cleanly, yielding 1-methyl-3-*tert*-butylacetate imidazolium chloride. Compound **6.2** differs from 1-methylimidazole as it has an additional tertiary nitrogen atom which also has an available lone pair of electrons. It is possible that the lone pair on the tertiary nitrogen could attack the *tert*-butyl chloroacetate to form a quaternary nitrogen species (Figure 6.7). This product may then decompose into further species, accounting for the mixture of products that were formed. Alternatively, the tertiary nitrogen could be causing the product to decompose

once the imidazolium species has been generated, again accounting for the mixture of products that were formed.

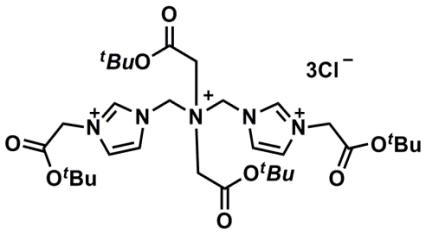

Figure 6.7 Proposed side product from the reaction of compound **6.2** with *tert*-butyl chloroacetate.

It was thought that reacting compound **6.1** with the already N-substituted imidazole, rather than proceeding through compound **6.2**, may reduce the problems associated with adding the acetate ester group to compound **6.2**. However, previous reactions with compound **6.1** had proved unsuccessful, due to its instability. Douthwaite *et al*. reported the preparation of amino(dichloroethyl) methyl benzene (compound **6.4**) as an intermediate in the formation of bis-imidazolium tertiary amine salts.[12] They reacted compound **6.4** with two equivalents of *tert*-butyl imidazole to yield the desired bis-imidazolium tertiary amine cleanly (Scheme 6.4). They found that it was necessary to protect the secondary amine of *bis*(2-dichloroethyl)amine with a benzyl group to prevent oligomerisation of the amine.

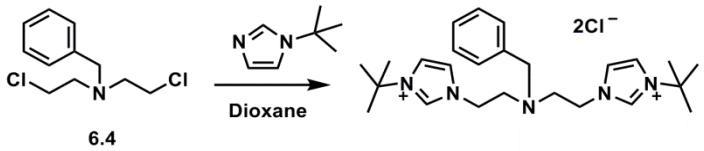

Scheme 6.4 Reported synthesis of bis-imidazolium tertiary amines.[12]

Compound **6.4** contains an extra CH_2 bridge between the tertiary amine and the chloride atoms compared to compound **6.1**. This alteration should increase the stability, as it is less likely that the imine will form. Compound **6.4** also incorporates the benzyl group on the amine rather than a *tert*-butyl acetate group, which would increase the number of synthetic steps to reach our (new) target compound (Scheme 6.5, compound **6.8**). We therefore attempted to add a *tert*-butyl acetate group to *bis*(2-dichloroethyl)amine, but the reaction was unsuccessful with none of the desired product being identified.

A proposed synthetic route to the new target compound (**6.8**) is shown in Scheme 6.5. The compound contains two CH_2 groups between the tertiary amine and

imidazolium groups, similar to DTPA, which contains two CH_2 groups between the nitrogen atoms.

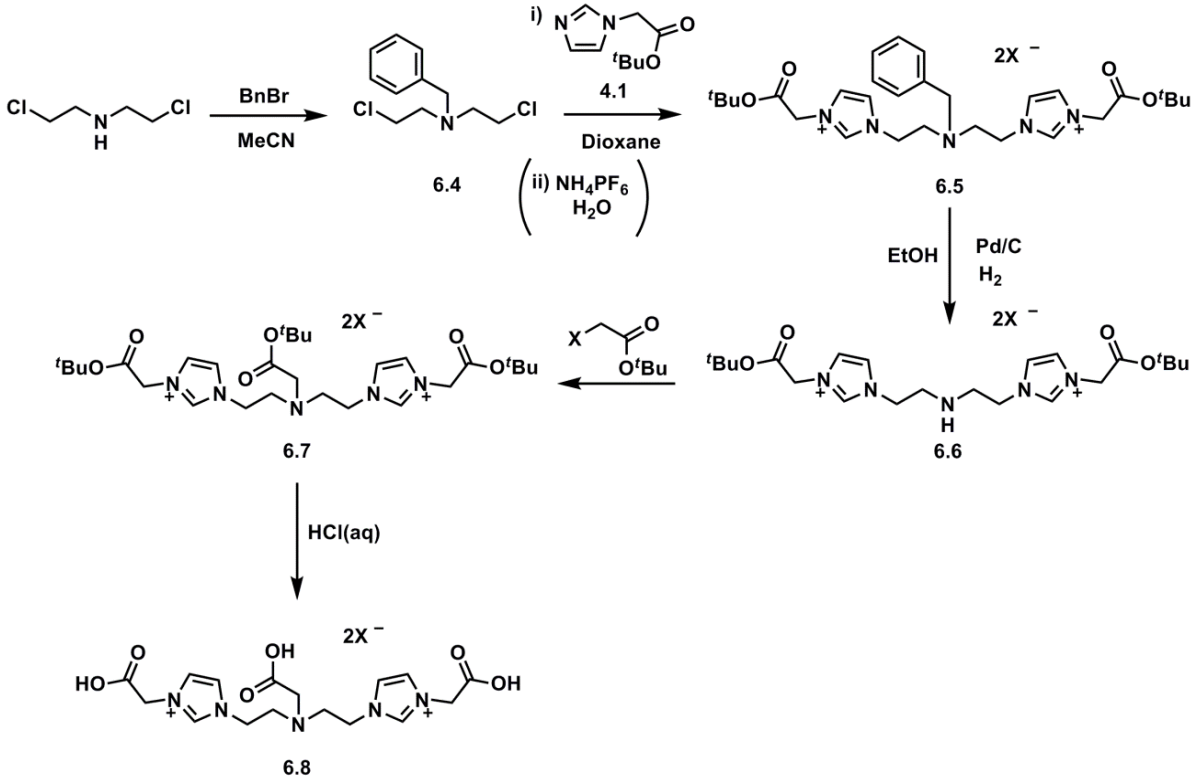

Scheme 6.5 Proposed synthesis of DTPA-inspired NHC ligand precursor **6.8** (X = Cl, Br, I, PF_6).

Compound **6.4** was synthesised in accordance with literature procedure.[12] *Bis*(2-chloroethylamine) hydrochloride was treated with sodium hydroxide to form the free amine, which was treated with benzyl bromide in the presence of excess potassium carbonate. The solution was filtered to remove the inorganic salts, and the solvent removed *in vacuo* to yield compound **6.4** as a yellow oil. When following the procedure outlined above, there was a large excess of benzyl bromide that remained in the reaction mixture, despite only a small excess (1.08 equivalents) initially being used. During the next step, reaction of this mixture with 1-*tert*-butyl acetate imidazole (**4.1**), lead to the formation of an undesired imidazolium salt, compound **6.9** (Figure 6.8).

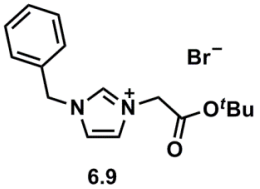

Figure 6.8 Product formed through the reaction of benzyl bromide with 1-methylimidazole *tert*-butyl chloroacetate.

It was therefore necessary to purify compound **6.4** further to remove any unreacted benzyl bromide. Firstly, the amount of benzyl bromide used in the reaction was reduced to less than one equivalent, as it was evident that an increased amount did not force the reaction to completion. In addition, once the reaction was complete, triethylamine was added which reacted with any remaining benzyl bromide to form the (N, N, N-triethylbenzyl)ammonium bromide salt. The triethylamine salt was precipitated from solution (DCM / petroleum ether), removed by filtration, and the solvent of the filtrate removed *in vacuo* to yield compound **6.4** as a colourless oil. Compound **6.4** was characterised by ^{1}H NMR and ^{13}C{^{1}H}NMR spectroscopy, combined with mass spectrometry, and was in accordance with the reported literature data.[12]

Compound **6.4** was reacted with 1-*tert*-butyl acetate imidazole (compound **4.1**) following the procedure outlined by Douthwaite et al. for the synthesis of bis-imidazolium tertiary amine salts.[12] Compound **6.4** and two equivalents of compound **4.1** were dissolved in 1,4-dioxane and the solution was heated at reflux (105 °C) for 12 hours. The solution was cooled to room temperature and the solvent removed *in vacuo*, to yield a yellow oil. The product was extracted into water and the water layer was washed with DCM followed by petroleum ether. The water was removed *in vacuo* to yield a pale yellow oil that solidified on washing with diethyl ether. Compound **6.5** was characterised by ^{1}H NMR and ^{13}C{^{1}H} NMR spectroscopy combined with mass spectrometry. The chloride counter ions were exchanged by reaction with ammonium hexafluorophosphate in water to afford the hexafluorophosphate salt of **6.5** as a white solid. Compound **6.5 PF_6** was characterised by ^{1}H NMR and ^{13}C{^{1}H} NMR spectroscopy, mass spectrometry and elemental analysis.

The ^{1}H NMR spectrum of compound **6.5 Cl** in MeOD-d_4 is displayed in Figure 6.9, with the relevant peaks assigned in Table 6.2. The ^{1}H NMR spectrum is as expected, with a characteristic resonance for the imidazolium C2 proton appearing downfield at δ = 9.10 ppm. The backbone imidazolium protons are observed as two separate resonances at δ = 7.61 ppm and δ = 7.59 ppm, with the resonances being too broad to display any resolved coupling between the inequivalent backbone imidazolium protons. The benzyl protons are observed as multiple resonances in the region of δ = 7.29 ppm to δ = 7.15 ppm. The CH_2 groups of the ethylene bridge appear as two separate triplet resonances at δ = 4.40 ppm and δ = 3.07 ppm, coupling with the inequivalent neighbouring CH_2 protons ($^{3}J_{HH}$ = 6 Hz).

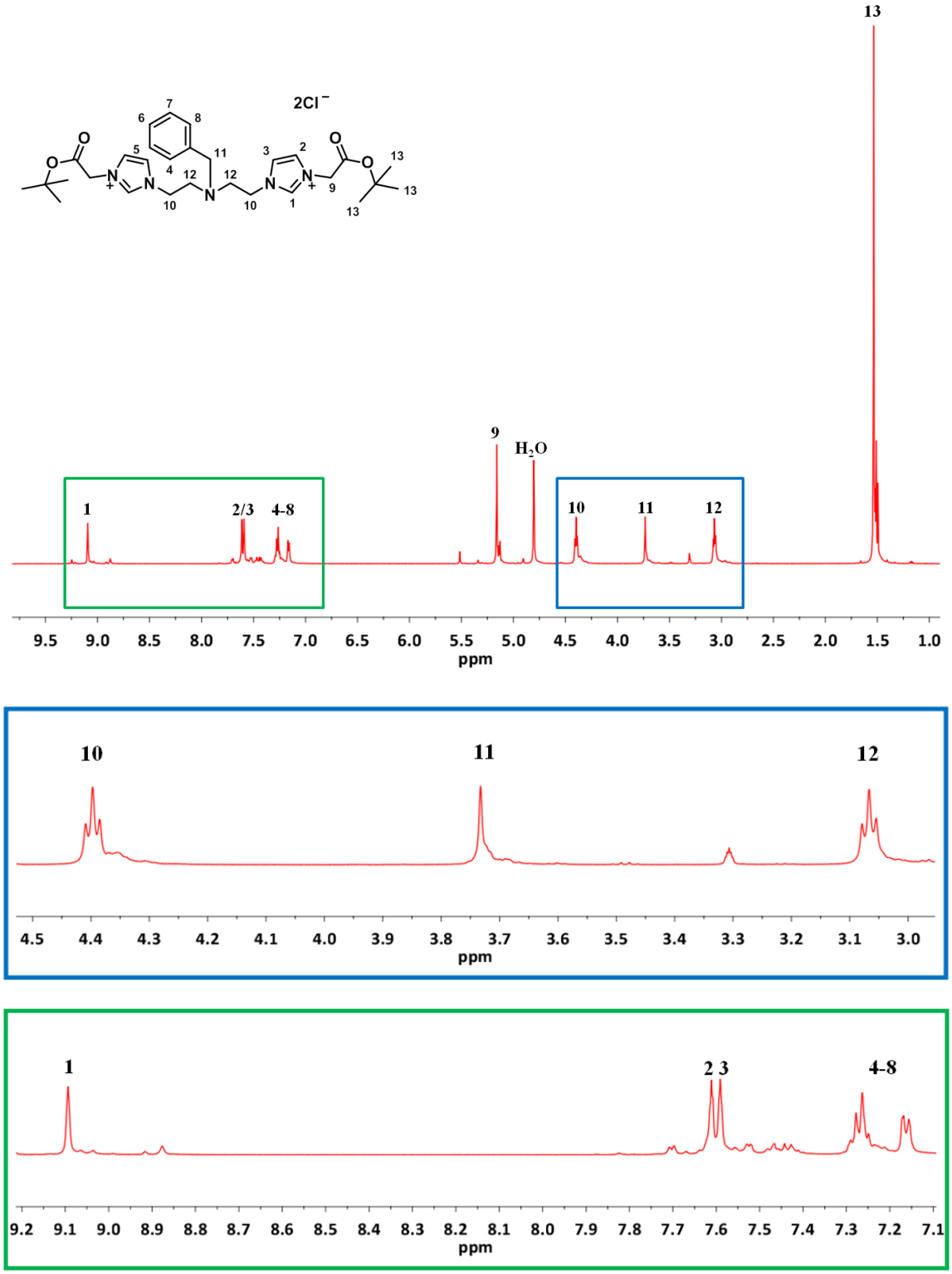

Figure 6.9 ^{1}H NMR spectrum (MeOD-d_4) of compound **6.5 Cl** at 298 K (top). Expansion in the region δ = 3.0 ppm to δ = 4.5 ppm (middle). Expansion in the region δ = 7.1 ppm to δ = 9.2 ppm (bottom).

Chemical shift (δ ppm) ^{1}H	Assignment
9.10 (s, 2H)	1
7.61 (s, 2H)	2 / 3
7.59 (s, 2H)	2 / 3
7.29 - 7.15 (m, 5H)	4-8
5.16 (s, 4H)	9
4.40 (t, 4H, $^3J_{HH}$ = 6 Hz)	10
3.74 (s, 2H)	11
3.07 (t, 4H, $^3J_{HH}$ = 6 Hz)	12
1.54 (s, 18H)	13

Table 6.2 ^{1}H NMR assignments for compound **6.5 Cl**.

The ^{1}H NMR spectrum of compound **6.5 PF_6** (MeOD-d_4) is consistent with the ^{1}H NMR data for **6.5 Cl** (MeOD-d_4). A change in the chemical shift is observed for the C2 protons, which is shifted upfield by 0.44 ppm to δ = 8.68 ppm. The hydrogen bonding interactions between the C2 proton and the non-coordinating anion (PF_6) are weaker than with the coordinating anion (Cl), resulting in the C2 proton experiencing a reduced deshielding effect. The formation of compound **6.5** was confirmed by mass spectrometry, with *m/z* observed for [**6.5**-Cl]$^+$ at 560.3, and [**6.5**-2Cl-H]$^+$ at 524.3. Similarly **6.5 PF_6** displayed *m/z* for [**6.5**-PF_6]$^+$ at 670.3.

The benzyl group on the amine of compound **6.5 Cl** was removed using Pd / C in ethanol at 70 °C for 24 hours. The mixture was filtered through celite and the solvent was removed *in vacuo* to yield compound **6.6** as a white hygroscopic solid, which was analysed by ^{1}H NMR and ^{13}C{^{1}H} NMR spectroscopy and mass spectrometry. The ^{1}H NMR spectrum of compound **6.5 Cl** in D_2O is displayed in Figure 6.10, with the relevant peaks assigned in Table 6.3.

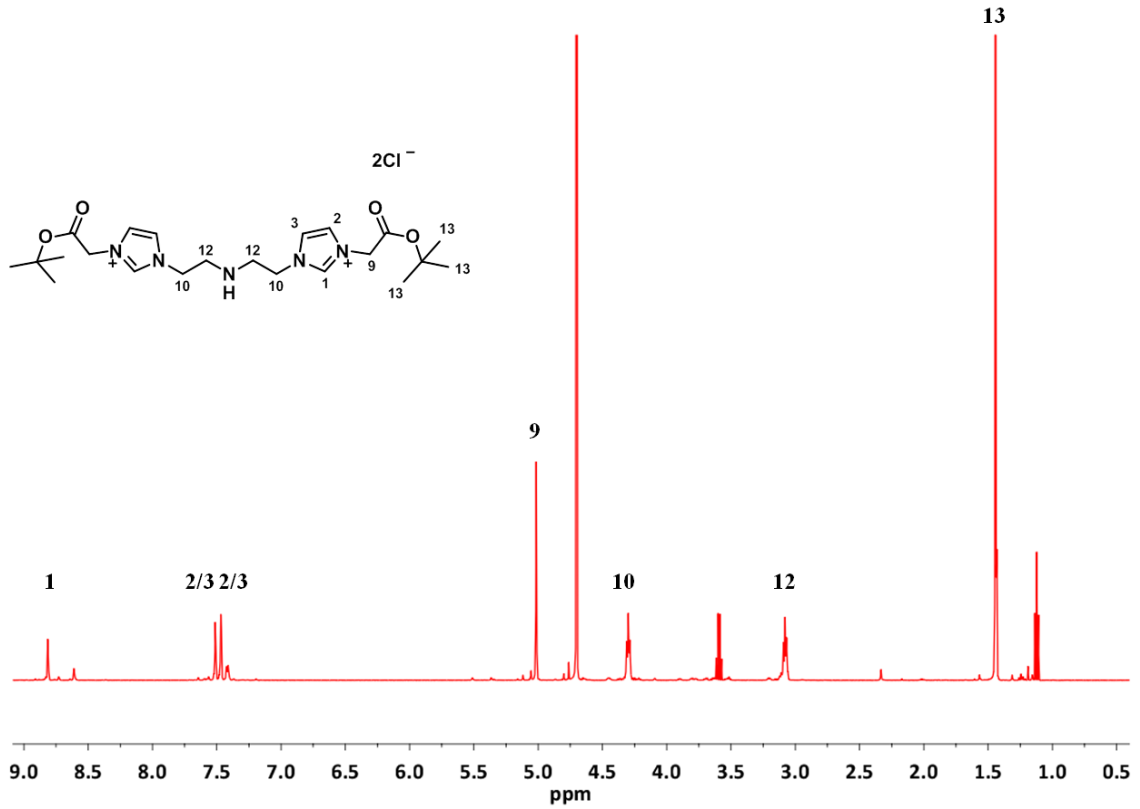

Figure 6.10 ^{1}H NMR spectrum (D_2O) of compound **6.6 Cl** at 298 K.

Chemical shift (δ ppm) ^{1}H	Assignment
8.98 (s, 2H)	1
7.68 (s, 2H)	2 / 3
7.63 (s, 2H)	2 / 3
5.19 (s, 4H)	9
4.46 (t, 4H, $^{3}J_{HH}$ = 6 Hz)	10
3.24 (t, 4H, $^{3}J_{HH}$ = 6 Hz)	12
1.61 (s, 18H)	13

Table 6.3 ^{1}H NMR assignments for compound **6.6 Cl**.

The ^{1}H NMR spectrum of compound **6.6** appears as expected, with loss of the proton resonances of the benzyl group between δ = 7.29 ppm and δ = 7.15 ppm, and δ = 3.74 ppm. The $^{13}C\{^{1}H\}$ NMR spectrum also appeared as expected with no low field resonances observed in the region for the benzylic carbons (δ = 130.5 ppm to δ = 128.6

ppm in compound **6.5**). The formation of compound **6.6** was confirmed by mass spectrometry with *m/z* for [**6.6**-2Cl-H]$^+$ observed at 470.3.

The same reaction was also attempted with compound **6.5 PF_6**. Once again the benzyl group was successfully removed, confirmed by ^{1}H NMR and ^{13}C{^{1}H} NMR spectroscopy. Interestingly, in this reaction, it appears that some of the *tert*-butyl groups of the acetate esters were also removed, with the proton resonance attributed to the *tert*-butyl groups at δ = 1.52 ppm being significantly reduced in intensity (Figure 6.11).

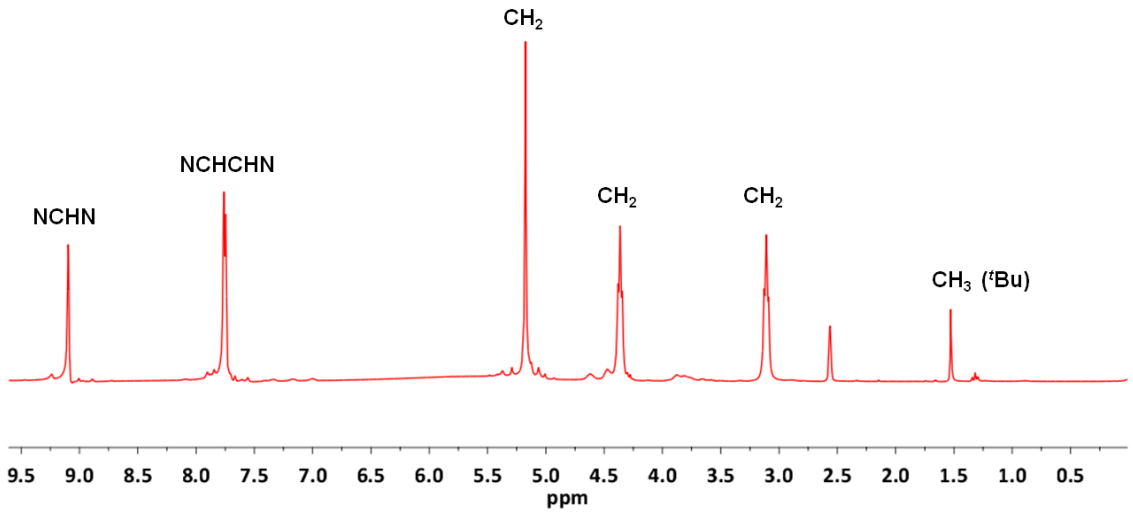

Figure 6.11 ^{1}H NMR spectrum (DMSO-d_6) of the product formed from the reaction of **6.5 PF_6** with Pd/C under a H_2 atmosphere.

The mass spectrometry data displayed a signal for the desired compound [**6.6**-PF_6]$^+$ at *m/z* 580.2. However, a signal was also observed for [**6.6**-2^{t}Bu-2PF_6]$^{2+}$ at *m/z* 161.6. Compounds often fragment during mass spectrometry experiments and it is not unusual to see the loss of *tert*-butyl groups. However, the significant reduction of the *tert*-butyl resonance in the ^{1}H NMR spectrum suggests that, in this case, it is likely that the *tert*-butyl groups have been removed from some of the material during this reaction. Therefore, compound **6.6 Cl** was used for further reactions.

Compound **6.6 Cl** was reacted with *tert*-butyl chloroacetate in an attempt to add the third *tert*-butyl acetate group to the secondary amine, to form compound **6.7 Cl**. The reaction was performed in acetonitrile and in the presence of potassium carbonate to 'mop up' the eliminated HCl and protect the *tert*-butyl groups of the acetate ester substituents. The product was analysed by ^{1}H NMR and ^{13}C{^{1}H} NMR spectroscopy, combined with mass spectrometry, but only starting material was identified from the reaction. The reaction was repeated using *tert*-butyl bromoacetate, as bromide is a better

leaving group than chloride, and the product was analysed by ^{1}H NMR spectroscopy and mass spectrometry. The major product of the reaction appeared to be the undesired imidazolium salt (Figure 6.12), indicating that fragmentation had occurred. The synthesis of compound **6.7 Cl** proved to be unsuccessful with none of the desired product being identified.

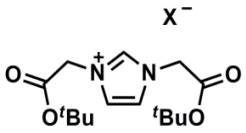

6.10

Figure 6.12 Product formed from the reaction of **6.7 Cl** with *tert*-butyl bromoacetate (X = Cl, Br).

Unfortunately, as the addition of the third *tert*-butyl acetate group to compound **6.6 Cl** was unsuccessful, the target ligand **6.8** was not synthesised. However, two novel NHC-ligand precursors were prepared (compounds **6.5** and **6.6**) that could be investigated as NHC ligand precursors. A third imidazolium amine ligand was also prepared by removing the *tert*-butyl groups from the acetate ester substituents of compound **6.5** to form a ligand with two carboxylic acid groups. Compound **6.5 PF_6** was dissolved in excess HCl (aq) and heated at reflux (110 °C) for 1 hour (Scheme 6.6). The solvent was removed *in vacuo* and the resultant solid was purified by washing with acetone and diethyl ether, and was dried *in vacuo* to isolate compound **6.11** as an off white solid, which was analysed by ^{1}H NMR and ^{13}C{^{1}H} NMR spectroscopy and mass spectrometry.

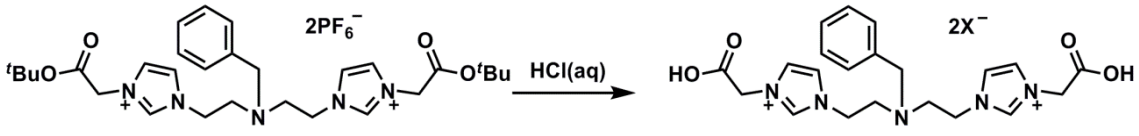

6.5 **6.11**

Scheme 6.6 Synthesis of compound **6.11** (X = Cl or PF_6).

The ^{1}H NMR spectrum of compound **6.11** appeared as expected, with the resonance attributed to the *tert*-butyl groups at δ = 1.54 ppm being absent. The formation of compound **6.11** was confirmed by mass spectrometry, with *m/z* for [**6.11**-2H-2X+Na]$^{+}$ at 434.2.

In conclusion, although the target DTPA inspired ligands (compounds **6.3** and **6.8**) were not synthesised, three novel DTPA-type NHC ligand precursors have been

prepared (compounds **6.5**, **6.6** and **6.11**), which incorporate different functional groups, and offer the potential to form a unique metal-NHC complexes.

6.2 Formation of metal-NHC complexes using a bis-imidazolium amine ligand (compound 6.5)

Douthwaite *et al.* were the first group to report the synthesis of an NHC-amine complex (Scheme 6.7).[12] They reacted a bis-imidazolium secondary amine (**6.12**) with Ag_2O to form a silver(I)-NHC complex (**6.13**), which was used as a ligand transfer agent to palladium(II). They isolated and crystallographically characterised the palladium(II)-complex **6.14**. The amine was then reduced to form a palladium(II)-NHC amido complex **6.15**. The same group later reported the synthesis of a palladium(II)-NHC complex using a bis-imidazolium tertiary amine NHC precursor (with a benzyl group on the amine). In this case the amine nitrogen does not from an interaction with the palladium centre (Figure 6.13, **A**).[13] Both these palladium-NHC complexes were found to be catalytically active in Heck reactions, displaying comparable activity to each other.

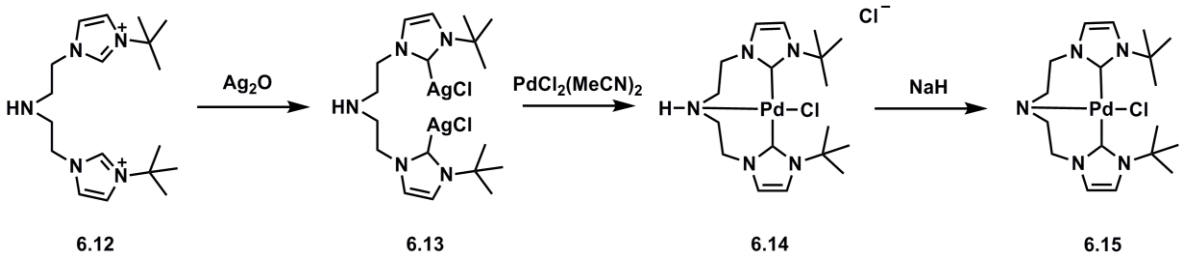

Scheme 6.7 Reported synthesis of a palladium-NHC amine complex.[12]

Hazari *et al*. later reported the synthesis of a related palladium(II)-NHC amine complex, which incorporates a further CH_2 linker between the amine and NHC groups (Figure 6.13, **B**).[14] The complex was crystallographically characterised and there was found to be no interaction between the amine and the palladium centre. The complex was catalytically active in both Heck and Suzuki reactions. However, the complex was not as active as those prepared by Douthwaite *et al*. for Heck reactions under the same conditions.

More recently, a rigid palladium(II)-NHC amido complex was reported by Cross *et al.* (Figure 6.13, **C**).[15] They prepared the palladium complex directly through reaction of the imidazolium salt with $Pd(OAc)_2$. They also report the preparation of a platinum(II) complex from the same ligand precursor.

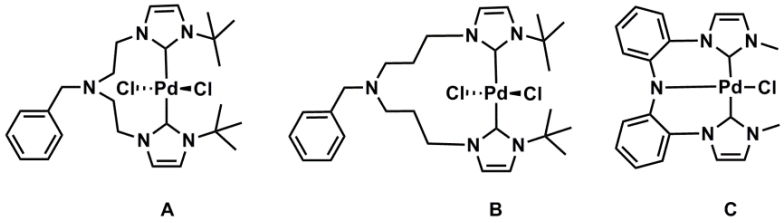

Figure 6.13 Palladium-NHC amine complexes using ligands with a similar architecture to compounds **6.5**, **6.6** and **6.11**.[13-15]

We initially explored the formation of metal-NHC complexes starting from the tertiary amine ligand precursor **6.5**. The protecting *tert*-butyl groups and benzyl group will prevent the interaction of any other part of the ligand with the metal centre.

6.2.1 Electrochemical synthesis of a copper(I)-NHC complex starting from imidazolium salt 6.5

Compound **6.5** has a similar architecture to the ligand reported by Douthwaite *et al*. (Figure 6.13, **A**), with the main difference being the incorporation of the *tert*-butyl acetate functionality on the imidazolium groups. We have found in previous investigations that, when using imidazolium precursors that are functionalised with acetate ester groups, the most common approaches reported in the literature for metal-NHC formation were unsuccessful. Under basic reaction conditions, the methylene groups of the acetate esters appear to deprotonate and cause undesired side reactions. However, the electrochemical method was successful for the synthesis of copper(I)-NHCs from imidazolium salts that were functionalised with acetate ester groups.[16] The electrochemical method was therefore explored with compound **6.5 PF_6** (Scheme 6.8).

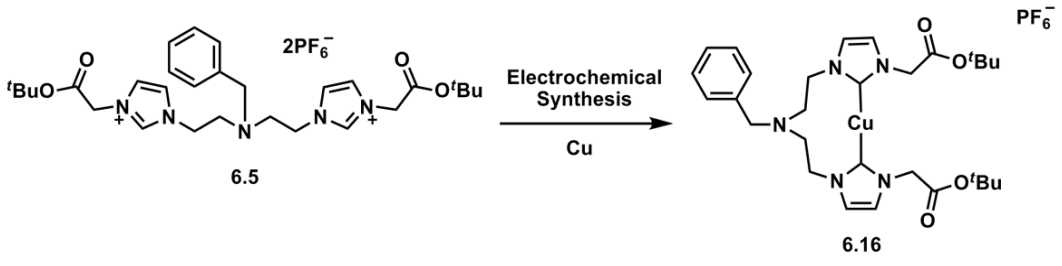

Scheme 6.8 Electrochemical synthesis of Cu(I)-NHC complex **6.16**.

Copper plates were used as both the sacrificial anode and cathode (1 × 3 cm), and the reaction was performed in anhydrous acetonitrile. Compound **6.5 PF_6** was added to the flask and degassed. Anhydrous acetonitrile was added (15 ml) and the solution was

degassed for 1 hour by bubbling argon through. The electrodes were inserted into the solution and a potential applied such to maintain a constant current of 50 mA. The reaction was monitored by ^{1}H NMR spectroscopy, and ended when the resonance for the C2 protons was no longer present in the ^{1}H NMR spectrum (25 minutes, 2 Q). The mixture was filtered to remove suspended copper particles, and the solvent removed *in vacuo* to yield complex **6.16** as an off white solid, which was characterised by ^{1}H NMR and ^{13}C{^{1}H} NMR spectroscopy combined with mass spectrometry. A ^{1}H NMR spectrum (MeCN-d_3) of the product is displayed in Figure 6.14.

It is evident that an NHC complex has formed due to the disappearance of the resonance attributed to the C2 protons observed at δ = 8.66 ppm (DMSO-d_6) in the imidazolium precursor **6.5 PF_6**. Signals are observed in the correct regions to be assigned as CH, CH_2 and CH_3 protons. However, there are five CH_2 and two CH_3 regions (integrate as 2.5:1), which is more than would be expected if one symmetrical complex was formed.

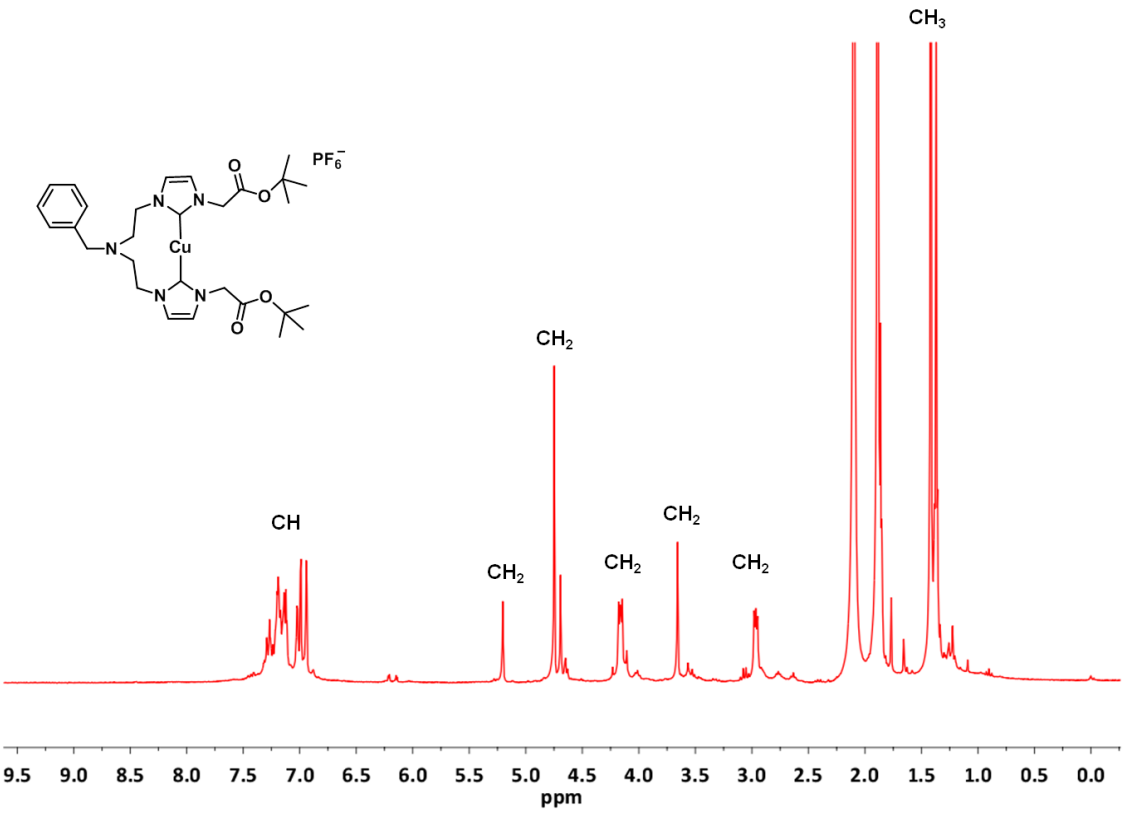

Figure 6.14 ^{1}H NMR spectrum (MeCN-d_3) of Cu(I)-NHC complex **6.16** at 298 K.

The ^{13}C{^{1}H} NMR spectrum of complex **6.16** displays a low field resonance at δ = 181.0 ppm, attributable to a C2 proton bound to copper. Again, as with the ^{1}H NMR

spectrum, there are six separate resonances assigned to carbons of CH_2 groups, and two resonances assigned to carbons of CH_3 groups. The mass spectrometry data confirmed the presence of the chelating copper complex with *m/z* observed for [**6.16**-PF_6]$^+$ at 586.25, which displays the correct splitting pattern for the +1 species (Figure 6.15). Crystallisations were attempted in a range of solvents / solvent systems, but no crystals were obtained that were suitable for analysis by single crystal X-ray diffraction. A crystal structure may have assisted in the assignment of the NMR spectra.

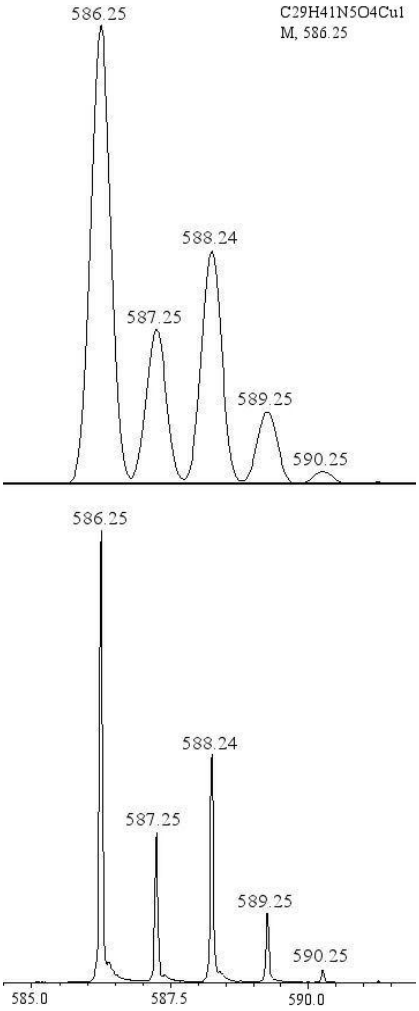

Figure 6.15 Mass spectrometry data of complex **6.16** (bottom), calculated for [**6.16**-PF_6]$^+$ (top).

6.2.2 Transmetallation from copper(I)-NHC complex 6.16 to palladium

An attractive route for the synthesis of a wide range of transition-metal NHC complexes is to use the direct NHC ligand transfer from one metal to another. As discussed previously, copper(I)-NHCs have been reported as carbene transfer agents to ruthenium(II), palladium(II), nickel(II) and gold(I).[17-19] The reaction of complex **6.16** with $PdCl_2(MeCN)_2$ was investigated (Scheme 6.9).

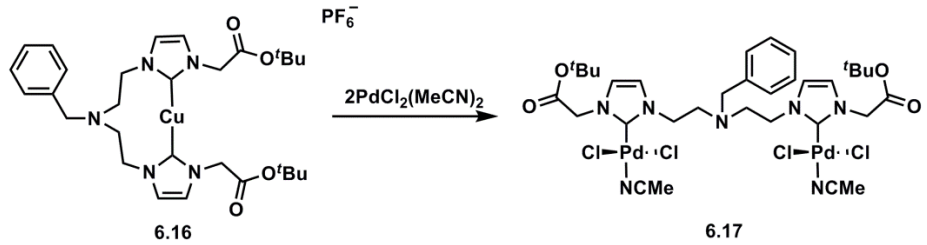

Scheme 6.9 Transmetallation reaction from copper(I) (complex **6.16**) to palladium(II) (suggested structure for the palladium(II)-NHC complex).

Complex **6.16** and $PdCl_2(MeCN)_2$ were stirred in DCM at room temperature for 12 hours. DCM is an attractive choice of solvent for transmetallation as the copper salts formed as by-products precipitate from DCM, which helps to drive the reaction to completion, and assists in the purification of the product. The solution was filtered to remove the inorganic salts and the solvent of the filtrate was removed *in vacuo*. The product was analysed by ^{1}H NMR spectroscopy and mass spectrometry, but the data could not be assigned to a desirable product. The reaction was repeated in acetonitrile, and the product purified by dissolving in DCM and filtering through celite. The solvent of the filtrate was removed and the product was analysed by ^{1}H NMR and $^{13}C\{^{1}H\}$ NMR spectroscopy combined with mass spectrometry. The ^{1}H NMR spectrum is displayed in Figure 6.16.

The ^{1}H NMR spectrum (MeCN-d_3) indicates the formation of a metal-NHC complex (or complexes) as there is no high field resonance for the C2 proton. The signals have shifted compared to the copper(I)-NHC complex, suggesting that transfer to palladium has occurred. The spectrum is very broad at low temperatures (243 K), becoming sharper on heating (323 K), with the broad resonance at $\delta = 2.65$ ppm (243 K) becoming two sharp resonances at 342 K. Although the spectra cannot be fully assigned, there are resonances in the correct regions to be assigned as CH, CH_2 and CH_3 protons of the desired product. The $^{13}C\{^{1}H\}$ NMR spectrum was also complicated, displaying a large number of resonances. However, no resonance was observed for the

C2 carbon bound to copper at δ = 181 ppm, and instead two low field resonances were observed at δ = 141 ppm and δ = 167 ppm. The resonance at δ = 141 ppm is characteristic of a palladium(II)-NHC complex that has a *trans*-coordinating two electron donor ligand such as $PdX_2(NHC)(py)$ or $PdX_2(NHC)(MeCN)$, whereas, the resonance at δ = 167 ppm is characteristic for a bidentate palladium(II)-NHC complex of the type $Pd(NHC)_2X_2$.[20, 21] The mass spectrometry data suggests the formation of a monodentate palladium-NHC complex bearing two palladium centres, with *m/z* at 842.0 for [**6.17**-2MeCN-Cl]$^+$ and *m/z* at 983.9 for [**6.17**+Na]$^+$.

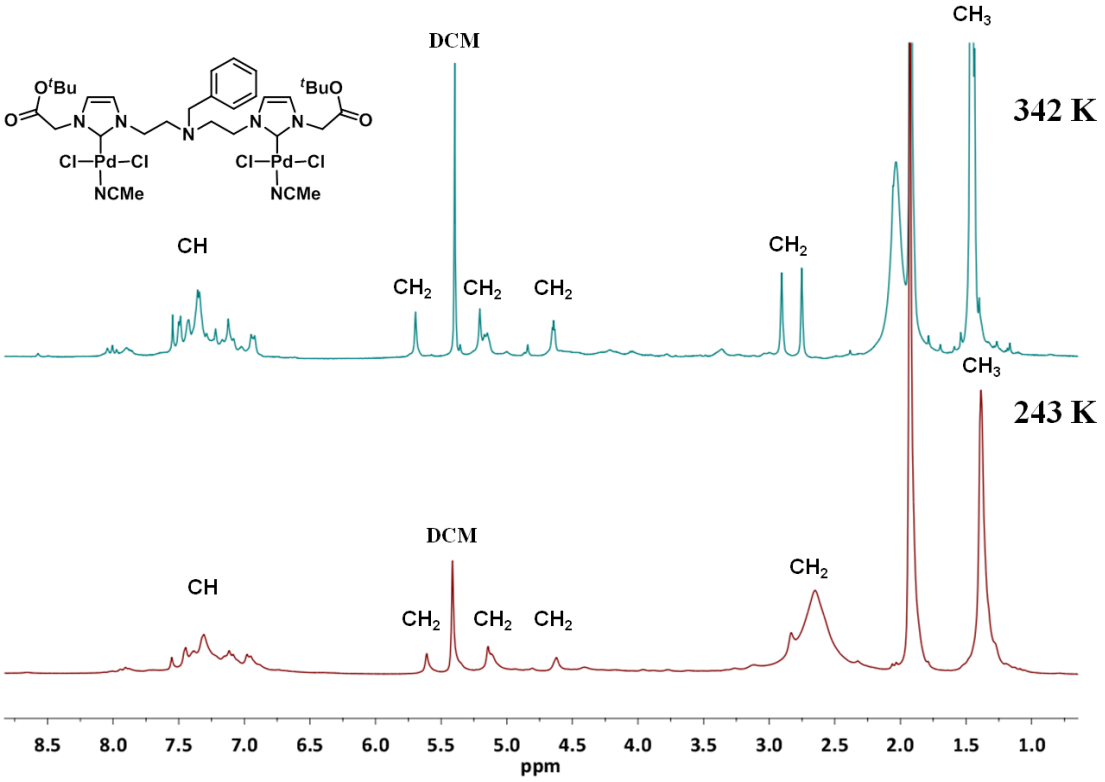

Figure 6.16 ^{1}H NMR spectrum (MeCN-d_3) of complex **6.17** at 243 K and 342 K.

Single crystals suitable for analysis by single crystal X-ray diffraction were obtained from the reaction mixture (MeCN / diethyl ether), but they were found to be copper(I) tetrakisacetonitrile hexafluorophosphate. Attempts were made to purify the product and remove the copper(I) salts but, to date, no crystals of a palladium complex have been obtained that are suitable for analysis by single crystal X-ray diffraction.

There are a number of products that could be formed in this transmetallation reaction, though only complex **6.17** has been identified in the mass spectrometry data. These include monomeric, dimeric, and oligomeric palladium(II) species, which may have *cis* or *trans* geometry about the palladium centres.[22] Some of the possible products

are displayed in Figure 6.17, where the carbenes in the bis-NHC complexes are coordinated in a *trans* fashion. If a mixture of products is formed in the reaction this may account for the broad and complicated ^{1}H NMR spectrum. Furthermore, it may account for the large number of signals that are seen in the $^{13}C\{^{1}H\}$ NMR spectrum. A similar finding was reported by Danopoulos *et al*. when they investigated the synthesis of bis-NHC complexes of palladium through transmetallation from silver. They observed mixtures of monomeric, dimeric, and oligomeric palladium(II) species which were inseparable.[23]

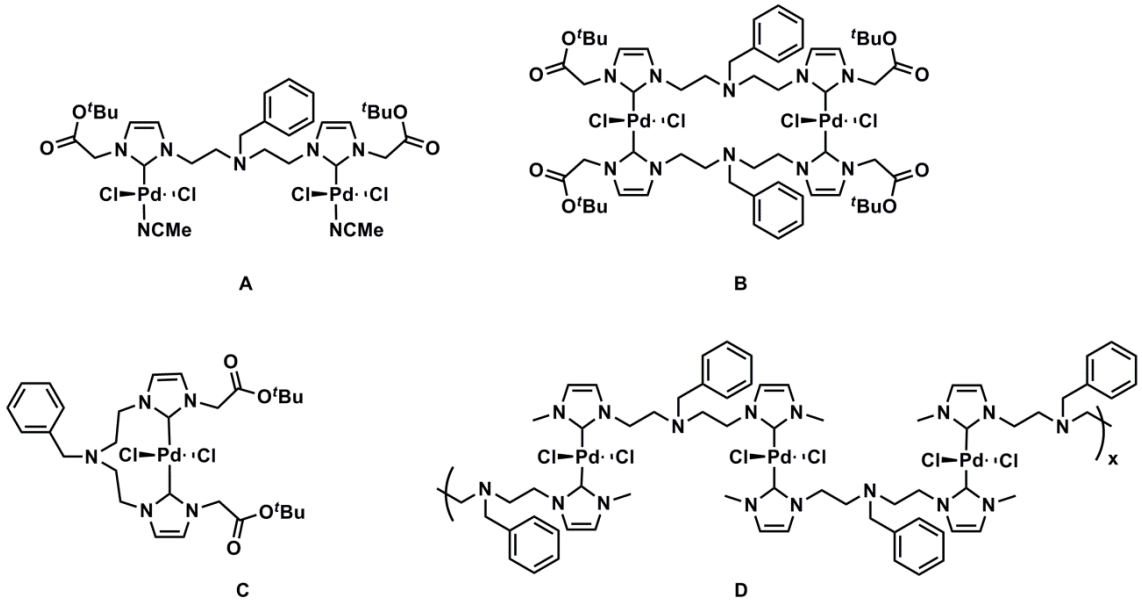

Figure 6.17 Possible products formed from the transmetallation reaction from copper(I) (complex **6.5**) to palladium(II).

6.3 Conclusion

In conclusion, although the synthesis of the target DTPA-type ligands (compounds **6.3** and **6.8**) was unsuccessful, three novel bis-imidazolium amine ligands were prepared (compounds **6.5**, **6.6** and **6.11**), which incorporate different functional groups and offer the potential to form unique metal-NHC complexes.

To date, only compound **6.5** has been investigated as a potential NHC-ligand precursor. The electrochemical approach was used to synthesise a copper(I)-NHC complex (complex **6.16**), which was used as a carbene transfer agent for the formation of a palladium(II)-NHC complex (**6.17**). Complex **6.17** appears to have a different structure to the palladium-NHC amine complexes that have been previously reported, with the monodentate $PdCl_2$(NHC)(MeCN) complex being identified. However, it

appears that complex **6.17** was not produced selectively and other products were formed during the transmetallation reaction.

6.4 Future work

Further work would include the purification and full characterisation of the products formed in the transmetallation reaction (Scheme 6.9). If the monodentate palladium-NHC complex **6.17** can be isolated from the reaction, this would be an interesting complex to test as a catalyst in the Heck reaction and compare with the bis-NHC complexes reported in the literature (Figure 6.13). Having an acetonitrile group *trans* to the NHC may improve the efficiency of the catalyst, as the acetonitrile molecule will be weakly bound owing to the strong *trans* effect of the NHC group.

The use of compounds **6.6** and **6.11** as NHC-ligand precursors should also be investigated. Compound **6.6** incorporates acetate ester functionalities, hence the electrochemical method would most likely be the best approach for the synthesis of metal-NHC complexes using this ligand precursor. Compound **6.11** incorporates acetic acid functionalities so the electrochemical route would not be a viable synthetic route for this ligand. We have previously observed that during electrochemical reactions, acetic acid groups appear to be eliminated from the compound. The use of a base (e.g. ^{n}BuLi), followed by coordination of the free NHC to a metal centre should be a suitable synthetic route for the formation of metal-NHC complexes using compound **6.11**. As compounds **6.6** and **6.11** incorporate different functional groups, for example carboxylate or an amine donor, it would be interesting to examine the resulting complexes in catalysis.

6.5 References

1. A. E. Frost, *Nature*, 1956, **178**, 322.
2. G. Schwarzenbach, *Helv. Chim. Acta*, 1952, **35**, 2344-2359.
3. H. J. Weinmann, R. C. Brasch, W. R. Press and G. E. Wesbey, *Am. J. Roentgenol.*, 1984, **142**, 619-624.
4. D. M. A. G. J. Ten and J. F. M. Wetzels, *Neth J Med*, 2008, **66**, 416-422.
5. J. L. Abraham and C. Thakral, *Eur J Radiol*, 2008, **66**, 200-207.
6. H. D. Roedler, D. Nosske, L. Ohlenschaeger, H. Schieferdecker, H. Doerfel and K. Renz, *Radiat. Prot. Dosim.*, 1989, **26**, 377-379.
7. E. H. Carbaugh, T. P. Lynch, C. N. Cannon and L. L. Lewis, *Health Phys.*, 2010, **99**, 539-546.
8. L. C. Song, J. H. Ge, X. F. Liu, L. Q. Zhao and Q. M. Hu, *J. Organomet. Chem.*, 2006, **691**, 5701-5709.
9. C. E. Willans, K. M. Anderson, P. C. Junk, L. J. Barbour and J. W. Steed, *Chem. Commun.*, 2007, 3634-3636.
10. L. D. S. Field, S.; Kalman, J. R., ed., *Organic Structure from Spectra*, John Wiley and sons Ltd. *(New York, U. S.)*, 1995.
11. F. P. Yi, H. Y. Sun, M. H. Pan, Y. Xu and J. Z. Li, *Chin. Chem. Lett.*, 2009, **20**, 275-278.
12. R. E. Douthwaite, J. Houghton and B. M. Kariuki, *Chem. Commun.*, 2004, 698-699.
13. J. Houghton, G. Dyson, R. E. Douthwaite, A. C. Whitwood and B. M. Kariuki, *Dalton Trans.*, 2007, 3065-3073.
14. J. D. Blakemore, M. J. Chalkley, J. H. Farnaby, L. M. Guard, N. Hazari, C. D. Incarvito, E. D. Luzik and H. W. Suh, *Organometallics*, 2011, **30**, 1818-1829.
15. W. B. Cross, C. G. Daly, R. L. Ackerman, I. R. George and K. Singh, *Dalton Trans.*, 2011, **40**, 495-505.
16. B. R. M. Lake, E. K. Bullough, T. J. Williams, A. C. Whitwood, M. A. Little and C. E. Willans, *Chem. Commun.*, 2012, **48**, 4887-4889.
17. M. R. L. Furst and C. S. J. Cazin, *Chem. Commun.*, 2010, **46**, 6924-6925.
18. G. Venkatachalam, M. Heckenroth, A. Neels and M. Albrecht, *Helv. Chim. Acta*, 2009, **92**, 1034-1045.
19. C. Chen, H. Qiu and W. Chen, *J. Organomet. Chem.*, 2012, **696**, 4166-4172.
20. K.-T. Chan, Y.-H. Tsai, W.-S. Lin, J.-R. Wu, S.-J. Chen, F.-X. Liao, C.-H. Hu and H. M. Lee, *Organometallics*, 2010, **29**, 463-472.
21. H. V. Huynh, Y. Han, J. H. H. Ho and G. K. Tan, *Organometallics*, 2006, **25**, 3267-3274.
22. E. Alcalde, R. M. Ceder, C. Lopez, N. Mesquida, G. Muller and S. Rodriguez, *Dalton Trans.*, 2007, 2696-2706.
23. R. M. Porter, S. Winston, A. A. Danopoulos and M. B. Hursthouse, *J. Chem. Soc., Dalton Trans.*, 2002, 3290-3299.

7 Synthesis of NHC ligand precursors that are inspired by the structural motif of DOTA: Ligand synthesis and metal complexation

1, 4, 7, 10-Tetraazacylododecane tetraacetic acid (DOTA) is a macrocyclic octadentate ligand that incorporates four tertiary nitrogen donors and four carboxylic acid donor groups (Figure 7.1, **A**). The ligand binds to metals and forms complexes with enhanced stability over similar complexes with non-chelating ligands. This enhanced stability is a consequence of both the chelating and macrocyclic effects, which are attributed to a combination of entropic and enthalpic factors that favour the formation of a rigid macrocyclic structure.[1] A major application for the DOTA ligand is in MRI, where DOTA is coordinated to gadolinium(III) and the complex is used as a contrast agent (Dotarem®).[2] MRI relies on the different distributions of water molecules in the examined tissue, and on the proton relaxational properties of the water molecules' longitudinal (T1) and transverse (T2) magnetic relaxational times.[3] Contrast agents alter the relaxational properties of the water molecules in the areas where they accumulate, enhancing the image produced in MRI. Ligands that bind to gadolinium and form stable complexes are vital, as dechelation of the gadolinium has been linked to a disease called NSF (nephrogenic systemic fibrosis), which can lead to serious and sometimes fatal complications.[4, 5] Therefore, the design of ligands that bind to gadolinium and form very stable complexes is vital. Most research performed so far has focused on varying the carboxylic acid functionalities of DOTA, which has often had a favourable increase in T1 relaxational times. There are fewer examples in the literature where the nitrogen donors of DOTA have been altered.[6] This is of interest as it could offer the possibility of more rigid ligands which will decrease the rotational rate and increase relaxivity. Furthermore, it may be possible to design more stable gadolinium chelates.

In this work, ligands have been designed that are inspired by the structural motif of DOTA. In the first target DOTA-type ligand, two of the tertiary nitrogen atom donors were replaced by imidazolium groups, offering the potential to form metal-NHC complexes from this ligand (Figure 7.1, **B**). The proposed macrocyclic hexadenate ligand (compound **7.2**) incorporates two tertiary nitrogen atom donors, two carboxylic acid groups and two imidazolium groups. However, the formation of the macrocyclic ligand **7.2** was unsuccessful. Our next approach involved the functionalisation of a pre-formed macrocyclic ligand with an imidazolium group (Figure 7.1, **C**). The potentially nonadentate ligand incorporates four tertiary nitrogen donors, four carboxylic acid

groups and one imidazolium group. A synthetic route for the formation of the DOTA-type ligand **C** is described (compound **7.17**, n = 3), and a gadolinium complex of the ligand was prepared (**7.19**). The efficiency of the gadolinium complex as a contrast agent was probed by measuring the relaxivity (*ri*).

A copper complex of the ligand was prepared electrochemically, which showed a mixed-valence complex, with a copper(I)-NHC and a copper(II) ion bound inside the macrocycle (**7.20**). This demonstrates the potential to coordinate this unique ligand to metals through two different types of binding sites.

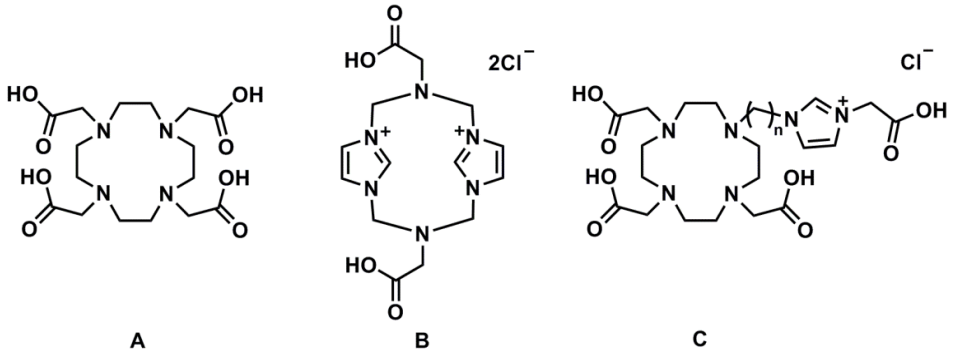

Figure 7.1 The structure of DOTA (A) and the novel DOTA inspired NHC-ligand precursors (B) and (C), (n = 1, 3).

7.1 Synthesis of DOTA inspired NHC ligand precursors

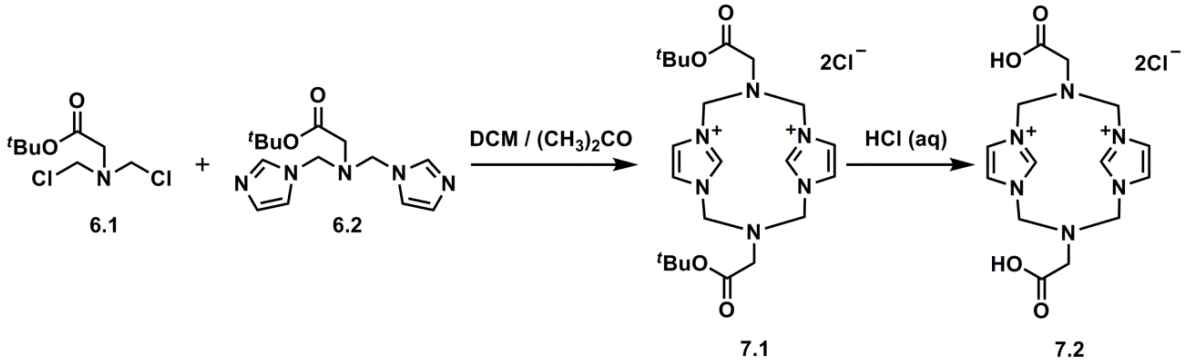

Scheme 7.1 Proposed synthesis of DOTA-inspired NHC ligand precursor (**7.2**).

The proposed synthetic route for the preparation of the DOTA-type ligand **7.2** is outlined in Scheme 7.1. The *tert*-butyl acetate ligand precursors (compounds **6.1** and **6.2**) were synthesised to prevent any competing reactions of the acetic acid group upon cyclisation. The aim was to remove the *tert*-butyl groups in the final step to form the target ligand (compound **7.2**). Preparation of the ligand precursors (amino(dichloromethyl) *tert*-butyl acetate (**6.1**) and amino(dimethyl-imidazole) *tert*-

butyl acetate (**6.2**)) was carried out as described in Chapter 6. Compounds **6.1** and **6.2** were added together slowly, under high dilution conditions, with a view to forming the cyclic product and minimising the formation of polymeric species. The reaction was attempted at different temperatures (30-70 °C), in different solvents (DCM / acetone), and the reaction time was varied (24-72 hours). In all cases, analysis by ^{1}H NMR spectroscopy (DMSO-d_6) suggested imidazolium species to have formed due to the shift in the C2 imidazole proton from δ = 7.45 ppm to between δ = 9.00 and δ = 9.50 ppm. However, a mixture of products was evident with no clear evidence for the formation of the target molecule. Analysis of the products by mass spectrometry did not provide any indication of the formation of the target macrocyclic molecule, or identifiable polymeric species. In addition, the experiments proved to be irreproducible, with repeated experiments producing different results each time.

As discussed in Chapter 6, compound **6.1** is unstable, requiring careful handling and storage at 4 °C. Compound **6.1** has the potential to form an imine, with the lone pair on the tertiary nitrogen of the amine attacking the adjacent carbon (Chapter 6, Figure 6.2). The formation of the imine in the above reactions was indicated by both mass spectrometry and infrared spectroscopy. It is likely that the instability of compound **6.1** was causing the problems in the cyclisation reaction.

The stability of compound **6.2** was examined to determine if it could also be degrading in a similar manner during the reaction. Compound **6.2** was dissolved in acetone-d_3 in an NMR tube and heated to 56 °C, with any reaction / degradation being followed over time (72 hours). Compound **6.2** was found to be stable to prolonged heating, with no significant changes being observed in the ^{1}H NMR spectrum. However, it is still possible that the lone pair of electrons on the tertiary amine of compound **6.2** is causing problems in the cyclisation reaction. Indeed, we have previously observed that when reacting compound **6.2** with *tert*-butyl chloroacetate, in an attempt to functionalise the neutral imidazole and form the imidazolium species, a complicated mixture of products was formed that appeared to include imidazolium and imidazole species (Chapter 6, Figure 6.6). We proposed that the lone pair on the tertiary nitrogen was either reacting with the *tert*-butyl chloroacetate to form the quaternary amine salt, that decomposed into further species. Or that the lone pair on the tertiary amine was causing the product to decompose once an imidazolium salt had formed. It is possible that a similar process was occurring in the cyclisation reaction.

Considering these findings, we decided to protect the amine with a more electron withdrawing group, to render it less basic. The benzoyl group was selected as it is more electron withdrawing than *tert*-butyl acetate. Compound **7.3** was synthesised in accordance with literature procedure.[7] Benzoyl chloride and hexamethylenetetramine were dissolved in xylene and the mixture was heated at 135 °C for 18 hours. The solvent was removed in *vacuo* to yield a yellow oil that was analysed by ^{1}H NMR spectroscopy. Compound **7.3** was identified in the ^{1}H NMR spectrum ($CDCl_3$), with the chemical shifts being consistent with the reported literature values.[7] However, the compound was not produced selectively and multiple products were formed. Attempts were made to distil the oil and isolate the pure product (96 °C / 10^{-2} torr), but the boiling point of compound **7.3** was too high at the vacuum achieved, and the mixture decomposed before the target compound was collected.

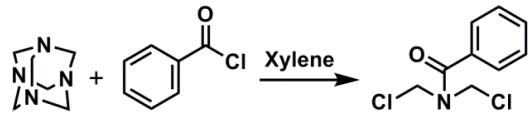

7.3

Scheme 7.2 Proposed product from the reaction of hexamethylenetetramine and benzoyl chloride.

The protecting group on the tertiary amine nitrogen was therefore altered to an acetyl group, as the boiling point of amino(dichloromethyl) acetyl (compound **7.4**) is lower (51 °C / 10^{-2} torr). Compound **7.4** was synthesised in accordance with the literature procedure.[7] Acetyl chloride and hexamethylenetetramine were added to a small ampoule and the solution was heated in a closed system at 120 °C for 5 hours. The solvent was removed *in vacuo* to yield a yellow oil. Distillation of the resultant oil yielded compound **7.4** as a colourless oil, which was analysed by ^{1}H NMR and ^{13}C{^{1}H} NMR spectroscopy, and was consistent with the reported literature values. The compound was too toxic and volatile for any further analysis to be obtained.[7]

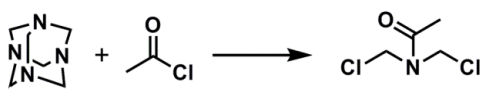

7.4

Scheme 7.3 Proposed product from the reaction of hexamethylenetetramine and acetyl chloride.

Compound **7.4** was reacted with imidazole in the presence of a base, in an attempt to prepare the bisimidazolium compound **7.5** (Scheme 7.4). The reaction proved unsuccessful, with starting material being identified in the product mixture.

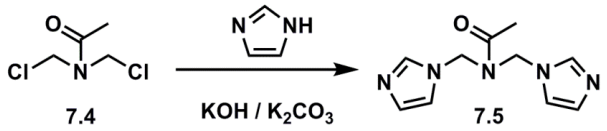

Scheme 7.4 Proposed product from the reaction of compound **7.4** with imidazole.

The formation of compound **6.2** (amino(dimethyl-imidazole) *tert*-butyl acetate) had also proved unsuccessful using the chloromethylated intermediate **6.1**. Therefore a direct approach was taken to prepare compound **6.2** starting from glycine *tert*-butyl ester hydrochloride ($H_2NCH_2CO_2{}^tBu$) and reacting this with two equivalents of formaldehyde and excess imidazole. The same approach was tried for the formation of compound **7.5** by reacting acetamide with formaldehyde and excess imidazole (Scheme 7.5). Again, the reaction proved to be unsuccessful with mostly starting material being isolated. Although the exact mechanism of this reaction is not known, the problem may be due to the increased electron withdrawing effect of the acetyl group deactivating the primary amine nitrogen lone pair.

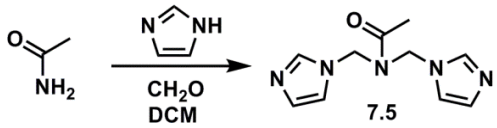

Scheme 7.5 Proposed product from the reaction between acetamide, formaldehyde and imidazole.

As the synthesis and purification of these compounds was proving challenging, we moved to a commercially available tertiary amine which is protected with an electron withdrawing group, namely N,N-*bis*(2-chloroethyl)-p-toluene sulfonamide (compound **7.6**). Although this compound contains chloroethyl rather than chloromethyl groups, the material is a solid so is easier to work with and can be obtained in 90 % purity. In addition, the extra CH_2 group should increase the stability as it is less likely that an imine will form. In the absence of a base, the reaction of compound **7.6** with excess imidazole produced only starting material. Therefore a base (KOH or K_2CO_3) was used to deprotonate the imidazole, followed by dropwise addition of a solution of compound **7.6** (Scheme 7.6). A small amount of imidazole species was isolated, even when using a large excess of base and prolonged heating at reflux. The ^1H NMR spectrum was complicated and suggested that more than one imidazole species was present. The desired product was identified in the mass spectrum with *m/z* 360.1 assigned as

[**7.7**+H]$^+$. However, other high mass species were also present, once again suggesting that the desired product was not produced selectively. Attempts were made to isolate the desired product from the reaction mixture, but these were unsuccessful.

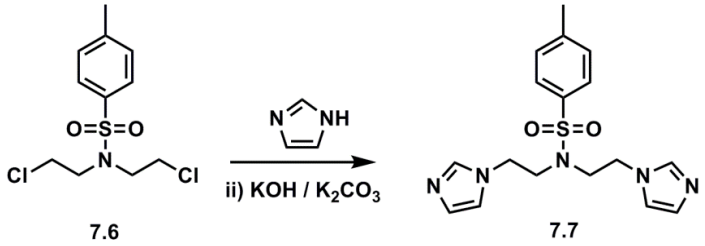

Scheme 7.6 Proposed product from the reaction of compound **7.6** and imidazole.

Although the data has not yet proved adequate to draw any direct conclusions as to what is occurring in these reactions, it is apparent that the nitrogen of the tertiary amine in these compounds is causing complications, even when protected by an electron withdrawing group. The reaction of imidazole with chloromethylated or bromomethylated compounds that do not contain an amine nitrogen usually proceed cleanly, often without the need for a base. This is a method used within our research group and there are examples contained within Chapters 2-4. The fact that this is proving so challenging must therefore be due to the inclusion of the amine functionality.

We therefore altered the structure of the target ligand to a preformed macrocyclic ligand functionalised with an imidazolium group (compound **7.12**). The starting material (compound **7.8**) incorporates three tertiary nitrogen atoms, which are functionalised with *tert*-butyl acetate groups, and a secondary nitrogen atom. The aim was to functionalise the secondary nitrogen with an imidazolium group to introduce a potential NHC moiety to the macrocycle. A proposed synthetic route is outlined in Scheme 7.7.

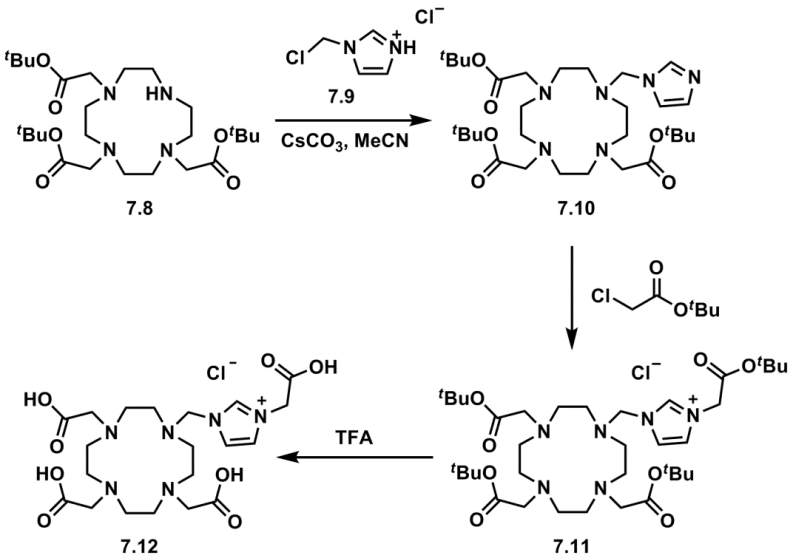

Scheme 7.7 Proposed synthesis of DOTA-inspired NHC ligand precursor (**7.12**).

Compound **7.8** was purchased from CheMatch and compound **7.9** was prepared in accordance with literature procedure.[8] Imidazole and paraformaldehyde were heated at 80 °C, in the presence of a catalytic amount of triethylamine, forming hydroxyl-methyl imidazole. This was reacted with thionyl chloride to yield compound **7.9** as the HCl salt, which was isolated as a white hygroscopic solid and characterised by ^{1}H NMR and $^{13}C\{^{1}H\}$ NMR spectroscopy combined with mass spectrometry.[8]

Compound **7.8** and compound **7.9** were added to a Schlenk flask and dissolved in acetonitrile, Cs_2CO_3 was added and the mixture was heated at reflux (85 °C) for 12 hours. The mixture was filtered to remove the inorganic salts and the solvent was removed *in vacuo* to yield a yellow oil. The isolated product was analysed by ^{1}H NMR and $^{13}C\{^{1}H\}$ NMR spectroscopy and mass spectrometry. The ^{1}H NMR spectrum ($CDCl_3$) of the product is displayed in Figure 7.2, and compared with that of the starting macrocyclic ligand compound **7.8**. The ^{1}H NMR spectrum of the product appears as expected, with a characteristic resonance for the C2 imidazole proton downfield at δ = 7.53 ppm. The imidazole backbone protons appear as one resonance at δ = 6.95 ppm, suggesting that the protons are coincidently in the same environment. The remainder of the spectrum is very similar to that of the un-functionalised macrocyclic compound **7.8**, displaying three broad resonances for the three inequivalent methylene protons of the macrocycle (**5**, **6**, **7**), and a low field resonance for the *tert*-butyl groups (**8**). The remaining two resonances at δ = 3.23 ppm and δ = 3.22 ppm are assigned as the

methylene protons of the acetate groups (**3**), and the methylene protons linking the macrocycle and the imidazole group (**4**). The formation of compound **7.10** was confirmed by mass spectrometry with a signal for [**7.10**+Na]$^+$ at *m/z* 617.4 (Figure 7.3).

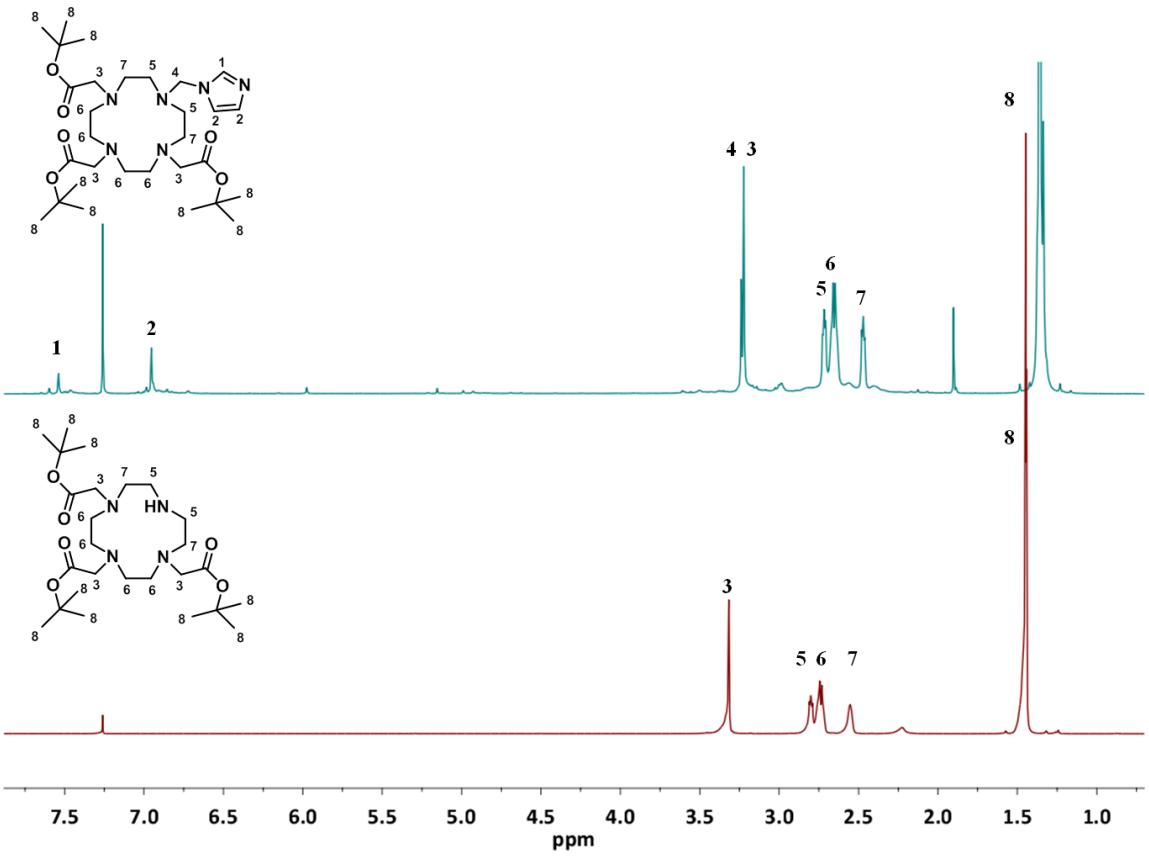

Figure 7.2 ^{1}H NMR spectra ($CDCl_3$) displaying compound **7.8** (bottom) and the product formed from the reaction between compound **7.8** and **7.9** (top) at 298 K.

Although the mass spectrum displays a signal for the expected compound (**7.10**), the starting macrocyclic ligand (**7.8**) is also observed at *m/z* 515.3 assigned as [**7.8**+H]$^+$. In addition, there is evidence of a macrocylic compound containing two methyl imidazole groups at *m/z* 697.4. The integrations from the ^{1}H NMR spectrum also suggest the presence of further products, with the imidazole resonances integrating to less than expected if compound **7.10** has formed exclusively in the reaction. The reaction time was increased from 12 hours to 72 hours, but analysis by ^{1}H NMR spectroscopy and mass spectrometry suggested that the same product mixture was formed. The purification of the product mixture was attempted by column chromatography (Silica gel, 10 % MeOH / $CHCl_3$) but the desired product was not isolated.

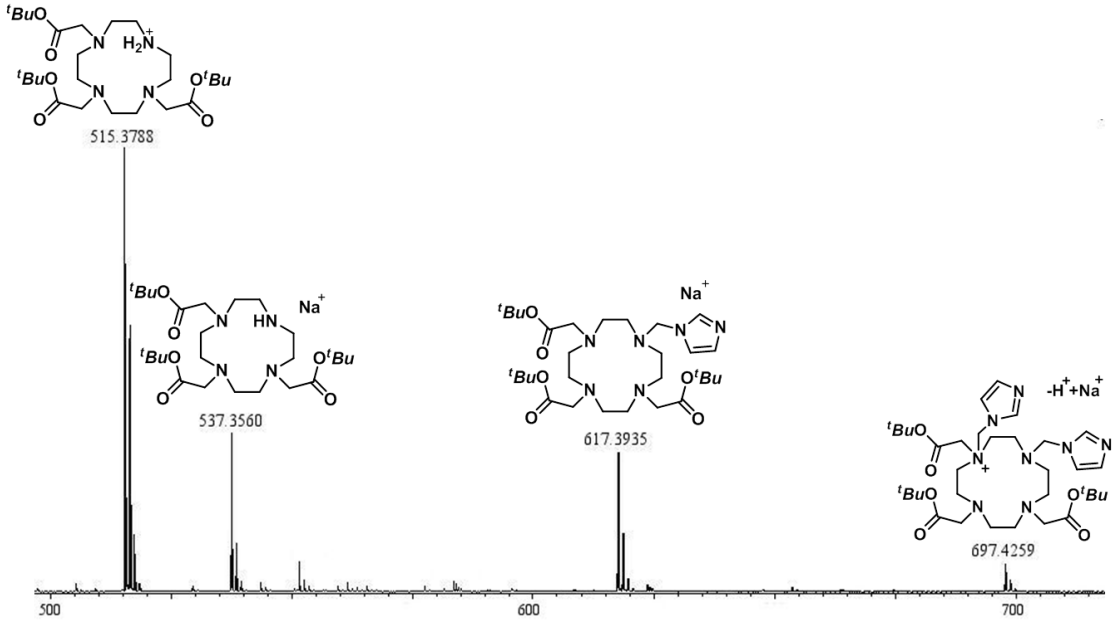

Figure 7.3 Mass spectrometry data displaying the products that were isolated from the reaction of **7.8** with **7.9**.

Therefore an approach was taken to react compound **7.8** with an imidazolium to prepare an imidazolium functionalised macrocyclic ligand directly (Scheme 7.8). The length of the alkyl chain on compound **7.14** can be varied depending on the required chain length between the macrocycle and imidazolium group. A propyl chain length was selected for ease of synthesis.

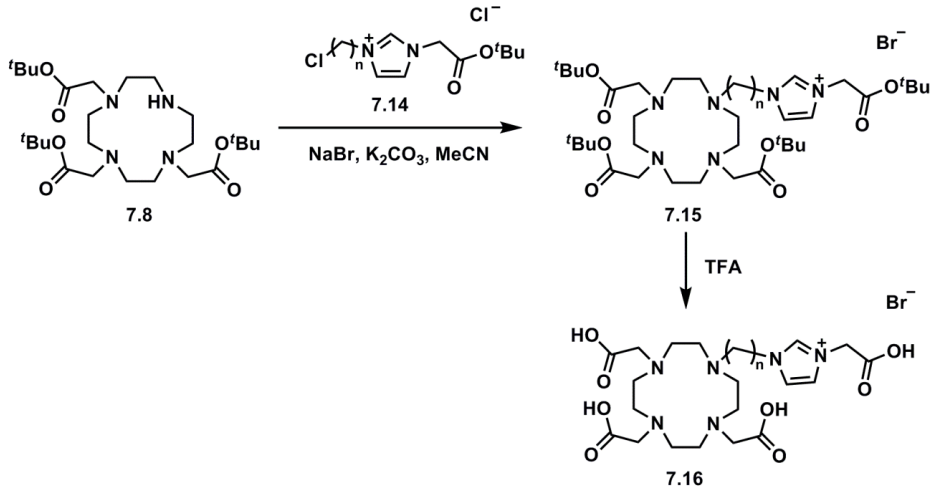

Scheme 7.8 Proposed synthesis of DOTA-inspired NHC ligand precursor **7.16** (n = 3).

The synthesis of compound **7.14** (where n = 3) was achieved through the reaction of *tert*-butyl chloroacetate with 1-propanol imidazole to yield compound **7.13**, which was

reacted with thionyl chloride to give compound **7.14** (Scheme 7.9). The addition of triethylamine was found to be necessary to neutralise the HCl formed in the reaction and protect the *tert*-butyl groups. The product was purified by recrystallisation from DCM / diethyl ether and was analysed by ^{1}H NMR and ^{13}C{^{1}H} NMR spectroscopy combined with mass spectrometry. The ^{1}H NMR spectrum appears as expected, with a characteristic low field resonance for the C2 imidazolium proton at δ = 9.29 ppm. The formation of compound **7.14** was confirmed by mass spectrometry with *m/z* at 259.1 assigned as [**7.14**-Cl]$^{+}$. It should be noted that compound **7.14** was isolated with the triethylamine chloride salt, which could not all be separated from the product, though this did not prove to be a problem in further reactions.

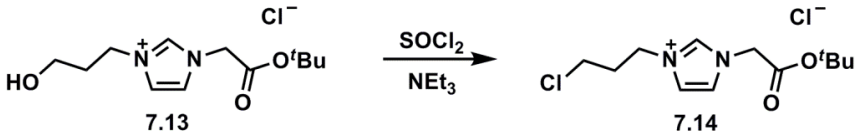

Scheme 7.9 Synthesis of compound **7.14**.

Compound **7.8** and compound **7.14** were added to a Schlenk flask and dissolved in acetonitrile. Cs_2CO_3 was added, and the mixture was heated at reflux (85 °C) for 12 hours. The solution was filtered to remove the inorganic salts and the solvent was removed *in vacuo.* Analysis of the isolated material by ^{1}H NMR spectroscopy and mass spectrometry showed that only starting material was present. The reaction conditions were varied (base, reaction vessel, addition of NaBr / NaI, temperature, reaction time). It was found that the desired product was formed in the highest yield when the reaction was performed in acetonitrile, in a sealed ampoule, with K_2CO_3 and NaBr added to the reaction mixture. The mixture was heated at 50 °C for 96 hours and the reaction was monitored by HPLC mass spectrometry. The product was identified in the HPLC mass spectrum at *m/z* 737.5 for [**7.15**-Br]$^{+}$ and *m/z* 396.3 for [**7.15**-Br+H]$^{2+}$. The mixture was filtered to remove the inorganic salts, and the solution was removed *in vacuo* to yield a yellow oil. The oil was washed with diethyl ether and dried *in vacuo* to yield a yellow hygroscopic solid. Analysis of the product by ^{1}H NMR spectroscopy and mass spectrometry indicated that the solid was a mixture of the starting material (**7.8**), and the desired product (**7.15**). Compound **7.15** was isolated from the reaction mixture using HPLC, and analysed by ^{1}H NMR and ^{13}C{^{1}H} NMR spectroscopy and mass spectrometry. The ^{1}H NMR spectrum of compound **7.15** is displayed in Figure 7.4.

The ^{1}H NMR spectrum of compound **7.15** ($CDCl_3$) appears as expected, with a

characteristic resonance for the imidazolium C2 proton downfield at δ = 10.04 ppm. The backbone imidazole protons appear as two separate resonances at δ = 8.34 ppm and δ = 7.35 ppm. The resonance at δ = 8.23 ppm has not been assigned, but is most likely due to formic acid from the HPLC separation. The methylene protons on the acetate tether of the imidazolium group appear as a singlet resonance at δ = 5.02 ppm, and a broad triplet resonance at δ = 4.64 ppm is assigned to the CH_2 group closest to the imidazolium group on the propyl chain. The remaining CH_2 protons appear as broad resonances between δ = 3.77 ppm and δ = 2.63 ppm. There are three resonances assigned to the CH_3 protons of the *tert*-butyl groups at δ = 1.47 ppm, δ = 1.45 ppm and δ = 1.43 ppm that integrate as 1:1:2. The formation of compound **7.15** was confirmed by mass spectrometry with *m/z* 841.4 assigned as [**7.15**+Na]$^+$, *m/z* 737.5 assigned as [**7.15**-Br]$^+$, and *m/z* 396.3 assigned as [**7.15**-Br+H]$^{2+}$. The purity of the compound was established by HPLC-MS and elemental analysis.

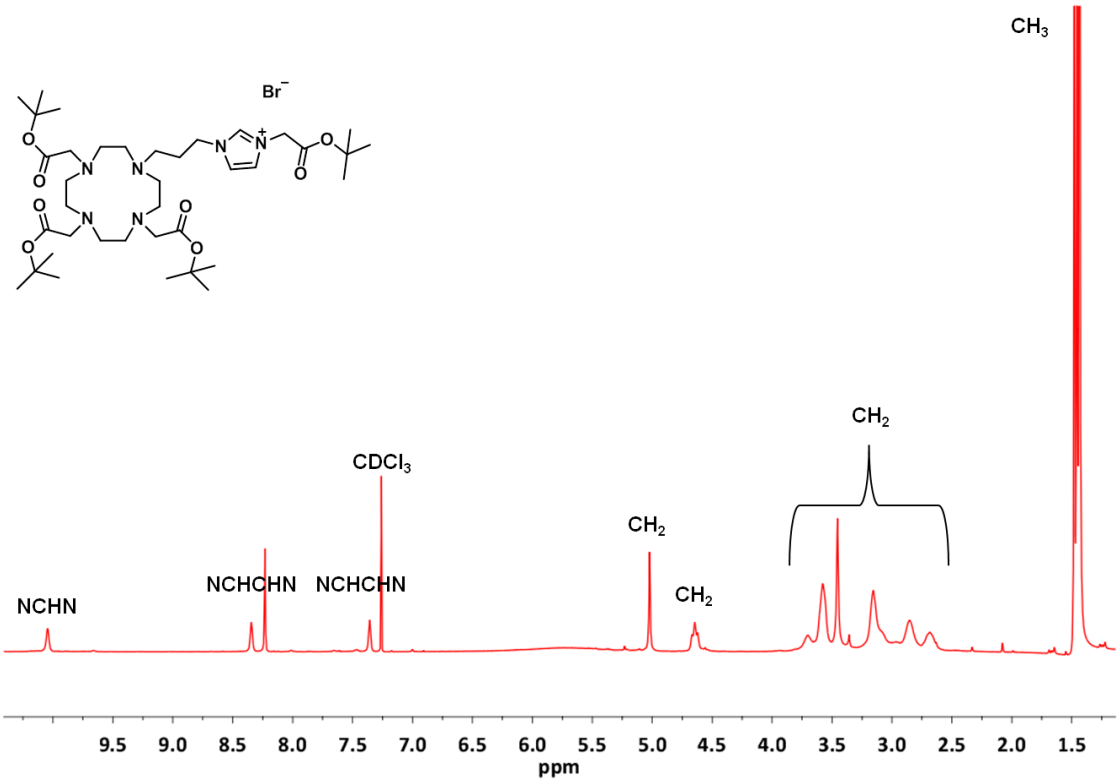

Figure 7.4 ^{1}H NMR spectrum ($CDCl_3$) of compound **7.15** at 298 K.

The *tert*-butyl protecting groups of compound **7.15** were removed by dissolving the compound in TFA and stirring the solution at room temperature for 12 hours. The TFA was removed *in vacuo* and the resultant oil was triturated with diethyl ether to yield a yellow solid. Compound **7.16** was analysed by ^{1}H NMR and ^{13}C{^{1}H} NMR

spectroscopy combined with mass spectrometry. The ^{1}H NMR spectrum appeared as expected, with the only difference between this and the ^{1}H NMR spectrum of compound **7.15** being the loss of the resonances assigned to the *tert*-butyl groups at δ = 1.47 ppm, 1.45 ppm and 1.43 ppm. The removal of the *tert*-butyl groups was further indicated by ^{13}C{^{1}H} NMR spectroscopy, with no resonance assigned to the *tert*-butyl groups (seen at δ = 27.99 ppm and 28.16 ppm in compound **7.15**), and mass spectrometry with *m/z* 513.3 assigned as [**7.16**-Br]$^{+}$.

7.2 Formation of a gadolinium complex using DOTA inspired NHC ligand precursor (7.17)

Magnetic resonance imagining (MRI) is a common imaging technique used in medical diagnostics. MRI relies on the different distribution and properties of water in the examined tissues, and on the proton relaxational properties of the water. As relaxational properties of water in different tissues can be very similar, or even identical, standard MRI techniques do not always produce images that can be used for diagnostics. Contrast agents modify the relaxational properties of water in areas where they accumulate, so the intensity of the MRI signal can be selectively enhanced through the administration of a contrast agent.

Gadolinium based contrast agents are used widely in clinical practice today. They consist of a gadolinium(III) metal centre surrounded by a chelating (e.g. Magnevist®) or macrocyclic (e.g. Dotarem®) organic ligand. Gadolinium(III) has seven unpaired electrons and a magnetic moment 657 times higher than that of a proton, making gadolinium(III) complexes highly paramagnetic. The proton nuclear spins of the surrounding water molecules interact with the local magnetic field generated by the paramagnetic metal ion. The effect is that both T1 (longitudinal), and T2 (transverse), magnetic relaxational times of the surrounding water molecules are shortened.[9, 10] The effect of the contrast agent on T1 dominate compared to T2 at the low concentrations that are used in diagnostics. Therefore, a T1 weighted image produces a brighter more defined picture.

The efficacy of a contrast agent at shortening T1 and T2 of the surrounding water molecules is dependent upon its relaxivity (*ri*), where the *i* refers to what is being measured, for T1 i =1 and for T2 i = 2.[1] The relaxivity of a contrast agent can be calculated by measuring *Ri*(obs) (which equates to 1 / *Ti*) at different concentrations of contrast agent (C). Plotting *Ri*(obs) against concentration (C) gives a linear graph, the gradient of which gives the relaxivity (*ri*). The relaxivity is also dependent on the strength of the magnetic field (Tesla) and the temperature of the solution, hence these parameters are reported with *ri* values. The relaxivity gives a measure of the change in the relaxation rate of water molecules in the presence of a contrast agent, and so provides a direct measure of the efficacy of a contrast agent. Two widely used commercially available contrast agents, Magnevist® and Dotarem®, have $r1$ = 3.3 mM^{-1} s^{-1} (1.5 T, 37 °C) and $r1$ = 2.9 mM^{-1} s^{-1} (1.5 T, 37 °C) respectively.[11]

$$Ri\ (obs) = \frac{1}{Ti(obs)} = \frac{1}{Ti(diam)} + riC$$

$$i = 1\ or\ 2$$

i = 1: effect of the contrast agent on T1

i = 2: effect of the contrast agent on T2

Ri = global relaxational rate constants of water in the system [s^{-1}]

Ti(diam) = relaxational time of water in the absence of contrast agent [s]

Ti(obs) = relaxational time of water in the presence of contrast agent [s]

C = concentration of the paramagnetic ion in the contrast agent [$mmol^{-1}$ L]

ri = relaxivity [mM^{-1} s^{-1}]

Figure 7.5 Equation to calculate the relaxivity of a contrast agent (*ri*).[1]

The main contributing factors towards the overall relaxivity are; a) the number of exchangeable water molecules that are bound to the metal ion, b) the time constant for the exchange of the metal bound water with the bulk water (inner sphere relaxation), c) the interaction of the surrounding bulk water molecules with the paramagnetic metal ion (outer sphere relaxation), and d) the rotational correlation time, which represents the tumbling of the complex.[3, 12] These properties can be altered by changing the ligand design. For example, hexadentate and heptadentate ligands have been designed that allow for two coordinated water molecules (most commercially available contrast agents are octadentate and incorporate one bound water molecule).[3, 13] These complexes have been shown to have up to twice the relaxivity of commercially available contrast agents. However, as they do not incorporate as many donor groups in the ligand, they are often not as stable as octadentate ligands.[3, 13] The rotational correlation time of a contrast agent can be altered by increasing the molecular weight or the rigidity of the ligand.[14] Different strategies have been used to increase the molecular weight such as attaching a DOTA / DTPA gadolinium complex to a sugar, an antibody, or even to a calixarene scaffold.[15-17]

To the best of our knowledge there are no examples in the literature of DOTA-

type ligands with a tethered imidazolium group, such as compound **7.16**. Our aim was to coordinate compound **7.16** to gadolinium and, after determining the structure of the complex, probe the relaxivity. Compound **7.16** is an octadentate ligand that incorporates four tertiary nitrogen donors and four carboxylic acid groups. There is also the potential to deprotonate the imidazolium in the presence of a base and coordinate through the NHC. Depending on the flexibility of the imidazolium tether, the fourth carboxylate donor on the imidazolium group may be too far removed to form an interaction with the gadolinium metal ion. Compound **7.16** was dissolved in water and 0.96 equivalents of $GdCl_3.6H_2O$ was added. The pH of the solution was increased to pH 6 by the slow addition of NaOH solution (0.1 M) with continuous stirring. The solution was stirred at room temperature for 24 hours and the solvent was removed *in vacuo* to yield a colourless oil which was analysed by mass spectrometry. The desired gadolinium complex **7.17** was observed in the mass spectrum with *m/z* 668.2 assigned as [**7.17**-Br]$^+$, and *m/z* 690.1 assigned as [**7.17**-Br-H+Na]$^+$ (Figure 7.7). We propose that the carboxylate donor of the imidazolium group does not interact with the gadolinium metal ion due to its distance from the metal centre. However, without the aid of a crystal structure, this cannot be confirmed.

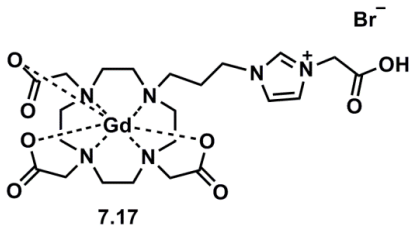

7.17

Figure 7.6 Suggested product from the reaction between compound **7.16** and $GdCl_3.6H_2O$. Any bound water molecules are omitted.

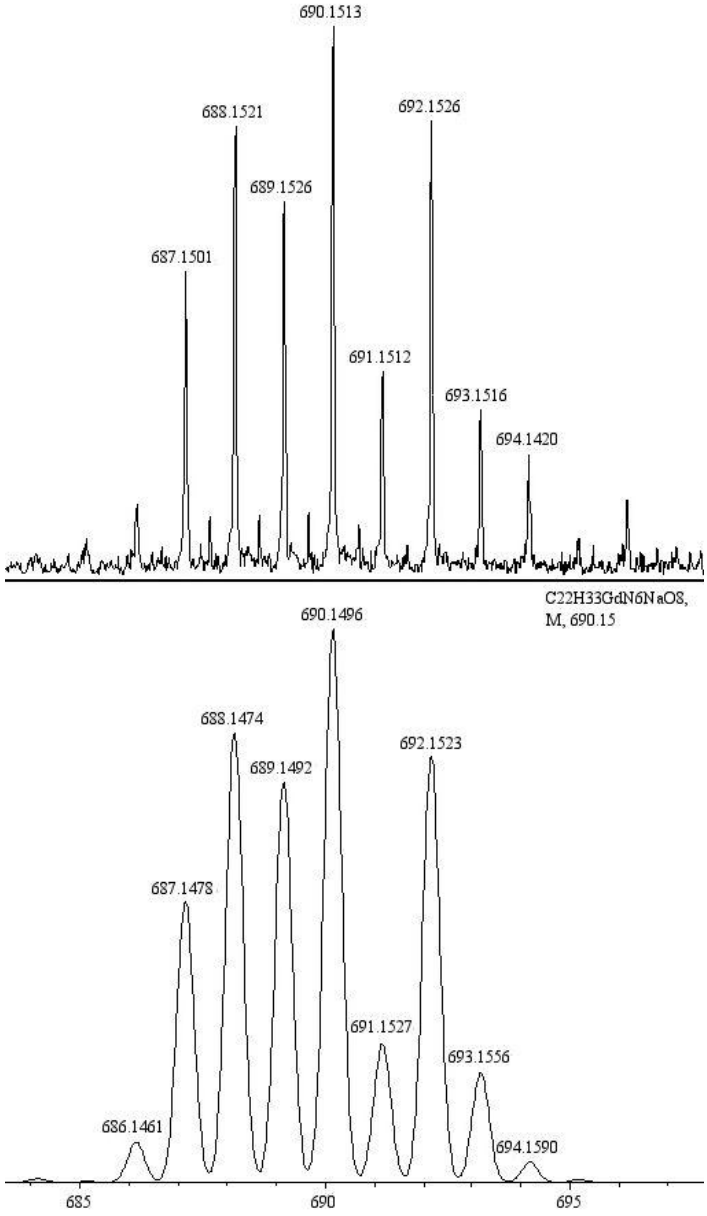

Figure 7.7 Mass spectrometry data of complex **7.17** (top) and calculated for [**7.17**-Br]$^+$ (bottom).

We were interested in measuring the relaxation properties of compound **7.17**. The assumption was made that, as less than one equivalent of $GdCl_3.6H_2O$ was used in the reaction, all the gadolinium in the solution was complexed by the ligand and there was no uncoordinated gadolinium. Therefore the amount of gadolinium that had been added to the reaction was used to calculate the concentration of gadolinium in the contrast agent. Five concentrations of the contrast agent were made up in deionised water in standard NMR tubes (50 mM, 25 mM, 16.66 mM, 8.33 mM, 2.5 mM). The T1 relaxational time of the water molecules was recorded at the different concentrations,

using a Maran Benchtop NMR analyser (20 MHz, 0.5 T, 23.8 ± 0.5 °C). Each T1 measurement was recorded three times and an average of the three results was taken. A graph was plotted of 1 / *T1* (s^{-1}) against concentration (mM), which showed the expected linear correlation (Figure 7.8). The gradient of the line was calculated to give a relaxivity (*r1*) = 5.70 mM^{-1} s^{-1} (0.5 T, 23.8 ± 0.5 °C). This result is very promising, as the relaxivity of complex **7.17** is larger than the commercially available Gd-DOTA contrast agent Dotarem® (*r1* = 3.3 mM^{-1} s^{-1} (1.5 T, 37 °C)).[11]

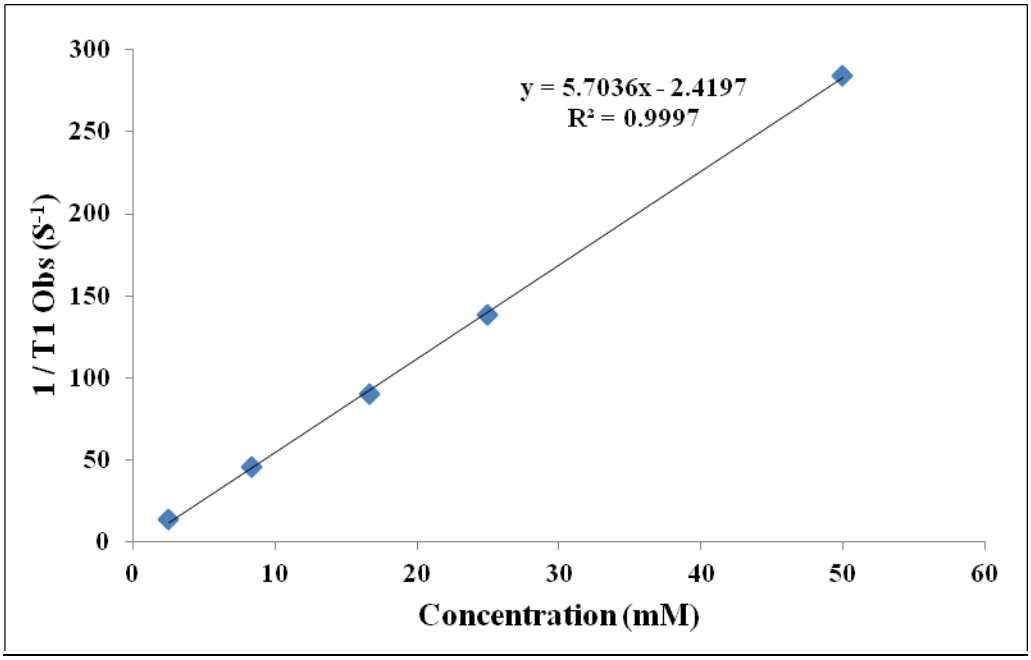

Figure 7.8 Plot of 1 / *T1* (s^{-1}) versus concentration (mM) of the gadolinium contrast agent.

The favourable *r1* (*r1* = 5.70 mM^{-1} s^{-1} (0.5 T, 23.8 ± 0.5 °C)) of complex **7.17** demonstrates that it has the potential to be used as a T1 contrast agent. However, these results are preliminary and several other factors need to be taken into account. The stability of the complex in solution needs to be examined to verify that the ligand remains coordinated to the gadolinium metal ion, and that gadolinium is not leached into solution. Other properties of the complex should also be examined such as the number of exchangeable water molecules. If the fourth carboxylate tether on the imidazolium group does not interact with the gadolinium centre then it is likely that the complex will have two water molecules coordinating to the gadolinium ion. This may account for the relatively high relaxivity that is observed, but may also cause problems with the stability of the complex. The number of coordinated water molecules can be determined in the solid state by single crystal X-ray crystallography. If single crystals

cannot be grown, the number of coordinated water molecules can be determined in solution based studies by preparing Eu(III) or Tb(III) analogues of the complex and measuring the luminescence lifetime in H_2O and D_2O. Comparison of luminescence lifetimes can be directly related to the number of coordinated water molecules in the inner sphere of a complex.[18]

Once these parameters have been measured, the effect of the imidazolium group on the ligand can be explored. As discussed previously (Chapter 2 and 3), imidazolium units offer the potential to be effective anion receptors due to the strong hydrogen bonding interactions they form with anions of the type $[(C\text{-}H)^{+}\cdots X^{-}]$. At present, complex **7.17** incorporates a bromide counter anion, which is a coordinating anion that will interact with the C2 imidazolium proton. This $[(C\text{-}H)^{+}\cdots X^{-}]$ interaction may influence the geometry of complex **7.17**. In the presence of other anions, such as the non-coordinating PF_6 anion, the geometry of the ligand may be different and this could have a direct effect on relaxivity. Therefore, we propose that complex **7.17** could find application as an anion sensing contrast agent.

7.3 Electrochemical synthesis of a copper-NHC complex using the DOTA inspired NHC-ligand precursor (7.15)

Compounds **7.15** and **7.16** may bind metals inside the macrocycle, in addition to having the potential to form a metal-NHC complex. The binding of metals inside the macrocycle has already been demonstrated through the synthesis of the gadolinium complex **7.17**. The formation of complex **7.17** requires the use of a base (NaOH), however, under aqueous reaction conditions the NHC would not be formed. Therefore, under these conditions, the metal is only coordinated to the ligand through the nitrogen and oxygen donors of the macrocycle. As an extension of this work, we were keen to demonstrate the potential of coordinating these compounds to metals through the formation of a metal-NHC bond. Ultimately, this offers the potential to form a bimetallic complex which could have some properties associated with the metal inside the macrocycle, and other properties due to the metal-NHC moiety.

We have found in previous investigations that the formation of metal-NHC complexes using imidazolium precursors that are functionalised with acetate ester, or acetic acid groups, can be problematic due to other acidic protons associated with these functional groups. However, the electrochemical synthetic method has overcome this problem when using imidazolium ligands with acetate ester groups. Therefore the

electrochemical method was explored using compound **7.15** and copper, and was followed as outlined previously (Scheme 7.10). The mixture was electrolysed for 25 minutes (2 Q), during which time the solution turned bright green. The solvent was removed *in vacuo* to yield a green solid, which was dissolved in DCM and filtered to remove the suspended copper particles. The solvent of the filtrate was removed *in vacuo* and compound **7.18** was analysed by ^{1}H NMR and ^{13}C{^{1}H} NMR spectroscopy, mass spectroscopy and elemental analysis.

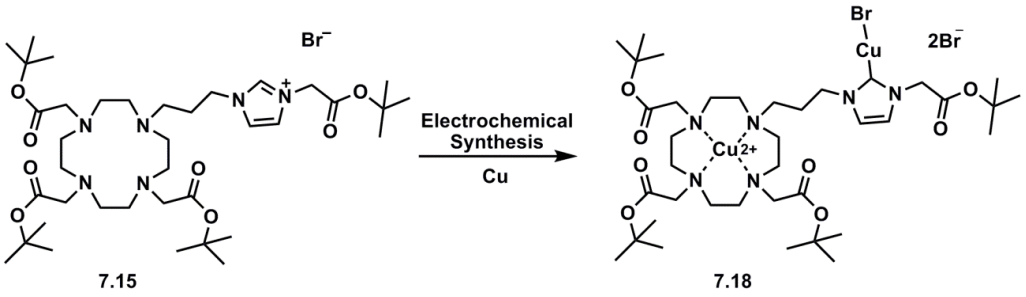

Scheme 7.10 Electrochemical synthesis of complex **7.18**.

Upon examination of the ^{1}H NMR spectrum it is evident that an NHC has formed due to the disappearance of the resonance attributed to the C2 proton observed at δ = 10.04 ppm in the imidazolium precursor **7.15** (Figure 7.9). The remainder of the spectrum appears as expected, with the backbone imidazolium protons as two separate resonances at δ = 7.21 ppm and δ = 7.13 ppm. The singlet resonance at δ = 4.84 ppm is assigned to the methylene protons of the acetate tether, and a broad triplet resonance at δ = 4.20 ppm is attributed to the CH_2 group nearest the carbene on the propyl chain. The CH_2 protons on the acetate groups of the macrocycle are at δ = 3.48 ppm. The remaining CH_2 protons on the macrocycle and on the propyl chain are observed between δ = 2.92 ppm to δ = 2.14 ppm as broad resonances. Upfield there is one resonance at δ = 1.45 ppm attributed to the CH_3 protons of the *tert*-butyl groups. The formation of the copper carbene was also indicated by ^{13}C{^{1}H} NMR spectroscopy which displays a low field resonance at δ = 177.2 ppm, indicative of a C2 carbon bound to copper.

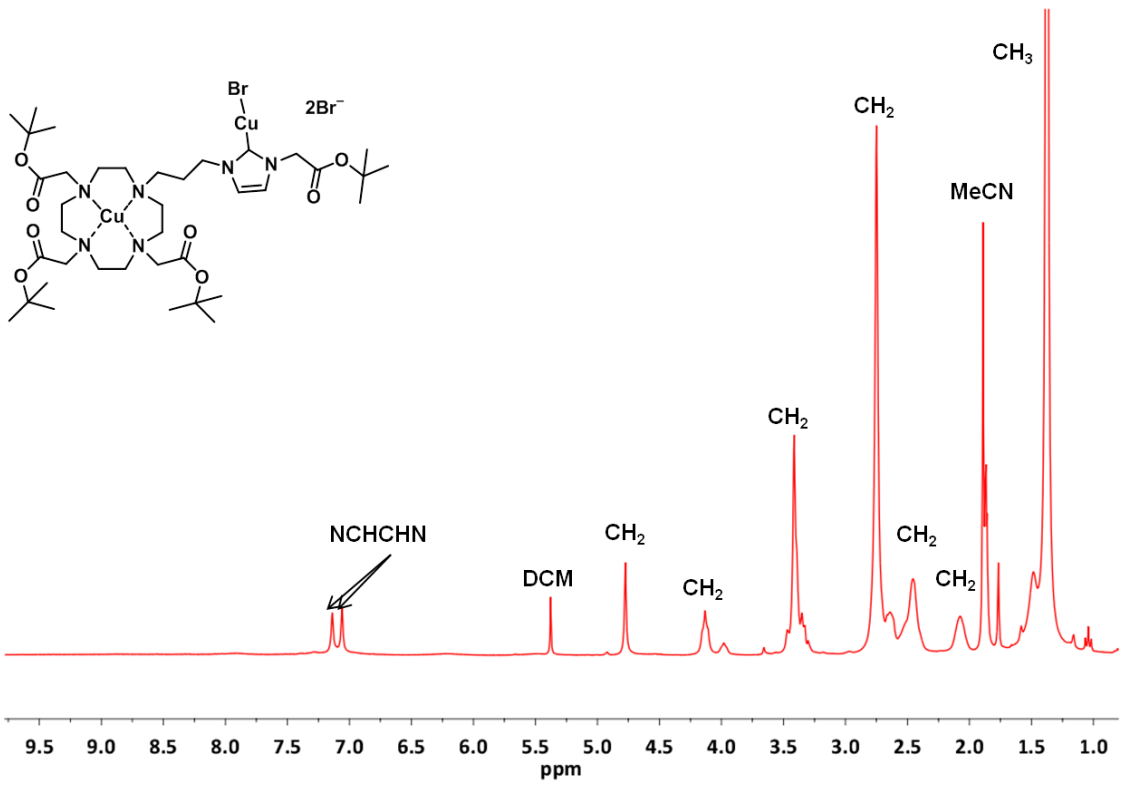

Figure 7.9 ^{1}H NMR spectrum (MeCN-d_3) of complex **7.18** at 298 K.

The mass spectrometry data is indicative of a mixed valence copper(I) / copper(II) complex, with *m/z* 1024.2 attributed to [**7.18**-Br]$^{+}$. The formation of a Cu(II) complex is also implied by the colour change that was observed during the reaction, with the solution turning from colourless to green. In previous work, the electrochemical method has produced only copper(I) species, which are stabilised by using acetonitrile as the solvent. We suspect that the redox potential of the copper is altered when it is bound inside the macrocycle, which may favour further oxidation of copper(I) to copper(II). Elemental analysis confirmed the formation of complex **7.18.**

The presence of the copper(II) ion was confirmed using EPR spectroscopy. The spectrum was recorded as a frozen glass of acetonitrile at 200 K, giving rise to an averaged spectrum of all orientations of the molecule. A typical four-line spectrum of copper(II) was recorded owing to the selection rule 2nI+1 (s = ½ and I = 3/2), whereby the unpaired electron spin interacts with the copper nucleus (Figure 7.10). The hyperfine coupling constants of the z-component (A_z) is 167 G and is in the range expected for a copper(II) nucleus (no hyperfine coupling was observed in the x, y component of this spectrum). The Landé splitting energy, the 'g factor', was calculated using the equation displayed in Figure 7.11, giving g_z = 2.25 and g_{xy} = 2.08, which are within

expectation.[19] The g values are such that $z > x = y$, which suggests that the geometry of the copper(II) centre is 'axial', therefore the unpaired electron is in the dx^2-y^2 or dxy orbital.[20] For copper(II) this is much more likely to be the dx^2-y^2 orbital, hence the geometry is either square-planar or square-pyramidal.

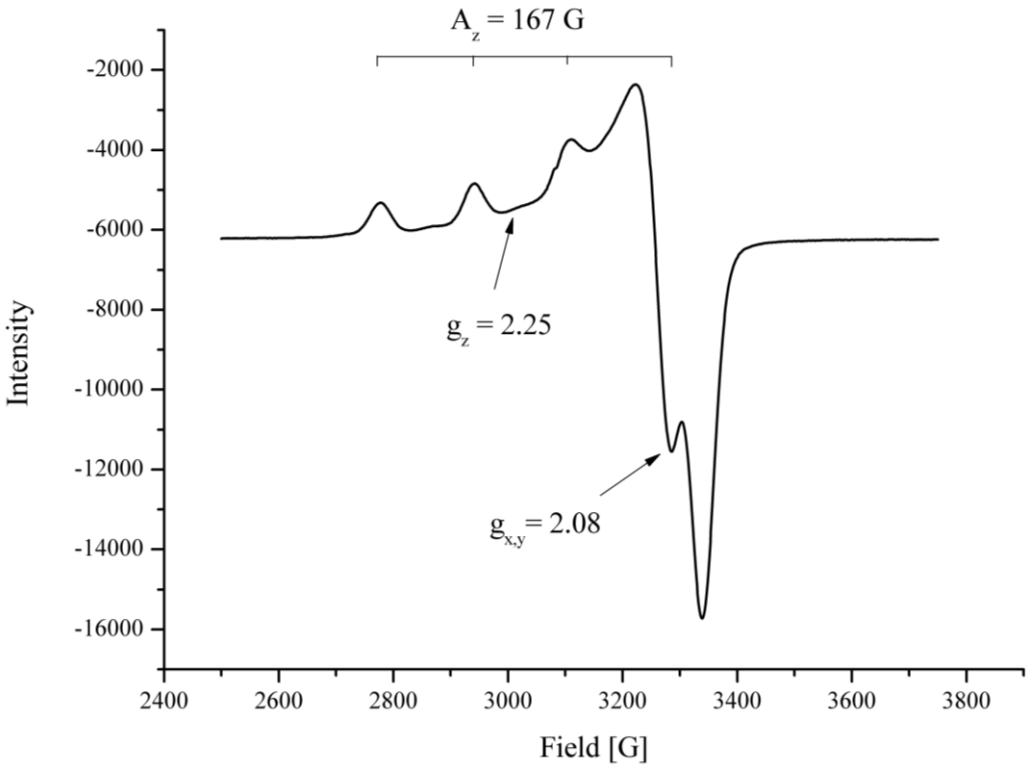

Figure 7.10 EPR spectrum (MeCN) of compound **7.18** recorded as a frozen glass at 200 K.

$$g = {}^{h\nu}/_{\beta B}$$

Figure 7.11 Relationship between Lande *g* factor and experimental conditions where *h* equals Planck's constant, *v* is the frequency of the instrument, *β* is the Bohr magneton and *B* is the experimental position of the absorbance peak.

7.4 Electrochemical synthesis of a gold complex using the DOTA inspired NHC-ligand precursor (7.15)

Gold complexes have been important in therapeutics for a number of years, being used to treat conditions such as rheumatoid arthritis. More recently gold complexes, including gold-NHCs, have been shown to have potential application as anticancer drugs, with some gold(I) and gold(III) complexes displaying good cytotoxicity.[21-23] As discussed in previous chapters, the electrochemical method has the potential to be extended for the synthesis of other transition metal-NHC complexes by simply substituting the copper anode for the desired transition metal anode. The electrochemical method was repeated with compound **7.15**, in this instance using a copper plate as the cathode, and gold wire as the anode. The mixture was electrolysed for 116 minutes, (6 Q). The solution was filtered to remove the suspended gold particles, and the solvent was removed *in vacuo* to yield a dark purple oil. The colour was most likely due to the presence of gold nanoparticles that were unable to be removed by filtration. The compound was analysed by ^{1}H NMR and ^{13}C{^{1}H} NMR spectroscopy, combined with mass spectrometry.

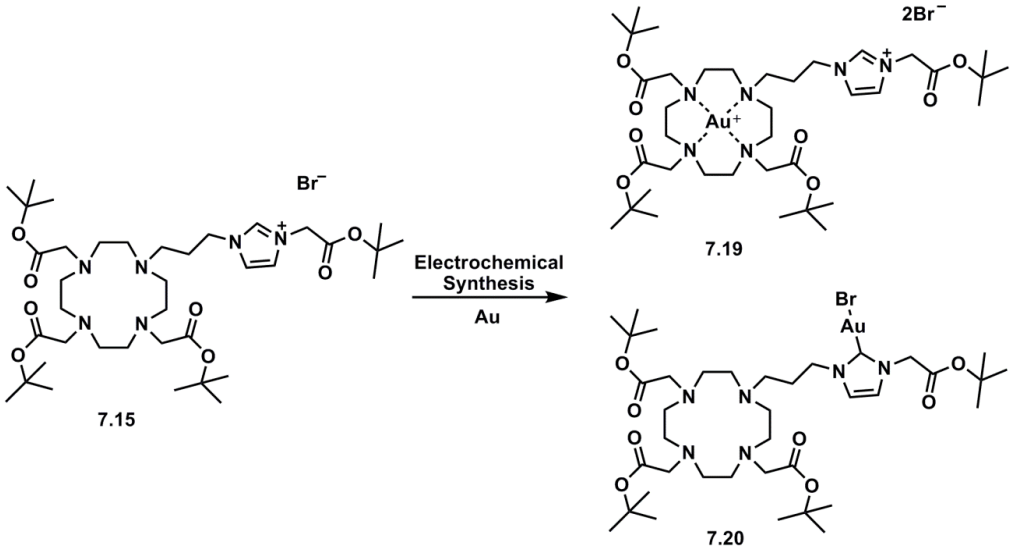

Scheme 7.11 Electrochemical synthesis of complex **7.19** / **7.20**.

Analysis by ^{1}H NMR spectroscopy (MeCN-d_3, DMSO-d_6, $CDCl_3$) was inconclusive, with the spectra appearing extremely broad in all cases. A gold mirror formed in the NMR tube over time, which may have contributed to the broadness of the spectra. The ^{13}C{^{1}H} NMR spectrum was complicated, displaying multiple resonances in the expected regions, and providing little insight into the complex that had been formed.

Mass spectrometry proved to be the most valuable analytical technique, with *m/z* 1015.40 with the correct splitting pattern to be assigned as [**7.15**+Au]$^{+}$. However, there are two possibilities as to the structure of the complex: either gold(I) is coordinated to the nitrogen atoms inside the macrocycle (complex **7.19**) with *m/z* at 1015.40 being assigned as [**7.19**-Br]$^{+}$, or the gold(I)-NHC complex (complex **7.20**) has been synthesised, with *m/z* 1015.40 being assigned as [**7.20**+H]$^{+}$. Unfortunately, without the aid of a crystal structure, the coordination of gold(I) to **7.15** has not yet been determined. However, the electrochemical method has proved to be a viable synthetic route for the formation of a gold(I) complex using ligand **7.15**.

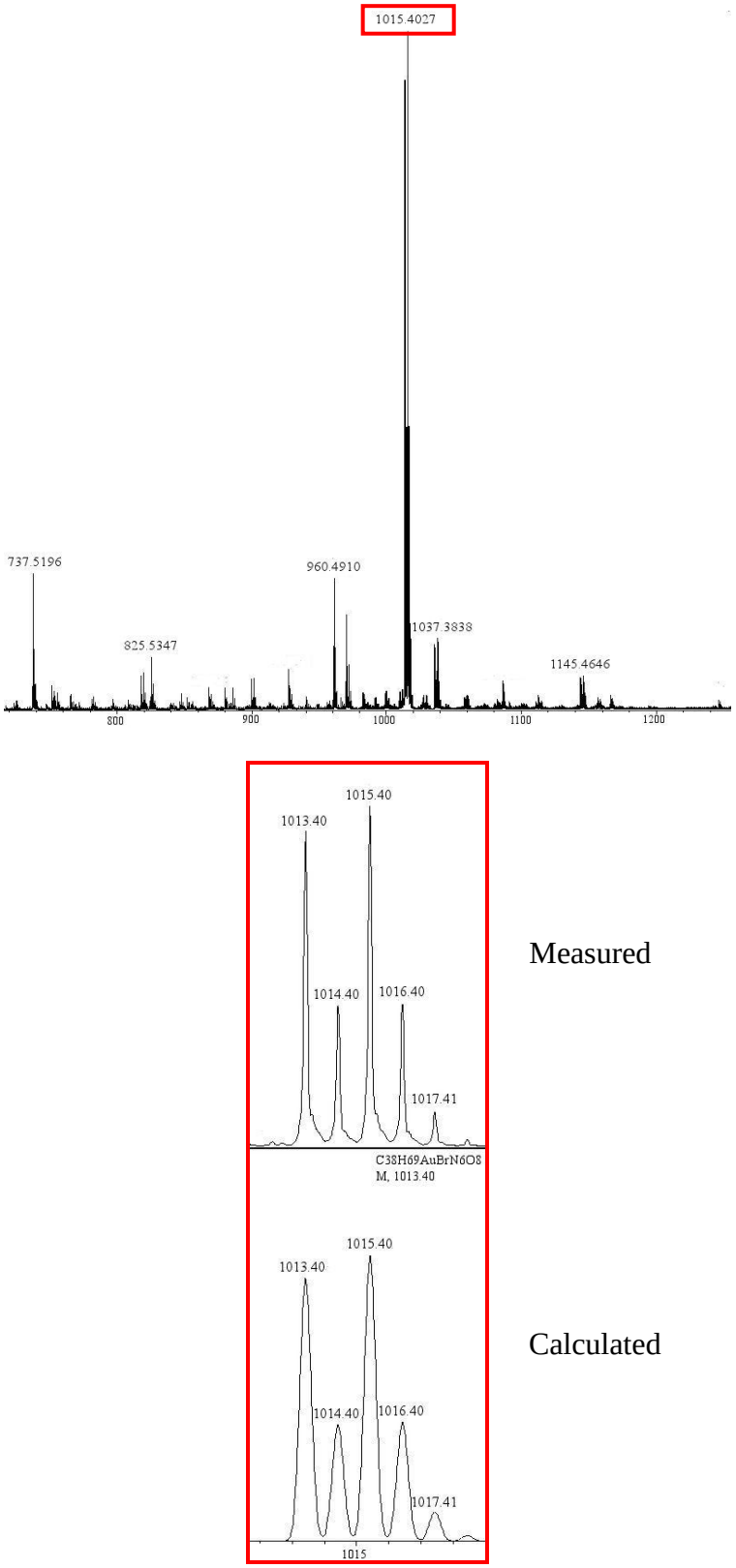

Figure 7.12 Mass spectrum of the product formed in the electrochemical method using compound **7.15** and gold (top). The expanded spectrum for the dominant peak and calculated for [**7.19**-Br]$^+$ / [**7.20**+H]$^+$(bottom).

7.5 Conclusion

In conclusion, a synthetic procedure has been successfully developed for the synthesis of novel imidazolium-functionalised DOTA-type ligands (compounds **7.15** and **7.16**). Compound **7.16** was coordinated to gadolinium and the potential of the complex (**7.17**) as a contrast agent was explored by measuring the relaxivity (*r1*). It was found that complex **7.17** has a relaxivity of (*r1*) = 5.70 mM^{-1} s^{-1} (0.5 T, 23.8 ± 0.5 °C), which is larger than that of the commercially available Gd-DOTA contrast agent Dotarem® (*r1* = 3.3 mM^{-1} s^{-1} (1.5 T, 37 °C)).[11]

The potential for the imidazolium-functionalised DOTA-type ligand to coordinate through an NHC in addition to the macrocycle was explored. It was found that the electrochemical synthetic approach yielded a mixed valence copper complex (**7.18**), where a copper(II) ion is coordinated inside the macrocycle, in addition to the formation of a copper(I)-NHC. The electrochemical method was extended to include gold as the sacrificial anode. A gold(I) complex was synthesised using ligand **7.15**, though the coordination geometry of the gold(I) could not be determined.

7.6 Future work

The work described in this Chapter is at an early stage and has the potential to be developed further. The use of complex **7.17** as an anion sensing contrast agent should be explored, which would involve fully determining the structure and stability of the complex, and examining the influence of the imidazolium tether. As imidazolium groups offer the potential to be effective anion receptors, the structure of the complex may change in the presence of different anions which may have a direct effect on the relaxivity (*r1*). MRI contrast agents have been reported that respond to changes in pH, the presence of metal ions, nitric oxide, lactate, glucose, and that detect enzymatic activity.[24-29] As anions are known to play important roles in biological systems, an anion sensing contrast agent could prove beneficial.

The introduction of the imidazolium functionality into the DOTA scaffold also offers the potential to prepare metal-NHC complexes of these ligands. This has been demonstrated in this work through the synthesis of the copper complex **7.18**. As an extension of this work, a complex could be prepared that has a gadolinium(III) ion bound inside the macrocycle (which would include coordination of the carboxylate groups) and a transition metal coordinated to the NHC group. This offers the potential

to synthesise a therapeutic contrast agent, which could also have anticancer or antimicrobial properties associated with the NHC complex.[30-32]

7.7 References

1. J.C.Dabrowiak, *Metals in medicine*, Wiley, 2009.
2. M. Bottrill, L. Kwok and N. J. Long, *Chem. Soc. Rev.*, 2006, **35**, 557-571.
3. P. Hermann, J. Kotek, V. Kubicek and I. Lukes, *Dalton Trans.*, 2008, 3027-3047.
4. D. M. A. G. J. ten and J. F. M. Wetzels, *Neth J Med*, 2008, **66**, 416-422.
5. J. L. Abraham and C. Thakral, *Eur J Radiol*, 2008, **66**, 200-207.
6. S. Aime, M. Botta, M. Fasano and E. Terreno, *Chem. Soc. Rev.*, 1998, **27**, 19-29.
7. H. Boehme, J. P. Denis and H. J. Drechsler, *Liebigs Annalen Der Chemie*, 1979, 1447-1455.
8. S. Julia, C. Martinezmartorell and J. Elguero, *Heterocycles*, 1986, **24**, 2233-2237.
9. N. Bloembergen, *J. Chem. Phys.*, 1957, **27**, 572-573.
10. N. Bloembergen, E. M. Purcell and R. V. Pound, *Phys. Rev.*, 1948, **73**, 679-712.
11. M. Rohrer, H. Bauer, J. Mintorovitch, M. Requardt and H.-J. Weinmann, *Invest Radiol*, 2005, **40**, 715-724.
12. E. Toth, L. Helm and A. E. Merbach, *Top. Curr. Chem.*, 2002, **221**, 61-101.
13. K. N. Raymond and V. C. Pierre, *Bioconjugate Chem.*, 2005, **16**, 3-8.
14. R. S. Ranganathan, M. E. Fernandez, S. I. Kang, A. D. Nunn, P. C. Ratsep, K. M. R. Pillai, X. Zhang and M. F. Tweedle, *Invest. Radiol.*, 1998, **33**, 779-797.
15. D. A. Fulton, E. M. Elemento, S. Aime, L. Chaabane, M. Botta and D. Parker, *Chem. Commun.*, 2006, 1064-1066.
16. D. T. Schuhle, M. Polasek, I. Lukes, T. Chauvin, E. Toth, J. Schatz, U. Hanefeld, M. C. A. Stuart and J. A. Peters, *Dalton Trans*, 2009, 185-191.
17. C. Burtea, S. Laurent, E. L. Vander, and R. N. Muller, *Contrast agents: Magnetic resonance.*, Handbook of experimental pharmacology, 2008, **185** (Pt 1), 135-165.
18. J. L. Major, G. Parigi, C. Luchinat and T. J. Meade, *Proc. Natl. Acad. Sci. U. S. A.*, 2007, **104**, 13881-13886.
19. B. J. Hathaway and D. E. Billing, *Coord. Chem. Rev.*, 1970, **5**, 143-207.
20. L. M. P. Lima, D. Esteban-Gomez, R. Delgado, C. Platas-Iglesias and R. Tripier, *Inorg. Chem.*, 2012, **51**, 6916-6927.
21. R. Rubbiani, I. Kitanovic, H. Alborzinia, S. Can, A. Kitanovic, L. A. Onambele, M. Stefanopoulou, Y. Geldmacher, W. S. Sheldrick, G. Wolber, A. Prokop, S. Woelfl and I. Ott, *J. Med. Chem.*, 2010, **53**, 8608-8618.
22. W. Liu, K. Bensdorf, M. Proetto, U. Abram, A. Hagenbach and R. Gust, *J. Med. Chem.*, 2011, **54**, 8605-8615.
23. C.-M. Che and R. W.-Y. Sun, *Chem. Commun.*, 2011, **47**, 9554-9560.
24. R. A. Moats, S. E. Fraser and T. J. Meade, *Angew. Chem., Int. Ed. Engl.*, 1997, **36**, 726-728.
25. J. L. Major, R. M. Boiteau and T. J. Meade, *Inorg. Chem.*, 2008, **47**, 10788-10795.
26. S. Aime, C. D. Delli, F. Fedeli and E. Terreno, *J. Am. Chem. Soc.*, 2002, **124**, 9364-9365.
27. G. Liu, Y. Li and M. D. Pagel, *Magn. Reson. Med.*, 2007, **58**, 1249-1256.
28. W.-h. Li, S. E. Fraser and T. J. Meade, *J. Am. Chem. Soc.*, 1999, **121**, 1413-1414.
29. S. Zhang, R. Trokowski and A. D. Sherry, *J. Am. Chem. Soc.*, 2003, **125**, 15288-15289.
30. D. C. F. Monteiro, R. M. Phillips, B. D. Crossley, J. Fielden and C. E. Willans, *Dalton Trans.*, 2012, **41**, 3720-3725.
31. K. M. Hindi, T. J. Siciliano, S. Durmus, M. J. Panzner, D. A. Medvetz, D. V. Reddy, L. A. Hogue, C. E. Hovis, J. K. Hilliard, R. J. Mallet, C. A. Tessier, C. L. Cannon and W. J. Youngs, *J. Med. Chem.*, 2008, **51**, 1577-1583.
32. M.-L. Teyssot, A.-S. Jarrousse, M. Manin, A. Chevry, S. Roche, F. Norre, C. Beaudoin, L. Morel, D. Boyer, R. Mahiou and A. Gautier, *Dalton Trans.*, 2009, 6894-6902.

8 Experimental

8.1 General Considerations

All manipulations were performed under an atmosphere of dry nitrogen or argon by means of standard Schlenk line or glovebox techniques unless otherwise stated. The gas was dried by passing through a twin-column drying apparatus containing molecular sieves (4Å) and P_2O_5. Anhydrous solvents were prepared by passing the solvent over activated alumina to remove water, copper catalyst to remove oxygen and molecular sieves to remove any remaining water, via the Dow-Grubbs solvent system. They were then degassed using standard freeze-pump-thaw techniques. Deuterated chloroform, acetonitrile and DMSO were dried over CaH_2, cannula filtered or distilled, and then freeze-pump-thaw degassed before use. Metal precursors, $PdCl_2(MeCN)_2$ and $[RuCl_2(cymene)]_2$ were prepared using literature procedures.[1, 2] All other reagents and solvents were used as supplied by Aldrich or Fisher, or prepared as outlined, without need for further purification. DO3AtBu was purchased from CheMatch and used as received. Propan-1-ol imidazole was purchased from CHESS and used as received.

HPLC was performed by Mr Martin Huscroft, School of Chemistry, University of Leeds, using Agilent 1260 Prep LC system, with Agilent 1260 prep scale fraction collector coupled with agilent 6100 series single quad mass spec and Chemstation Software. Solvents used were methanol / water + 0.1 % formic acid, gradient 50-95 % methanol + 0.1 % formic acid. The time was 8 minutes at a flow of 20 mL / min. The column used was water XBridge Prep C18 5 m OBD 19 × 100 mm.

8.2 Characterisation

^1H and $^{13}C\{^1H\}$ NMR spectra were recorded either by the author, or by Mr. Simon Barrett, School of Chemistry, University of Leeds, using a Bruker DPX300 spectrometer (operating frequency 300.1 MHz for ^1H and 75.48 MHz for ^{13}C) or on a Bruker DRX500 spectrometer (operating frequency 500.13 MHz for ^1H and 125.03 MHz for $^{13}C\{^1H\}$). Chemical shift values are quoted in parts per million (ppm, δ) and coupling constants *J* are quoted in Hertz (Hz). Multiplicities are reported as singlet (s), doublet (d), triplet (t), quartet (q), quintet (quintet), broad (br) or multiplet (m). Attribution of the ^1H and $^{13}C\{^1H\}$ signals was performed using two dimensional $^1H^1H$ and $^1H^{13}C$ correlation techniques.$^{13}C\{^1H\}$ resonances were also confirmed using $^{13}C\{^1H\}$ DEPT experiments.

Microanalyses were performed by Mr. Martin Huscroft and Mr. Ian Blakeley, School of Chemistry, University of Leeds, using a Carlo Erba Elemental Analyser MOD 1106 spectrometer.

Mass spectra were collected by Ms. Tanya Marinko-Covell or Dr. Stuart Warriner, School of Chemistry, University of Leeds, either on a Bruker Daltonics (micro T.O.F.) instrument operating in the electrospray mode, or a GCT Premier (T.O.F.) instrument operating in electron impact mode, using methanol, DMSO, or acetonitrile as the solvent.

X-ray diffraction data were collected by Mr. Colin Kilner or Dr. Marc Little, School of Chemistry, University of Leeds, on a Bruker Nonius X8 diffractometer fitted with an Apex II detector with Mo-K_α radiation (λ = 0.71073 Å). Crystals were mounted under oil on glass fibres. Data sets were corrected for absorption using a multiscan method, and the structures were solved by direct methods using SHELXS-97 and refined by full-matrix least squares on F^2 using SHELXL-97, interfaced through the program X-Seed.[3, 4] Molecular graphics for all structures were generated using POV-RAY in the X-Seed program.

The structure of compound **4.2** and complex **4.6** contained significant void space, and residual electron density was too diffuse to adequately model, hence SQUEEZE routine of the program PLATON was employed in these cases.[5]

X-band electron paramagnetic resonance spectra were recorded by Mr. Jonathan Loughrey, School of Chemistry, University of Leeds, using a Bruker EMX spectrometer (Bruker Biospin GmbH) fitted with a frequency counter. Spectra were recorded and viewed using the WINEPR software package (Bruker Analytische Messtechnik GmbH). Samples were cooled to 200 K using a continuous-flow cryostat and liquid nitrogen coolant.

8.3 Experimental for Chapter 2

8.3.1 4-Hydroxy-tert-butyl calix[4]arene (2.1)[6]

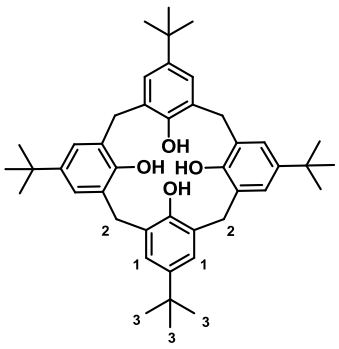

4-*Tert*-butylphenol (25.00 g, 0.166 mmol), formaldehyde (18 mL, 0.24 mmol, 37-41 % solution) and sodium hydroxide (0.265 g, 0.0066 mmol, 0.040 equiv) were added to a round bottomed flask and heated for 7 hours maintaining the temperature between 110-120 °C. During this time the solution thickened and became a hard yellow solid. The solid was broken into pieces and stored in the oven at 50 °C (mass of precursor = 27.5 g). The precursor (16.0 g) was suspended in diphenyl ether (510 mL) in a three necked round bottom flask that was fitted with a mechanical stirrer, a nitrogen inlet and a condenser. During the first phase of the reaction the condenser was left off the reaction setup whilst the heat was gradually increased and nitrogen was blown rapidly over the mixture to aid the removal of water. Once water evolution stopped and the temperature of the solution had reached around 220 °C, the condenser was put in place and the mixture heated at reflux (257 °C) for 2 hours under nitrogen. The solution was allowed to cool to room temperature. Ethyl acetate (600 mL) was added and the suspension stirred for 30 minutes then left to stand for 30 minutes. The precipitate was collected by reduced pressure filtration, washed with ethyl acetate (2 × 60 mL) then acetic acid (1 × 80 mL) and collected as a white solid (11.80 g) which was a mixture of the 4-*tert*-butylcalix[4]arene and 4-*tert*-butylcalix[8]arene. The white solid was added to toluene (150 mL) and heated at reflux (115 °C) for 30 minutes then filtered whilst hot. Upon cooling the 4-*tert*-butylcalix[4]arene precipitated from the toluene solution as white crystals and was collected by reduced pressure filtration (Yield: 5.60 g, 40 %).

^{1}H NMR (500 MHz, $CDCl_3$, 300 K): δ = 10.27 (s, 4H, OH), 6.98 (s, 8H, **1**), 4.19 (d, $^{3}J_{H-H}$ = 13 Hz, 4H, **2**), 3.42 (d, $^{3}J_{H-H}$ = 13 Hz, 4H, **2**), 1.12 (s, 36H, **3**).

^{13}C{^{1}H} NMR (125 MHz, $CDCl_3$, 300 K): δ = 147.09 (quaternary, Ar), 144.99 (quaternary, Ar), 127.87 (CH, Ar), 126.00 (quaternary, Ar), 33.03 (quaternary, ^{t}Bu), 31.81 (CH_2), 31.34 (CH_3).

ESI+MS *m/z* 666.5 $[M+NH_4]^+$

EI+HRMS calcd. for $C_{44}H_{60}N_1O_4$ $[M+NH_4]^+$: 666.4517. Found: 666.4538

8.3.2 4-Hydroxy calix[4]arene (2.2)[7]

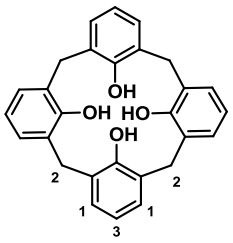

4-Hydroxy-*tert*-butyl calix[4]arene (**2.1**) (5.00 g, 6.75 mmol) was added to a three necked round bottom flask and the reagent and apparatus were degassed. Anhydrous toluene (150 mL) was added and the mixture heated at 65 °C, with stirring, for 20 minutes. The solution was cooled to 55 °C, treated with anhydrous $AlCl_3$ (5.40 g, 37 mmol) and heated for 2 hours at 55 °C. The mixture was cooled to room temperature before being poured into ice (250 g), washed with 1M HCl solution (2 × 250 mL) and the organic phase separated. The aqueous phase was washed with dichloromethane (2 × 150 mL) and the organic layers combined, dried over $CaCl_2$, filtered, and the solvent removed *in vacuo* to yield a yellow oil. This was triturated with diethyl ether (500 mL) to yield a white solid (Yield: 1.89 g, 66 %).

^{1}H NMR (300 MHz, $CDCl_3$, 300 K): δ = 10.24 (s, 4H, OH), 7.30-6.72 (m, 12H, **1**, **3**), 4.32 (br d, 4H, **2**), 3.61 (br d, 4H, **2**).

^{13}C{^{1}H} NMR (75 MHz, $CDCl_3$, 300 K): δ = 149.33 (quaternary, Ar), 129.29 (quaternary, Ar), 128.21 (CH, Ar), 122.86 (CH, Ar), 32.13 (CH_2).

ESI+MS *m/z* 442.2 $[M+NH_4]^+$

EI+HRMS calcd. for $C_{28}H_{28}N_1O_4$ $[M+NH_4]^+$: 442.2013. Found: 442.2023

8.3.3 Bromomethylated 4-hydroxy calix[4]arene (2.3)[8]

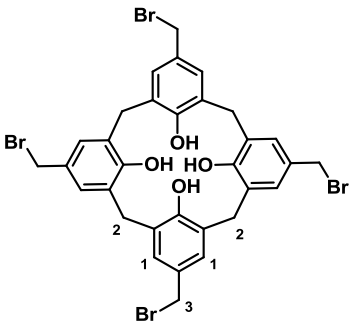

Zn powder (0.115 g, 1.77 mmol) was added to glacial acetic acid (62 mL) in a round bottom flask, followed by HBr (33 % wt in acetic acid, 7.5 mL) and stirred for 30 minutes. 4-Hydroxy calix[4]arene (**2.2**) (1.50 g, 3.54 mmol), paraformaldehyde (5.6 g, 187 mmol) and HBr solution (37 mL) were added and the mixture heated at 90 °C for 72 hours. The solution was allowed to cool before the precipitate was collected under reduced pressure filtration, washed with water (2 × 20 mL) and dried by washing with diethyl ether (2 × 30 mL). The product was collected as a white solid (Yield: 2.06 g, 73 %).

^{1}H NMR (300 MHz, $CDCl_3$, 300 K): δ = 10.02 (s, 4H, OH), 7.03 (s, 8H, **1**), 4.25 (s, 8H, **3**), 4.14 (br d, 4H, **2**), 3.16 (br d, 4H, **2**).

$^{13}C\{^{1}H\}$ NMR (75 MHz, $CDCl_3$, 300 K): δ = 147.91 (quaternary, Ar), 130.68 (quaternary, Ar), 128.93 (CH, Ar), 127.26 (quaternary, Ar), 32.25 (CH_2), 30.56 (CH_2).

ESI+MS *m/z* 637.2 $[M-2Br+H]^+$

8.3.4 Tetrakis(methylimidazole) calix[4]arene (2.4)[9, 10]

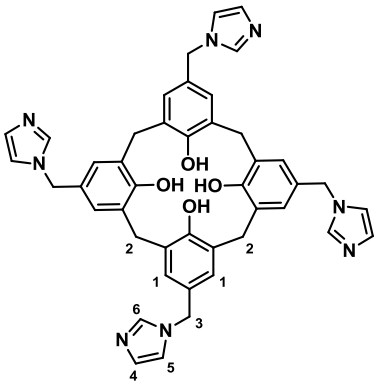

Bromomethylated-4-hydroxy calix[4]arene (**2.3**) (2.00 g, 2.53 mmol) and imidazole (6.88 g, 101.2 mmol) were added to a Schlenk flask and the reagents degassed. Anhydrous methanol (70 mL) was added and the solution heated at 75 °C for 72 hours. The reaction mixture was allowed to cool before water (100 mL) was added resulting in the formation of a white precipitate. The precipitate was collected by reduced pressure filtration, washed with water (2 × 50 mL) and dried by washing with diethyl ether (2 × 50 mL). The product was collected as an off white solid (Yield: 0.40 g, 21 %).

^{1}H NMR (300 MHz, DMSO-d_6, 300 K): δ = 7.95 (s, 4H, **6**), 7.72 (s, 4H, **4** / **5**), 7.06 (s, 4H, **4** / **5**), 6.80 (s, 8H, **1**), 4.91 (s, 8H, **3**), 4.22 (br d, 4H, **2**), 3.13 (br d, 4H, **2**), OH resonance not observed.

$^{13}C\{^{1}H\}$ NMR (75 MHz, DMSO-d_6, 300K): δ = 154.94 (quaternary, Ar), 137.01 (CH, NCN), 130.76 (quaternary, Ar), 127.47 (CH), 126.94 (CH), 126.30 (quaternary, Ar), 120.38 (CH), 50.28 (CH_2), 32.61 (CH_2).

ESI+MS *m/z* 745.3 $[M+H]^+$, 767.3 $[M+Na]^+$

EI+HRMS calcd. for $C_{44}H_{41}N_8O_4$ $[M+H]^+$: 745.3245. Found: 745.3228

EI+HRMS calcd. for $C_{44}H_{40}N_8NaO_4$ $[M+Na]^+$:767.3065. Found: 767.3039

Anal.calcd. for $C_{44}H_{40}N_8O_4.3H_2O$: C, 66.15 %; H, 5.80 %; N, 14.03 %. Found: C, 66.50 %; H, 5.50 %; N, 14.65%.

Recrystallisation from chloroform resulted in colourless prism crystals suitable for single crystal X-ray diffraction analysis.

Tetrakis(methylimidazolium) calix[4]arene Br (2.5 Br)[11]

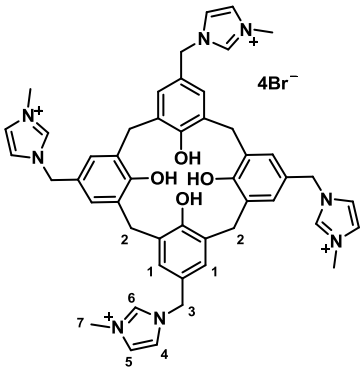

Bromomethylated-4-hydroxy calix[4]arene (**2.3**) (1.00 g, 1.26 mmol) was added to a Schlenk flask and the reagent degassed. Anhydrous DCM (50 mL) was added, followed by 1-methyl imidazole (0.46 mL, 5.60 mmol). The solution was stirred at room temperature for 12 hours. The product precipitated from solution as a white solid that was collected by filtration, washed with DCM (3 × 20 mL), and dried *in vacuo* (Yield: 1.20 g, 84 %).

^{1}H NMR (500 MHz, DMSO-d_6, 300 K): δ = 9.31 (s, 4H, **6**), 7.80 (s, 4H, **4** / **5**), 7.70 (s, 4H, **4** / **5**), 7.17 (s, 8H, **1**), 5.12 (s, 8H, **3**), 3.86 (s, 12H, **7**), bridging CH_2 resonances are not observed due to ring inversion at room temperature rendering them broad, OH resonance not observed.

^{13}C{^{1}H} NMR (125 MHz, DMSO-d_6, 300K): δ = 152.97 (quaternary, Ar), 136.21 (CH, NCN), 129.65 (quaternary, Ar), 128.78 (CH), 123.53 (CH), 121.91 (CH), 51.73 (CH_2), 35.64 (CH_3).

ESI+MS *m/z* 1147.1 $[M+Na]^+$, 936.2 $[M-2Br-H]^+$, 881.3 $[M-3Br-2H]^+$

Colourless crystals suitable for single crystal X-ray diffraction analysis were grown by the vapour diffusion of diethyl ether into a methanol solution of **2.5 Br**.

8.3.5 Tetrakis(methylimidazolium) calix[4]arene PF_6 (2.5 PF_6)[11]

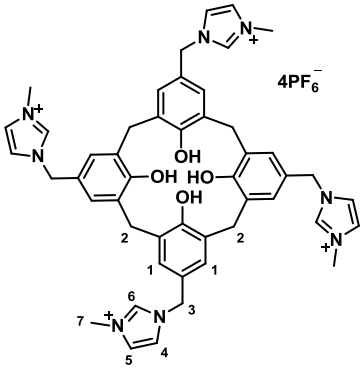

Tetrakis(methylimidazolium) calix[4]arene Br (**2.5 Br**) (0.58 g, 5.15 mmol) was dissolved in H_2O (10 mL) and a H_2O solution (10 mL) of NH_4PF_6 (0.24 g, 1.4 mmol) was added dropwise with stirring. The mixture was stirred for 30 minutes, filtered, and the solid washed with water (3 × 5 mL) followed by diethyl ether (3 × 5 mL), and dried in air. The product was collected as a white solid (Yield: 0.55 g, 87 %).

^{1}H NMR (500 MHz, DMSO-d_6, 300 K): δ = 9.03 (s, 4H, **6**), 7.70 (s, 4H, **4** / **5**), 7.67 (s, 4H, **4** / **5**), 7.11 (s, 8H, **1**), 5.09 (s, 8H, **3**), 3.86 (s, 12H, **7**), bridging CH_2 resonances are not observed due to ring inversion at room temperature rendering them broad, OH resonance not observed.

^{1}H NMR (500 MHz, MeCN-d_3, 248 K): δ = 8.47 (s, 4H, **6**), 7.32 (s, 4H, **4** / **5**), 7.26 (s, 4H, **4** / **5**), 7.15 (s, 8H, **1**), 5.03 (s, 8H, **3**), 4.17 (d, 4H, $^{2}J_{HH}$ = 13.8 Hz, **2**), 3.78 (s, 12H, **7**), 3.50 (d, 4H, $^{2}J_{HH}$ = 13.8 Hz, **2**).

^{13}C{^{1}H} NMR (125 MHz, DMSO-d_6, 300K): δ = 152.14 (quaternary, Ar), 136.14 (CH, NCN), 129.36 (quaternary, Ar), 128.83 (CH), 123.84 (CH), 122.11 (CH), 51.77 (CH_2), 38.96 (CH_3).

ESI+MS *m/z* 1239.3 $[M\text{-}PF]^{+}$

EI+HRMS calcd. for $C_{48}H_{52}F_{18}N_8O_4P_3$ $[M\text{-}PF_6]^{+}$: 1239.3031. Found: 1239.3047

Anal.calcd. for $C_{48}H_{52}F_{24}N_8O_4P_4.2H_2O$: C, 40.57 %; H, 3.88 %; N, 7.99 %. Found: C, 40.95 %; H, 3.85 %; N, 7.80 %.

8.3.6 ^{1}H NMR spectroscopic titration experiments

^{1}H NMR spectroscopic titration experiments were carried out by the author using a Bruker DPX300 spectrometer running at 300.1 MHz at room temperature. All chemical shifts are reported in ppm. A specific concentration of host, typically 15-23 mM, was made up in a single NMR tube in DMSO-d_6 (0.8 mL). The anions as their tetrabutylammonium salts, were made up to 1 mL, 10 times the concentration of the host, with DMSO-d_6. 20 μL aliquots of the guest were added to the NMR tube and the spectra recorded after each addition.

8.4 Experimental for Chapter 3

8.4.1 Mesityl calix[4]arene (3.1)[12]

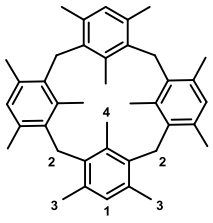

α-Chloroisodurene (5.00 g, 29.6 mmol) was dissolved in anhydrous dichloromethane (60 mL) in a round bottom flask. Tin chloride (1M in DCM, 6 mL, 6 mmol) was added resulting in a red solution and the slow formation of a precipitate. The mixture was heated at reflux (40 °C) for two hours then allowed to cool to room temperature before water (60 mL) was added and the mixture stirred for 30 minutes. The dichloromethane layer containing a precipitate was extracted. The water layer was washed with dichloromethane (3 x 15 mL) and the dichloromethane layers combined. The solvent was removed *in vacuo* to yield a cream solid (4.85 g, 40 %).

^{1}H NMR (300 MHz, DMSO-d_6, 300 K): δ = 6.72 (s, 4H, **1**), 3.81 (s, 8H, **2**), 2.26 (s, 24H, **3**), 1.12 (s, 12H, **4**).

$^{13}C\{^{1}H\}$ NMR (75 MHz, DMSO-d_6, 300 K): δ = 137.64 (quaternary, Ar), 135.91 (quaternary, Ar), 133.25 (quaternary, Ar), 130.34 (CH, Ar), 31.92 (CH_2), 21.45 (CH_3), 17.98 (CH_3).

ESI+MS *m/z* 551.4 $[M+Na]^+$

EI+HRMS calcd. for $C_{40}H_{48}Na$ $[M+Na]^+$: 551.3648. Found: 551.3663

8.4.2 Bromomethylated mesityl calix[4]arene (3.2)[8]

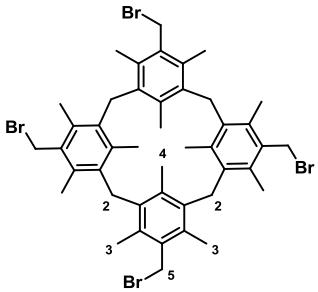

Zinc powder (0.18 g, 2.85 mmol) was added to glacial acetic acid (100 mL) in a round bottom flask, followed by HBr (33 % wt in acetic acid, 12 mL) and stirred for 30 minutes. Mesityl calix[4]arene (**3.1**) (3.00 g, 5.67 mmol), paraformaldehyde (9.00 g, 3 mmol) and HBr solution (60 mL) were added and the mixture heated at 90 °C for 72 hours. The solvent was removed *in vacuo* to yield a white solid that was washed with water (3 x 10 mL) followed by diethyl ether (3 x 10mL) and dried *in vacuo* (Yield: 5.0 g, 97 %).

^{1}H NMR (300 MHz, DMSO-d_6, 300 K): δ = 4.56 (s, 8H, **5**), 3.90 (s, 8H, **2**), 2.36 (s, 24H, **3**), 1.01 (s, 12H, **4**).

$^{13}C\{^{1}H\}$ NMR (75 MHz, DMSO-d_6, 300 K): δ = 138.47 (quaternary, Ar), 137.03 (quaternary, Ar), 133.67 (quaternary, Ar), 132.32 (quaternary, Ar), 33.44 (CH_2), 33.29 (CH_2), 19.08 (CH_3), 17.07 (CH_3).

8.4.3 Methyl-imidazole mesityl calix[4]arene (3.3)[9, 13]

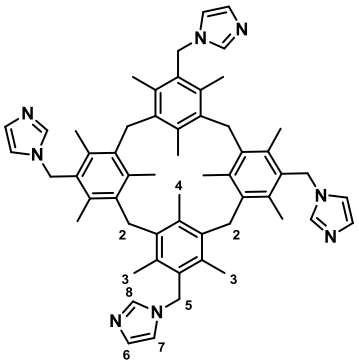

Bromomethylated-mesityl calix[4]arene (**3.2**) (1.50 g, 1.67 mmol) and imidazole (4.60 g, 66.9 mmol) were added to a Schlenk flask and the reagents degassed. Anhydrous methanol was added (50 mL) and the reaction heated at reflux (75 °C) for 72 hours. The solution was allowed to cool and the solvent was removed *in vacuo*. The product was extracted into chloroform (3 × 30 mL) from water (50 mL) and the chloroform layer washed with water (50 mL). The solvent was removed *in vacuo* to yield a cream solid (0.43 g, 30 %).

^{1}H NMR (500 MHz, DMSO-d_6, 300 K): δ = 7.47 (s, 4H, **8**), 6.96 (s, 4H, **6** / **7**), 6.81 (s, 4H, **6** / **7**), 5.32 (s, 8H, **5**), 4.06 (s, 8H, **2**), 2.38 (s, 24H, **3**), 1.19 (s, 12H, **4**).

$^{13}C\{^{1}H\}$ NMR (125 MHz, DMSO-d_6, 300 K): δ = 137.89 (quaternary, Ar), 136.43 (CH, Im), 135.41 (quaternary, Ar), 133.13 (quaternary, Ar), 129.66 (quaternary, Ar), 128.30 (CH, Im), 118.39 (CH, Im), 45.80 (CH_2), 32.66 (CH_2), 17.88 (CH_3) 16.86 (CH_3).

ESI+MS *m/z* 425.3 $[M+2H]^{2+}$, 849.5 $[M+H]^{+}$

EI+HRMS calcd. for $C_{56}H_{66}N_8$ $[M+2H]^{2+}$: 425.2700. Found: 425.2699

8.4.4 Propanol-tethered methyl-imidazolium mesityl calix[4]arene Br (3.4 Br)

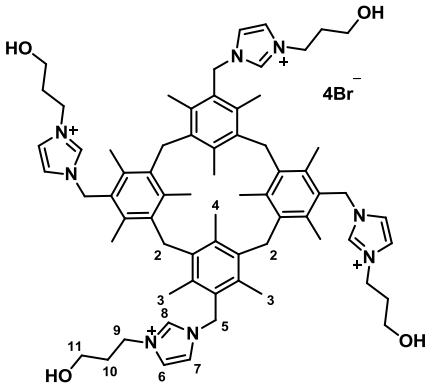

Bromomethylated mesityl calix[4]arene (**3.2**) (0.20 g, 0.22 mmol) was added to a Schlenk flask and the reagent degassed. Anhydrous DCM (10 mL) was added followed by a DCM solution (2 mL) of 1-(3-hydroxypropyl)-1H-imidazole (0.12 g, 0.94 mmol). The resultant solution was stirred at room temperature for 48 hours, during which time the product precipitated from solution as a white solid. The solution was filtered and the solid was washed with DCM (3 × 5 mL) and dried *in vacuo* (Yield: 0.25 g, 81 %).

^{1}H NMR (500 MHz, DMSO-d_6, 300 K): δ = 8.93 (s, 4H, **8**), 7.83 (s, 4H, **6** / **7**), 7.46 (s, 4H, **6** / **7**), 5.53 (s, 8H, **5**), 4.70 (t, 4H, $^{3}J_{HH}$ = 6.5 Hz, OH), 4.24 (t, 8H, $^{3}J_{HH}$ = 6.5 Hz, **9**), 4.02 (s, 8H, **2**), 3.38 (q, 8H, $^{3}J_{HH}$ = 6.5 Hz, **11**), 2.34 (s, 24H, **3**), 1.92 (quintet, 8H, $^{3}J_{HH}$ = 6.5 Hz, **10**), 1.12 (s, 12H, **4**).

$^{13}C\{^{1}H\}$ NMR (125 MHz, DMSO-d_6, 300 K): δ = 138.62 (quaternary, Ar), 136.88 (quaternary, Ar), 136.04 (CH, Im), 134.42, (quaternary, Ar) 129.97 (quaternary, Ar), 123.24 (CH, Im), 122.35 (CH, Im), 57.64 (CH_2), 55.41 (CH_2), 49.20 (CH_2), 46.98 (CH_2), 32.74 (CH_2), 18.86 (CH_3), 17.61 (CH_3).

ESI+MS *m/z* 1325.5 $[M-Br]^{+}$

EI+HRMS calcd. for $C_{68}H_{92}N_8O_4Br_3$ $[M-Br]^{+}$: 1325.4766. Found: 1325.4764

Anal.cald. for $C_{68}H_{92}Br_4N_8O_4.CH_2Cl_2$: C, 55.62 %, H, 6.39 %, N, 7.52 %. Found: C, 55.20 %, H, 6.70 %, N, 7.20 %.

8.4.5 Propanol-tethered methyl-imidazolium mesityl calix[4]arene PF_6 (3.4 PF_6)

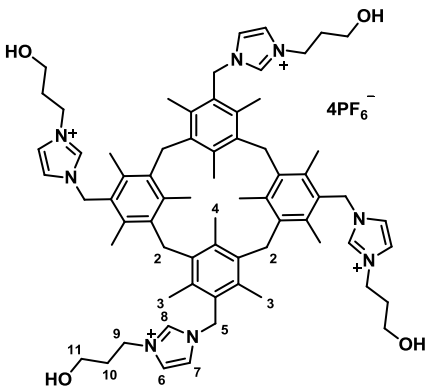

Propanol-tethered methyl-imidazolium mesityl calix[4]arene Br (**3.4 Br)** (0.20 g, 0.14 mmol) was dissolved in methanol (10 mL) and a methanol solution (10 mL) of NH_4PF_6 (0.24 g, 1.4 mmol) was added to the solution dropwise with stirring. The mixture was stirred for 30 minutes then filtered to isolate the solid. The solid was washed with methanol (3 × 5 mL) and dried in air. The product was collected as a white solid (Yield: 0.15 g, 63 %).

^{1}H NMR (500 MHz, DMSO-d_6, 300 K): δ = 8.83 (s, 4H, **8**), 7.78 (s, 4H, **6** / **7**), 7.45 (s, 4H, **6** / **7**), 5.49 (s, 8H, **5**), 4.69 (br, 4H, **OH**), 4.24 (t, 8H, $^3J_{HH}$ = 6.3 Hz, **9**), 4.02 (s, 8H, **2**), 3.34 (br, 8H, **11**), 2.34 (s, 24H, **3**), 1.90 (quintet, 8H, $^3J_{HH}$ = 6.3 Hz, **10**), 1.13 (s, 12H, **4**).

^{13}C{^{1}H} NMR (125 MHz DMSO-d_6, 300 K): δ = 138.48 (quaternary, Ar), 136.77 (quaternary, Ar), 135.87 (CH, Im), 134.25 (quaternary, Ar), 127.75 (quaternary, Ar), 123.12 (CH, Im), 122.22 (CH, Im), 57.54 (CH_2), 48.99 (CH_2), 46.87 (CH_2), 33.31 (CH_2), 32.70 (CH_2), 18.71 (CH_3), 17.61 (CH_3).

ESI+MS *m/z* 1519.62 $[M\text{-}PF_6]^+$; 687.3 $[M\text{-}2PF_6]^{2+}$

EI+HRMS calcd. for $C_{68}H_{92}N_8O_4F_{18}P_3$ $[M\text{-}PF_6]^+$: 1519.6161. Found: 1519.6136

Anal.cald. for $C_{68}H_{92}F_{24}N_8O_4P_4$: C, 49.04 %; H, 5.57 %; N, 6.73 %. Found: C, 49.35 %, H, 5.65 %, N, 6.55 %.

Colourless crystals of **3.4 3Cl.PF_6** and **3.4 4Br** suitable for single crystal X-ray diffraction were grown by slow evaporation of saturated acetonitrile solutions of compound **3.4 PF_6** with four equivalents NBu_4^+ X^- (where X = Cl or Br).

8.4.6 ^{1}H NMR spectroscopic titration experiment

The ^{1}H NMR spectroscopic titration experiments were carried out by the author using a Bruker DPX300 spectrometer running at 300.1 MHz, at room temperature. The chemical shifts are reported in ppm. Compound **3.4 PF_6** (0.01 g, 6.02 × 10^{-6} moles) was made up in a single NMR tube in MeCN-d_3 (0.5 mL). Tetrabutylammonium bromide (0.00234 g, 7.25 × 10^{-5} moles) was dissolved in MeCN-d_3 (1 mL), approximately 10

times the concentration of the host. 10 µL aliquots of the guest were added to the NMR tube and the spectra recorded after each addition.

8.4.7 Reaction of compound 3.4 Br with Ag_2O in methanol

Propanol-tethered methyl-imidazolium mesityl calix[4]arene Br (**3.4 Br**) (0.45 g, 0.32 mmol) was added to a Schlenk flask containing 3Å molecular sieves and the reagent was degassed. Anhydrous methanol was added (25 mL) followed by Ag_2O (0.09 g, 0.38 mmol). The resultant suspension was stirred at room temperature, in the dark, for 2 hours. The mixture was filtered through celite and the solvent removed *in vacuo* to yield an off white solid (0.15 g).

^{1}H NMR (300 MHz, DMSO-d_6, 300 K): δ = 7.80 (s, 4H, **CH**), 7.44 (s, 4H, **CH**), 5.50 (s, 8H, **CH_2**), 4.21 (m, 8H, **CH_2**), 4.01 (s, 8H, **CH_2**), 3.38 (m, 8H, **CH_2**), 2.34 (s, 24H, **CH_3**), 1.91 (m, 8H, **CH_2**), 1.12 (s, 12H, **CH_3**).

^{13}C{^{1}H} NMR (75 MHz, DMSO-d_6, 300 K): δ = 138.47 (quaternary), 136.88 (quaternary), 134.27 (quaternary), 123.08 (CH), 122.16 (CH), 57.46 (CH_2), 48.93 (CH_2), 46.82 (CH_2), 33.30 (CH_2), 32.76 (CH_2), 18.68 (CH_3), 17.52 (CH_3).

8.4.8 Reaction of compound 3.4 Br with Ag_2O in THF / methanol (1:1)

Propanol-tethered methyl-imidazolium mesityl calix[4]arene Br (**3.4 Br**) (0.45 g, 0.32 mmol) was added to a Schlenk flask that contained 3Å molecular sieves and the reagent was degassed. Anhydrous THF was added (15 mL) followed by anhydrous methanol dropwise (approximately 5 mL) until the compound was dissolved in solution. Ag_2O (0.09 g, 0.38 mmol) was added and the resultant suspension was stirred at room temperature, in the dark, for 12 hours. The mixture was filtered through celite and the solvent removed *in vacuo* to yield a yellow film (0.20 g).

^{1}H NMR (500 MHz, MeOD-d_4, 300 K): δ = 7.61 (s, 4H, **CH**), 7.27 (s, 4H, **CH**), 5.50 (s, 8H, **CH_2**), 4.24 (t, 8H, $^2J_{HH}$= 7 Hz, **CH_2**), 4.04 (s, 8H, **CH_2**), 3.46 (m, 8H, **CH_2**), 2.32 (s, 24H, **CH_3**), 1.96 (m, 8H, **CH_2**), 1.51 (s, 12H, **CH_3**).

^{13}C{^{1}H} NMR (125 MHz, MeOD-d_4, 300 K): δ = 182.39 (quaternary), 138.47 (quaternary), 136.88 (quaternary), 134.27 (quaternary), 129.04 (quaternary), 123.08 (CH), 122.16 (CH), 57.46 (CH_2), 48.93 (CH_2), 46.82 (CH_2), 33.30 (CH_2), 32.76 (CH_2), 18.68 (CH_3), 17.52 (CH_3).

8.4.9 Reaction of 3.4 Br with Cu_2O

Propanol-tethered methyl-imidazolium mesityl calix[4]arene Br (**3.4 Br**) (0.69 g, 0.5 mmol) and Cu_2O (0.42, 3 mmol) were added a Schlenk flask containing 3Å molecular sieves, and the reagents were degassed. Anhydrous acetonitrile (20 mL) was added and the suspension heated at 90 °C for 120 hours, under an atmosphere of argon. The solvent was removed *in vacuo* to yield a red solid. The product was dissolved in anhydrous acetone, filtered, and the solvent removed *in vacuo* to yield a pale yellow solid (Yield: 0.01 g), which was found to be a mixture of copper-NHC complexes.

^{1}H NMR (300 MHz, acetone-d_6, 300 K): δ = 8.79 (s, **CH**), 7.83 (s, **CH**), 7.55 (s, **CH**), 7.35 (s, **CH**), 7.04 (s, **CH**), 7.02 (s, **CH**), 6.13 (s, **CH_2**), 5.77 (s, **CH_2**), 5.47 (s, **CH_2**), 4.45 (t, **CH_2**), 4.26 (br, **CH_2**), 4.14 (br, **CH_2**), 3.6 (br, **CH_2**), 2.49 (br, **CH_3**), 2.47 (br, **CH_3**), 2.42 (s, **CH_3**), 1.85 (m, **CH_2**), 1.24-1.29 (br, **CH_3**).

ESI+MS *m/z* 1678.1 $[3.4\text{-}4H+4Cu+Na]^+$; 1593.2 $[3.4\text{-}3H+3Cu\text{-}Br+2MeCN]^+$; 1449.3 $[3.4\text{-}2H+2Cu\text{-}Br]^+$; 1385.4 $[3.4\text{-}H+Cu\text{-}Br]^+$

8.5 Experimental for Chapter 4

8.5.1 1-Tert-butylacetate imidazole (4.1)[14]

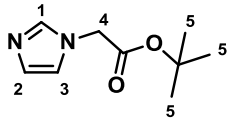

To a solution of imidazole (1.00 g, 14.7 mmol) in ethyl acetate (16 mL) in a round bottom flask was added powered potassium carbonate (2.80 g, 20.5 mmol) and the mixture was heated to reflux (76 °C). *Tert*-butyl chloroacetate (2.1 mL, 14.7 mmol) dissolved in ethyl acetate (5 mL) was added dropwise to the refluxing solution. The reaction was heated at reflux (76 °C) for 12 hours. The reaction was allowed to cool and then quenched with cold water (10 mL). The ethyl acetate layer was separated and the aqueous layer washed with ethyl acetate (2 × 10 mL). The ethyl acetate layers were combined, washed with brine (20 mL), and dried over sodium sulphate. The solution was filtered, and the filtrate was removed *in vacuo* to yield a yellow solid. The solid was stirred with hexane (5 mL) at room temperature for one hour, filtered, and the solid washed further with hexane (2 × 2 mL) to afford the target compound (Yield: 1.02 g, 55 %). The product was purified by column chromatography (10 % MeOH / chloroform, I_2 active by TLC).

^{1}H NMR (300 MHz, DMSO-d_6, 300 K): δ = 7.40 (s, 1H, **1**), 6.98 (s, 1H, **2** / **3**), 6.87 (s, 1H, **2** / **3**), 4.52 (s, 2H, **4**) 1.39 (s, 9H, **5**).

$^{13}C\{^{1}H\}$ NMR (75 MHz, DMSO-d_6, 300 K): δ = 166.3 (quaternary, COO^{t}Bu,), 138.7 (CH), 129.8 (CH), 120.3 (CH), 83.4 (quaternary, ^{t}Bu,), 49.5 (CH_2), 28.3 (CH_3).

ESI+MS *m/z* 183.1 $[M+H]^+$

EI+HRMS calcd. for $C_9H_{15}N_2O_2$ $[M+H]^+$: 183.1128. Found: 183.1136.

Anal.cald. for $C_9H_{15}N_2O_2$: C, 59.32 %; H, 7.74 %; N, 15.37 %. Found: C, 59.25 %, H, 7.80 %, N, 15.45 %.

8.5.2 Acetate-tethered methyl-imidazolium-mesityl calix[4]arene Br (4.2 Br)

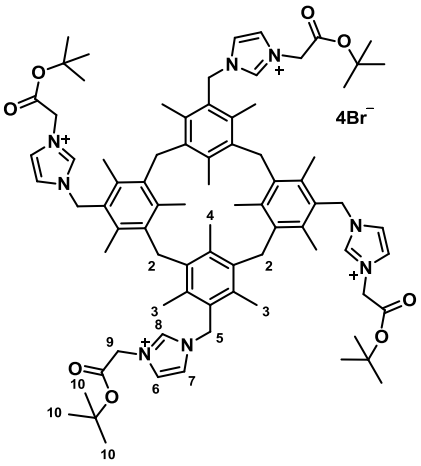

Bromomethylated mesityl calix[4]arene (**3.3**) (0.30 g, 0.33 mmol) was added to Schlenk flask and the reagent was degassed. Anhydrous THF was added (10 mL) followed by a THF solution (10 mL) of 3-(*tert*-butyl)-acetic acid imidazole (**4.1**) (0.26 g, 1.4 mmol). The resultant solution was stirred at room temperature for 48 hours. The product precipitated from solution as a white solid that was collected by filtration, washed with anhydrous THF (2 × 5 mL), and dried *in vacuo* (Yield: 0.25 g, 46 %).

^{1}H NMR (500 MHz, DMSO-d_6, 300 K): δ = 8.92 (s, 4H, **8**), 7.81 (s, 4H, **6** / **7**), 7.57 (s, 4H, **6** / **7**), 5.62 (s, 8H, **5**), 5.13 (s, 8H, **9**), 4.01 (s, 8H, **2**), 2.34 (s, 24H, **3**), 1.43 (s, 36H, **10**), 1.14 (s, 12H, **4**).

$^{13}C\{^{1}H\}$ NMR (125 MHz, DMSO-d_6, 300 K): δ = 166.08 (quaternary, COO^{t}Bu), 138.49 (quaternary, Ar), 136.91 (CH, Im), 136.83 (quaternary, Ar), 134.83 (quaternary, Ar), 127.83 (quaternary, Ar), 124.42 (CH, Im), 121.97 (CH, Im), 93.34 (quaternary, ^{t}Bu), 50.13 (CH_2), 48.90 (CH_2), 32.91 (CH_2), 28.01 (CH_3), 18.73 (CH_3), 17.53 (CH_3).

ESI+MS *m/z* 734.4 $[M-2Br]^{2+}$

EI+HRMS calcd. for $C_{80}H_{110}N_8O_8Br_2$ $[M-2Br]^+$: 734.3401. Found: 734.3382.

Colourless crystals suitable for single crystal X-ray diffraction analysis were grown by slow diffusion of ethyl acetate into a DMSO solution of compound **4.2 Br**.

8.5.3 Acetate-tethered methyl-imidazolium-mesityl calix[4]arene PF_6 (4.2 PF_6)

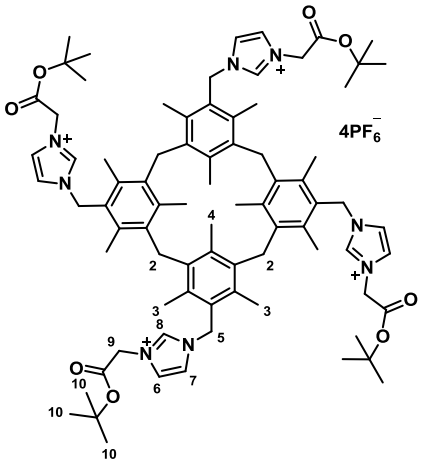

Acetate-tethered methyl-imidazolium-mesityl calix[4]arene bromide (**4.2 Br**) (0.2 g, 0.14 mmol) was dissolved in methanol (10 mL) and a methanol solution (10 mL) of NH_4PF_6 (0.24 g, 1.4 mmol) was added to the solution dropwise with stirring. The mixture was stirred for 30 minutes then filtered to isolate the solid. The solid was washed with methanol (3 × 5 mL) and dried in air. The product was collected as a white solid (Yield: 0.15 g, 63 %).

^{1}H NMR (500 MHz, DMSO-d_6, 300 K): δ = 8.80 (s, 4H, **8**), 7.73 (s, 4H, **6** / **7**), 7.49 (s, 4H, **6** / **7**), 5.55 (s, 8H, **5**), 5.07 (s, 8H, **9**), 4.02 (s, 8H, **2**), 2.34 (s, 24H, **3**), 1.45 (s, 36H, **10**), 1.12 (s, 12H, **4**).

^{13}C{^{1}H} NMR (125 MHz, DMSO-d_6, 300 K): δ = 165.76 (quaternary, COO^tBu), 138.09 (quaternary, Ar), 136.56 (CH, Im), 136.44 (quaternary, Ar), 133.91 (quaternary, Ar), 127.37 (quaternary, Ar), 124.07 (CH, Im), 121.64 (CH, Im), 82.98 (quaternary, ^{t}Bu), 50.07 (CH_2), 48.87 (CH_2), 32.87 (CH_2), 27.72 (CH_3), 18.73 (CH_3), 17.53 (CH_3).

ESI+MS *m/z* 1744.7 $[M\text{-}PF_6]^+$; 799.4 $[M\text{-}2PF_6]^{2+}$

EI+HRMS calcd. for $C_{80}H_{108}N_8O_8P_3F_{18}$ $[M\text{-}PF_6]^+$: 1744.6543. Found: 1744.7286.

Anal.cald. for $C_{80}H_{108}F_{24}N_8O_8P_4$: C, 50.85 %; H, 5.76 %; N, 5.93 %. Found: C, 49.90 %; H, 5.60 %; N, 5.65 %.

8.5.4 Acetic acid- tethered methyl-imidazolium-mesityl calix[4]arene Br (4.3 Br)

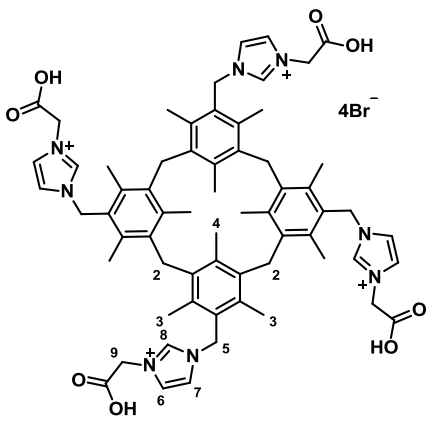

A HCl solution (37 %, 4 mL, 50 mmol) of acetate tethered mesityl calix[4]arene Br (**4.2 Br**) (1.00 g, 0.62 mmol) was heated at reflux (110 °C) for one hour. The solution was cooled to room temperature and the solvent removed *in vacuo*. The resultant solid was washed with acetone (2 × 10 mL), followed by diethyl ether (2 × 10 mL) and dried *in vacuo* to yield a crystalline yellow solid (0.71 g, 71 %).

^{1}H NMR (500 MHz, DMSO-d_6, 300 K): δ = 8.87 (s, 4H, **8**), 7.79 (s, 4H, **6** / **7**), 7.57 (s, 4H, **6** / **7**), 5.80 (s, 8H, **5**), 5.13 (s, 8H, **9**), 4.01 (s, 8H, **2**), 2.35 (s, 24H, **3**), 1.12 (s, 12H, **4**).

^{13}C{^{1}H} NMR (125 MHz, DMSO-d_6, 300 K): δ= 166.08 (quaternary, COOH), 138.30 (quaternary, Ar), 136.52 (CH, Im), 136.44 (quaternary, Ar), 133.93 (quaternary, Ar), 127.46 (quaternary, Ar), 124.07 (CH, Im), 121.56 (CH, Im), 49.80 (CH_2), 48.88 (CH_2), 32.87 (CH_2), 18.33 (CH_3), 17.14 (CH_3).

ESI+MS *m/z* 1081.5 $[M\text{-}4Br\text{-}3H]^+$

EI+HRMS calcd. for $C_{64}H_{73}N_8O_8$ $[M\text{-}4Br\text{-}3H]^+$: 1081.5551. Found: 1081.5513

Anal.cald. for $C_{64}H_{76}N_8O_8Br_4.H_2O$: C, 54.02 %; H, 5.53 %; N, 7.87 %. Found: C, 54.50 %, H, 5.80 %, N, 7.25 %.

8.5.5 Acetic acid-tethered methyl-imidazolium-mesityl calix[4]arene PF_6 (4.3 PF_6)

Acetic acid-tethered methyl-imidazolium-mesityl calix[4]arene Br (**4.3 Br**) (0.20 g, 0.14 mmol) was dissolved in methanol (10 mL) and a methanol solution (10 mL) of NH_4PF_6 (0.24 g, 1.4 mmol) was added to the solution dropwise with stirring. The mixture was stirred for 30 minutes then filtered to isolate the solid. The solid was washed with methanol (3 × 5 mL) and dried in air. The product was collected as a white solid (Yield: 0.16 g, 68 %).

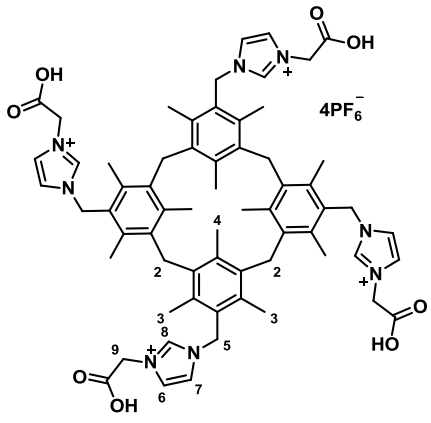

^{1}H NMR (500 MHz, DMSO-d_6, 300 K): δ = 8.71 (s, 4H, **8**), 7.69 (s, 4H, **6** / **7**), 7.45 (s, 4H, **6** / **7**), 5.54 (s, 8H, **5**), 4.87 (s, 8H, **9**), 4.02 (s, 8H, **2**), 2.35 (s, 24H, **3**), 1.13 (s, 12H, **4**).

^{13}C{^{1}H} NMR (125 MHz, DMSO-d_6, 300 K): δ = 167.46 (quaternary, COOH), 138.11 (quaternary, Ar), 136.45 (CH, Im), 136.24 (quaternary, Ar), 133.90 (quaternary, Ar), 127.43 (quaternary, Ar), 124.04 (CH, Im), 121.21 (CH, Im), 50.75 (CH_2), 48.69 (CH_2), 32.89 (CH_2), 18.30 (CH_3), 17.05 (CH_3).

ESI+MS *m/z* 1227.53 $[M\text{-}2PF_6\text{-}2H]^+$; 1373.51 $[M\text{-}2PF_6\text{-}H]^+$

EI+HRMS calcd. for $C_{64}H_{75}N_8O_8P_2F_{12}$ $[M\text{-}2PF_6\text{-}H]^+$: 1373.4991. Found: 1373.5125

8.5.6 1-Methyl-3-tert-butylacetate imidazolium chloride (4.4)

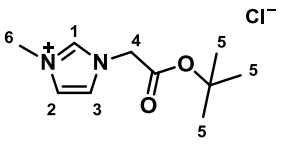

1-Methylimidazole (1.60 mL, 20 mmol) and *tert*-butyl 2-chloroacetate (2.90 mL, 20 mmol) were added to a Schlenk flask. The mixture was stirred at room temperature for 18 hours during which time the mixture solidified. The target compound was recrystallised from DCM / hexane as a white solid, which was washed with diethyl ether (2 × 10 mL) and dried *in vacuo* (Yield: 3.59 g, 77 %).

^{1}H NMR (300 MHz, DMSO-d_6, 300 K): δ = 9.31 (s, 1H, **1**), 7.78 (s, 2H, **2**, **3**), 5.22 (s, 2H, **4**), 3.91 (s, 3H, **6**), 1.44 (s, 9H, **5**).

^{13}C{^{1}H} NMR (75 MHz, DMSO-d_6, 300 K): δ = 165.80 (quaternary, COO^{t}Bu,), 137.70 (CH), 123.60 (CH), 123.10 (CH), 82.90 (quaternary, ^{t}Bu), 49.50 (CH_2), 35.70 (CH_3), 27.60 (CH_3).

ESI+MS *m/z* 197.1 $[M\text{-}Cl]^+$

EI+HRMS calcd. for $C_{10}H_{17}N_2O_2$ $[M–Cl]^+$: 197.1285. Found: 197.1307.

8.5.7 Copper(I)-(1-methyl-3-tert-butlyacetate)-N-heterocyclic carbene Cl (4.5)[15]

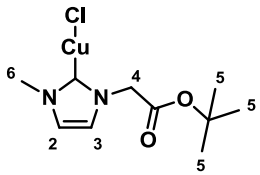

1-Methyl-3-*tert*-butylacetate imidazolium chloride (**4.4**) (0.23 g, 1 mmol) was added to a three-necked round-bottomed flask. Anhydrous MeCN (15 mL) was added and the copper electrodes (1 x 3 cm^2) were inserted in to the reaction mixture. The mixture was electrolysed at 50 mA for 50 minutes (2Q), under an atmosphere of argon. The mixture was filtered, and the solvent was removed *in vacuo*, to yield an off white solid (Yield: 0.14 g, 48 %).

^{1}H NMR (500 MHz, $CDCl_3$, 300 K): δ = 6.98 (s, 1H, **2** / **3**), 6.93 (s, 1H, **2** / **3**), 4.78 (s, 2H, **4**), 3.81 (s, 3H, **6**), 1.45 (s, 9H, **5**).

^{13}C{^{1}H} NMR (125 MHz, $CDCl_3$, 300 K): δ = 178.00 (quaternary, Cu-C), 166.47 (quaternary, COO^{t}Bu), 122.02 (CH), 83.72 (quaternary, ^{t}Bu), 52.60 (CH_2), 38.29 (CH_3), 28.00 (CH_3).

ESI+MS *m/z* 300.1 $[M\text{-}Cl+MeCN]^+$

EI+HRMS calcd. for $C_{12}H_{19}CuN_3O_2$ $[M–Cl+MeCN]^+$: 300.0768. Found: 300.0761.

Anal.cald. for $C_{10}H_{19}CuN_3O_{2.}1/3DCM$: C, 38.36 %; H, 5.19 %; N, 8.66 %. Found: C, 38.40 %, H, 5.15 %; N, 8.70 %.

8.5.8 Tetrakis-(p-copper(I)-N-heterocyclic carbene) mesityl calix[4]arene (4.6)

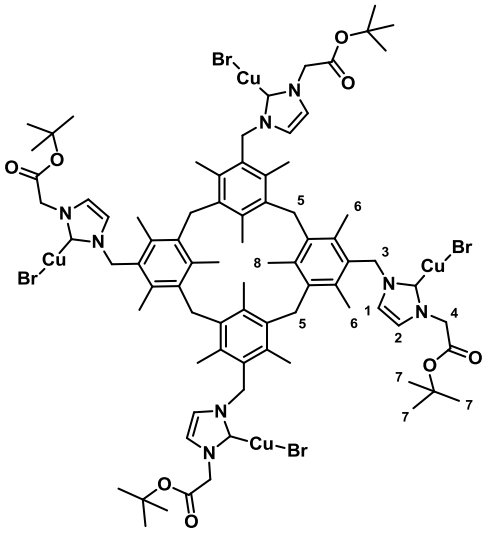

Acetate-tethered methyl-imidazolium-mesityl calix[4]arene Br (**4.2**) (0.81 g, 0.5 mmol) was added to a three-necked round-bottomed flask. Anhydrous MeCN (15 mL) was added and the copper electrodes (1 × 3 mL) were inserted into the reaction mixture. The potential was adjusted so that a current of 10 mA was maintained. The mixture was electrolysed for 1920 minutes (6 Q) under an atmosphere of argon, filtered, and the solvent removed *in vacuo* to yield a pale yellow solid (Yield: 0.2 g, 21 %).

^{1}H NMR (300 MHz, MeCN-d_3, 300 K): δ = 7.08 (s, 4H, **1** / **2**), 6.69 (s, 4H, **1** / **2**), 5.37 (s, 8H, **3**), 4.79 (s, 8H, **4**), 4.03 (s, 8H, **5**), 2.34 (s, 24H, **6**), 1.44 (s, 36H, **7**), 1.18 (s, 12H, **8**).

^{13}C{^{1}H} NMR (75 MHz, $CDCl_3$, 300K): δ = 178.65 (quaternary, Cu-C), 166.57 (quaternary, COO^tBu), 138.84 (quaternary, Ar), 137.21 (quaternary, Ar), 133.80 (quaternary, Ar), 128.13 (quaternary, Ar), 121.58 (CH), 119.72 (CH), 83.74 (quaternary, ^{t}Bu), 67.98 (CH_2), 65.85 (CH_2), 53.08 (CH_2), 50.88 (CH_2), 33.42 (CH_2), 28.09 (CH_3), 25.62 (CH_2), 18.68 (CH_3), 17.69 (CH_3).

ESI+MS *m/z* 1879.2 $[M+H]^+$

EI+HRMS calcd. for $C_{80}H_{104}Cu_4N_8O_8Br_4$ $[M+H]^+$: 1879.1929. Found: 1879.0310.

Anal. Calcd. for $C_{80}H_{105}Br_4Cu_4N_8O_8.2CH_2Cl_2$: C, 48.56; H, 5.43; N, 5.39. Found: C, 48.30; H, 5.40; N, 5.25.

8.5.9 Tetrakis-p-(palladium(II)-N-heterocyclic carbene) mesityl calix[4]arene (4.7)

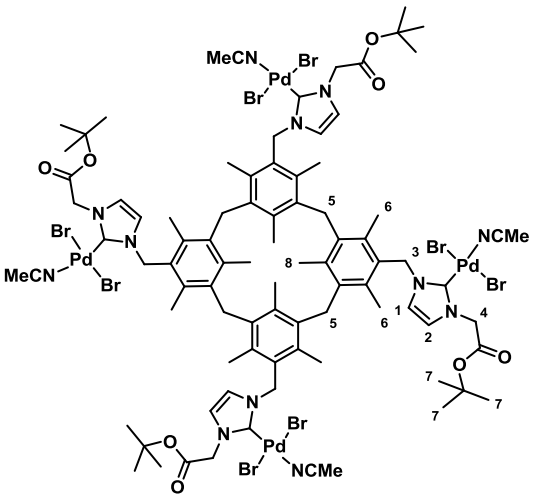

Tetrakis-(*p*-copper(I)-N-heterocyclic carbene) mesityl calix[4]arene (**4.6**) (1.00 g, 0.5 mmol) was added to a Schlenk flask. KBr (1.20 g, 20 mmol) was added followed by anhydrous DCM (5 mL). $PdCl_2(MeCN)_2$ (0.55 g, 2.15 mmol) was added to the reaction and the mixture was stirred at room temperature for 12 hours. The solvent was removed *in vacuo* before acetonitrile (20 mL) was added to dissolve the product. The mixture was filtered through a celite plug and the solvent reduced *in vacuo* (5 mL). Diethyl ether (5 mL) was added to precipitate the product as a yellow solid that was collected by gravity filtration and dried by washing with diethyl ether (2 × 10 mL). The product was purified by the filtration of an acetonitrile solution of **4.7** through a silica plug. The solvent was removed *in vacuo* to yield a red solid (0.59 g, 47 %).

^{1}H NMR (300 MHz, CD_3CN, 300 K): δ = 7.11 (s, 4H, **1** / **2**), 6.14 (s, 4H, **1** / **2**), 5.60 (s, 8H, **3**), 5.20 (s, 8H, **4**), 4.05 (s, 8H, **5**), 2.30 (s, 24H, **6**), 1.46 (s, 36H, **7**), 1.24 (s, 12H, **8**).

^{13}C{^{1}H} NMR (125 MHz, $CDCl_3$, 300 K): δ = 167.26 (quaternary, COO^tBu), 147.31 (quaternary, Pd-C), 139.86 (quaternary, Ar), 138.10 (quaternary, Ar), 135.74 (quaternary, Ar), 129.32 (quaternary, Ar), 124.60 (CH), 120.76 (CH), 83.73 (quaternary, ^{t}Bu), 53.74 (CH_2), 52.65 (CH_2), 34.02 (CH_2), 28.51 (CH_3), 19.25 (CH_3), 18.28 (CH_3).

ESI+MS *m/z* 992.8 $[M\text{-}4^tBu\text{-}2Br]^{2+}$

EI+HRMS calcd. for $C_{64}H_{72}Br_6N_8O_8Pd_4$ $[M\text{-}4^tBu\text{-}2Br]^{2+}$: 992.8344; Found: 992.8370.

Anal. Calcd. for: $C_{80}H_{104}Br_8N_8O_8Pd_4$: C, 40.53; H, 4.42; N; 4.73. Found: C, 38.25, H, 4.30, N, 4.75.

Yellow plate crystals suitable for single crystal X-ray diffraction analysis were grown by slow diffusion of pentane into an acetonitrile solution of compound **4.7**.

8.5.10 Tetrakis-p-(rhodium(I)-N-heterocyclic carbene) mesityl calix[4]arene (4.8)

Tetrakis-(*p*-copper(I)-N-heterocyclic carbene) mesityl calix[4]arene (**4.6**) (0.08 g, 0.042 mmol) was added to a small ampoule followed by KBr (0.04 g, 0.42 mmol) and anhydrous chloroform (1 mL). $[Rh(COD)Cl]_2$ (0.042 g, 0.084 mmol) was added and the mixture stirred at room temperature for 12 hours. The solution was filtered and the solvent removed *in vacuo* to yield the target complex as a yellow solid (Yield: 0.06 g, 61 %). The ^{1}H NMR and $^{13}C\{^{1}H\}$ NMR spectra were too complicated to be fully assigned.

^{1}H NMR (300 MHz, $CDCl_3$, 300 K): δ = 6.79 (**CH**), 6.14 (**CH**), 5.87 (**CH_2**), 5.63 (**CH_2**), 5.42 (**CH_2**), 5.05 (**CH_2**), 4.64 (**CH_2**), 4.58 (**CH_2**), 4.22 (**CH_2**), 3.98 (**CH_2**), 2.30 (**CH_3**), 1.93 (**CH_3**), 1.15 (**CH_3**).

$^{13}C\{^{1}H\}$ NMR (75 MHz, $CDCl_3$, 300 K): δ = 182.15 (quaternary, Rh-C, d, $2J^{13}_{C\text{-}Rh}$ = 50.1 Hz), 167.30 (quaternary, $COO^{t}Bu$,), 137.41 (quaternary, Ar), 135.57 (quaternary, Ar), 133.02 (quaternary, Ar), 127.89 (quaternary, Ar), 120.22 (CH), 118.55 (CH), 98.01 (quaternary, ^{t}Bu), 97.64 (quaternary, ^{t}Bu), 81.96 (CH_2), 77.84 (CH_2), 68.14 (CH_2), 66.95 (CH_2), 64.82 (CH_2), 52.43 (CH_2), 52.02 (CH_2), 49.56 (CH_2), 31.95 (CH_2), 29.88 (CH_2), 27.95 (CH_2), 17.75 (CH_3), 16.70 (CH_3).

ESI+MS *m/z* 1154.8 $[M\text{-}2Br]^{2+}$; 2389.4 $[M\text{-}Br]^{+}$

EI+HRMS Calcd. for $C_{112}H_{152}Br_3N_8O_8Rh_4$ $[M\text{-}Br]^{+}$: 2389.5464; Found: 2389.4319.

EI+HRMS Calcd. for $C_{112}H_{152}Br_2N_8O_8Rh_4$ $[M\text{-}2Br]^{2+}$: 1154.8166; Found: 1154.8408.

8.5.11 1-Methyl-3-acetic acid imidazolium chloride (4.9)

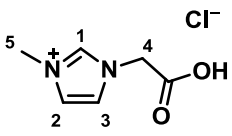

A HCl solution (37 %, 2 mL, 22 mmol) of 1-methyl-2-*tert*-butylacetate imidazolium chloride (**4.4**) (3.90 g, 20 mmol) was heated at reflux (110 °C) for one hour. The solution was allowed to cool to room temperature and the solvent was removed in vacuo. The resultant solid was washed with acetone (2 × 10 mL), followed by diethyl ether (2 × 10 mL), and dried *in vacuo* to yield an off white solid (2.30 g, 82 %).

^{1}H NMR (500 MHz, DMSO-d_6, 300 K): δ = 9.33 (s, 1H, **1**), 7.80 (s, 1H, **2** / **3**), 7.78 (s, 1H, **2** / **3**), 5.24 (s, 2H, **4**), 3.93 (s, 3H, **5**).

$^{13}C\{^{1}H\}$ NMR (125 MHz, DMSO-d_6, 300 K): δ = 167.96 (quaternary, COOH), 137.65 (CH), 123.67 (CH), 123.12 (CH), 49.69 (CH_2), 35.65 (CH_3).

ESI+MS *m/z* 141.1 $[M\text{-}Cl]^+$

EI+HRMS calcd. for $C_6H_9N_2O_2$ $[M–Cl]^+$: 141.0659. Found: 141.0693.

8.5.12 Reaction of compound 4.9 with Ag_2O in DCM / methanol

1-Methyl-3-acetic acid imidazolium chloride (**4.9**) (1.70 g, 10 mmol) was added to a Schlenk flask containing 4Å molecular sieves and the reagent was degassed. Anhydrous DCM was added (40 mL) followed by anhydrous methanol (20 mL). Ag_2O (3.50 g, 15 mmol) was added to the solution and the resultant suspension was stirred at room temperature in the dark, for 12 hours. The mixture was filtered through celite and the celite was washed with DCM / methanol (1:1) solution (3 × 10 mL). The solvent was removed *in vacuo* to yield an off white solid (Yield: 0.5 g).

^{1}H NMR (500 MHz, MeOD-d_4, 300 K): δ = 7.52 (s, 1H, **CH**), 7.50 (s, 1H, **CH**), 4.74 (s, 2H, **CH_2**), 3.92 (s, 3H, **CH_3**).

^{13}C{^{1}H} NMR (125 MHz, MeOD-d_4, 300 K): δ = 171.02 (quaternary, COOH), 124.88 (CH), 123.97 (CH), 36.28 (CH_3).

ESI+MS *m/z* 141.1 $[4.9\text{-}Cl]^+$

8.5.13 Reaction of compound 4.9 with Ag_2O in methanol

1-Methyl-3-acetic acid imidazolium chloride (**4.9**) (1.70 g, 10 mmol) was added to a Schlenk flask that contained 4Å molecular sieves and the reagent degassed. Anhydrous methanol was added (50 mL) followed by Ag_2O (3.50 g, 15 mmol). The resultant suspension was stirred at room temperature, in the dark, for 12 hours. The mixture was filtered through celite and the celite was washed with methanol (3 × 10 mL). The solvent was removed *in vacuo*, to yield a white solid (Yield: 1.00 g). At least two carbene products were observed in the NMR spectrum.

Compound 1; **^{1}H NMR** (300 MHz, MeOD-d_4, 300 K): δ = 7.56 (s, 1H, **CH**), 7.53 (s, 1H, **CH**), 4.77 (s, 2H, **CH_2**), 3.95 (s, 3H, **CH_3**). Compound 2; δ = 7.53 (s, 1H, **CH**), 7.24 (s, 1H, **CH**), 4.73 (s, 2H, **CH_2**), 3.90 (s, 3H, **CH_3**).

ESI+MS *m/z* 141.1 $[4.9\text{-}Cl]^+$; 433.9; 492.0; 566.9.

Colourless crystals suitable for single crystal X-ray diffraction analysis were grown in the dark by vapour diffusion of diethyl ether into a methanol solution of the product formed in the reaction. The X-ray crystal structure revealed a zwitterion (compound **4.10**).

8.6 Experimental for Chapter 5

General protocol used for the Suzuki-Miyaura reactions. Phenyl boronic acid was reacted with either 4-chlorotoluene or 4-bromotoluene, and the conditions applied were the same as those reported by Brenner *et al* and Dinares *et al*.[16, 17] The yields were determined by ^{1}H NMR spectroscopy using 1,4-dimethoxybenzene as a standard. Phenyl boronic acid (0.183 g, 1.5 mmol), Cs_2CO_3 (0.625 g, 2 mmol) and an acetonitrile solution of compound **5** (or palladium source and ligand **3**) were added to a carousel reactor and the solvent was removed *in vacuo*. Reaction solvent was added (3 mL) followed by the aryl halide (1 mmol). The mixture was stirred vigorously at 80 °C, for 2 hours, under an atmosphere of nitrogen. The hot mixture was filtered through a pad of celite, and the celite washed with the reaction solvent (2 mL). 1,4-Dimethoxybenzene (0.069 g, 0.5 mmol) was added to the filtrate and the solvent removed *in vacuo*. The mixture was analysed by ^{1}H NMR spectroscopy and the product yields were determined by comparing the intensity of the methyl signal of the product (δ = 2.41 ppm) with that of the 1,4-dimethoxybenzene (δ = 3.78 ppm).

8.7 Experimental for Chapter 6

8.7.1 (Dichloromethyl) amino-tert-butylacetate (6.1)

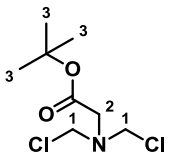

Glycine *tert*-butyl ester hydrochloride (0.419 g, 2.5 mmol) and paraformaldehyde (0.195 g, 6.5 mmol) were added to a Schlenk flask and the reagents degassed. Anhydrous dichloromethane (7 mL) was added and the solution stirred for 1 hour at room temperature. The solution was cooled to 0 °C in an ice bath and $SOCl_2$ (0.73 mL, 10 mmol), was added dropwise, purified by distillation (59-64 °C).[18] The solvent was removed *in vacuo* to yield a yellow oil that solidifies in the fridge. The sample was purified by extraction into anhydrous diethyl ether (Yield: 0.21 g, 50 %).

^{1}H NMR (500 MHz, $CDCl_3$, 300 K): δ = 5.18 (s, 4H, **1**), 3.59 (s, 2H, **2**), 1.41 (s, 9H, **3**).

^{13}C{^{1}H} NMR (125 MHz, $CDCl_3$, 300 K): δ = 168.44 (quaternary, $COO^{t}Bu$), 82.94 (quaternary, ^{t}Bu), 71.60 (CH_2), 50.90 (CH_2), 28.04 (CH_3).

ESI+MS *m/z* 192.2 $[M\text{-}Cl]^+$

EI+HRMS calcd. for $C_8H_{15}NO_2Cl$ $[M\text{-}Cl]^+$: 192.0787. Found: 192.0786.

8.7.2 (Dimethylimidazole) amino-tert-butylacetate (6.2)

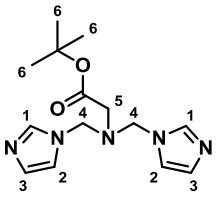

Glycine *tert*-butyl ester hydrochloride (0.67 g, 4 mmol) and imidazole (1.02 g, 15 mmol) were added to a Schlenk flask containing 4Å molecular sieves and the reagents were degassed. Formaldehyde (37-41 wt %, 0.7 mL, 10 mmol) in anhydrous ethanol (2 mL) was added followed by anhydrous dichloromethane (15 mL). The mixture was stirred at room temperature for 72 hours. The product was extracted into chloroform (3 x 30 mL) from water (30 mL). The chloroform layer was washed with water (50 mL), dried over $CaCl_2$, and filtered. The chloroform was removed *in vacuo* to yield a yellow oil. Diethyl ether (30 mL) was added to the oil and the solution stored in the fridge (4 °C) for 24 hours. The product precipitated from solution as a crystalline white solid that was collected by reduced pressure filtration, washed with diethyl ether (5 x 10 mL) and dried in air (Yield: 0.40 g, 35 %).

^{1}H NMR (500 MHz, $CDCl_3$, 300 K): δ = 7.63 (s, 2H, **1**), 7.12 (s, 2H, **2** / **3**), 6.97 (s, 2H, **2** / **3**), 4.93 (s, 4H, **4**), 3.35 (s, 2H, **5**), 1.44 (s, 9H, **6**).

^{13}C{^{1}H} NMR (125 MHz, $CDCl_3$, 300 K): δ = 169.13 (quaternary, COO^tBu), 137.43 (CH), 130.14 (CH), 118.80 (CH), 82.64 (quaternary, ^tBu), 63.01 (CH_2), 51.35 (CH_2), 28.12 (CH_3).

ESI+MS *m/z* 292.2 $[M+H]^+$

EI+HRMS calcd. for $C_{14}H_{22}N_5O_2$ $[M+H]^+$: 292.1768. Found: 292.1761

Anal.calcd. for $C_{14}H_{21}N_5O_2$: C, 57.71%; H, 7.27%; N, 24.04%. Found: C, 57.15%; H, 7.20%; N, 23.75%.

Colourless crystals suitable for single crystal X-ray diffraction analysis were grown by slow evaporation of a saturated chloroform solution of compound **6.2**.

8.7.3 1-methyl-3-acetic acid imidazolium tetrafluroborate and related imidazolium species[19]

1-Methylimidazole (0.8 mL, 10 mmol) and chloroacetic acid (0.945 g, 10 mmol) were added to a Schlenk flask and heated at 70 °C for 12 hours. The mixture was allowed to cool to room temperature and the resultant oil was washed with anhydrous diethyl ether (3 × 2 mL). Sodium tetrafluoroborate (1.098 g, 10 mmol) was added followed by anhydrous acetonitrile (20 mL) and the suspension was heated at reflux (84 °C) for 24

hours. Once cooled, the solution was filtered to remove the white precipitate, and the solvent was removed from the filtrate *in vacuo*, to yield a yellow oil that was assigned by ^{1}H NMR spectroscopy and mass spectrometry to be a mixture of products (Figure 8.1).

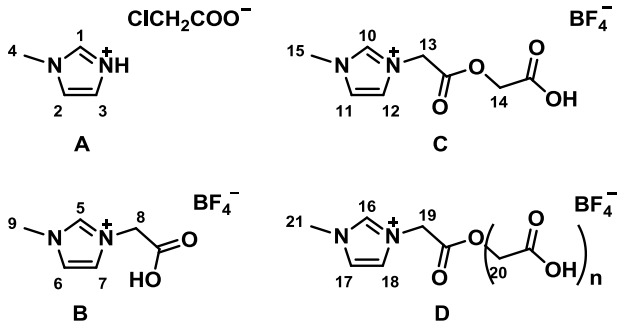

Figure 8.1 Products formed in the reaction between 1-methyl imidazole and chloroacetic acid (n = 2-6).

^{1}H NMR (500 MHz, d_6-DMSO, 300 K): δ = 9.10 (s, 1H, **C10**), 9.03 (s, 1.6H, **B5**), 8.91 (s, 1.8H, **A1**), 7.71 (d, $^{3}J_{H\text{-}H}$= 1.45 Hz, 1H, **C12**), 7.70 (d, $^{3}J_{H\text{-}H}$= 1.45 Hz, 1H, **C11**), 7.68 (m, 1.6H, **B7**), 7.66 (m, 1.6H, **B6**), 7.62 (br, 1.8H, **A3**), 7.59 (br, 1.8H, **A2**), 5.38 (s, 2H, **C13**), 5.08 (s, 3.2H, **B8**), 4.74 (s, 2H, **C14**), 3.92 (s, 3H, **C15**), 3.09 (s, 4.8H, **B9**), 3.86 (s, 5.4H, **A4**).

ESI+MS *m/z* 141.1 $[B]^{+}$; 199.1 $[C]^{+}$; 257.1 [D (n=2)]$^{+}$; 315.1 [D (n=3)]$^{+}$; 373.1 [D (n=4)]$^{+}$; 4.31.1 [D (n=5)]$^{+}$; 489.1 [D (n=6)]$^{+}$

EI+HRMS calcd. for $C_6H_9N_2O_2$ $[B]^{+}$: 141.0659 Found: 141.0695

8.7.4 Bis(2-dichloroethyl) amino benzyl (6.4)[20]

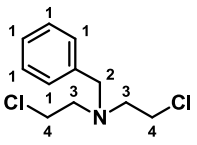

An aqueous solution (12.5 mL) of bis(2-dichloroethyl)amine hydrochloride (5.00 g, 0.028 mol) was poured into an aqueous solution of sodium hydroxide (12.5 mL, 0.031 mol) and the mixture was stirred for 5 minutes. The organic phase was separated, dissolved in acetonitrile (12.5 mL), and dried over $MgSO_4$ for 1 hour. The resulting filtrate was poured into a mixture of potassium carbonate (13.0 g, 0.13 mol) in acetonitrile (12.5 mL), and an acetonitrile solution (7.5 mL) of benzyl bromide (2.41 mL, 0.02 mol) was added. The mixture was stirred at room temperature for 12 hours, filtered to remove the undissolved inorganic solids, and the solvent was removed *in vacuo* to yield a yellow oil. A mixture of triethylamine (2.26 mL) in 40-60 petroleum ether (12.5 mL) was added to the oil, generating a white precipitate. The mixture was stirred at room temperature for 1 hour,

filtered to remove the triethylamine salt, and the solvent was removed *in vacuo* to yield a yellow oil. DCM (5 mL) was added to dissolve the oil followed by petroleum ether dropwise (approximately 4 mL), until the solution became cloudy. The mixture was cooled in the fridge for 12 hours, filtered to remove the precipitate, and concentrated *in vacuo* to yield compound **6.4** as a colourless oil (3.2 g, 49 %).

^{1}H NMR (300 MHz, $CDCl_3$, 300 K): δ = 7.25-7.38 (m, 5H, **1**), 3.74 (s, 2H, **2**), 3.50 (t, $^{3}J_{HH}$= 7 Hz, 4H, **3**), 2.93 (t, $^{3}J_{HH}$= 7 Hz, 4H, **4**).

^{13}C{^{1}H} NMR (75 MHz, $CDCl_3$, 300 K): δ = 138.93 (*ipso*-C_6H_5), 129.14 (CH), 128.88 (CH), 128.67 (CH), 128.52 (CH), 127.47 (CH), 58.90 (CH_2), 56.48 (CH_2), 42.09 (CH_2).

ESI+MS *m/z* 232.0 $[M+H]^+$

EI+HRMS calcd. for $C_{11}H_{16}NCl_2$ $[M+H]^+$: 232.0654. Found: 232.0662.

8.7.5 Bis[2-imidazolium(3-tert-butylacetate)ethyl]amino benzyl Cl (6.5 Cl)

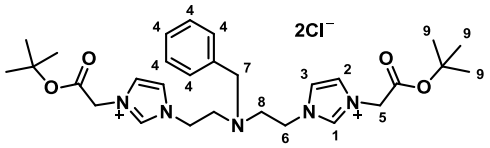

Bis(2-dichloroethyl) amino benzyl (**6.4**) (1 mL, 2.80 g, 12.1 mmol) and 1-*tert*-butylacetate imidazole (**4.1**) (4.43 g, 24.2 mmol) were added to a Schlenk flask. Anhydrous 1,4-dioxane (14 mL) was added and the mixture was heated at reflux (105 °C) for 12 hours. The solution was cooled to room temperature and the solvent was removed *in vacuo* to yield a yellow oil. The product was extracted into H_2O (10 mL), and the H_2O layer was washed with DCM (4 × 5 mL), followed by petroleum ether (2 × 5 mL). The H_2O was removed *in vacuo* to yield a pale yellow oil that, when washed with diethyl ether (2 × 5 mL) and dried *in vacuo*, solidified as an off-white hygroscopic solid (Yield: 1.12 g, 16 %).

^{1}H NMR (500 MHz, MeOD-d_4, 300 K): δ = 9.10 (s, 2H, **1**), 7.61 (s, 2H, **2** / **3**), 7.59 (s, 2H, **2** / **3**), 7.29-7.15 (m, 5H, **4**), 5.16 (s, 4H, **5**), 4.40 (t, 4H, $^{3}J_{HH}$ = 6 Hz, **6**), 3.74 (s, 2H, **7**), 3.07 (t, 4H, $^{3}J_{HH}$ = 6 Hz, **8**), 1.54 (s, 18H, **9**).

^{13}C{^{1}H} NMR (75 MHz, D_2O, 300 K): δ =167.19 (quaternary, COO^{t}Bu), 139.34 (*ipso*-C_6H_5), 138.79 (CH), 130.52 (CH), 129.74 (CH), 129.65 (CH), 128.65 (CH), 128.03 (CH), 125.10 (CH), 123.57 (CH), 85.26 (quaternary, ^{t}Bu), 59.48 (CH_2), 54.61 (CH_2), 51.60 (CH_2), 49.16 (CH_2), 28.35 (CH_3).

ESI+MS *m/z* 560.3 $[M-Cl]^+$

EI+HRMS calcd. for $C_{29}H_{43}Cl_1N_5O_4$ $[M-Cl]^+$: 560.2998. Found: 560.3022.

8.7.6 Bis[2-imidazolium(3-tert-butylacetate)ethyl]amino benzyl PF_6 (6.5 PF_6)

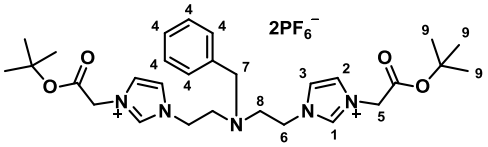

Bis[2-imidazolium(3-*tert*-butylacetate)ethyl] amino benzyl Cl (**6.5 Cl**) (0.80 g, 1.43 mmol) was dissolved the minimum amount of H_2O and a H_2O solution (5 mL) of NH_4PF_6 (2.19 g, 13.4 mmol) was added dropwise with stirring. A white precipitate formed immediately. The mixture was stirred at room temperature for 30 minutes, and filtered to isolate the solid. The solid was washed with H_2O (3 × 10 mL) followed by diethyl ether (3 × 10 mL) and dried *in vacuo.* Compound **6.5 PF_6** was collected as a colourless crystalline solid (Yield: 0.9 g, 82 %).

^{1}H NMR (500 MHz, MeOD-d_4, 300 K): δ = 8.68 (s, 2H, **1**), 7.48 (s, 2H, **2**), 7.41 (s, 2H, **3**), 7.26-7.17 (m, 5H, **4**), 5.01(s, 4H, **5**), 4.25 (br, 4H, **6**), 3.72 (s, 2H, **7**), 3.02 (br, 4H, **8**), 1.52 (s, 18H, **9**).

^{13}C{^{1}H} NMR (125 MHz, MeOD-d_4, 300 K): δ = 165.77 (quaternary, COO^tBu), 138.43 (*ipso*-C_6H_5), 137.09 (CH), 129.05 (CH), 128.85 (CH), 128.65 (CH), 128.22 (CH), 127.11 (CH), 123.53 (CH), 122.08 (CH), 83.11 (quaternary, ^{t}Bu), 57.04 (CH_2), 52.30 (CH_2), 49.94 (CH_2), 46.93 (CH_2), 27.37 (CH_3).

ESI+MS *m/z* 670.3 $[M\text{-}PF_6]^+$

EI+HRMS calcd. for $C_{29}H_{43}F_6N_5O_4P_1$ $[M\text{-}PF_6]^+$: 670.2951. Found: 670.2952.

Anal.calcd. for $C_{29}H_{43}F_{12}N_5O_4P_2$: C, 42.71 %; H, 5.31 %; N, 8.59 %. Found: C, 42.50 %; H, 5.25 %; N, 8.45 %.

8.7.7 Bis[2-imidazolium(3-tert-butylacetate)ethyl]amine Cl (6.6 Cl)

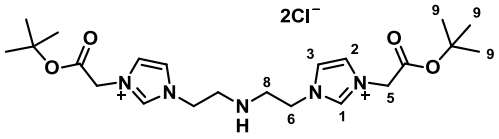

Bis[2-imidazolium(3-*tert*-butylacetate)ethyl] amino benzyl Cl (**6.5 Cl**) (0.2 g, 0.33 mmol) was added to a small ampoule and the reagent degassed. A small spatula of Pd / C was added followed by anhydrous ethanol (3 mL). The ampoule was freeze-pump-thaw degassed and back-filled with H_2 (gas). The mixture was heated with stirring at 70 °C for 24 hours in a closed ampoule. The solution was cooled to room temperature and filtered through a plug of celite. The celite was washed with ethanol (3 × 10 mL) and the volatiles were removed from the filtrate *in vacuo* to yield a white hygroscopic solid (0.33 g, 50 %).

^{1}H NMR (300 MHz, D_2O, 300 K): δ = 8.98 (s, 2H, **1**), 7.68 (s, 2H, **2** / **3**), 7.63 (s, 2H, **2** / **3**), 5.19 (s, 4H, **5**), 4.46 (t, 4H, $^{3}J_{HH}$= 6 Hz, **6**), 3.24 (t, 4H, $^{3}J_{HH}$= 6 Hz, **8**), 1.61 (s, 18 H, **9**).

^{13}C{^{1}H} NMR (75 MHz, D_2O, 300 K): δ = 166.94 (quaternary, COO^{t}Bu), 136.00 (CH), 123.81 (CH), 122.42 (CH), 85.78 (^{t}Bu), 57.44 (CH_2), 50.61 (CH_2), 47.34 (CH_2), 27.10 (CH_3).

ESI+MS *m/z* 470.3 $[M\text{-}Cl]^+$

EI+HRMS calcd. for $C_{22}H_{37}N_5O_4Cl$ $[M\text{-}Cl]^+$: 470.2529. Found: 470.2540

8.7.8 Bis[2-imidazolium(3-tert-butylacetate)ethyl]amine PF_6 (6.6 PF_6)

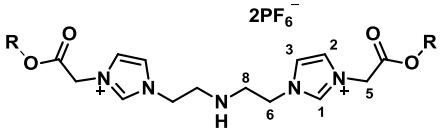

Bis[2-imidazolium(3-*tert*-butylacetate)ethyl] amino benzyl PF_6 (**6.5 PF_6**) (0.20 g, 0.33 mmol) was added to a small ampoule and the reagent degassed. A small spatula of Pd / C was added followed by anhydrous ethanol (3 mL). The ampoule was freeze-pump-thaw degassed and back-filled with H_2 (g). The mixture was heated with stirring at 70 °C for 24 hours in a sealed ampoule. The solution was cooled to room temperature and filtered through a plug of celite. The celite was washed with ethanol (3 × 10 mL) and the volatiles were removed from the filtrate *in vacuo* to yield a white hygroscopic solid (0.33 g, 50 %). It appeared that some of the *tert*-butyl groups were also removed during the reaction, with only small resonances observed for the CH_3 groups in the ^{1}H NMR and ^{13}C{^{1}H} NMR spectra.

^{1}H NMR (300 MHz, DMSO-d_6, 300 K): δ = 9.10 (s, 2H, **NCHN**), 7.76 (s, 2H, **NCHC**), 7.75 (s, 2H, **NCHC**), 5.17 (s, 4H, **CH_2**), 4.36 (t, $^{3}J_{HH}$ = 5.4 Hz, 4H, **CH_2**), 3.11 (t, $^{3}J_{HH}$ = 5.4 Hz, 4H, **CH_2**), 1.52 (s, 0.55H, **CH_3**).

^{13}C{^{1}H} NMR (75 MHz, D_2O, 300 K): δ = 168.26 (quaternary), 137.33 (CH), 123.61 (CH), 122.25 (CH), 49.70 (CH_2), 48.00 (CH_2), 46.97 (CH_2), 27.59 (CH_3).

ESI+MS *m/z* 580.2 $[6.6\text{-}PF_6]^+$; 161.6 $[6.6+2^{t}Bu\text{-}2PF_6]^{2+}$

8.7.9 Bis[2-imidazolium(3-tert-butyl-acetic-acid)ethyl]amine PF_6 (6.11)

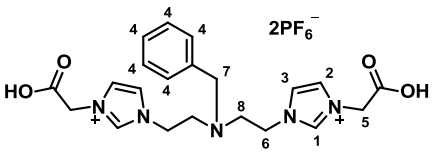

A HCl solution (37 %, 0.5 mL, 1.3 mmol) of bis[2-imidazolium(3-*tert*-butylacetate)ethyl]amine PF_6 (**6.5 PF_6**) (0.40 g, 0.49 mmol) was heated at reflux (110 °C) for one hour. The solution was allowed to cool to room temperature and the

solvent was removed *in vacuo*. The resultant solid was washed with acetone (2 × 10 mL), followed by diethyl ether (2 × 10 mL) and dried *in vacuo* to yield an off white solid (0.25 g, 72 %).

^{1}H NMR (300 MHz, DMSO-d_6, 300 K): δ = 9.31 (s, 2H, **1**), 7.77 (s, 2H, **2** / **3**), 7.71 (s, 2H, **2** / **3**), 7.51-7.20 (m, 5H, **4**), 5.19 (s, 4H, **5**), 4.49 (br, 4H, **6**), 3.87 (br, 2H, **7**), 3.10 (br, 4H, **8**).

^{13}C{^{1}H} NMR (75 MHz, DMSO-d_6, 300 K): δ = 168.08 (quaternary, COOH), 137.34 (*ipso*-C_6H_5), 137.29 (CH), 129.31 (CH), 128.27 (CH), 123.64 (CH), 122.11 (CH), 57.01 (CH_2), 52.20 (CH_2), 51.99 (CH_2), 49.74 (CH_2).

ESI+MS *m/z* 434.2 $[M\text{-}2X\text{-}2H^{+}+Na]^{+}$

EI+HRMS calcd. for $C_{21}H_{25}N_5O_4Na$ $[M\text{-}2X\text{-}2H^{+}+Na]^{+}$: 434.1799. Found: 434.1796.

8.7.10 Copper(I)-N-heterocyclic carbene complex using ligand 6.5 PF (6.16)

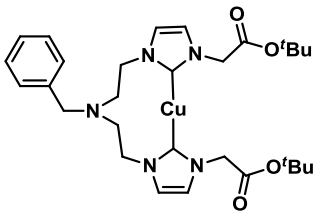

Bis[2-imidazolium(3-*tert*-butylacetate)ethyl]amine PF_6 (**6.5 PF_6**) (0.20 g, 0.24 mmol) was added to a three-necked round-bottomed flask. Anhydrous MeCN (15 mL) was added and the copper electrodes (1 × 3 mL) were inserted into the reaction mixture. The potential was adjusted so that a current of 50 mA was maintained. The mixture was electrolysed for 25 minutes (2 Q) under an argon atmosphere, filtered, and the solvent removed *in vacuo*. The product was purified by precipitation from DCM / diethyl ether to yield a pale yellow solid (0.17 g, 96 %).

^{1}H NMR (300 MHz, MeCN-d_3, 300 K): δ = 7.35-7.04 (m, 5H, **C_5H_5**), 7.02 (br, 1H, **NCHN**), 6.67 (br, 1H, **NCHN**), 5.32 (s, 1H, **CH_2**), 4.78 (s, 2H, **CH_2**), 4.72 (s, 1H, **CH_2**), 4.19 (m, 4H, **NCH_2CH_2N**), 3.69 (s, 2H, **CH_2**), 2.99 (m, 4H, **NCH_2CH_2N**), 1.45 (s, 10H, **CH_3**), 1.40 (s, 8H, **CH_3**).

^{13}C{^{1}H} NMR (125 MHz, MeCN-d_3, 125 K): δ = 181.05 (quaternary, Cu-C), 168.48 (quaternary, COO^{t}Bu), 138.40 (quaternary), 137.46 (quaternary), 130.88 (CH), 129.96 (CH), 129.34 (CH), 128.78 (CH), 128.64 (CH), 123.46 (CH), 122.77 (CH), 121.98 (CH), 121.98 (CH), 83.55 (^{t}Bu), 58.21 (CH_2), 56.04 (CH_2), 55.90 (CH_2), 53.43 (CH_2), 53.40 (CH_2), 47.79 (CH_2), 28.72 (CH_3), 28.17 (CH_3).

ESI+MS *m/z* 586.2 $[M\text{-}PF_6]^{+}$

EI+HRMS calcd. for $C_{29}H_{41}CuN_5O_4$ $[M\text{-}PF_6]^{+}$: 586.2449. Found: 586.2449.

8.7.11 Palladium-N-heterocyclic carbene complex(es) using ligand 6.5 (6.17)

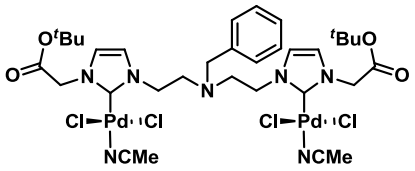

Compound **6.5 PF_6** (0.20 g, 0.24 mmol) was added to a three-necked round-bottomed flask. Anhydrous MeCN (15 mL) was added and the copper electrodes (1 × 3 mL) were inserted into the reaction mixture. The potential was adjusted so that a current of 50 mA was maintained. The mixture was electrolysed for 25 minutes (2 Q) under an argon atmosphere and then the electrodes were removed from the reaction mixture. $PdCl_2(MeCN)_2$ (0.125 g, 0.48 mmol) was added to the reaction flask and the mixture was stirred at room temperature for 48 hours. The solution was filtered and the solvent was removed *in vacuo* to yield a yellow solid. The product was purified by dissolving in DCM and filtering through celite (Yield: 0.12 g).

^{1}H NMR and ^{13}C{^{1}H} NMR were too broad and complicated to be assigned (see results and discussion section for more details).

ESI+MS *m/z* 842.0 $[M\text{-}2MeCN\text{-}Cl]^+$; 983.9 $[M+Na]^+$

EI+HRMS calcd. for $C_{29}H_{41}Cl_3N_5O_4Pd_2$ $[M\text{-}2MeCN\text{-}Cl]^+$: 840.0289. Found: 842.0306.

8.8 Experimental for Chapter 7

8.8.1 Bis(chloromethyl)amino benzoyl (7.3)[21]

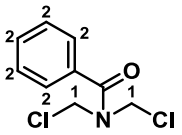

Benzoylchloride (7.05 g, 50 mmol) and hexamethylenetetramine (1.15 g, 8.3 mmol) were dissolved in xylol (50 mL) and the mixture was heated at reflux (135 °C) for 18 hours. The mixture was concentrated *in vacuo* to yield a yellow oil. Distillation of the oil (96 °C / 10^{-2} torr) was attempted to isolate the pure product, however the boiling point of the product was too high and the mixture decomposed before it could be collected.^{1}H NMR data confirmed the product was present in the sample mixture and was consistent with that of the literature.[21]

^{1}H NMR (300 MHz, $CDCl_3$, 300 K): δ = 7.53 (m, 5H, **2**), 5.40 (s, 4H, **1**).

8.8.2 Bis(chloromethyl)amino acetyl (7.4)[21]

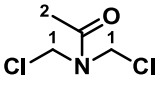

Acetyl chloride (3 mL, 3.90 g, 50 mmol) and hexamethylenetetramine (1.15 g, 8 mmol) were added to a Schlenk flask. The reaction vessel was sealed and the mixture was heated at 120 °C for 5 hours. Distillation of the resultant oil (80 °C / 10^{-1}) yielded bis(chloromethyl)amino acetyl as a colourless oil.

^{1}H NMR (500 MHz, $CDCl_3$, 300 K): δ = 5.46 (s, 4H, **1**), 2.32 (s, 3H, **2**).

^{13}C{^{1}H} NMR (125 MHz, $CDCl_3$, 300 K): δ = 168.97 (quaternary, COMe), 58.4 (CH_2), 54.3 (CH_2), 20.67 (CH_3).

8.8.3 1-Methanol imidazole[22]

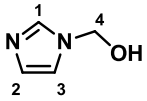

Imidazole (3.00 g, 44 mmol) and paraformaldehyde (1.46 g, 49 mmol) were added to a Schlenk flask followed by three drops of triethylamine. The flask was sealed and the solids were heated at 80 °C for 1 hour with gentle stirring, during which time the solids melted. The mixture was cooled to room temperature to yield a white solid. The product was purified by recrystallisation from DCM / hexane (Yield: 2.45 g, 57 %).

^{1}H NMR (300 MHz, $CDCl_3$, 300 K): δ = 7.37 (s, 1H, **1**), 7.01 (s, 1H, **2** / **3**), 6.89 (s, 1H, **2** / **3**), 5.34 (s, 2H, **4**), OH resonances not observed.

^{13}C{^{1}H} NMR (75 MHz, $CDCl_3$, 300 K): δ = 136.18 (CH), 128.40 (CH), 118.64 (CH), 70.07 (CH_2), OH resonance not observed.

ESI+MS *m/z* 91.02 $[M+H]^+$; 121.03 $[M+Na]^+$

EI+HRMS calcd. for $C_4H_6N_2NaO$ $[M+Na]^+$: 121.0372. Found: 121.0386.

8.8.4 1-Chloromethylimidazole (7.9)[22]

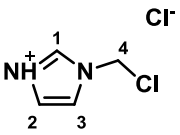

1-Methanolimidazole (1.00 g, 0.01 mol) was dissolved in anhydrous chloroform (25 mL) in a Schlenk flask. Thionyl chloride (1.4 mL, 0.19 mol) was added and the mixture was stirred at room temperature for 12 hours. The solvent was removed *in vacuo* and the solid was dried *in vacuo* for two hours. The product was purified by recrystallisation from ethanol / diethyl ether (Yield: 0.625 g, 53 %).

^{1}H NMR (300 MHz, D_2O, 300 K): δ = 9.08 (s, 1H, **1**), 7.75 (s, 1H, **2** / **3**), 7.65 (s, 1H, **2** / **3**), 6.07 (s, 2H, **4**).

^{13}C{^{1}H} NMR (75 MHz, D_2O, 300 K): δ = 135.98 (CH), 121.82 (CH), 120.56 (CH), 54.18 (CH_2).

ESI+MS *m/z* 117.02 $[M]^+$

EI+HRMS calcd. for $C_4H_6N_2Cl$ $[M]^+$: 117.0220. Found: 117.0230.

8.8.5 Synthesis of compound 7.10

DO3AtBu (0.16 g, 0.31 mmol) was added to a Schlenk flask and the reagent degassed. 1-Chloromethylimidazole (**7.9**) (0.036 g, 0.31 mmol) and Cs_2CO_3 (0.33 g, 3.22 mmol) were added, followed by anhydrous acetonitrile (10 mL). The mixture was heated at 85 °C for 12 hours. The solution was cooled to room temperature and filtered to remove the inorganic salts. The filtrate was concentrated *in vacuo* to yield a yellow oil, which was assigned by ^{1}H NMR spectroscopy and mass spectrometry to be a mixture of compounds (Figure 8.2).

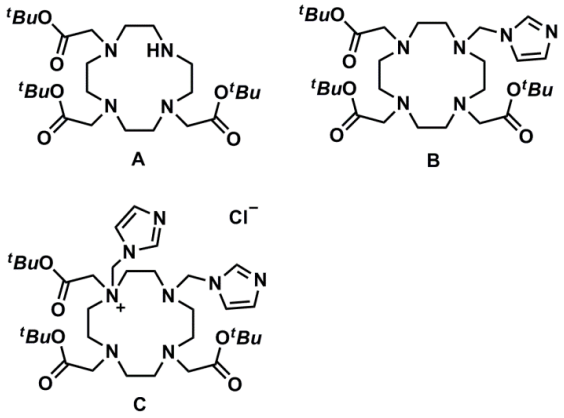

Figure 8.2 Compounds identified in the reaction between DO3AtBu and compound **7.10**.

^{1}H NMR (500 MHz, $CDCl_3$, 300 K): δ = 7.53 (s, 1H, **NCHN**), 6.95 (s, 2H, **NCHCHN**), 3.23 (s, 4H, **CH_2**), 3.22 (s, 8H, **CH_2**), 2.71 (m, 9H, **CH_2**), 2.64 (m, 20H, **CH_2**), 2.46 (m, 9H, **CH_2**), 1.35 (s, 80H, **CH_3**).

^{13}C{^{1}H} NMR (125 MHz, $CDCl_3$, 300 K): δ = 169.50 (quaternary, COO^{t}Bu), 169.40 (quaternary, COO^{t}Bu), 134.91 (CH), 133.52 (CH), 129.03 (CH), 116.42 (CH), 78.96 (quaternary, ^{t}Bu), 78.92 (quaternary, ^{t}Bu), 55.37 (CH_2), 50.62 (CH_2), 48.80 (CH_2), 45.6 (CH_2), 26.41 (CH_3), 26.29 (CH_3).

ESI+MS *m/z* 515.37 $[A+H]^+$, 617.39 $[B+Na]^+$, 697.42 $[C-H-Cl+Na]^+$

8.8.6 1-Propanol-3-tert-butylaceate imidazolium chloride (7.13)

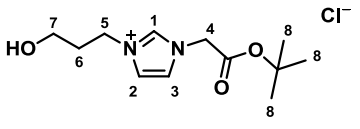

1-(3-Hydroxypropyl)-1H-imidazole (1.00 g, 7.9 mmol) and *tert*-butyl chloroacetate (1.25 mL, 8.7 mmol) were added to a Schlenk flask. The reagents were stirred for 12 hours at room temperature. The resultant oil was washed with diethyl ether (2 × 5 mL) and dried *in vacuo*. The product was isolated as a white solid (Yield: 1.94 g, 88 %).

^{1}H NMR (300 MHz, DMSO-d_6, 300 K): δ = 9.21 (s, 1H, **1**), 7.82 (s, 1H, **2** / **3**), 7.74 (s, 1H, **2** / **3**), 5.14 (s, 2H, **4**), 4.79 (br, 1H, **OH**), 4.30 (t, 2H, $^{3}J_{HH}$ = 6.5 Hz, **5**), 3.40 (q, 2H, $^{3}J_{HH}$ = 6.5 Hz, **7**), 1.94 (quintet, 2H, $^{3}J_{HH}$ = 6.5 Hz, **6**), 1.45 (s, 9H, **8**).

^{13}C{^{1}H} NMR (75 MHz, DMSO-d_6, 300 K): δ = 165.73 (quaternary, COO^{t}Bu), 137.42 (CH), 123.19 (CH), 122.17 (CH), 83.00 (quaternary, ^{t}Bu) , 56.86 (CH_2), 49.98 (CH_2), 46.38 (CH_2), 32.33 (CH_2), 27.63 (CH_3).

ESI+MS *m/z* 241.2 $[M\text{-}Cl]^+$

EI+HRMS calcd. for $C_{12}H_{21}N_2O_3$ $[M\text{-}Cl]^+$: 241.1547. Found: 241.1590.

8.8.7 1-Chloropropyl-3-tert-butylacetate imidazolium chloride (7.14)

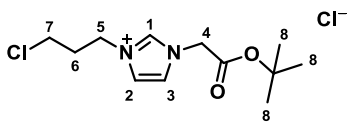

Compound **7.13** (0.6 g, 2.16 mmol) was added to a Schlenk flask and the reagent was degassed. The solid was dissolved in anhydrous chloroform (20 mL) and triethylamine (0.3 mL, 2.15 mmol) was added. $SOCl_2$ (0.19 mL, 2.15 mmol) was added dropwise and the resultant solution was stirred at room temperature for 12 hours. The solvent was removed *in vacuo* and the product was dried *in vacuo* for two hours. The product was purified by recrystallisation from DCM / diethyl ether, and was isolated with the triethylammonium chloride salt (Yield: 0.8 g).

^{1}H NMR (300 MHz, DMSO-d_6, 300 K): δ = 9.29 (s, 1H, **1**), 7.86 (s, 1H, **2** / **3**), 7.78 (s, 1H, **2** / **3**), 5.16 (s, 2H, **4**), 4.38 (t, 2H, $^{3}J_{HH}$ = 6.5 Hz, **5**), 3.65 (t, 2H, $^{3}J_{HH}$ = 6.5 Hz, **7**), 2.29 (quintet, 2H, $^{3}J_{HH}$ = 6.5 Hz, **6**), 1.45 (s, 9H, **8**).

^{13}C{^{1}H} NMR (75 MHz, DMSO-d_6, 300 K): δ = 165.69 (quaternary, COO^{t}Bu), 137.58 (CH), 122.93 (CH), 122.06 (CH), 82.96 (quaternary, ^{t}Bu), 50.0 (CH_2), 46.58 (CH_2), 45.18 (CH_2), 31.99 (CH_2), 27.60 (CH_3).

ESI+MS *m/z* 259.1 $[M\text{-}Cl]^+$

EI+HRMS calcd. for $C_{12}H_{20}ClN_2O_2$ $[M\text{-}Cl]^+$: 259.1218. Found: 259.1218

.

8.8.8 Synthesis of compound 7.15

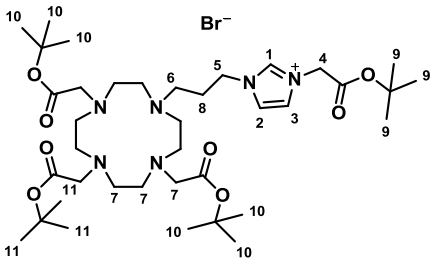

DO3AtBu (1.00 g, 1.9 mmol), NaBr (0.40 g, 3.8 mmol) and K_2CO_3 (1.22 g, 9.5 mmol) were added to a small ampoule and the reagents degassed. Anhydrous acetonitrile (20 mL) was added, followed by 1-chloropropyl-3-*tert*-butylacetate imidazolium chloride (**7.14**) (0.83 g, 2.85 mmol). The ampoule was sealed and the mixture was heated at 50 °C for 96 hours, with stirring. The mixture was cooled to room temperature and filtered to remove the inorganic salts. The filtrate was concentrated *in vacuo* to yield a yellow oil, which solidified on washing with diethyl ether (20 mL). The product was purified by HPLC (methanol / water + 0.1 % formic acid), and was isolated as a pale yellow solid (Yield: 0.55 g, 48 %).

^{1}H NMR (300 MHz, $CDCl_3$, 300 K): δ = 10.04 (s, 1H, **1**), 8.34 (s, 1H, **2** / **3**), 7.35 (s, 1H, **2** / **3**), 5.02 (s, 2H, **4**), 4.64 (br t, 2H, **5**), 3.70 (br, 2H, **6**), 3.64-2.76 (m, 22H, **7**), 2.68 (br, 2H, **8**), 1.47 (s, 9H, **9** / **11**), 1.45 (s, 9H, **9** / **11**), 1.43 (s, 18H, **10**).

^{13}C{^{1}H} NMR (75 MHz, $CDCl_3$, 300 K): δ = 170.47 (quaternary, COO^{t}Bu), 164.52 (quaternary, COO^{t}Bu), 163.27 (quaternary, COO^{t}Bu), 137.77 (CH), 123.75 (CH), 122.86 (CH), 84.85 (quaternary, ^{t}Bu), 82.13 (quaternary, ^{t}Bu), 56.06 (CH_2), 55.5 (CH_2), 53.0 (CH_2), 51.8 (CH_2), 50.72 (CH_2), 49.87 (CH_2), 48.71 (CH_2), 47.00 (CH_2), 28.15 (CH_3), 27.98 (CH_3).

ESI+MS *m/z* 841.4 $[M+Na]^+$, 737.5 $[M-Br]^+$, 369.3 $[M-Br+H]^{2+}$

EI+HRMS calcd. for $C_{38}H_{69}N_6O_8$ $[M-Br]^+$: 737.5171. Found: 737.5178.

Anal.calcd. for $C_{38}H_{69}BrN_6O_8.4H_2O$: C, 51.28 %; H, 8.72 %, N, 9.44 %. Found: C, 51.40 %; H, 8.20 %; N, 9.35 %.

8.8.9 Synthesis of compound 7.16

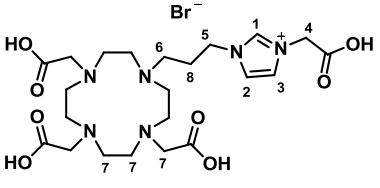

Compound **7.15** (0.208 g, 0.25 mmol) was dissolved in TFA (2 mL) and the mixture was stirred at room temperature for 12 hours. The TFA was removed *in vacuo* to yield a yellow oil, which when triturated with diethyl ether became a yellow solid. The product was not purified at this stage and was used as isolated, with the yield assumed as 100 %.

^{1}H NMR (300 MHz, D_2O, 300 K): δ = 8.90 (s, 1H, **1**), 7.56 (s, 1H, **2** / **3**), 7.51 (s, 1H, **2** / **3**), 5.10 (s, 2H, **4**), 4.33 (br t, 2H, **5**), 3.63-2.84 (m, 24H, **6**, **7**), 2.37 (br, 2H, **8**).

^{13}C{^{1}H} NMR (75 MHz, D_2O, 300 K): δ = 174.30 (quaternary, COOH), 169.70 (quaternary, COOH), 168.39 (quaternary, COOH), 136.95 (CH), 124.05 (CH), 122.25 (CH), 54.38 (CH_2), 52.95 (CH_2), 51.9 (CH_2), 51.53 (CH_2), 50.1 (CH_2), 49.14 (CH_2), 47.57 (CH_2), 46.56 (CH_2), 42.17 (CH_2).

ESI+MS *m/z* 513.3 $[M\text{-}Br]^+$

8.8.10 Synthesis of gadolinium complex 7.17

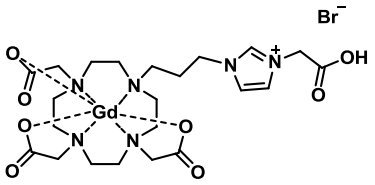

Compound **7.16** (0.13 g, 0.25 mmol) was dissolved in water (5 mL). $GdCl_3.6H_2O$ (0.09 g, 0.24 mmol) was added and the pH of the solution was adjusted to pH 6 by addition of NaOH solution (0.1 M, 1.8 mL). The solution was stirred at room temperature for 24 hours. The product was purified by HPLC (methanol / water) and isolated as a colourless oil.

ESI+MS *m/z* 668.2 $[7.19\text{-}Br]^+$, 690.1 $[7.19\text{-}Br+Na]^+$

EI+HRMS calcd. for $C_{22}H_{33}N_6GdO_8Na$ $[7.19\text{-}Br+Na]^+$: 690.1496. Found: 690.1513.

8.8.11 Relaxivity measurements using complex 7.17

T1 measurements were recorded with the assistance of Dr. Julie Fisher, School of Chemistry, University of Leeds, using a Maran Benchtop NMR analyser operating at 20 MHz, field strength of 0.5 T, at a temperature of 23.8 ± 0.5 °C. Five known concentrations of contrast agent were made up from a neat solution (50 mM) in deionised water, in standard NMR tubes (50 mM, 25 mM, 16.66 mM, 8.33 mM and 2.5 mM). Each T1 measurement was recorded three times and an average of the three results was taken.

8.8.12 Synthesis of copper complex 7.18

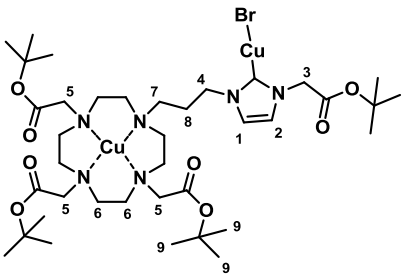

Compound **7.15** (0.20 g, 0.24 mmol) was added to a three-necked round-bottomed flask. Anhydrous MeCN (15 mL) was added and the copper electrodes (1 × 3 mL) were inserted into the reaction mixture. The potential was adjusted so that a current of 30 mA

was maintained. The mixture was electrolysed for 25 minutes (2 Q) under an argon atmosphere, and then the solvent was removed *in vacuo*. The solid was dissolved in DCM, filtered, and the solvent removed *in vacuo* to yield a green solid (Yield: 0.055 g, 59 %).

^{1}H NMR (300 MHz, MeCN-d_3, 300 K): δ = 7.21 (s, 1H, **1** / **2**), 7.13 (s, 1H, **1** / **2**), 4.84 (s, 2H, **3**), 4.20 (br t, 2H, **4**), 3.48 (s, 6H, **5**), 2.92-2.14 (br, 20H, **6**, **7, 8**), 1.45 (br s, 36 H, **9**).

^{13}C{^{1}H} NMR (75 MHz, MeCN-d_3, 300 K): δ = 177.21 (quaternary, Cu-C), 168.86 (quaternary, COO^{t}Bu), 168.80 (quaternary, COO^{t}Bu), 166.94 (quaternary, COO^{t}Bu), 122.11 (CH), 120.66 (CH), 82.05 (quaternary, ^{t}Bu), 80.77 (quaternary, ^{t}Bu), 55.30 (CH_2), 55.18 (CH_2), 51.97 (CH_2), 51.63 (CH_2), 49.90 (CH_2), 49.06 (CH_2), 48.81 (CH_2), 27.06 (CH_3), 27.03 (CH_3), 26.88 (CH_3).

ESI+MS *m/z* 1024.2 $[M\text{-}Br]^+$

EI+HRMS calcd. for $C_{38}H_{68}N_6Br_2O_8Cu_2$ $[M\text{-}Br]^+$: 1020.2052. Found: 1022.2044.

Anal.calcd. for $C_{38}H_{68}Br_3Cu_2N_6O_8$: C, 41.35 %; H, 6.21 %, N, 7.61 %. Found: C, 41.10 %; H, 6.50 %; N, 7.75 %.

8.8.13 Synthesis of gold complex (7.19 / 7.20)

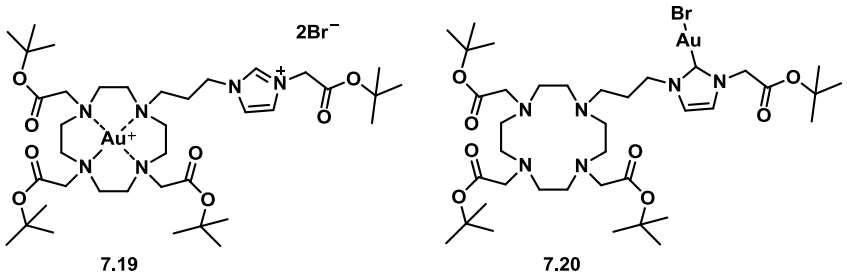

7.19 7.20

Compound **7.15** (0.20 g, 0.24 mmol) was added to a three-necked round-bottomed flask. Anhydrous MeCN (15 mL) was added and the copper cathode (1 × 3 mL) and gold anode (gold wire, 0.5 mm) were inserted into the reaction mixture. The potential was adjusted so that a current of 30 mA was maintained. The mixture was electrolysed for 116 minutes (6 Q) under an argon atmosphere. The mixture was filtered, and the solvent was removed *in vacuo* to yield a dark purple oil.

^{1}H NMR and ^{13}C{^{1}H} NMR were too broad and complicated to be assigned (see results and discussion section for more details).

ESI+MS *m/z* 1015.4 $[7.16+Au]^+$

EI+HRMS calcd. for $C_{38}H_{69}Au_1Br_1N_6O_8$ $[7.16+Au]^+$: 1015.4003. Found: 1015.4027.

8.9 References

1. F. R. Hartley, S. G. Murray and C. A. McAuliffe, *Inorg. Chem.*, 1979, **18**, 1394-1397.
2. M. A. Bennett and A. K. Smith, *J. Chem. Soc., Dalton Trans.*, 1974, 233-241.
3. G. M. Sheldrick, *Acta Crystallogr., Sect. A: Found. Crystallogr.*, 2008, **A64**, 112-122.
4. L. J. Barbour, *J. Supramol. Chem.*, 2003, **1**, 189-191.
5. d. S. P. Van and A. L. Spek, *Acta Crystallogr., Sect. A: Found. Crystallogr.*, 1990, **A46**, 194-201.
6. C. D. Gutsche, M. Iqbal and D. Stewart, *J. Org. Chem.*, 1986, **51**, 742-745.
7. C. D. Gutsche, J. A. Levine and P. K. Sujeeth, *J. Org. Chem.*, 1985, **50**, 5802-5806.
8. L.-M. Yang, Y.-S. Zheng and Z.-T. Huang, *Synth. Commun.*, 1999, **29**, 4451-4460.
9. C. E. Willans, K. M. Anderson, P. C. Junk, L. J. Barbour and J. W. Steed, *Chem. Commun.*, 2007, 3634-3636.
10. C. D. Gutsche and K. C. Nam, *J. Am. Chem. Soc.*, 1988, **110**, 6153-6162.
11. E. K. Bullough, C. A. Kilner, M. A. Little and C. E. Willans, *Org. Biomol. Chem.*, 2012, **10**, 2824-2829.
12. T. T. Wu and J. R. Speas, *J. Org. Chem.*, 1987, **52**, 2330-2332.
13. J. Ehrhart, J. M. Planeix, N. Kyritsakas-Gruber and M. W. Hosseini, *Dalton Trans.*, 2009, 2552-2557.
14. S. K. Singh, N. Manne, P. C. Ray and M. Pal, *Beilstein J. Org. Chem.*, 2008, **4**, 42.
15. B. R. M. Lake, E. K. Bullough, T. J. Williams, A. C. Whitwood, M. A. Little and C. E. Willans, *Chem. Commun.*, 2012, **48**, 4887-4889.
16. I. Dinares, d. M. C. Garcia, M. Font-Bardia, X. Solans and E. Alcalde, *Organometallics*, 2007, **26**, 5125-5128.
17. E. Brenner, D. Matt, M. Henrion, M. Teci and L. Toupet, *Dalton Trans.*, 2011, **40**, 9889-9898.
18. L. Friedman and W. P. Wetter, *J. Chem. Soc. A.*, 1967, **1**, 36-37.
19. F. P. Yi, H. Y. Sun, M. H. Pan, Y. Xu and J. Z. Li, *Chin. Chem. Lett.*, 2009, **20**, 275-278.
20. R. E. Douthwaite, J. Houghton and B. M. Kariuki, *Chem. Commun.*, 2004, 698-699.
21. H. Boehme, J. P. Denis and H. J. Drechsler, *Liebigs Annalen Der Chemie*, 1979, 1447-1455.
22. S. Julia, C. Martinezmartorell and J. Elguero, *Heterocycles*, 1986, **24**, 2233-2237.

9 Supplementary information

Contents

9.1 NMR data for the compounds reported in Chapter 2

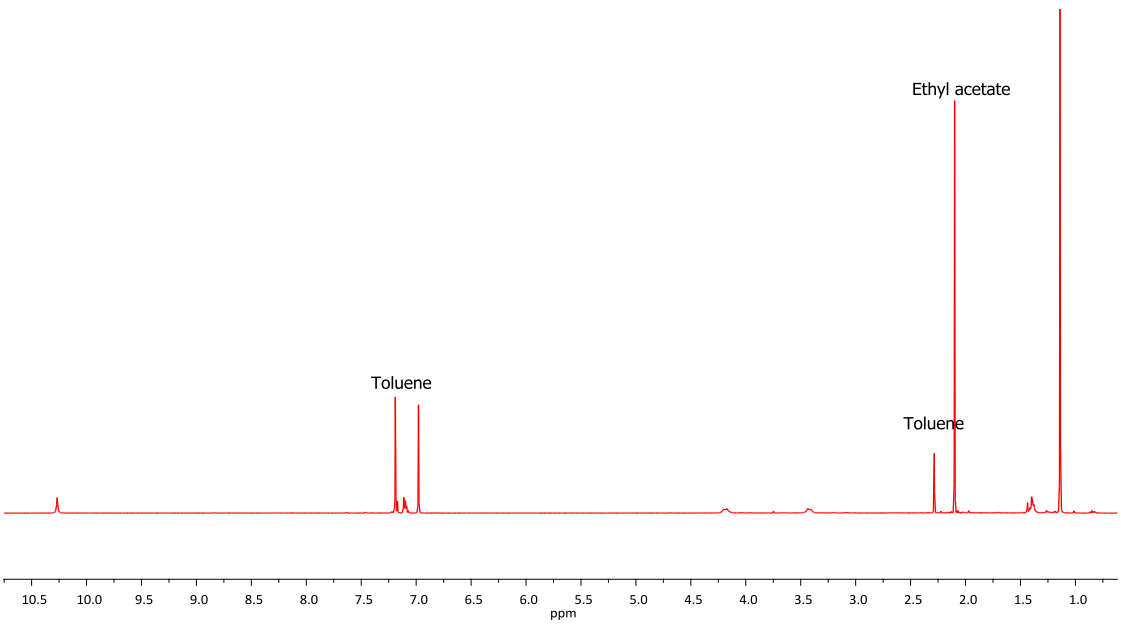

Figure 1 ^{1}H NMR spectrum ($CDCl_3$) of compound **2.1** at 298 K.

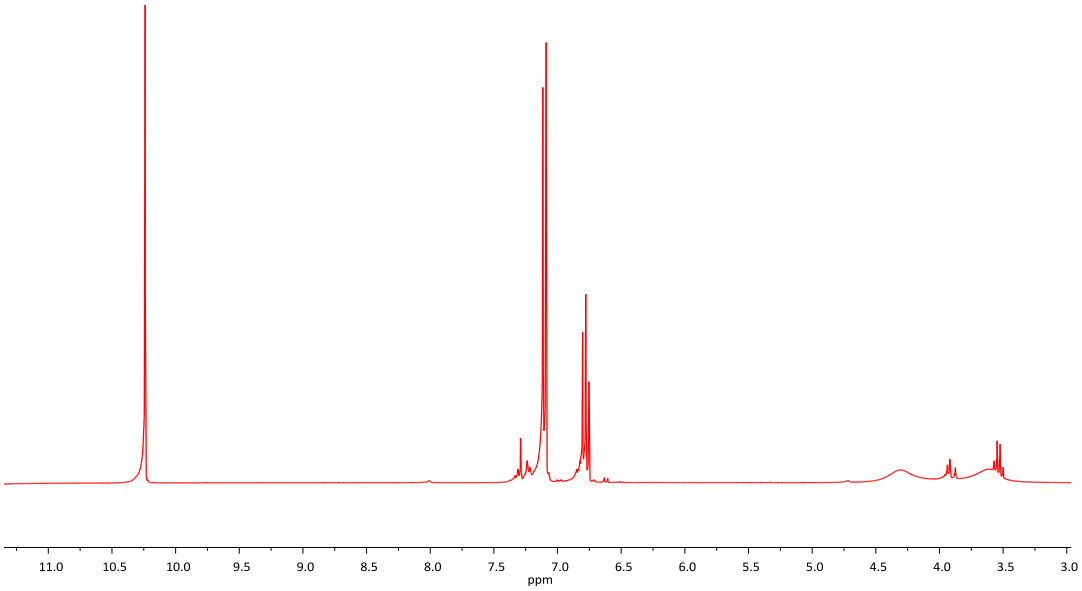

Figure 2 ^{1}H NMR spectrum ($CDCl_3$) of compound **2.2** at 298 K.

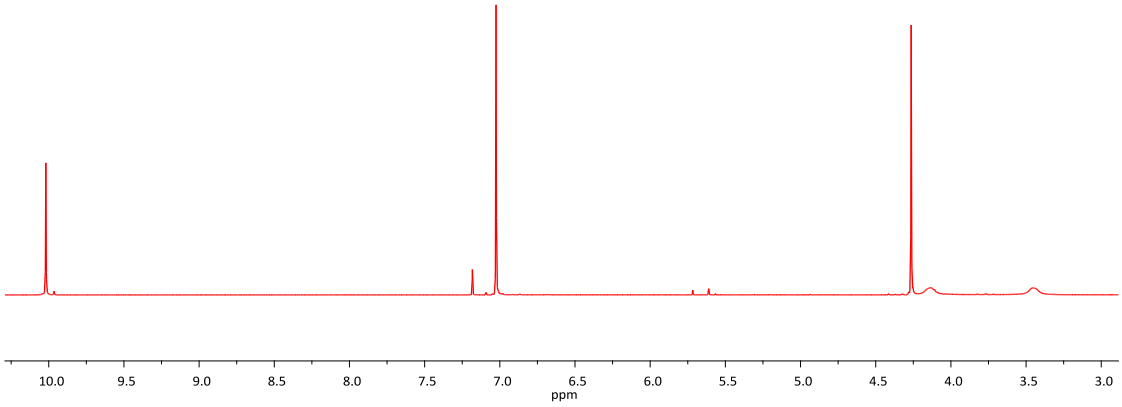

Figure 3 ^{1}H NMR spectrum ($CDCl_3$) of compound **2.3** at 298 K.

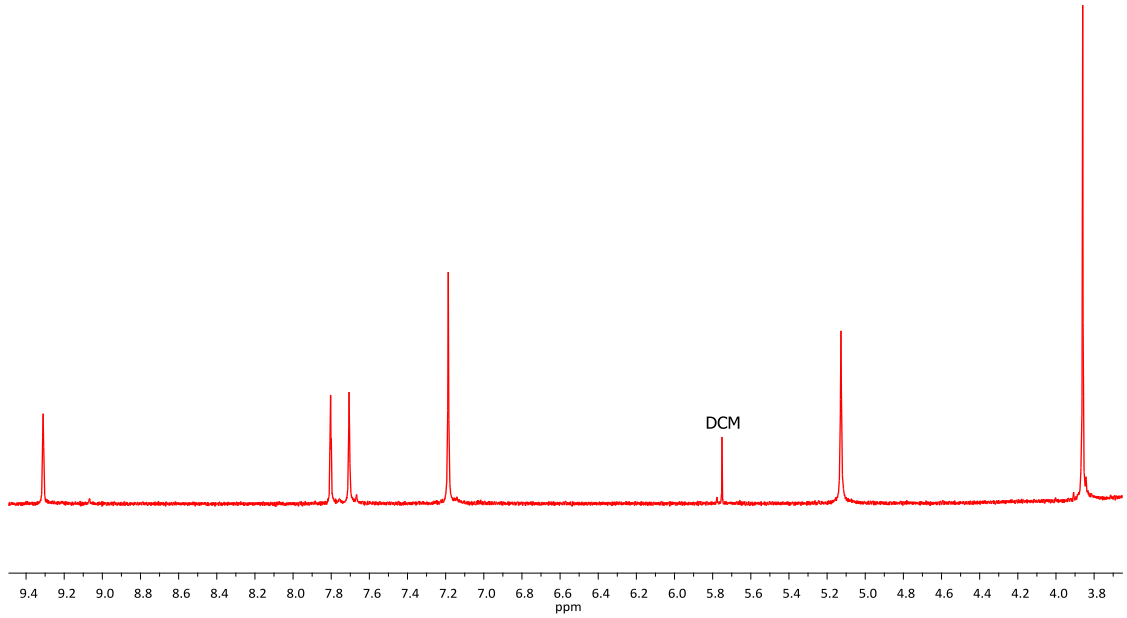

Figure 4 ^{1}H NMR spectrum (DMSO-d_6) of compound **2.5 Br** at 298 K.

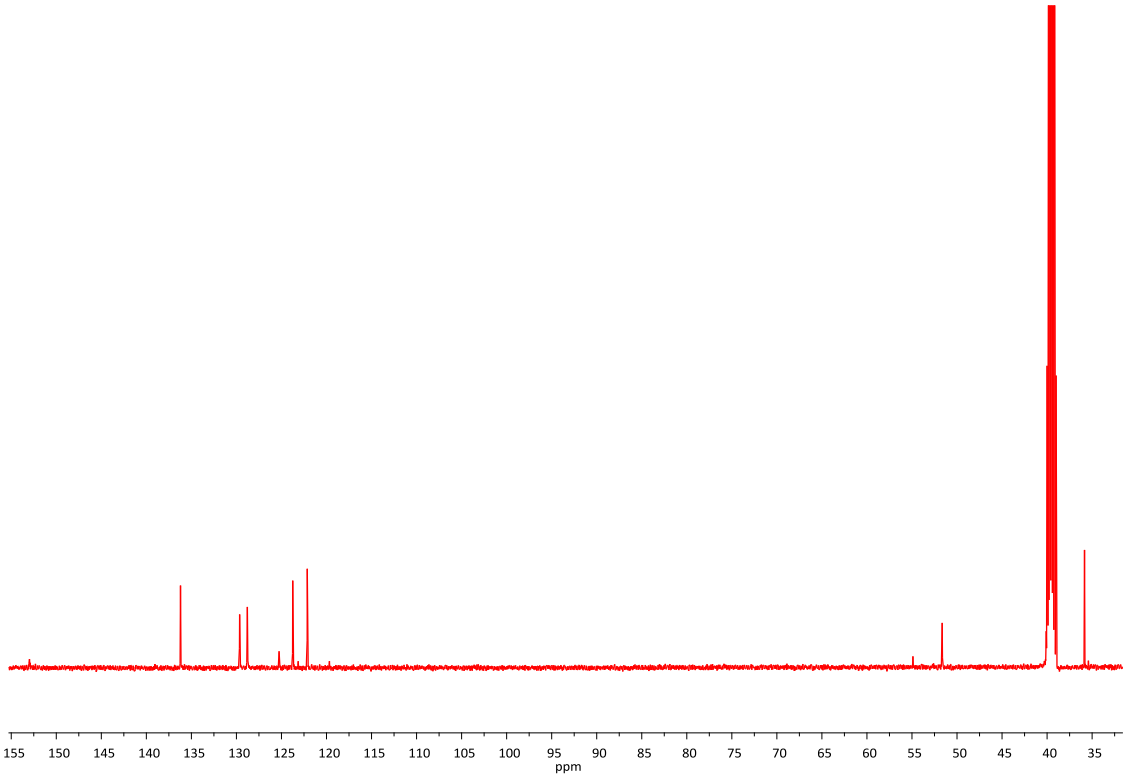

Figure 5 ^{13}C{^{1}H} NMR spectrum (DMSO-d_6) of compound **2.5 Br** at 298 K.

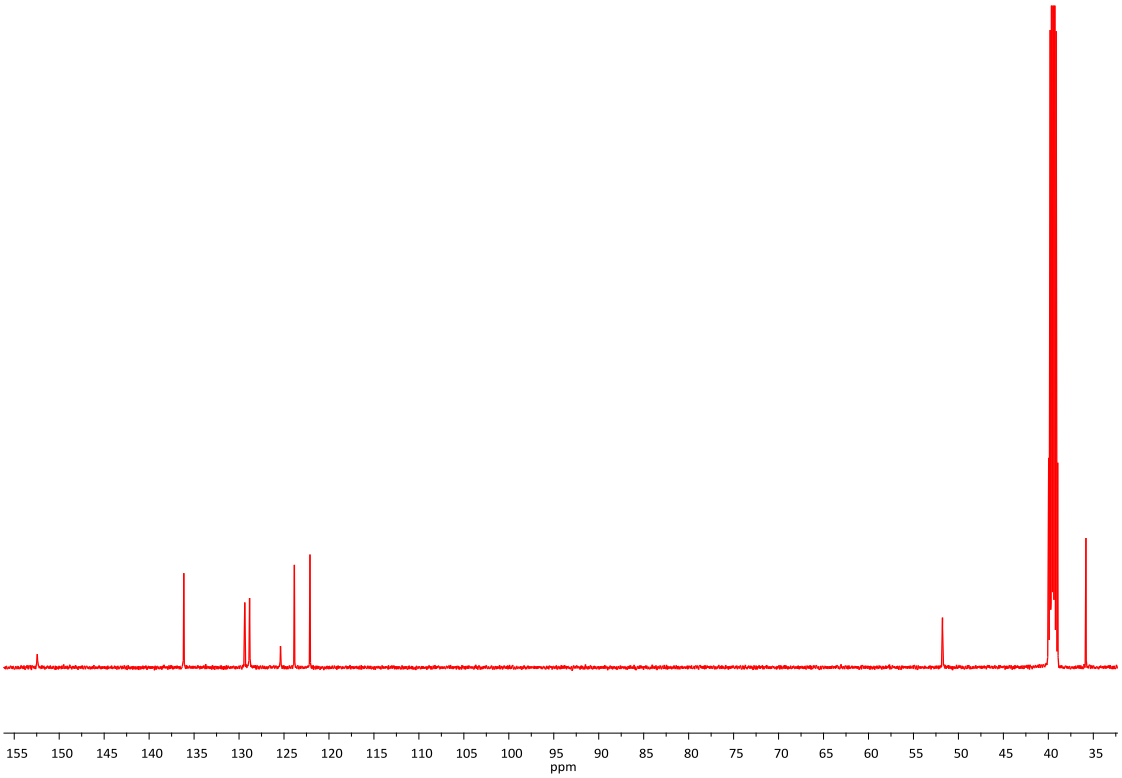

Figure 6 $^{13}C\{^{1}H\}$ NMR spectrum (DMSO-d_6) of compound **2.5 PF_6** at 298 K.

9.2 NMR data for the compounds reported in Chapter 3

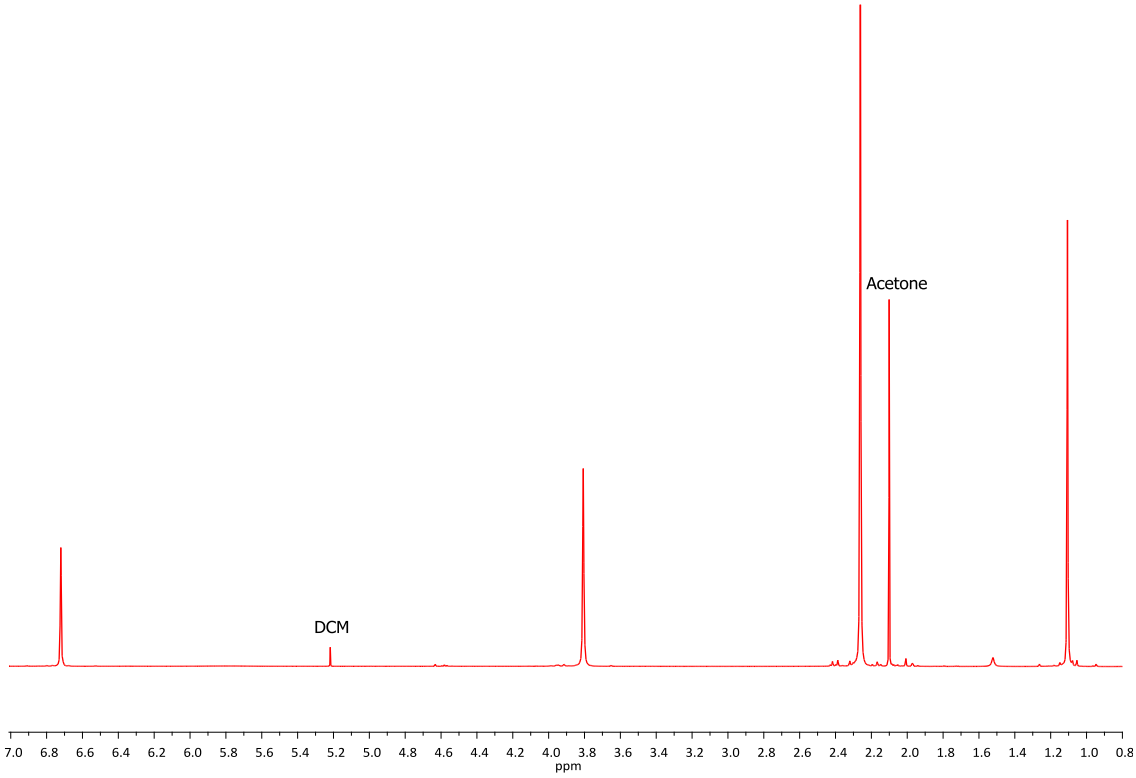

Figure 7 ^{1}H NMR spectrum (DMSO-d_6) of compound **3.1** at 298 K.

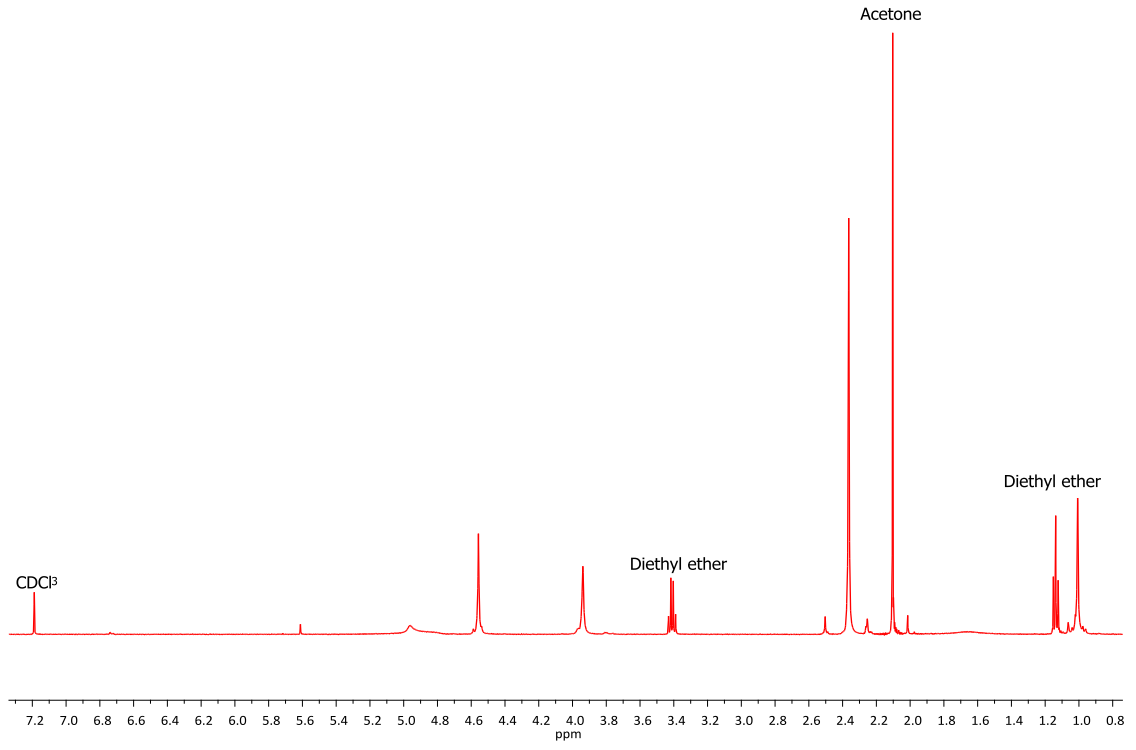

Figure 8 ^{1}H NMR spectrum ($CDCl_3$) of compound **3.2** at 298 K.

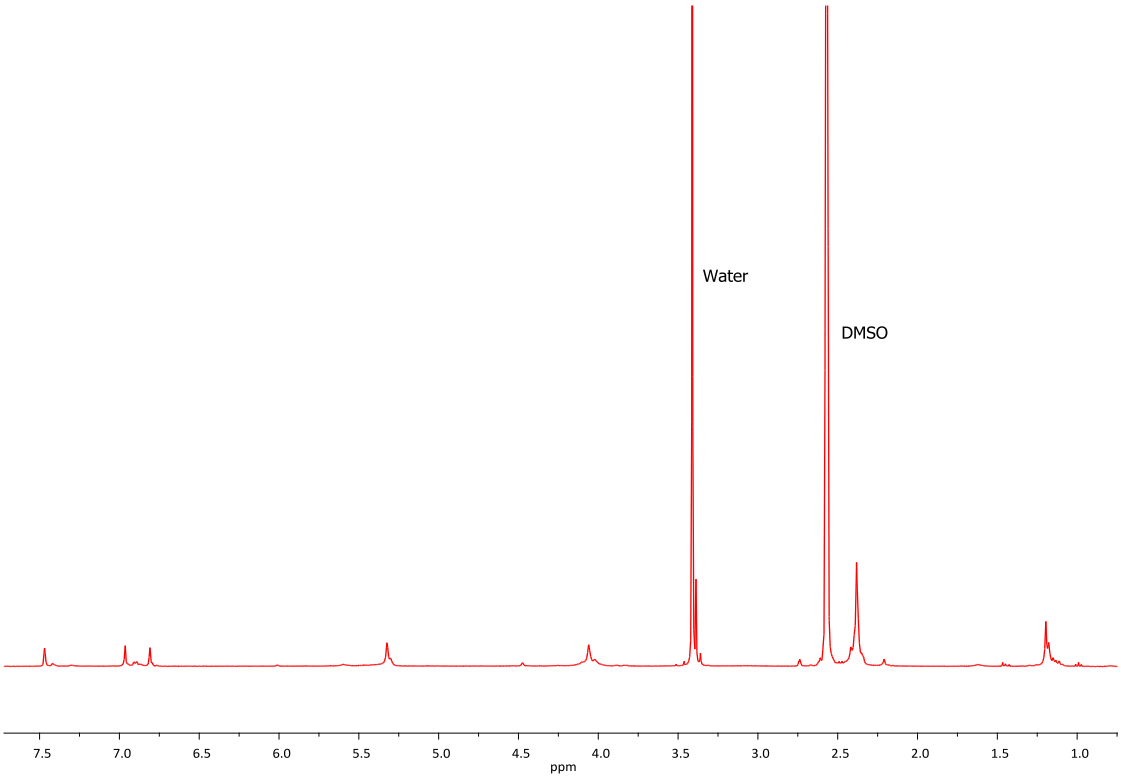

Figure 9 ^{1}H NMR spectrum (DMSO-d_6) of compound **3.3** at 298 K.

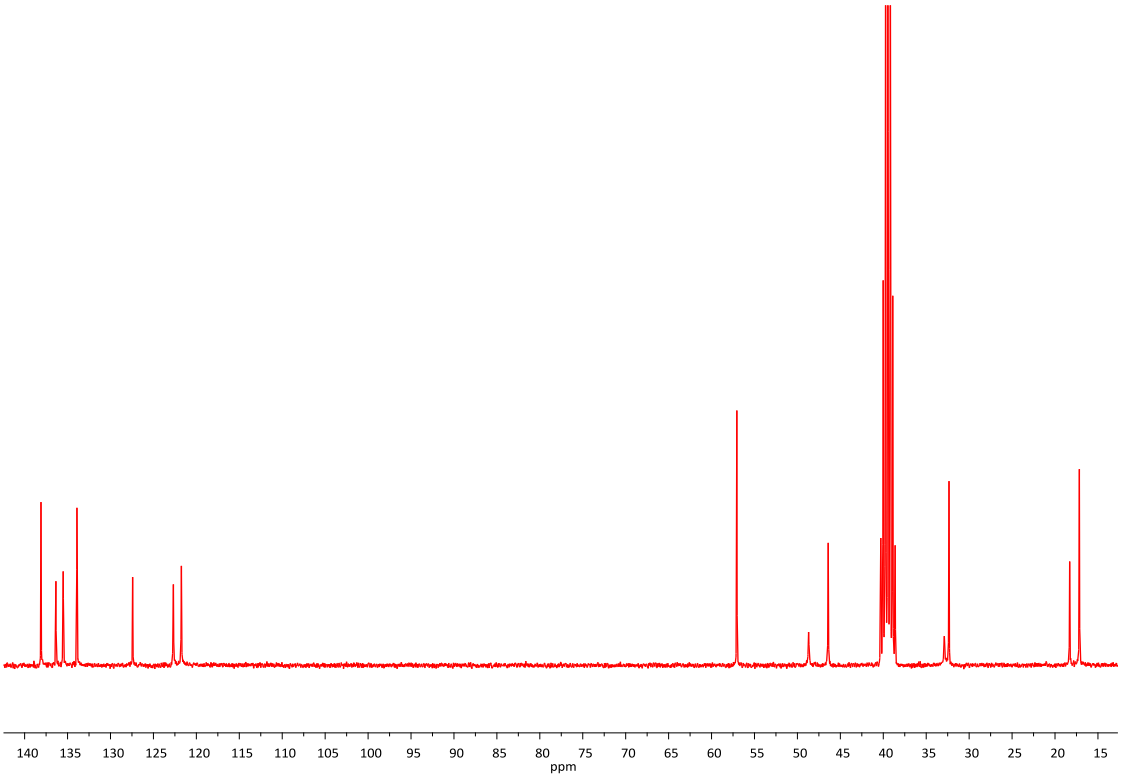

Figure 10 ^{13}C{^{1}H} NMR spectrum (DMSO-d_6) of compound **3.4 Br** at 298 K.

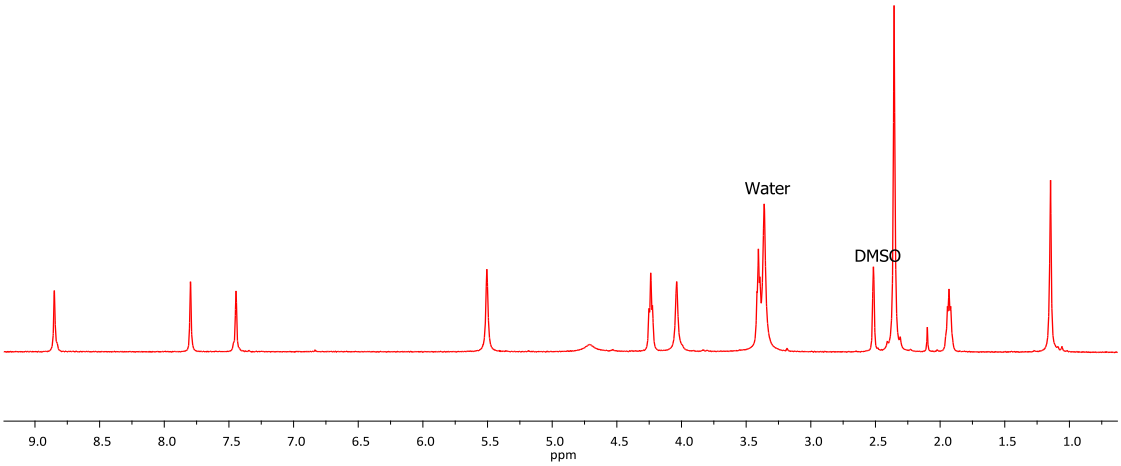

Figure 11 ^{1}H NMR spectrum (DMSO-d_6) of compound **3.4 PF_6** at 298 K.

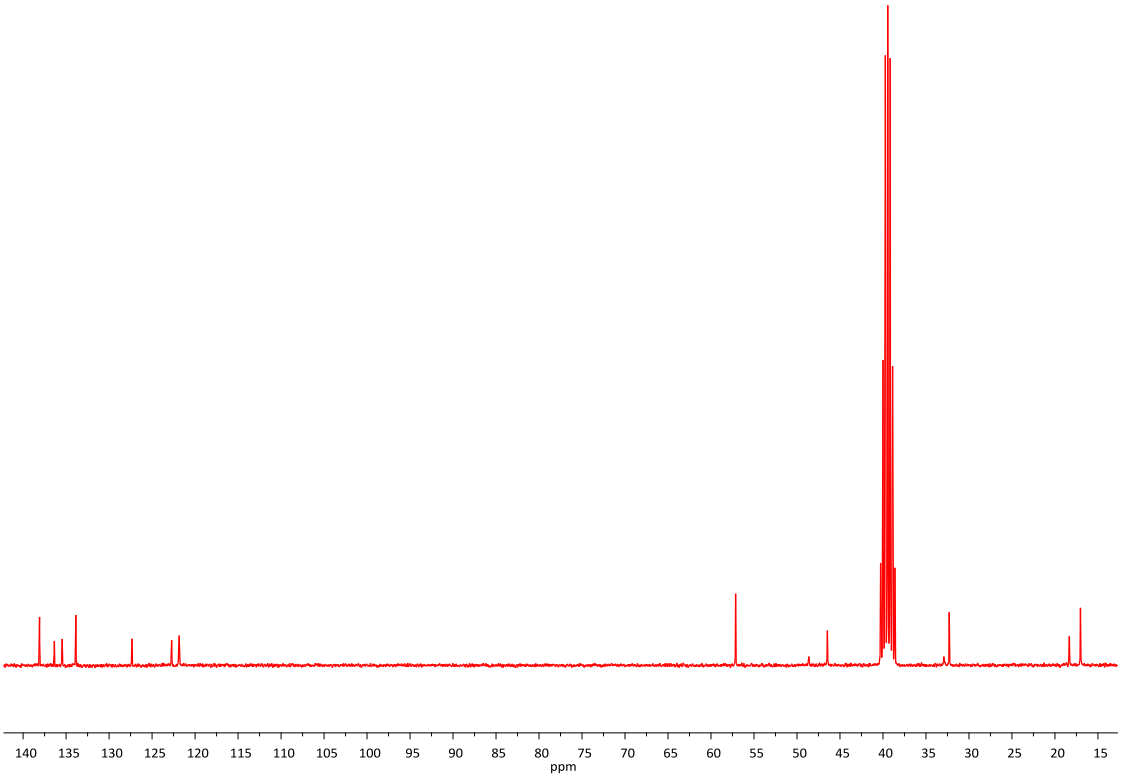

Figure 12 $^{13}C\{^{1}H\}$ NMR spectrum (DMSO-d_6) of compound **3.4 PF_6** at 298 K.

9.3 NMR data for the compounds / complexes reported in Chapter 4

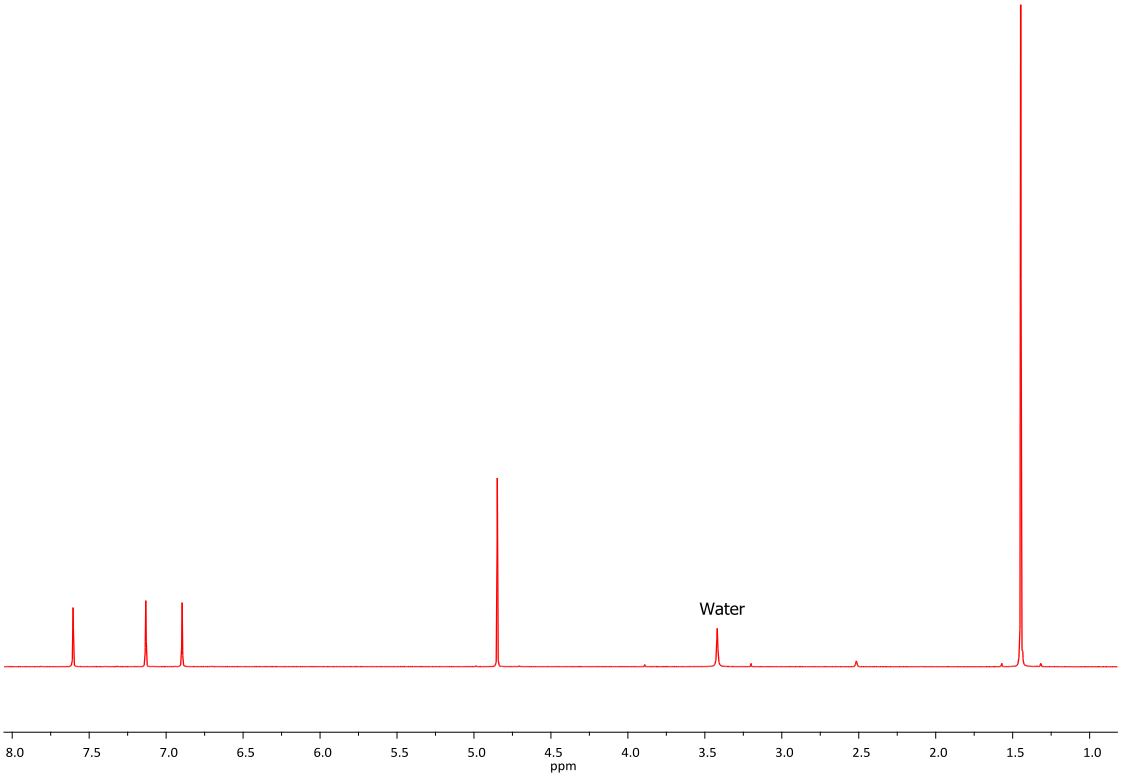

Figure 13 ^{1}H NMR spectrum (DMSO-d_6) of compound **4.1** at 298 K.

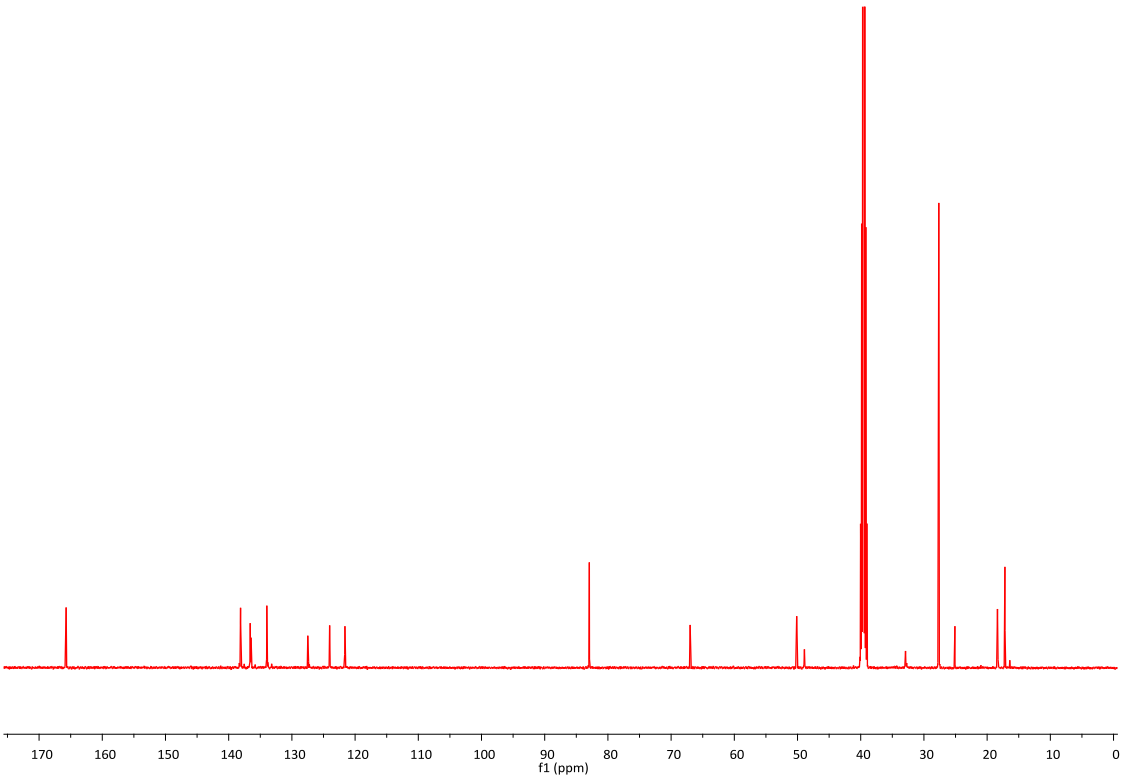

Figure 14 ^{13}C{^{1}H} NMR spectrum (DMSO-d_6) of compound **4.2 Br** at 298 K.

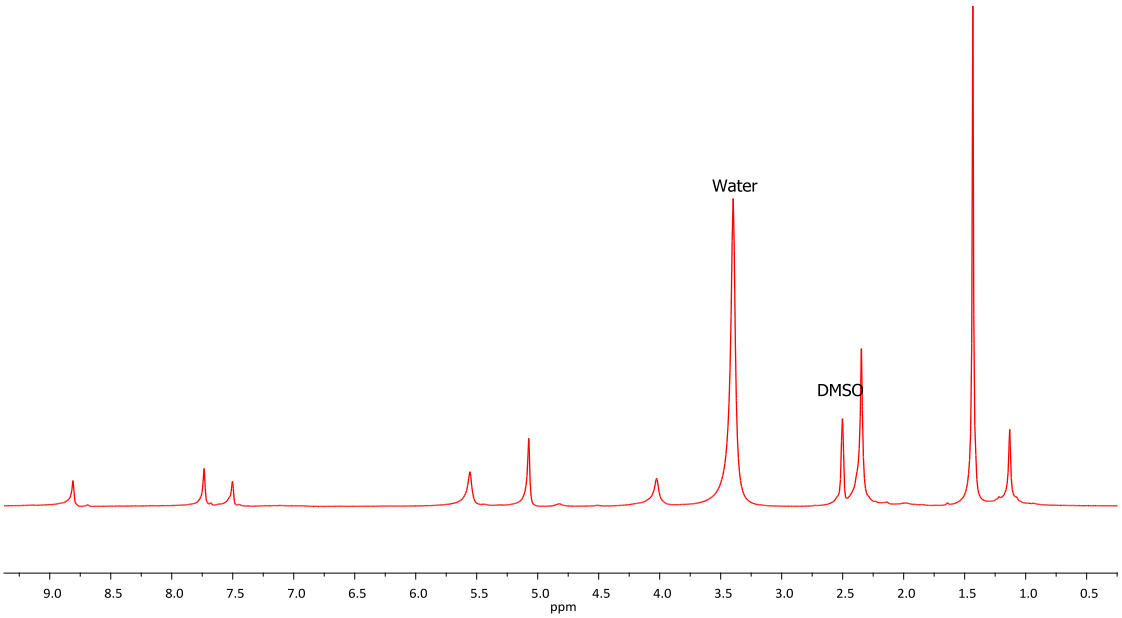

Figure 15 ^{1}H NMR spectrum (DMSO-d_6) of compound **4.2 PF_6** at 298 K.

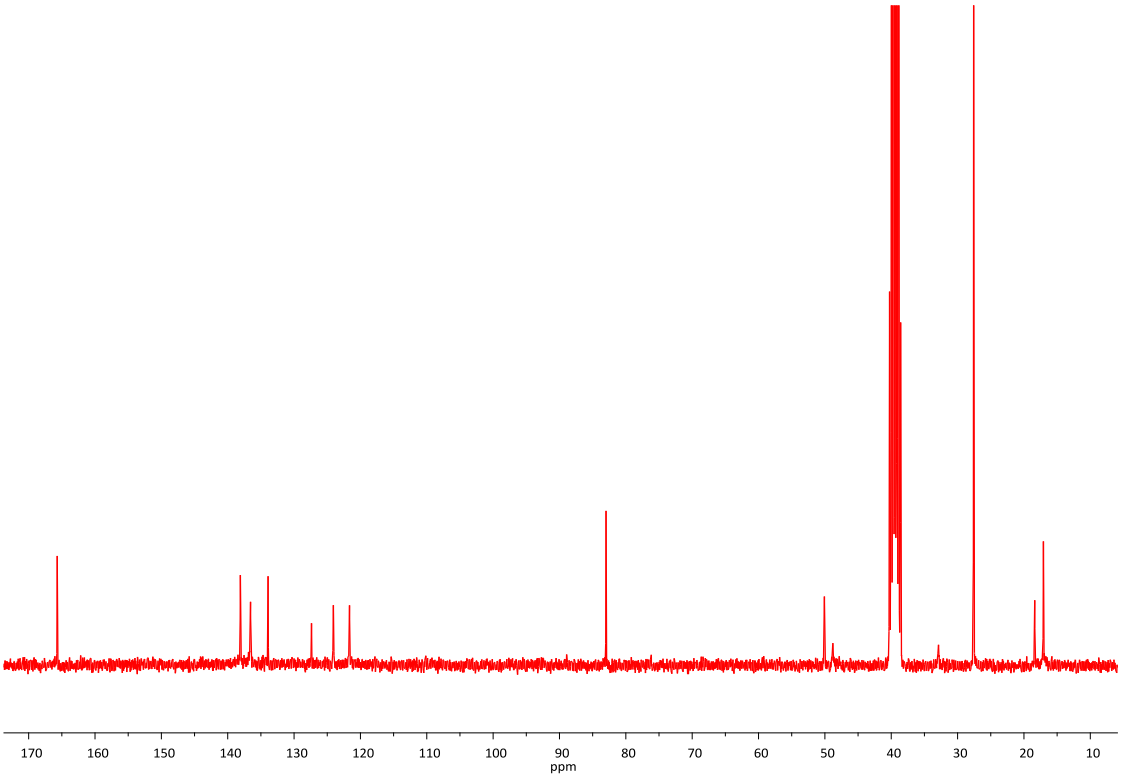

Figure 16 $^{13}C\{^{1}H\}$ NMR spectrum (DMSO-d_6) of compound **4.2 PF_6** at 298 K.

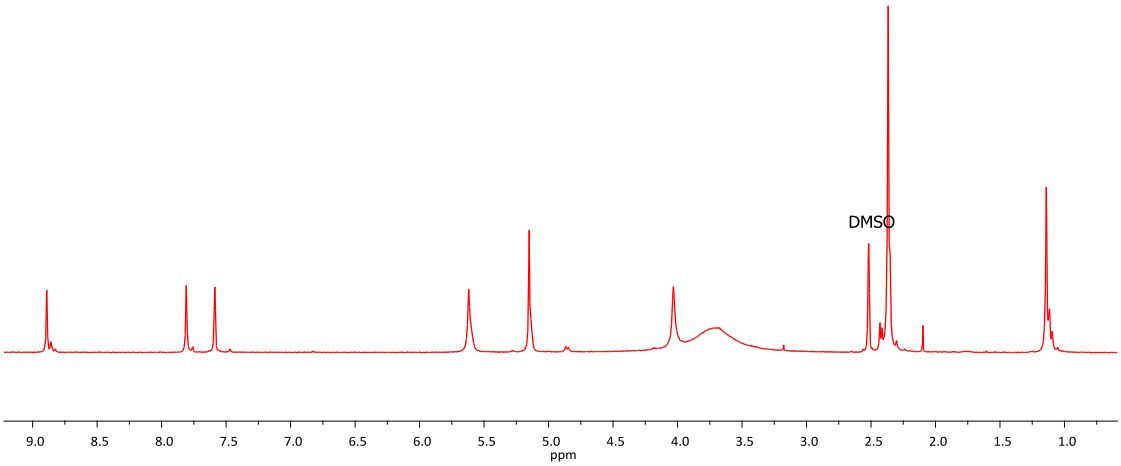

Figure 17 ^{1}H NMR spectrum (DMSO-d_6) of compound **4.3 Br** at 298 K.

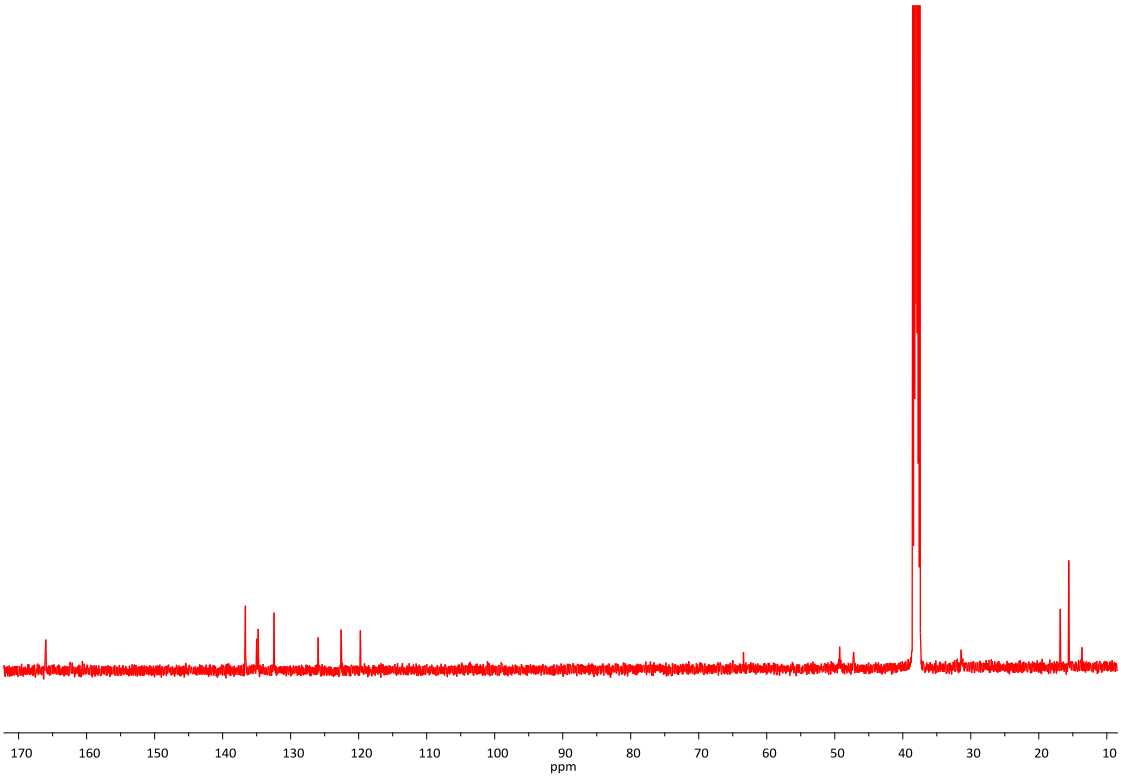

Figure 18 ^{13}C{^{1}H} NMR spectrum (DMSO-d_6) of compound **4.3 Br** at 298 K.

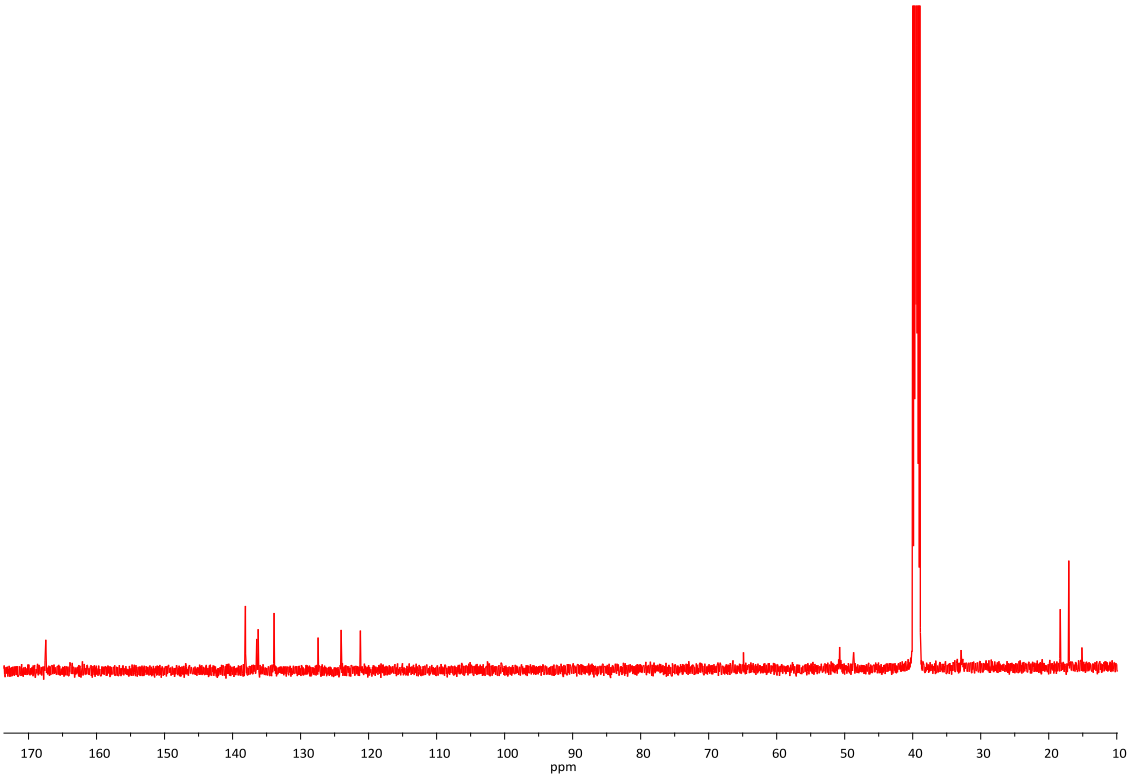

Figure 19 $^{13}C\{^{1}H\}$ NMR spectrum (DMSO-d_6) of compound **4.3** $\mathbf{PF_6}$ at 298 K.

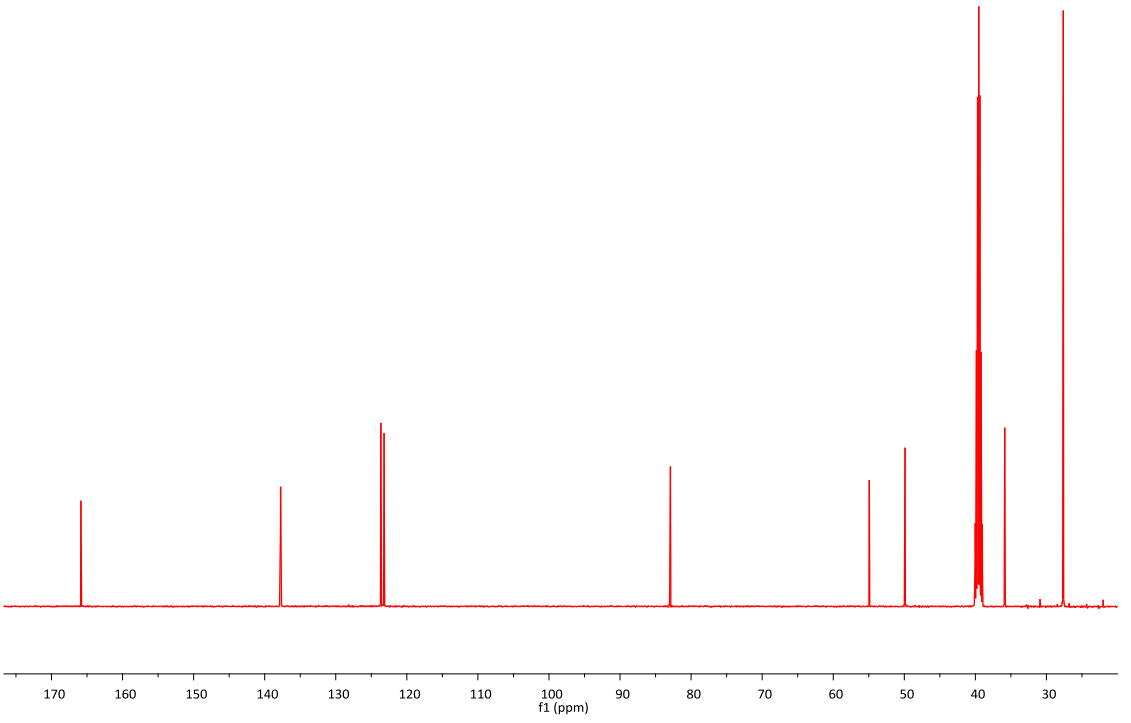

Figure 20 $^{13}C\{^{1}H\}$ NMR spectrum (DMSO-d_6) of compound **4.4** at 298 K.

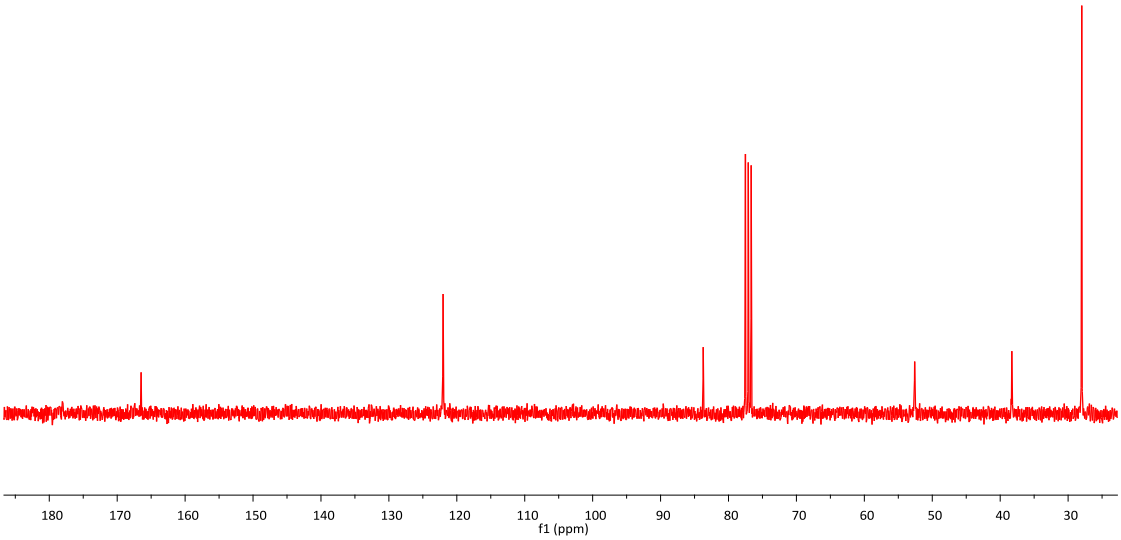

Figure 21 $^{13}C\{^{1}H\}$ NMR spectrum ($CDCl_3$) of complex **4.5** at 298 K.

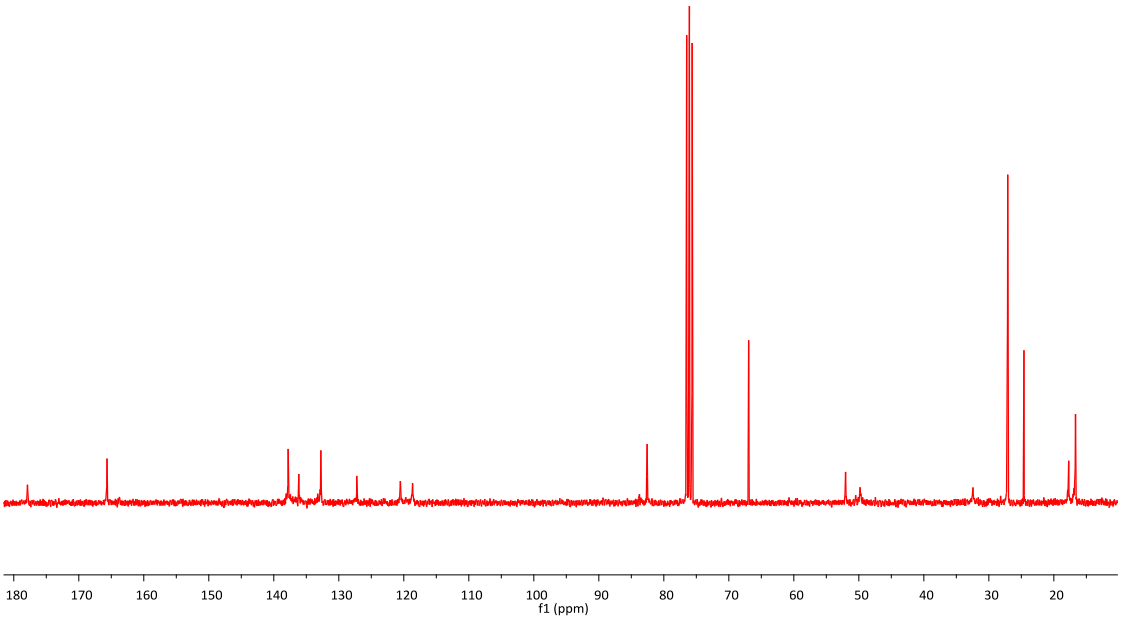

Figure 22 $^{13}C\{^{1}H\}$ NMR spectrum ($CDCl_3$) of complex **4.6** at 298 K.

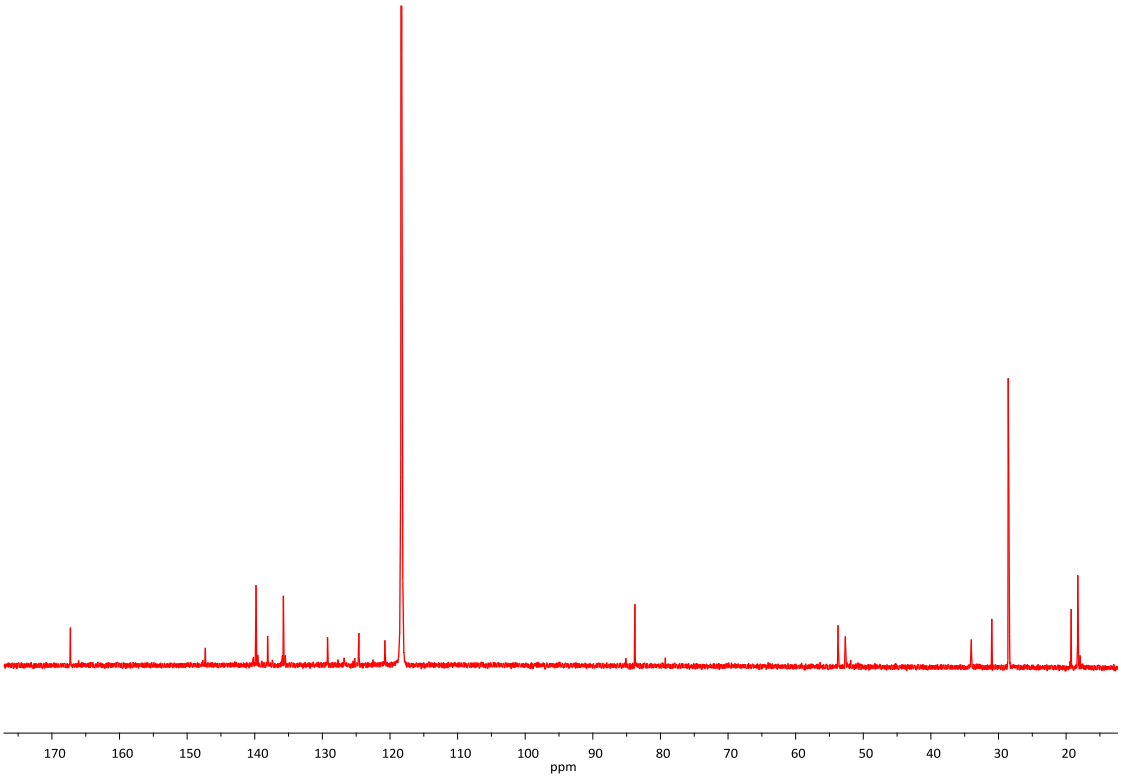

Figure 23 $^{13}C\{^{1}H\}$ NMR spectrum ($CDCl_3$) of complex **4.7** at 298 K.

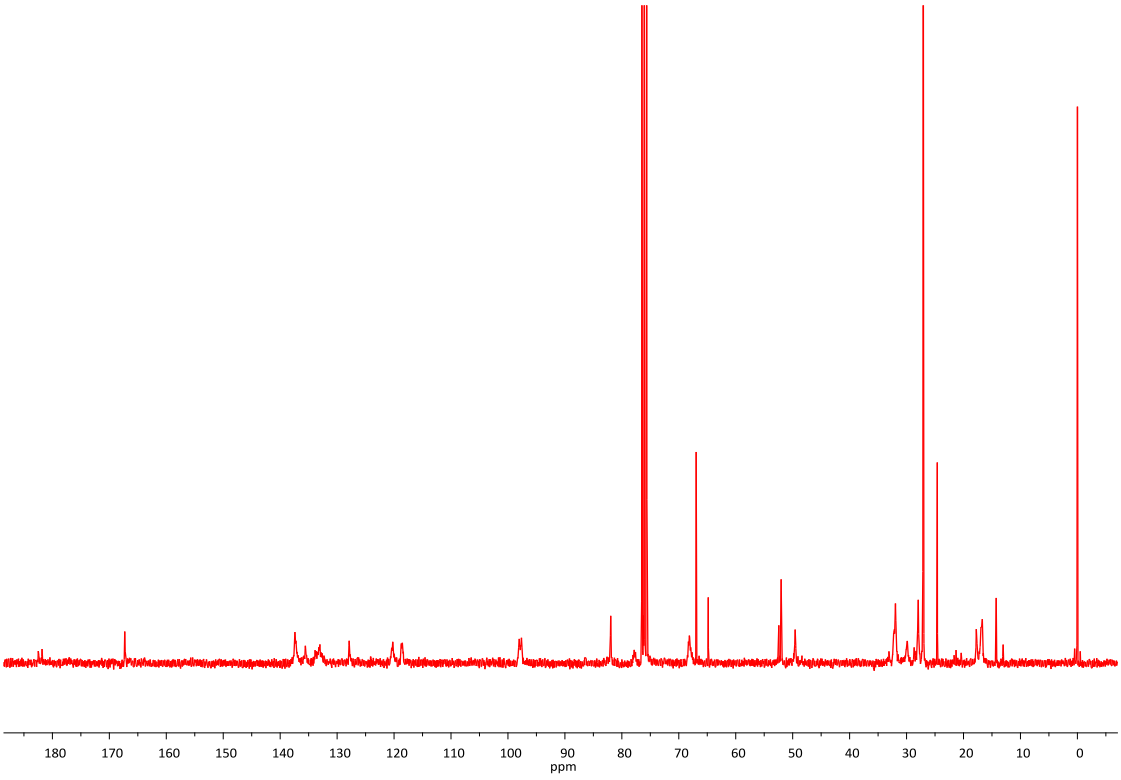

Figure 24 $^{13}C\{^{1}H\}$ NMR spectrum ($CDCl_3$) of complex **4.8** at 298 K.

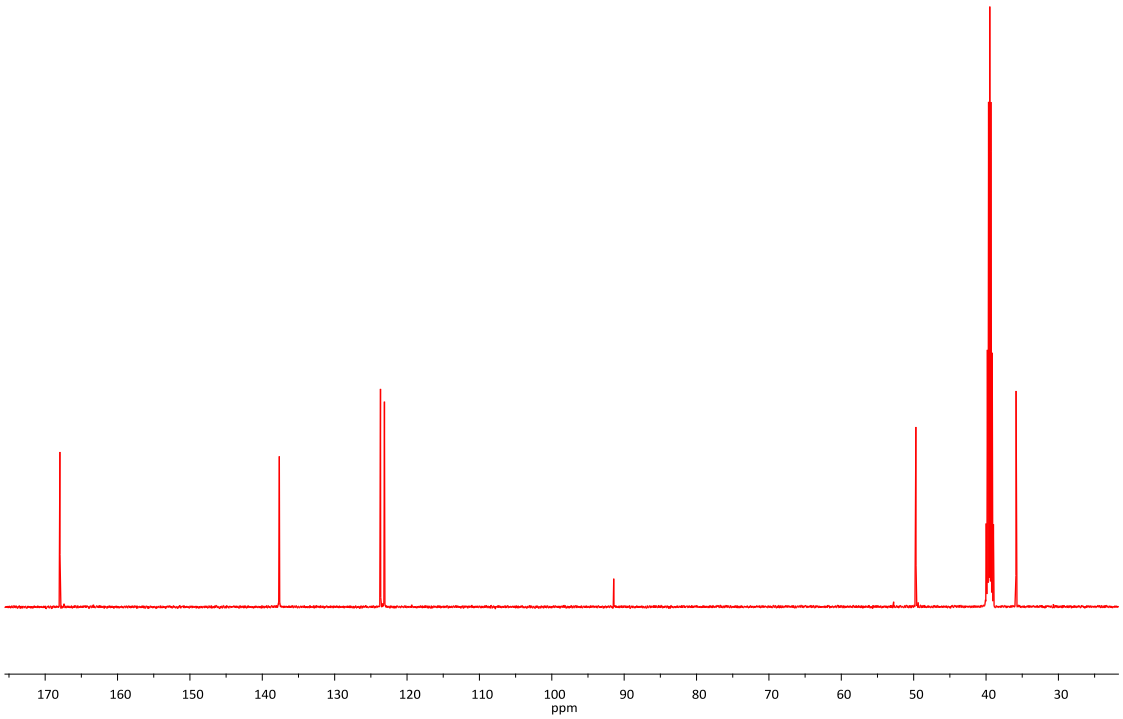

Figure 25 $^{13}C\{^{1}H\}$ NMR spectrum (DMSO-d_6) of compound **4.9** at 298 K.

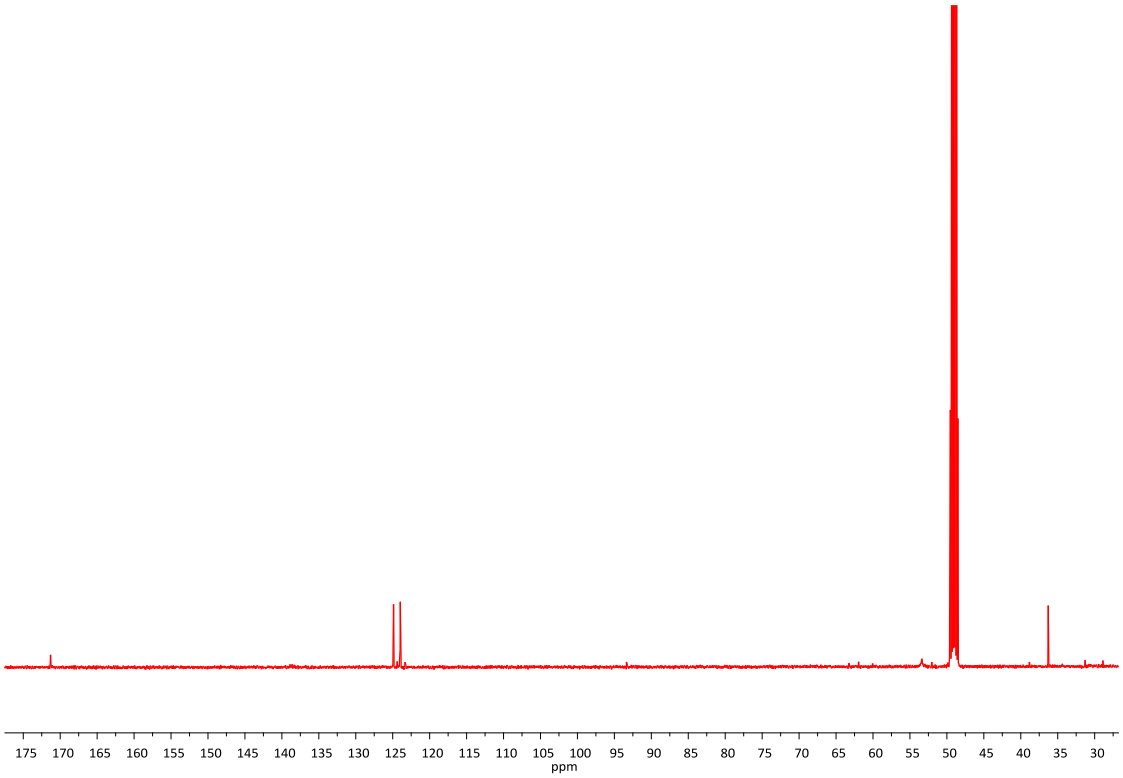

Figure 26 $^{13}C\{^{1}H\}$ NMR spectrum (MeOD-d_4) of the product formed in the reaction of compound **4.9** with Ag_2O in DCM / methanol.

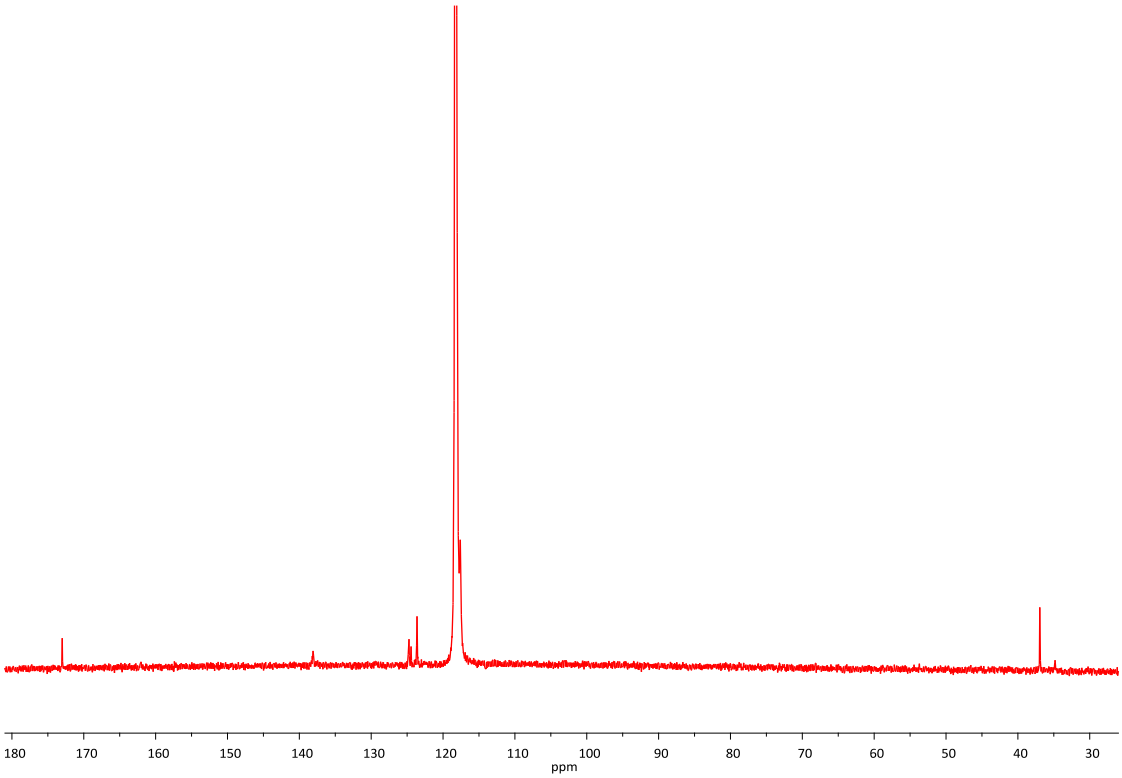

Figure 27 $^{13}C\{^{1}H\}$ NMR spectrum (MeCN-d_3) of the product formed in the electrochemical reaction of compound **4.9 a**t 298 K.

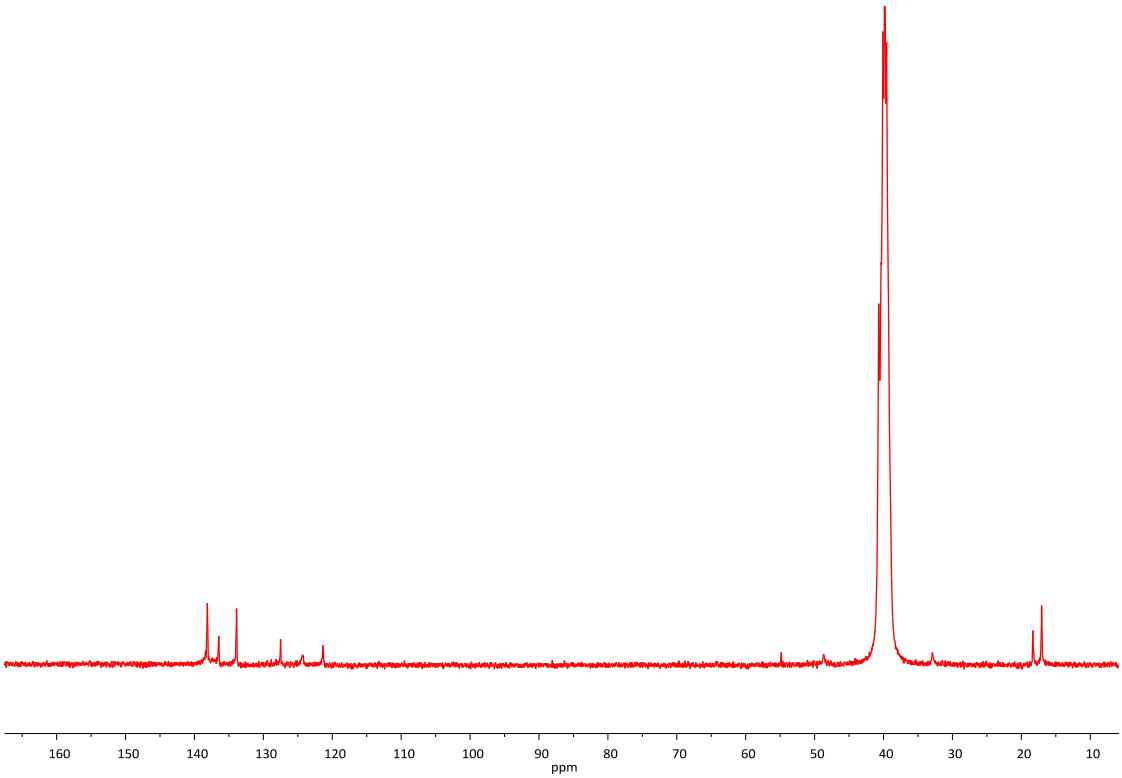

Figure 28 $^{13}C\{^{1}H\}$ NMR spectrum (DMSO-d_6) of the product formed in the electrochemical reaction of **4.3 PF_6** at 298 K.

9.4 NMR data for the compounds / complexes reported in Chapter 6

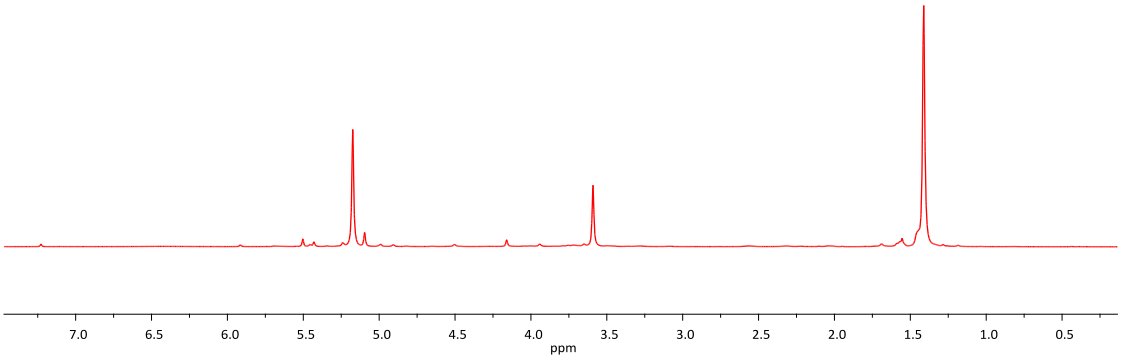

Figure 29 ^{1}H NMR spectrum ($CDCl_3$) of compound **6.1** at 298 K.

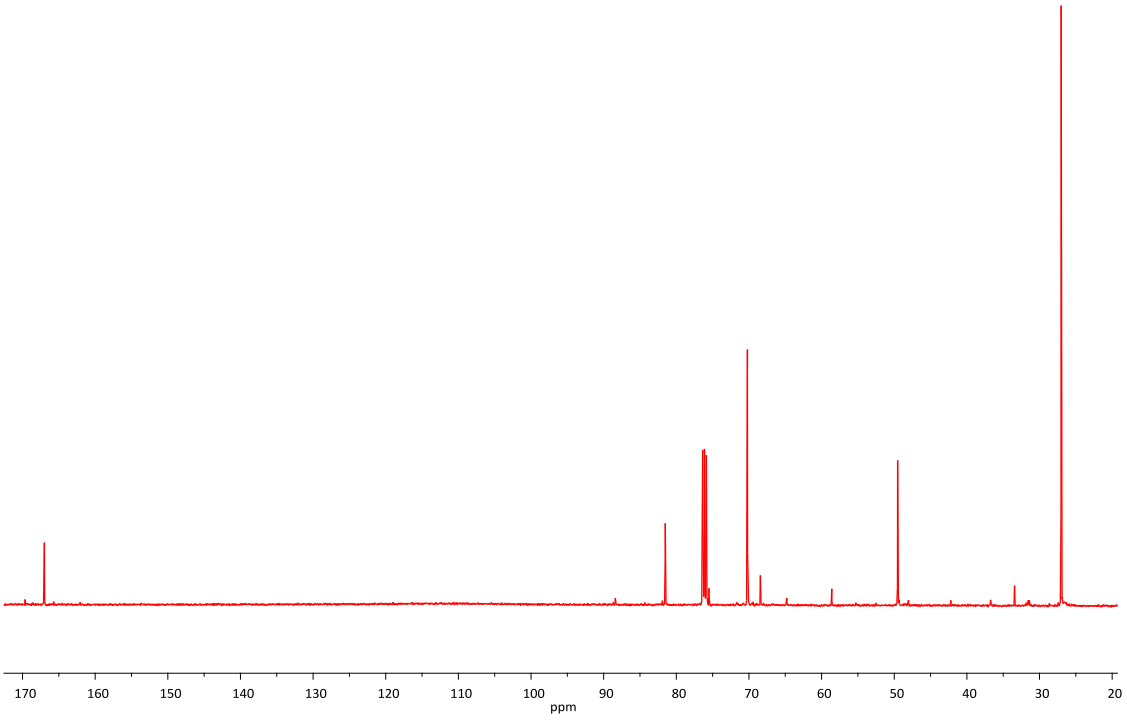

Figure 30 $^{13}C\{^{1}H\}$ NMR spectrum ($CDCl_3$) of compound **6.1** at 298 K.

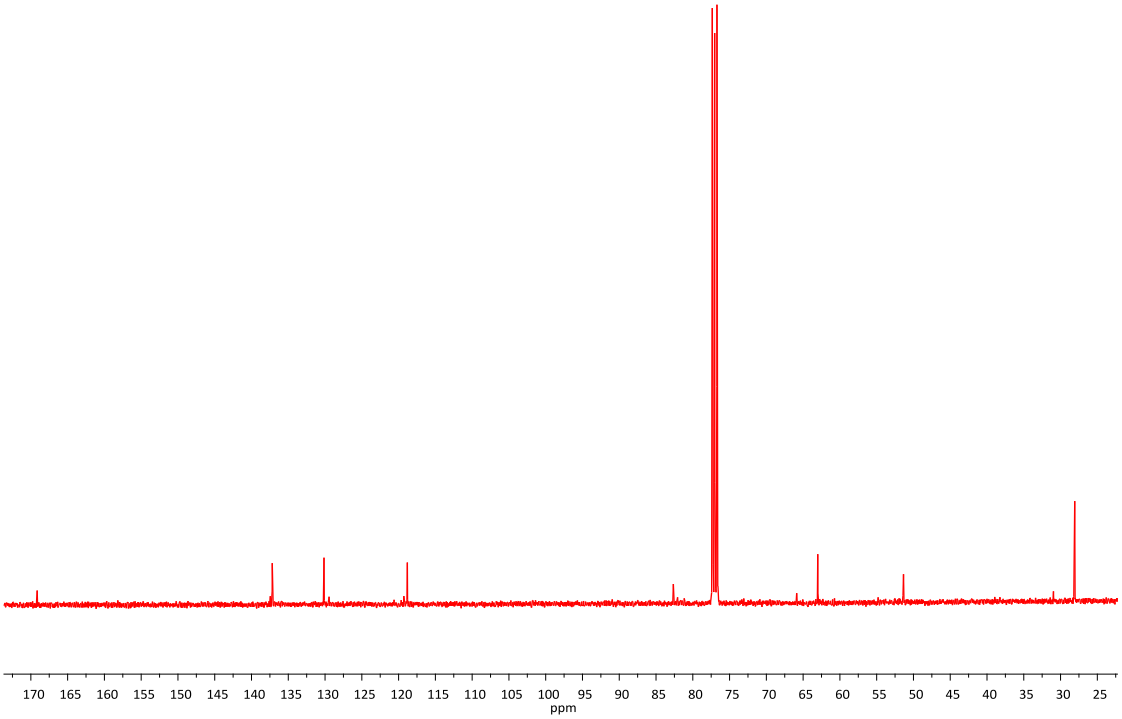

Figure 31 $^{13}C\{^{1}H\}$ NMR spectrum ($CDCl_3$) of compound **6.2** at 298 K.

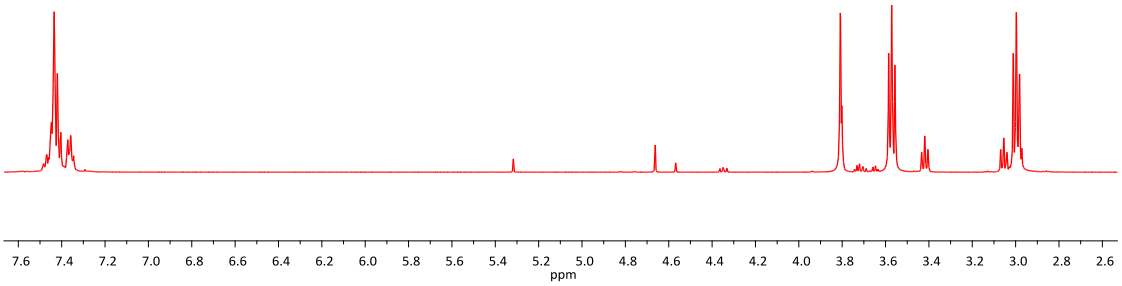

Figure 32 ^{1}H NMR spectrum ($CDCl_3$) of compound **6.4** at 298 K.

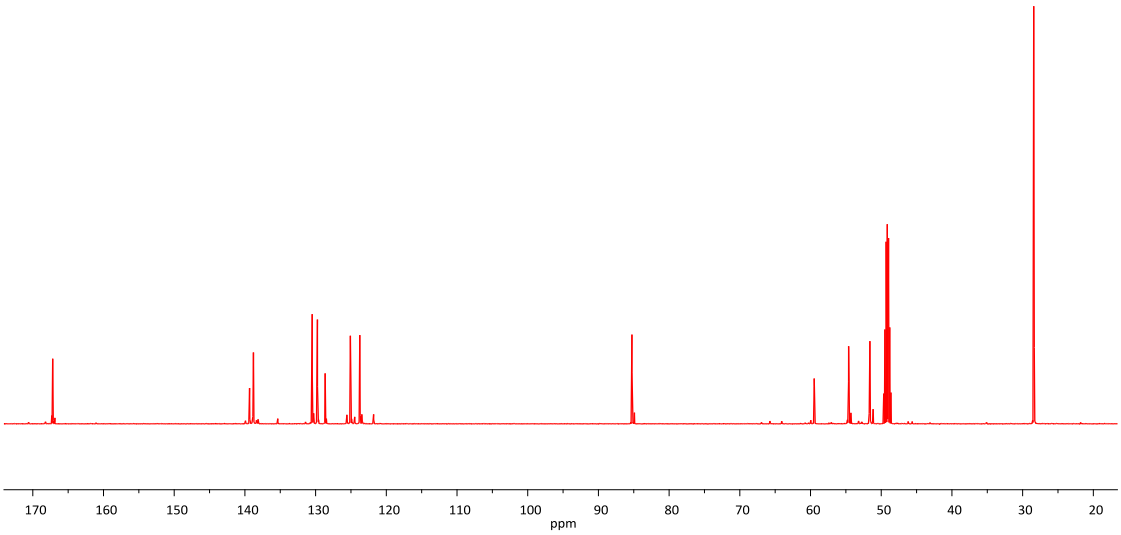

Figure 33 $^{13}C\{^{1}H\}$ NMR spectrum (MeOD-d_4) of compound **6.5 Cl** at 298 K.

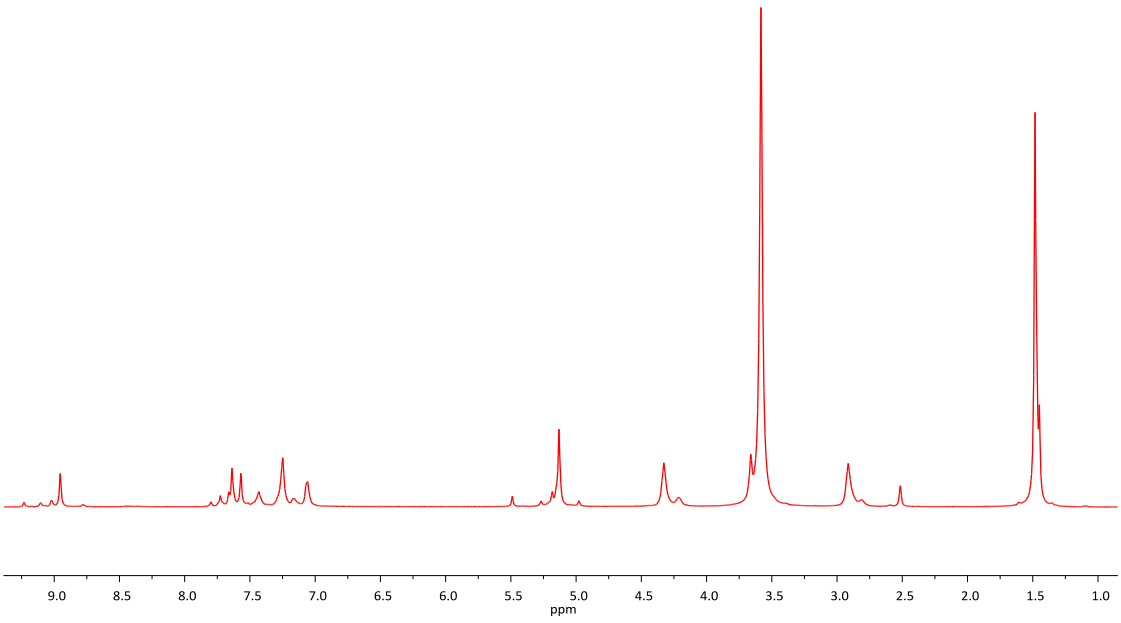

Figure 34 ^{1}H NMR spectrum (DMSO-d_6) of compound **6.5 PF_6** at 298 K.

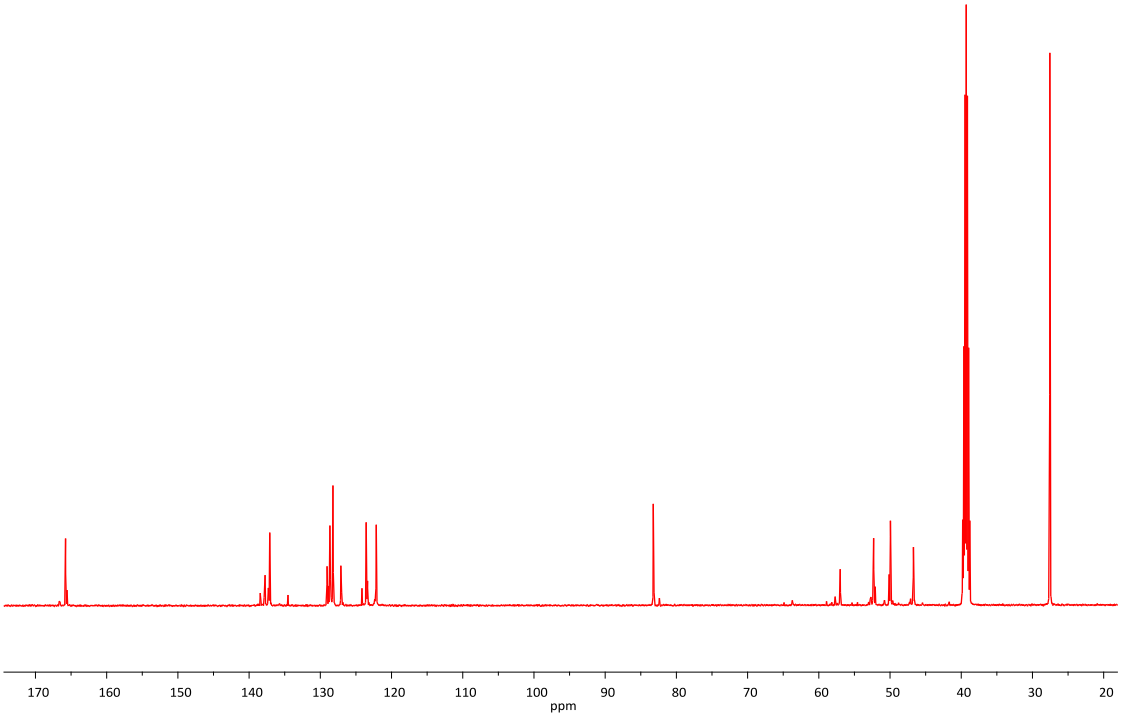

Figure 35 $^{13}C\{^{1}H\}$ NMR spectrum ($DMSO\text{-}d_6$) of compound **6.5** $\mathbf{PF_6}$ at 298 K.

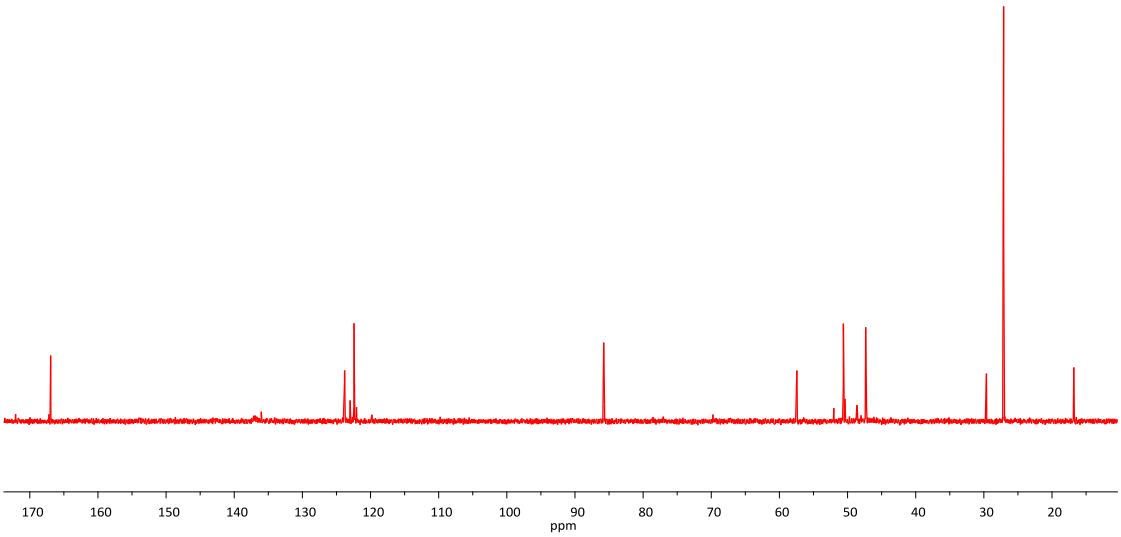

Figure 36 $^{13}C\{^{1}H\}$ NMR spectrum (D_2O) of compound **6.6 Cl** at 298 K.

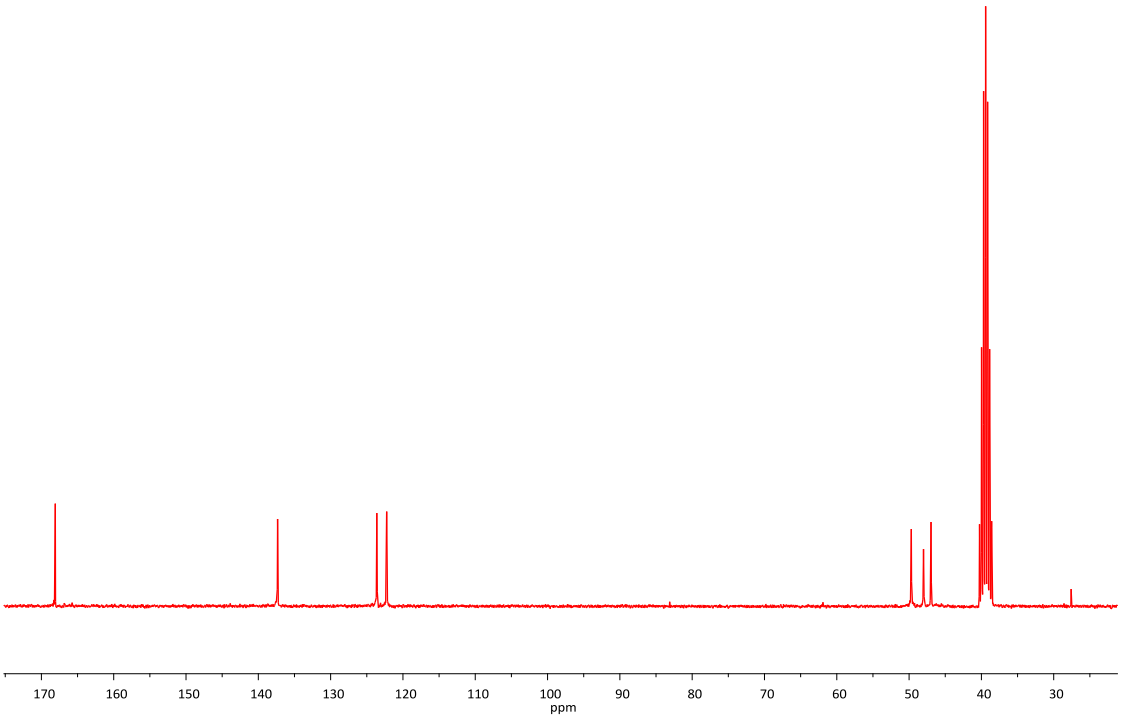

Figure 37 $^{13}C\{^{1}H\}$ NMR spectrum (D_2O) of compound **6.6** $\mathbf{PF_6}$ at 298 K.

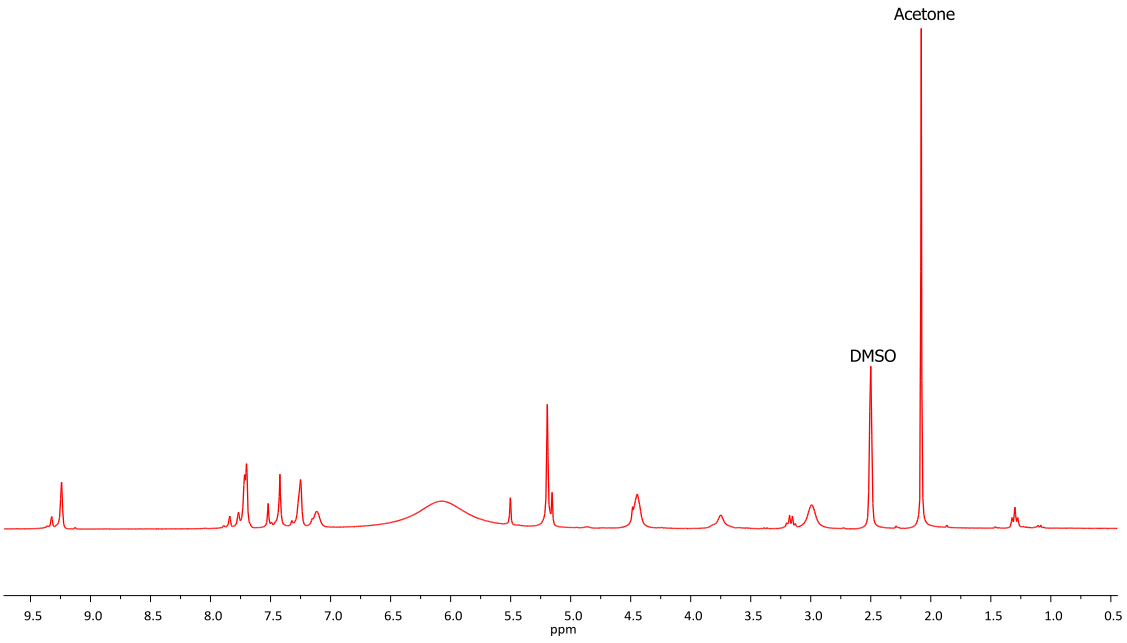

Figure 38 ^{1}H NMR spectrum (DMSO-d_6) of compound **6.11** at 298 K.

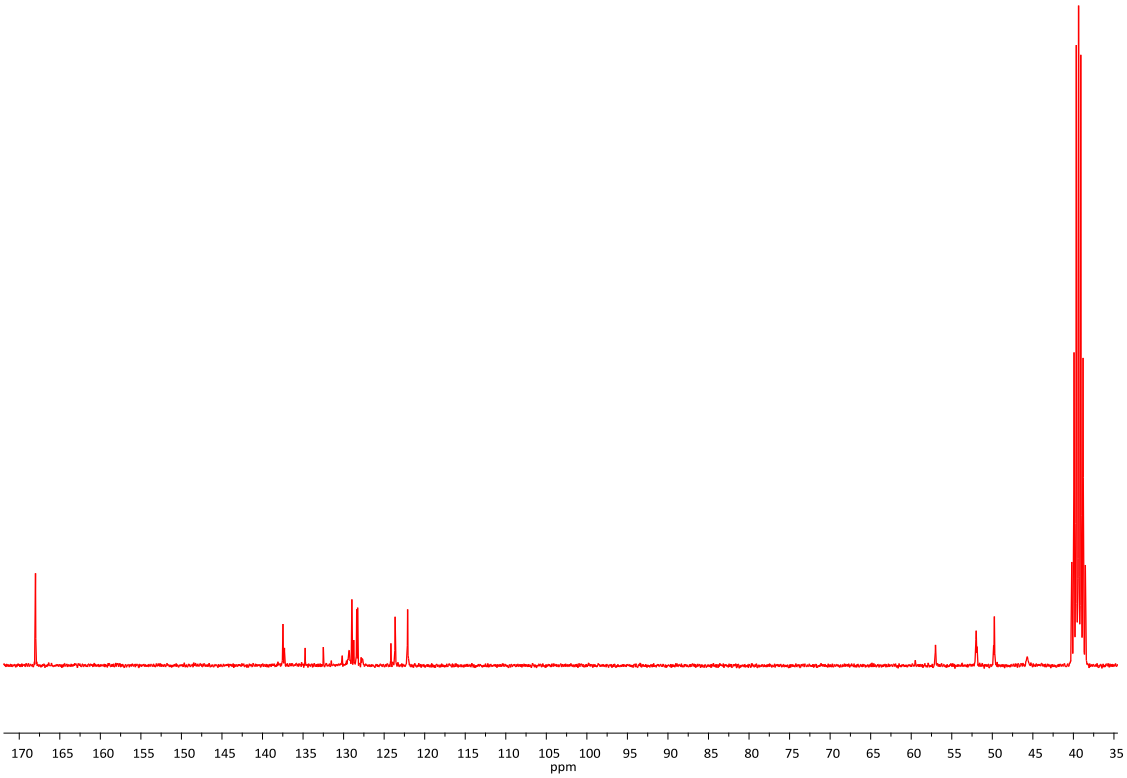

Figure 39 $^{13}C\{^{1}H\}$ NMR spectrum (DMSO-d_6) of compound **6.11** at 298 K.

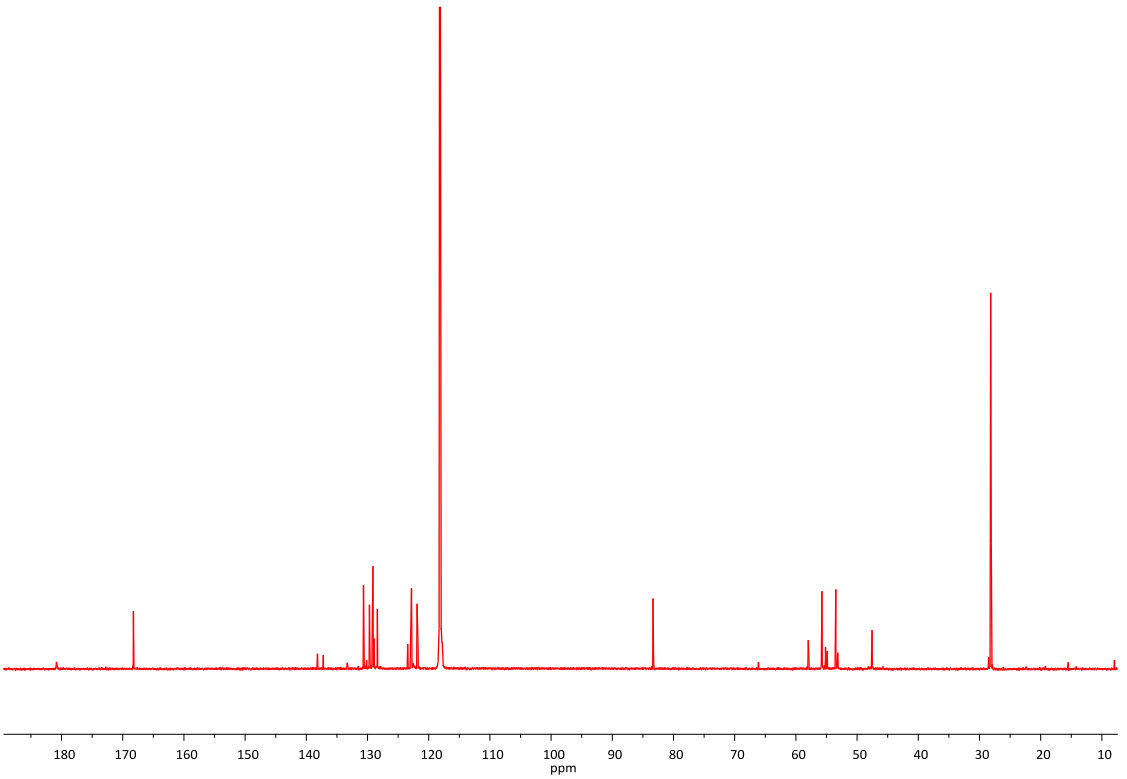

Figure 40 $^{13}C\{^{1}H\}$ NMR spectrum (MeCN-d_3) of complex **6.16** at 298 K.

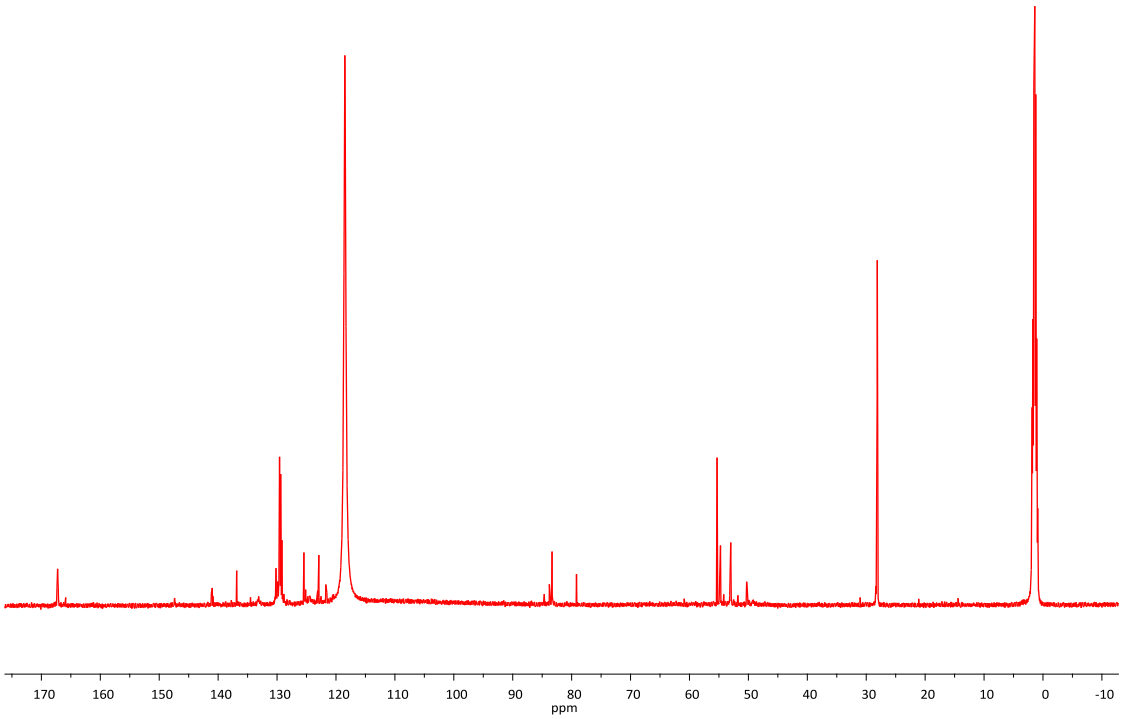

Figure 41 $^{13}C\{^{1}H\}$ NMR spectrum (MeCN-d_3) of complex **6.17** at 298 K.

9.5 NMR data for the compounds / complexes reported in Chapter 7

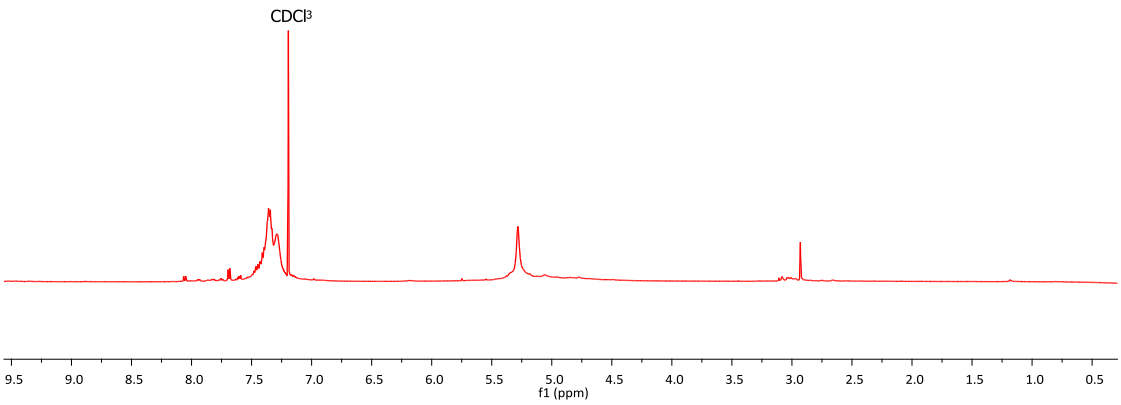

Figure 42 ^{1}H NMR spectrum ($CDCl_3$) of compound **7.3** at 298 K.

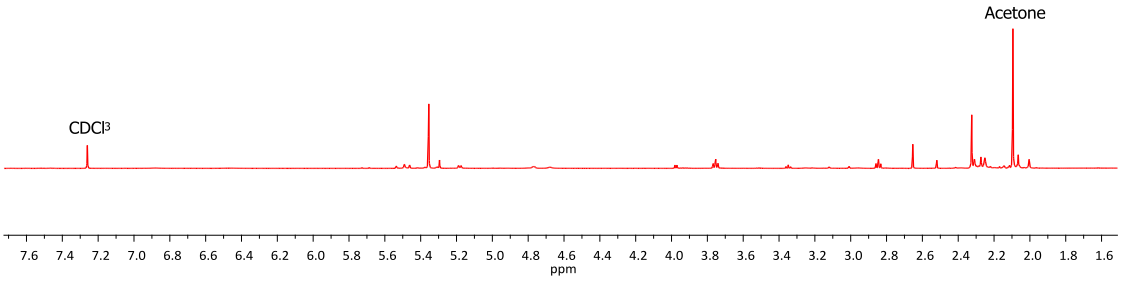

Figure 43 ^{1}H NMR spectrum ($CDCl_3$) of compound **7.4** at 298 K.

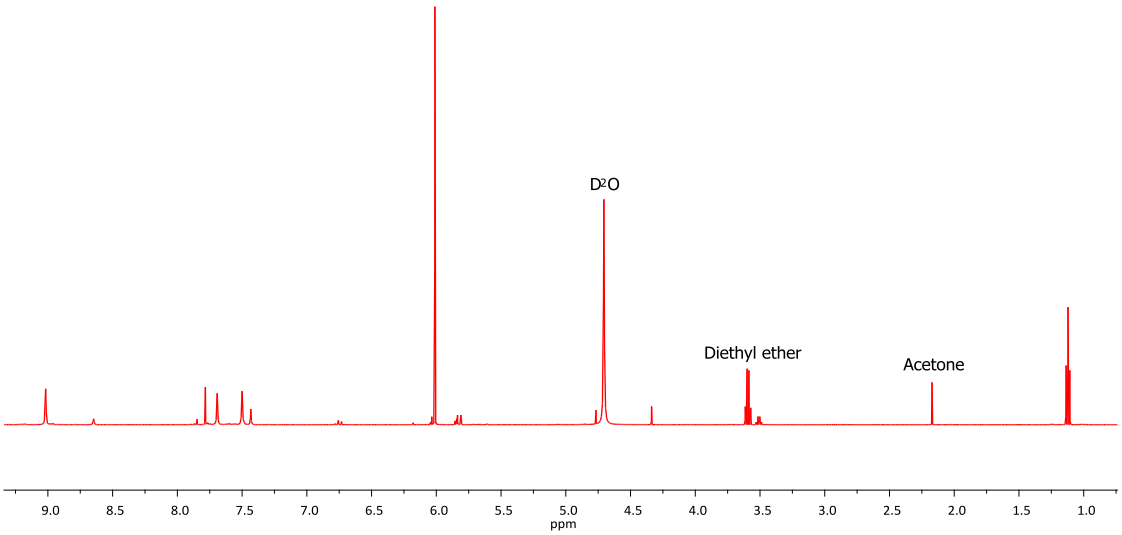

Figure 44 ^{1}H NMR spectrum (D_2O) of compound **7.9** at 298 K.

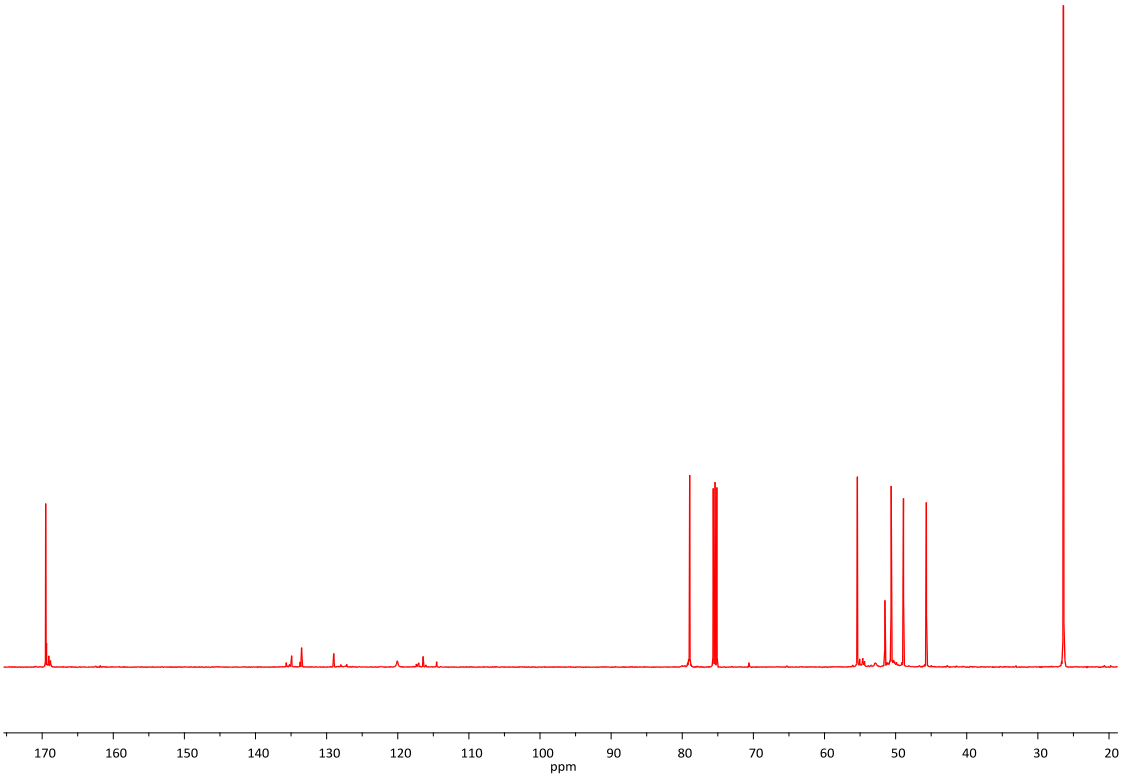

Figure 45 $^{13}C\{^{1}H\}$ NMR spectrum ($CDCl_3$) of compound **7.9** at 298 K.

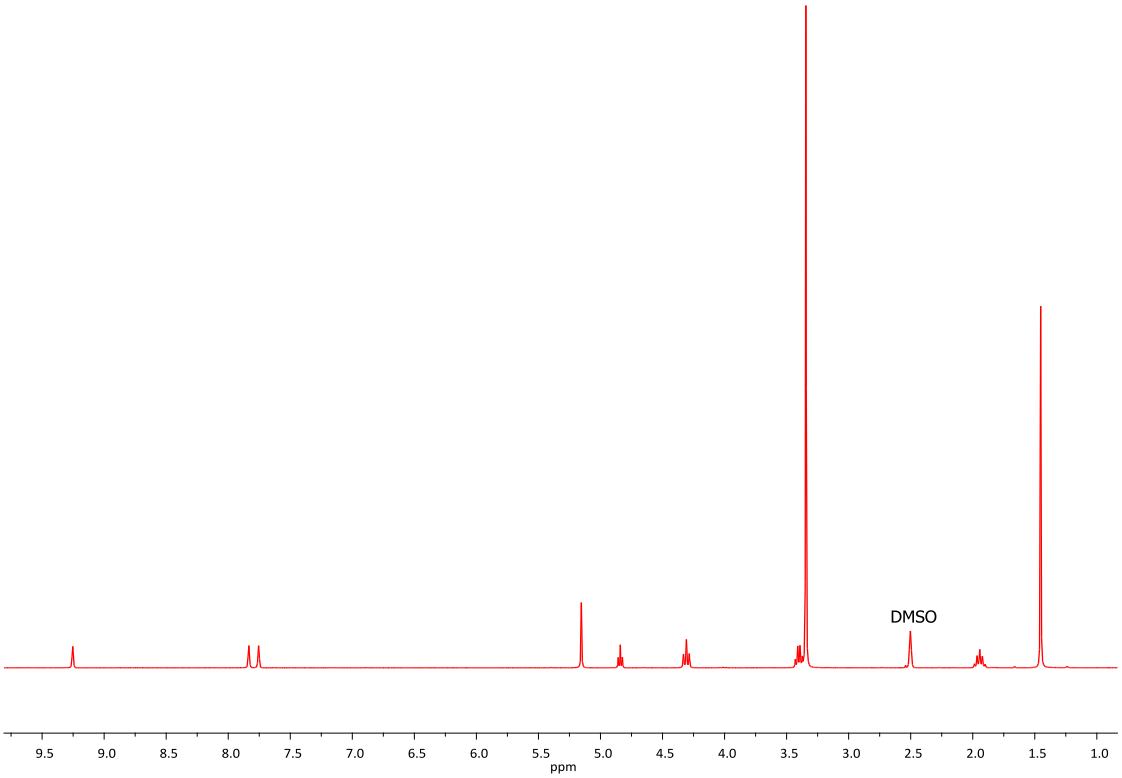

Figure 46 ^{1}H NMR spectrum (DMSO-d_6) of compound **7.13** at 298 K.

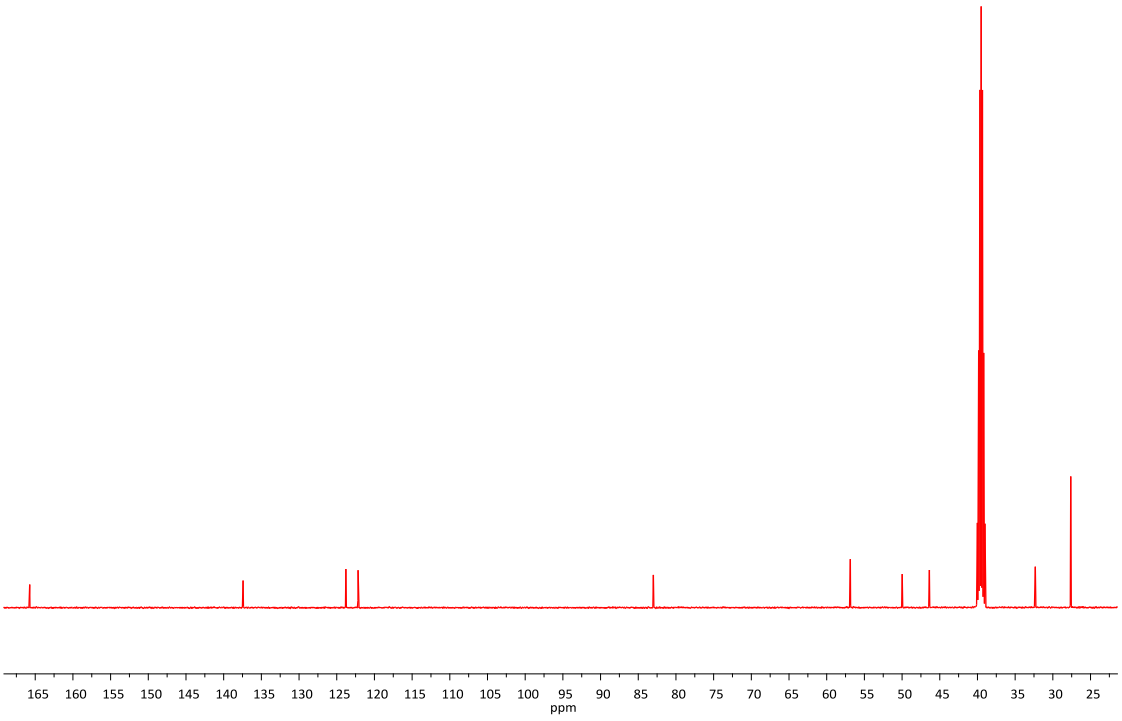

Figure 47 ^{13}C{^{1}H} NMR spectrum (DMSO-d_6) of compound **7.13** at 298 K.

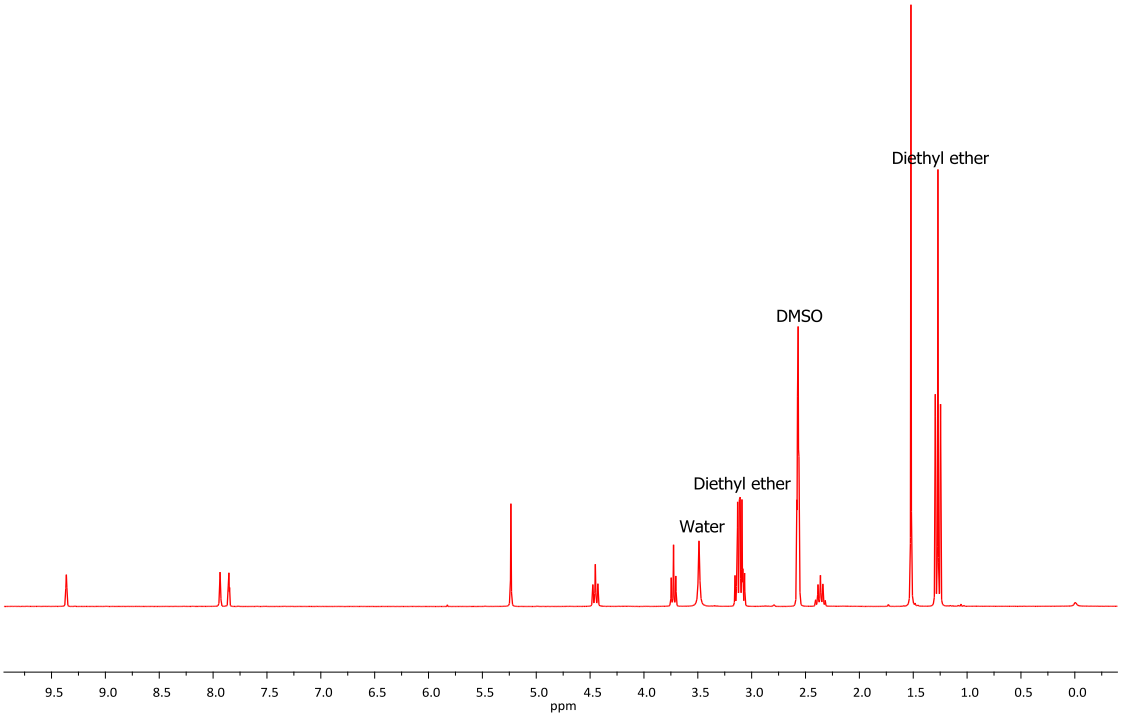

Figure 48 ^{1}H NMR spectrum (DMSO-d_6) of compound **7.14** at 298 K.

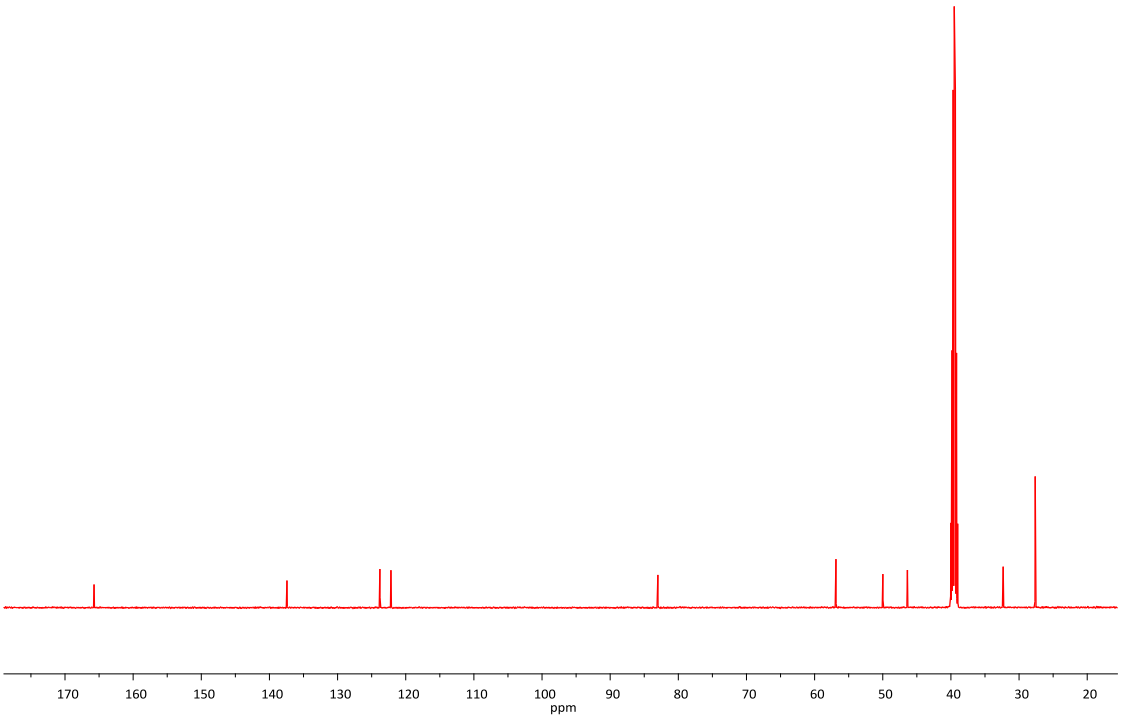

Figure 49 ^{13}C{^{1}H} NMR spectrum (DMSO-d_6) of compound **7.14** at 298 K.

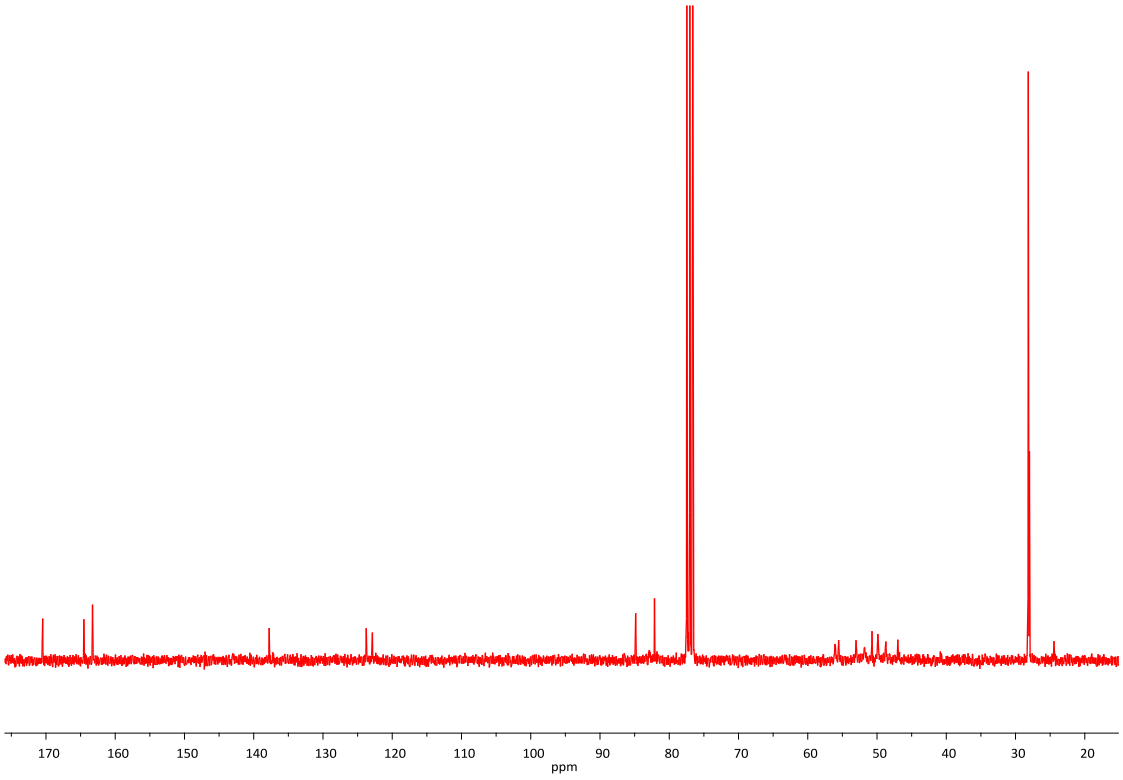

Figure 50 $^{13}C\{^{1}H\}$ NMR spectrum ($CDCl_3$) of compound **7.15** at 298 K.

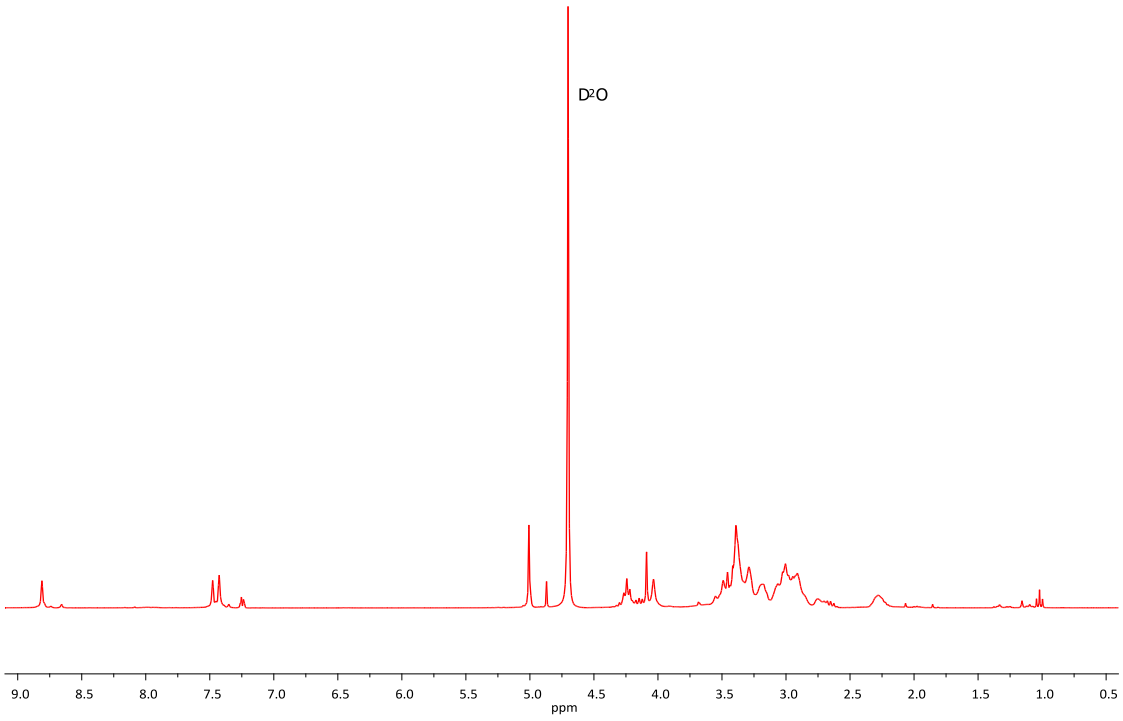

Figure 51 ^{1}H NMR spectrum (D_2O) of compound **7.16** at 298 K.

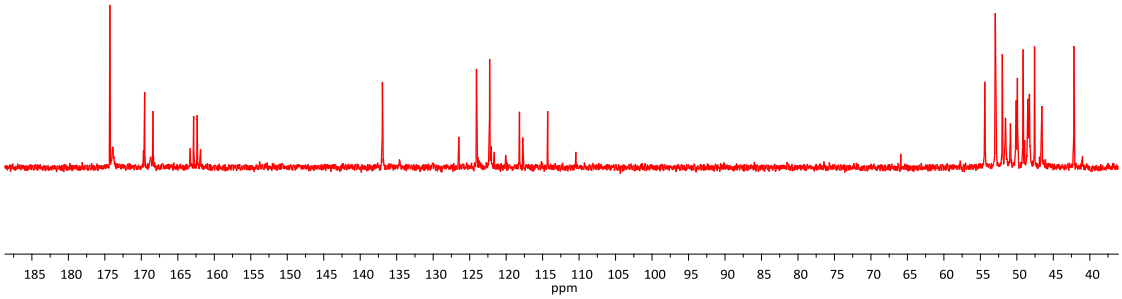

Figure 52 $^{13}C\{^{1}H\}$ NMR spectrum (D_2O) of compound **7.16** at 298 K.

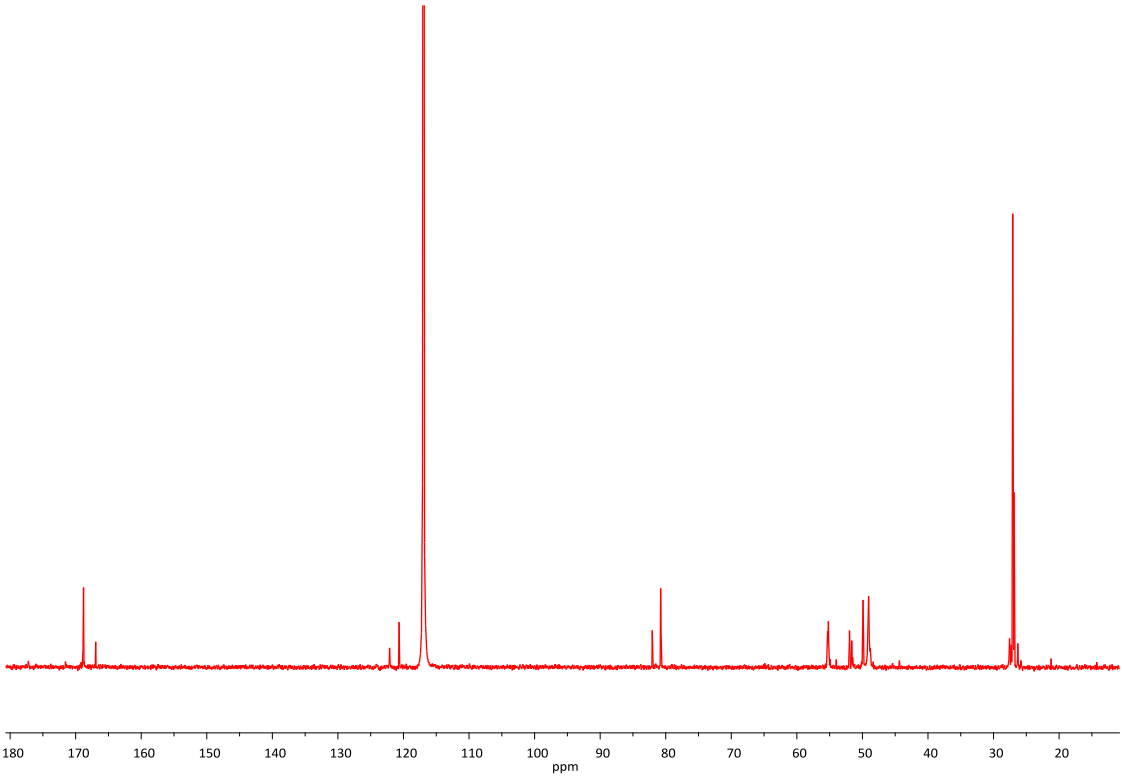

Figure 53 $^{13}C\{^{1}H\}$ NMR spectrum (MeCN-d_3) of complex **7.18** at 298 K.

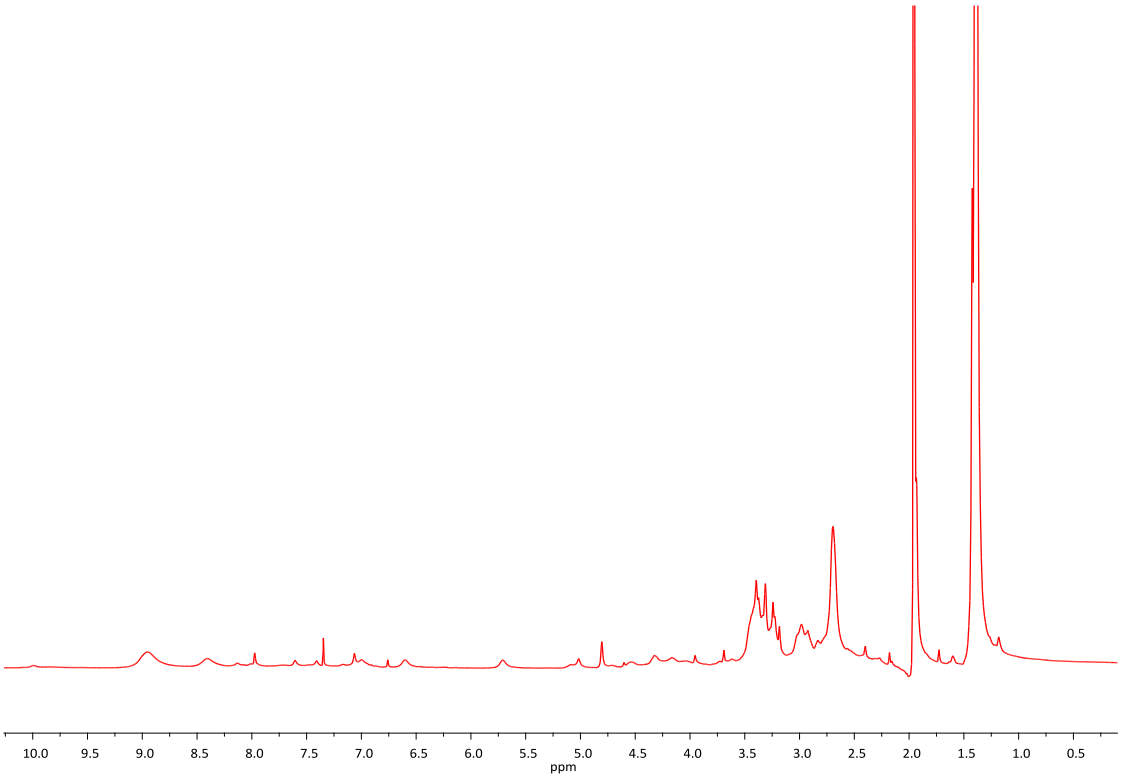

Figure 54 ^{1}H NMR spectrum (MeCN-d_3) of complex **7.19** / **7.20** at 298 K.

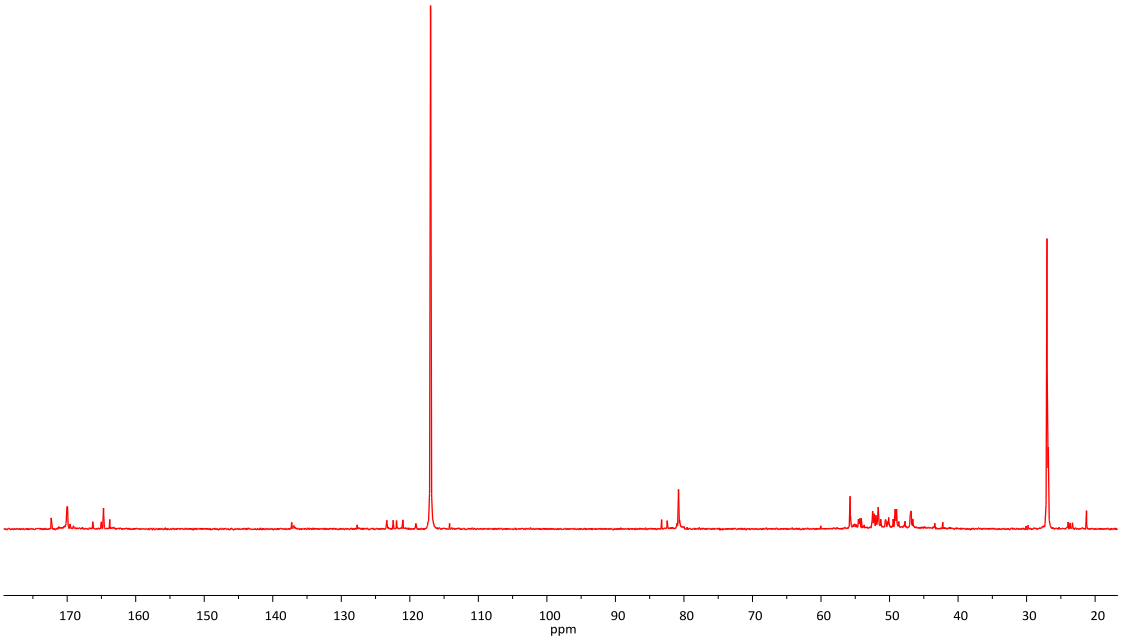

Figure 55 ^{13}C{^{1}H} NMR spectrum (MeCN-d_3) of complex **7.19** / **7.20** at 298 K.

9.6 Example spreadsheet for NMR titration experiments

NMR Titrations

RMM of Host	1384.83	
Mass of Host	0.0201	g
No. of moles of Host	1.45E-05	moles
Host solution volume	0.8	ml
RMM of Guest	322.37	
Mass of Guest	**0.0637**	g
No. of moles of Guest	1.98E-04	moles
Guest solution volume	1.0	ml

Spectrum Number	Volume of Guest added (ml)	Total volume (ml)	Concentrations		Equivalents of Guest	Observed Chemical Shift (ppm)		
			Host	Guest		[Proton 1]	[Proton 2]	[Proton 3]
1	0.000	0.800	0.018143	0.000000	0.000000	9.04	7.67	7.02
2	0.010	0.810	0.017919	0.002439	0.136140	9.06	7.68	7.03
3	0.020	0.820	0.017701	0.004819	0.272280	9.08	7.68	7.03
4	0.030	0.830	0.017487	0.007142	0.408420	9.09	7.68	7.04
5	0.040	0.840	0.017279	0.009409	0.544559	9.11	7.69	7.04
6	0.050	0.850	0.017076	0.011623	0.680699			
7	0.060	0.860	0.016877	0.013786	0.816839	9.13	7.71	7.05
8	0.070	0.870	0.016683	0.015899	0.952979			
9	0.080	0.880	0.016494	0.017964	1.089119	9.15	7.72	7.05
10	0.090	0.890	0.016308	0.019982	1.225259			
11	0.100	0.900	0.016127	0.021955	1.361398	9.17	7.72	7.07
12	0.110	0.910	0.015950	0.023886	1.497538			
13	0.120	0.920	0.015777	0.025774	1.633678	9.18	7.73	7.08
14	0.130	0.930	0.015607	0.027621	1.769818			
15	0.140	0.940	0.015441	0.029430	1.905958	9.2	7.74	7.08
16	0.150	0.950	0.015278	0.031200	2.042098	9.21	7.74	7.08
17	0.160	0.960	0.015119	0.032933	2.178237			
18	0.170	0.970	0.014963	0.034631	2.314377	9.22	7.75	7.09
19	0.180	0.980	0.014811	0.036294	2.450517			
20	0.190	0.990	0.014661	0.037923	2.586657	9.23	7.75	7.09
21	0.200	1.000	0.014514	0.039520	2.722797			
22	0.210	1.010	0.014371	0.041085	2.858937	9.24	7.76	7.1
23	0.220	1.020	0.014230	0.042619	2.995076			

9.7 Hyp NMR data

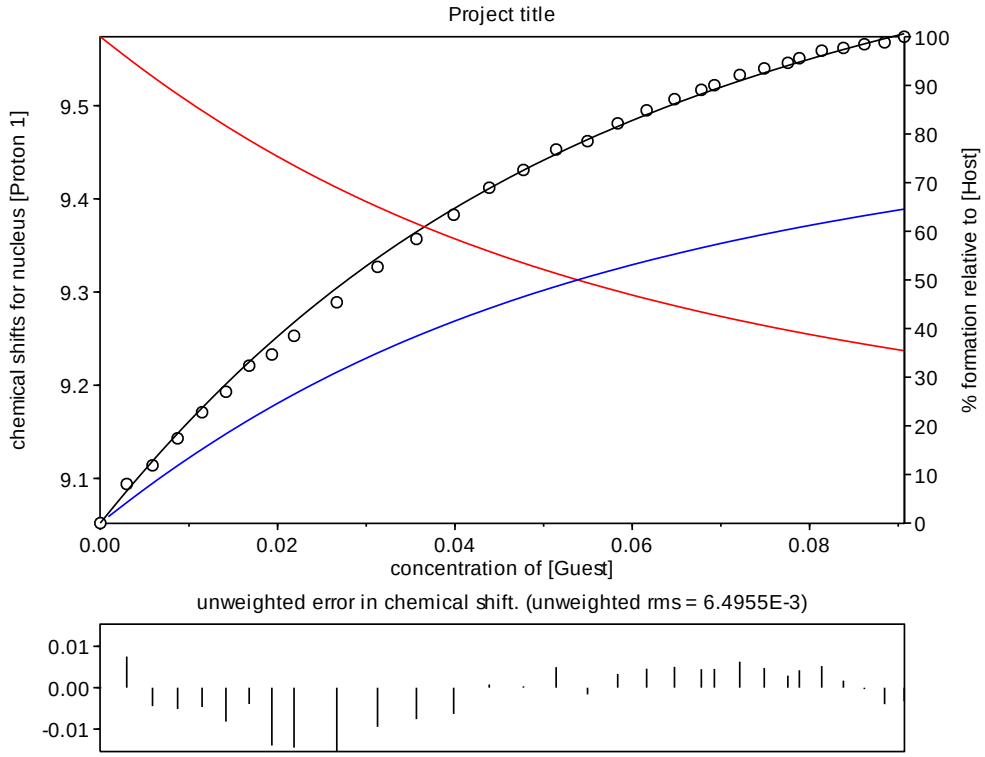

Figure 56 HypNMR fitting data for Cl^- binding by compound **2.5** PF_6.

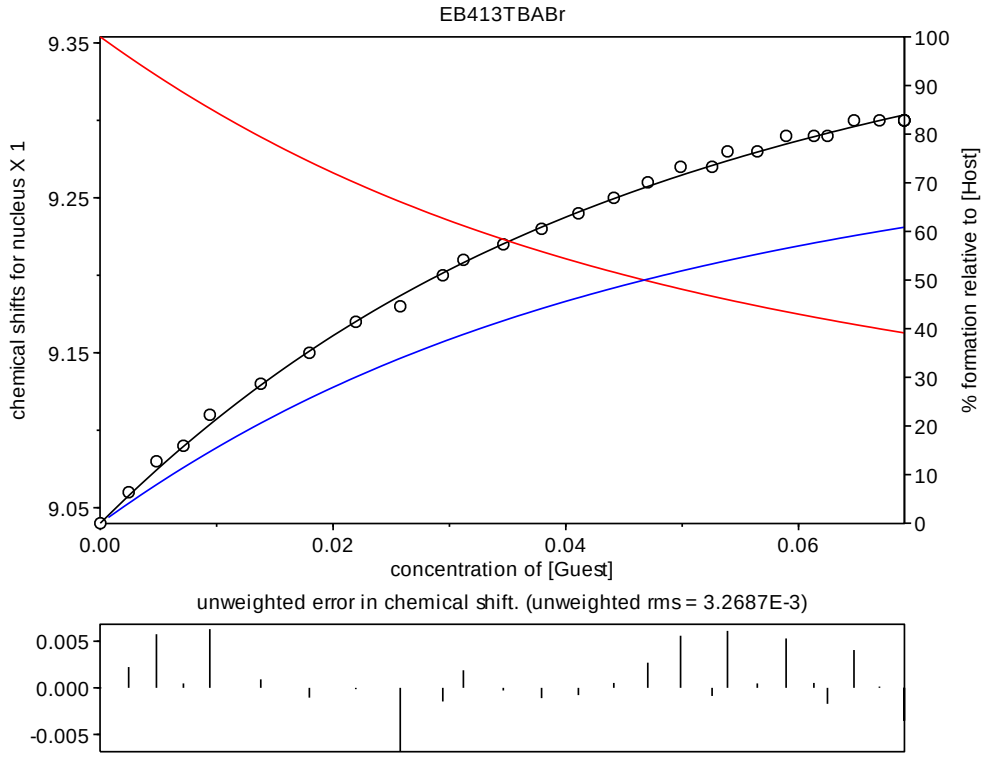

Figure 57 HypNMR fitting data for Br^- binding by compound **2.5** PF_6.

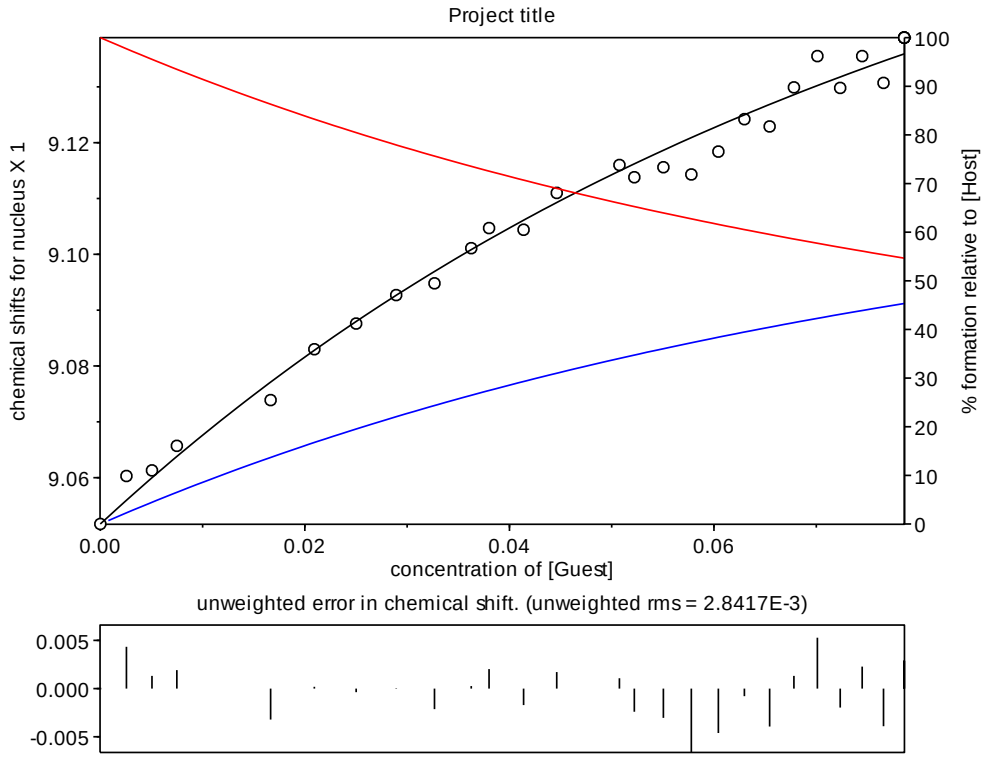

Figure 58 HypNMR fitting data for NO_3^- binding by compound **2.5 PF_6**.

9.8 Crystallography Data tables

Details of data collections and structural refinements of compound **2.4**, **2.5 Br**, **3.4 4Br**, **3.4 3Cl.PF_6**, **4.2 Br**, **4.10**, **6.2** and complex **4.7**.

Identification code	Compound **2.4**
Empirical formula	$C_{45}H_{44}Cl_3N_8O_{5.5}$
Formula weight	891.23
Temperature/K	150(2)
Crystal system	monoclinic
Space group	$P2_1/c$
a/Å	10.0579(8)
b/Å	40.788(3)
c/Å	10.7646(9)
α/°	90.00
β/°	101.688(4)
γ/°	90.00
Volume/Å^3	4324.5(6)
Z	4
ρ_{calc}mg/mm^3	1.369
M/mm^{-1}	0.270
F(000)	1860.0
Crystal size/mm^3	0.18 × 0.11 × 0.09
2Θ range for data collection	4 to 54.38°
Index ranges	$-11 \leq h \leq 12$, $-52 \leq k \leq 50$, $-13 \leq l \leq 13$
Reflections collected	61030
Independent reflections	9587[$R(int)$ = 0.0443]
Data/restraints/parameters	9587/197/662
Goodness-of-fit on F^2	1.031
Final R indexes [I>=2σ (I)]	R_1 = 0.0492, wR_2 = 0.1009
Final R indexes [all data]	R_1 = 0.0799, wR_2 = 0.1133
Largest diff. peak/hole / e Å^{-3}	0.57/-0.60

Identification code	Compound **2.5 Br**
Empirical formula	$C_{27}H_{37.14}Br_2N_4O_{4.5}$
Formula weight	649.57
Temperature/K	150(2)
Crystal system	monoclinic
Space group	$C2/m$
a/Å	17.580(2)
b/Å	39.483(5)
c/Å	11.7189(15)
α/°	90.00
β/°	130.147(4)

γ/°	90.00
Volume/Å^3	6217.9(14)
Z	8
ρ_{calc}mg/mm^3	1.388
M/mm^{-1}	2.645
F(000)	2665.0
Crystal size/mm^3	0.46 × 0.37 × 0.15
2*Θ* range for data collection	4.12 to 52.22°
Index ranges	-21 ≤ h ≤ 15, -47 ≤ k ≤ 48, -11 ≤ l ≤ 14
Reflections collected	36408
Independent reflections	6241[*R(int)* = 0.0669]
Data/restraints/parameters	6241/0/346
Goodness-of-fit on F^2	1.039
Final *R* indexes [*I*>=2*σ* (*I*)]	R_1 = 0.0651, wR_2 = 0.1935
Final *R* indexes [all data]	R_1 = 0.1132, wR_2 = 0.2229
Largest diff. peak/hole / e Å^{-3}	1.84/-0.95

Identification code	Compound **3.4 4Br**
Empirical formula	$C_{69.2}H_{94.8}Br_4N_{8.6}O_{4.5}$
Formula weight	1438.78
Temperature/K	150(2)
Crystal system	triclinic
Space group	*P*-1
a/Å	14.5208(7)
b/Å	16.3118(8)
c/Å	16.8001(7)
α/°	89.050(2)
β/°	74.817(2)
γ/°	65.845(2)
Volume/Å^3	3485.5(3)
Z	2
ρ_{calc}mg/mm^3	1.371
M/mm^{-1}	2.362
F(000)	1492.0
Crystal size/mm^3	0.32 × 0.25 × 0.24
2*Θ* range for data collection	3.48 to 56.36°
Index ranges	-19 ≤ h ≤ 19, -21 ≤ k ≤ 21, -22 ≤ l ≤ 21
Reflections collected	119266
Independent reflections	17035[*R(int)* = 0.0503]
Data/restraints/parameters	17035/66/834
Goodness-of-fit on F^2	1.027
Final *R* indexes [*I*>=2*σ* (*I*)]	R_1 = 0.0435, wR_2 = 0.1105
Final *R* indexes [all data]	R_1 = 0.0805, wR_2 = 0.1272
Largest diff. peak/hole / e Å^{-3}	1.38/-1.22

Identification code	Compound **3.4 3Cl.PF_6**
Empirical formula	$C_{72}H_{100}Cl_3F_6N_{10}O_5P$
Formula weight	1436.94
Temperature/K	150(2)
Crystal system	triclinic
Space group	*P*-1
a/Å	15.3602(7)
b/Å	16.4401(6)
c/Å	17.6345(12)
α/°	115.124(3)
β/°	105.512(3)
γ/°	101.167(2)
Volume/Å^3	3636.1(3)
Z	2
ρ_{calc}mg/mm^3	1.312
M/mm^{-1}	0.220
F(000)	1524.0
Crystal size/mm^3	0.24 × 0.18 × 0.14
2*Θ* range for data collection	2.94 to 56.46°
Index ranges	$-20 \leq h \leq 20$, $-21 \leq k \leq 21$, $-23 \leq l \leq 23$
Reflections collected	136919
Independent reflections	17815[*R(int)* = 0.0347]
Data/restraints/parameters	17815/40/888
Goodness-of-fit on F^2	1.039
Final *R* indexes [$I>=2\sigma(I)$]	R_1 = 0.0901, wR_2 = 0.2587
Final *R* indexes [all data]	R_1 = 0.1196, wR_2 = 0.2871
Largest diff. peak/hole / e Å^{-3}	3.70/-1.96

Identification code	Compound **4.2 Br**
Empirical formula	$C_{342}H_{502}Br_{16}N_{32}O_{44}S_{11}$
Formula weight	7392.92
Temperature/K	150(2)
Crystal system	triclinic
Space group	*P*-1
a/Å	18.4774(16)
b/Å	22.3850(19)
c/Å	27.557(2)
α/°	99.003(4)
β/°	98.530(4)
γ/°	96.578(4)
Volume/Å^3	11021.8(16)
Z	1
ρ_{calc}mg/mm^3	1.114
M/mm^{-1}	1.562

$F(000)$	3862.0
Crystal size/mm^3	0.15 × 0.12 × 0.08
2Θ range for data collection	2.6 to 45°
Index ranges	$-18 \leq h \leq 19$, $-24 \leq k \leq 24$, $-29 \leq l \leq 28$
Reflections collected	108088
Independent reflections	28814[*R(int)* = 0.0630]
Data/restraints/parameters	28814/153/1959
Goodness-of-fit on F^2	1.147
Final *R* indexes [$I>=2\sigma(I)$]	R_1 = 0.0949, wR_2 = 0.2802
Final *R* indexes [all data]	R_1 = 0.1237, wR_2 = 0.3059
Largest diff. peak/hole / e Å^{-3}	2.78/-1.46

Identification code	Complex **4.7**
Empirical formula	$C_{206}H_{277}Br_{16}N_{39}O_{16}Pd_8$
Formula weight	5685.43
Temperature/K	150(2)
Crystal system	monoclinic
Space group	*C*2/*c*
a/Å	42.542(6)
b/Å	24.032(4)
c/Å	14.441(2)
α/°	90.00
β/°	95.272(7)
γ/°	90.00
Volume/Å^3	14701(4)
Z	2
ρ_{calc}mg/mm^3	1.284
M/mm^{-1}	2.703
$F(000)$	5684.0
Crystal size/mm^3	0.32 × 0.27 × 0.05
2Θ range for data collection	3.34 to 48.88°
Index ranges	$-49 \leq h \leq 49$, $-27 \leq k \leq 24$, $-16 \leq l \leq 16$
Reflections collected	88980
Independent reflections	12096[*R(int)* = 0.0612]
Data/restraints/parameters	12096/126/701
Goodness-of-fit on F^2	1.110
Final *R* indexes [$I>=2\sigma(I)$]	R_1 = 0.0907, wR_2 = 0.2486
Final *R* indexes [all data]	R_1 = 0.1069, wR_2 = 0.2566
Largest diff. peak/hole / e Å^{-3}	1.47/-1.36

Appendix

Identification code	Compound **4.10**
Empirical formula	$C_6H_8N_2O_2$
Formula weight	140.14
Temperature/K	150(2)
Crystal system	orthorhombic
Space group	$Pca2_1$
a/Å	15.887(2)
b/Å	4.9335(7)
c/Å	8.7022(12)
α/°	90.00
β/°	90.00
γ/°	90.00
Volume/Å^3	682.07(16)
Z	4
ρ_{calc}mg/mm^3	1.365
M/mm^{-1}	0.105
F(000)	296.0
Crystal size/mm^3	0.3 × 0.3 × 0.07
2*Θ* range for data collection	6.94 to 53.02°
Index ranges	$-19 \leq h \leq 15$, $-6 \leq k \leq 5$, $-10 \leq l \leq 10$
Reflections collected	4732
Independent reflections	1382[*R(int)* = 0.0377]
Data/restraints/parameters	1382/1/92
Goodness-of-fit on F^2	1.028
Final *R* indexes [$I>=2\sigma(I)$]	R_1 = 0.0458, wR_2 = 0.1030
Final *R* indexes [all data]	R_1 = 0.0688, wR_2 = 0.1122
Largest diff. peak/hole / e Å^{-3}	0.51/-0.14
Flack parameter	0(2)

Identification code	Compound **6.2**
Empirical formula	$C_{14}H_{21}N_5O_2$
Formula weight	291.36
Temperature/K	150(2)
Crystal system	Monoclinic
Space group	$P2_1/c$
a/Å	5.5038(4)
b/Å	27.370(2)
c/Å	10.4978(8)
α/°	90
β/°	101.568(3)
γ/°	90
Volume/Å^3	1549.3(2)
Z	14
ρ_{calc}mg/mm^3	1.249

Appendix

M/mm^{-1}	0.087
F(000)	624
Crystal size/mm^3	0.41 × 0.09 × 0.05
2Θ range for data collection	2.48 to 27.36°
Index ranges	$-6 \leq h \leq 7$, $-34 \leq k \leq 35$, $-13 \leq l \leq 13$
Reflections collected	13342
Independent reflections	3479[$R(int)$ = 0.0617]
Data/restraints/parameters	3479/0/193
Goodness-of-fit on F^2	1.018
Final R indexes [I>=2σ (I)]	R_1 = 0.0428, wR_2 = 0.1018
Final R indexes [all data]	R_1 = 0.0650, wR_2 = 0.1134
Largest diff. peak/hole / e Å^{-3}	0.305/-0.229